



Modelling and Analysis of Marine Operations

APRIL 2011

*This document has been amended since the main revision (April 2011), most recently in December 2012.
See "Changes" on page 3.*

The electronic pdf version of this document found through <http://www.dnv.com> is the officially binding version

FOREWORD

DNV is a global provider of knowledge for managing risk. Today, safe and responsible business conduct is both a license to operate and a competitive advantage. Our core competence is to identify, assess, and advise on risk management. From our leading position in certification, classification, verification, and training, we develop and apply standards and best practices. This helps our customers safely and responsibly improve their business performance. DNV is an independent organisation with dedicated risk professionals in more than 100 countries, with the purpose of safeguarding life, property and the environment.

DNV service documents consist of among others the following types of documents:

- *Service Specifications*. Procedural requirements.
- *Standards*. Technical requirements.
- *Recommended Practices*. Guidance.

The Standards and Recommended Practices are offered within the following areas:

- A) Qualification, Quality and Safety Methodology
- B) Materials Technology
- C) Structures
- D) Systems
- E) Special Facilities
- F) Pipelines and Risers
- G) Asset Operation
- H) Marine Operations
- J) Cleaner Energy
- O) Subsea Systems
- U) Unconventional Oil & Gas

© Det Norske Veritas AS April 2011

Any comments may be sent by e-mail to rules@dnv.com

CHANGES

General

This document supersedes DNV-RP-H103, April 2010.

Text affected by the main changes in this edition is highlighted in red colour. However, if the changes involve a whole chapter, section or sub-section, normally only the title will be in red colour.

Amendment December 2012

- **Sec.6 Landing on Seabed and Retrieval**
 - Equation in item 6.2.3.8 moved back to its original location.

Main changes in April 2011

- **General**
 - The layout has been changed to one column in order to improve electronic readability.
- **Sec.5 Deepwater Lowering Operations**
 - Figure 5-5 has been updated.

Editorial Corrections

In addition to the above stated main changes, editorial corrections may have been made.

CONTENTS

1.	General.....	6
1.1	Introduction.....	6
1.2	Objective.....	6
1.3	Relationship to other codes.....	6
1.4	References.....	6
1.5	Abbreviations.....	6
1.6	Symbols.....	6
2.	General Methods of Analysis	11
2.1	Introduction.....	11
2.2	Description of waves.....	11
2.3	Wave loads on large volume structures	16
2.4	Wave Loads on small volume structures	22
2.5	References	26
3.	Lifting through Wave Zone – General.....	27
3.1	Introduction.....	27
3.2	Loads and load effects	27
3.3	Hydrodynamic coefficients	39
3.4	Calculation methods for estimation of hydrodynamic forces	43
3.5	Moonpool operations	49
3.6	Stability of lifting operations	56
3.7	References.....	57
4.	Lifting through Wave Zone – Simplified Method.....	58
4.1	Introduction.....	58
4.2	Static weight.....	58
4.3	Hydrodynamic forces.....	59
4.4	Accept criteria.....	66
4.5	Typical load cases during lowering through water surface	67
4.6	Estimation of hydrodynamic parameters	69
4.7	Snap forces in slings or hoisting line	72
4.8	References.....	75
5.	Deepwater Lowering Operations.....	75
5.1	Introduction.....	75
5.2	Static forces on cable and lifted object	76
5.3	Dynamic forces on cable and lifted object	80
5.4	Heave compensation	89
5.5	Fibre rope properties	91
5.6	References	93
6.	Landing on Seabed and Retrieval	94
6.1	Introduction.....	94
6.2	Landing on seabed	94
6.3	Installation by suction and levelling	102
6.4	Retrieval of foundations.....	103
6.5	References.....	104
7.	Towing Operations.....	104
7.1	Introduction.....	104
7.2	Surface tows of large floating structures	105
7.3	Submerged tow of 3D objects and long slender elements	115
7.4	References.....	121
8.	Weather Criteria and Availability Analysis	122
8.1	Introduction.....	122
8.2	Environmental parameters	122
8.3	Data accuracy.....	123
8.4	Weather forecasting	125
8.5	Persistence statistics.....	125
8.6	Monitoring of weather conditions and responses	128
8.7	References.....	129
9.	Lifting Operations.....	130
9.1	Introduction.....	130
9.2	Light lifts.....	130
9.3	Heavy lifts.....	132

9.4	Hydrodynamic coupling.....	136
9.5	Lift-off of an object	137
9.6	References.....	139
Appendix A. Added Mass Coefficients		140
Appendix B. Drag Coefficients		144
Appendix C. Physical Constants.....		150

1 General

1.1 Introduction

The present Recommended Practice (RP) gives guidance for modelling and analysis of marine operations, in particular for lifting operations including lifting through wave zone and lowering of objects in deep water to landing on seabed.

1.2 Objective

The objective of this RP is to provide simplified formulations for establishing design loads to be used for planning and execution of marine operations.

1.3 Relationship to other codes

This Recommended Practice should be considered as guidelines describing how to apply the requirements of “*Rules for Planning and Execution of Marine Operations*” issued by Det Norske Veritas, 1996.

Section 4 “Lifting through wave zone – simplified method” in the present RP substitutes the sub-section; *Sec.2 Design Loads* in *Pt.2 Ch.6 Sub Sea Operations* in the “*Rules for Planning and Execution of Marine Operations*”.

These Rules are presently being converted to following new DNV Offshore Standards (planned October 2010):

DNV-OS-H101	Marine Operations, General
DNV-OS-H102	Marine Operations, Loads and Design
DNV-OS-H201	Load Transfer Operations
DNV-OS-H202	Sea Transports
DNV-OS-H203	Transit and Positioning of Mobile Offshore Units
DNV-OS-H204	Offshore Installation Operations
DNV-OS-H205	Lifting Operations
DNV-OS-H206	Subsea Operations

More general information on environmental conditions and environmental loads is given in; *DNV-RP-C205 Environmental Conditions and Environmental Loads (April 2007)*.

1.4 References

References are given at the end of each chapter. These are referred to in the text.

1.5 Abbreviations

<i>DAF</i>	Dynamic Amplification Factor
<i>HF</i>	high frequency
<i>J</i>	Jonswap
<i>LF</i>	low frequency
<i>LTF</i>	linear transfer function
<i>PM</i>	Pierson-Moskowitz
<i>RAO</i>	Response Amplitude Operator
<i>WF</i>	wave frequency

1.6 Symbols

1.6.1 Latin symbols

a	fluid particle acceleration
a_{ct}	characteristic single amplitude vertical acceleration of crane tip
a_r	relative acceleration
a_w	characteristic wave particle acceleration
A	cross-sectional area
A	nominal area of towline
A_{exp}	projected cross-sectional area of towed object
A_h	area of available holes in bucket
A_{ij}	added mass
A_{33}^{∞}	infinite frequency vertical added mass
A_{33}^0	zero-frequency vertical added mass
A_b	bucket area
A_C	wave crest height

A_p	projected area
A_s	friction area per meter depth of penetration
A_t	skirt tip area
A_T	wave trough depth
A_W	water plane area
A_x	x-projected area of lifted object
A_γ	normalizing factor in Jonswap spectrum
B	beam/breadth
B_{ij}	wave generation damping
B_{11}	wave drift damping
$B_{33}^{(1)}$	linear heave damping coefficient
$B_{33}^{(2)}$	quadratic heave damping coefficient
B_1	linear damping coefficient
B_2	quadratic damping coefficient
c	wave phase speed
c'	equivalent winch damping
c_c	linear damping of heave compensator
c_L	sound of speed
C_A	added mass coefficient
C_b	block coefficient
C_B	centre of buoyancy
C_D	drag coefficient
C_{Df}	cable longitudinal friction coefficient
C_{Dn}	drag coefficient for normal flow
C_{Dx}	drag coefficient for horizontal flow
C_{DS}	steady drag coefficient
C_{Dz}	drag coefficient for vertical flow
C_d	damping coefficient
C_e	water exit coefficient
C_F	force centre
c_F	fill factor
C_G	centre of gravity
C_L	lift coefficient
C_M	mass coefficient ($=1+C_A$)
C_s, C_b	moonpool damping coefficients
C_{s1}	linearised moonpool damping coefficients
C_S	slamming coefficient
C_{ij}	hydrostatic stiffness
d	water depth
d	depth of penetration
d_i	diameter of flow valve
D	diameter
D	diameter of propeller disk
D_c	cable diameter
$D(\theta)$	wave spectrum directionality function
E	modulus of elasticity
EI	bending stiffness
E_k	fluid kinetic energy
f	wave frequency ($=\omega/2\pi$)
f	friction coefficient for valve sleeves
$f(z)$	skin friction at depth z
f_{drag}	sectional drag force
f_N	sectional normal force
f_L	sectional lift force
f_T	sectional tangential force
F_{line}	force in hoisting line/cable

F_B	buoyancy force
F_{D0}	horizontal drag force on lifted object
F_ρ	buoyancy force
F_C	steady force due to current
F_I	inertia force
$F_\lambda(t)$	marginal distribution of “calm” period t
F_{wd}	wave generation damping force
F_{WD}	wave drift force
F_d	drag force
F_d	dynamic force in cable
F_h	depth Froude number
F_w	wave excitation force
F_s	slamming force
F_e	water exit force
g	acceleration of gravity
GM_L	longitudinal metacentric height
GM_T	transverse metacentric height
h	gap between soil and skirt tip
H	wave height ($=A_C+A_T$)
$H(\omega, \theta)$	motion transfer function
H_L	motion transfer function for lifted object
H_b	breaking wave height
H_{m0}	significant wave height
H_s	significant wave height
I	area moment of inertia of free surface in tank
k	wave number
k	roughness height
k	total towline stiffness
k'	equivalent winch stiffness coefficient
k_{flow}	pressure loss coefficient
k_s	stiffness of soft sling
k_c	stiffness of crane master
k_c	stiffness of heave compensator
k_f	skin friction correlation coefficient
k_t	tip resistance correlation coefficient
k_V	vertical cable stiffness
k_E	vertical elastic cable stiffness
k_E	elastic towline stiffness
k_G	vertical geometric cable stiffness
k_G	geometric towline stiffness
k_H	horizontal stiffness for lifted object
k_U	soil unloading stiffness
K	stiffness of hoisting system
KC	Keulegan-Carpenter number
KC_{por}	“Porous Keulegan-Carpenter number”
k_{ij}	wave number
K_{ij}	mooring stiffness
L	unstretched length of cable/towline
L_b	length of towed object
L_s	stretched length of cable
L_{sleeve}	length of valve sleeves
M	mass of lifted object
m	mass per unit length of cable
m'	equivalent winch mass
m_a	added mass per unit length
m_c	mass of heave compensator

M_f	dynamic amplification factor
M_G	moment of towing force
M_{ij}	structural mass matrix
M_n	spectral moments
M_s^{tow}	mass of towed object
M_s^{tug}	mass of tug
N	number of wave maxima
N_c	number of “calm” periods
N_s	number of “storm” periods
p	perforation ratio
p_{FK}	undisturbed (Froude-Krylov) pressure
p_w	hydrodynamic pressure inside bucket
$q_c(z)$	cone penetration resistance
q_{flow}	flow of water out of bucket
$q_t(d)$	tip resistance at depth of penetration
Q_{skirt}	skirt penetration resistance
Q_{soil}	force transferred to the soil
Q_{sc}	static soil resistance
Q_{sd}	design bearing capacity
r	structural displacement
\dot{r}	structural velocity
\ddot{r}	structural acceleration
\mathbf{r}_0^{tow}	position of towline end on tow
\mathbf{r}_0^{tug}	position of towline end on tug
R	reflection coefficient
R	distance from COG to end of bridle lines
Re	Reynolds number
R_{max}	most probable largest maximum load
r_{ij}	radii of gyration
s	submergence of cylinder
$S(\omega)$	wave energy spectrum
$S_L(\omega)$	response spectrum of lifted object
S	projected area
S	area of circumscribed circle of towline cross-section
S	wave steepness
S	water plane area
T	wave period
T	draft
T_b	draft of towed object
T_c	total duration of “calm” periods
T_s	total duration of “storm” periods
$T(s)$	quasi-static tension at top of the cable as function of payout s
T_C	estimated contingency time
T_{ct}	period of crane tip motion
T_j, T_n	natural periods (eigenperiods)
T_2, T_{m01}	mean wave period
T_z, T_{m02}	zero-up-crossing period
T_p	spectrum peak period
T_{POP}	planned operation time
T_R	operation reference period
T_z	zero-up-crossing period
T_0	resonance period (eigenperiod)
T_0	towline tension
T_{0h}	horizontal resonance period (eigenperiod)
U	towing speed
$U(r, x)$	velocity in thruster jet

U_c	current velocity
U_0	flow velocity through propeller disk
v	fluid particle velocity
v_3	vertical water particle velocity
\dot{v}_3	vertical water particle acceleration
\dot{v}	fluid particle acceleration
v_c	mean (constant) lowering velocity
v_{ct}	characteristic single amplitude vertical velocity of crane tip
v_{ff}	free fall velocity
v_{flow}	velocity of water out of bucket
v_{imp}	landing impact velocity
v_m	maximum wave velocity
v_r	relative velocity
v_s	slamming impact velocity
v_w	characteristic wave particle velocity
$V(t)$	displaced volume
V_R	velocity parameter
V_R	reference volume
V_0	displaced volume of object in still water
w	submerged weight per unit length of cable/towline
W	submerged weight of lifted object
W	submerged weight of towline
W_0	weight of lifted object in air
\dot{x}_j	velocity of lifted object in direction j
\ddot{x}_j	acceleration of lifted object in direction j
x_w	winch pay-out coordinate
$x(s)$	horizontal towline coordinate
$z(s)$	horizontal towline coordinate
z_{ct}	motion of crane tip
z_m	vertical oscillation amplitude
z_m	maximum (positive) sag of towline
z_{max}	squat

1.6.2 Greek symbols

α	towline direction
α_{int}	interaction efficiency factor
β	beta parameter ($=Re/KC$)
β	wave direction
Δ	non-dimensional roughness
Δz_G	vertical geometric displacement
Δz_E	vertical elastic displacement
ε	random phase
ε	mass ratio
δ	static deflection (sag) of beam
δ_{mob}	vertical soil displacement to mobilize Q_{sd}
$\dot{\delta}_{soil}$	rate of change of soil displacement
γ	peak shape parameter in Jonswap spectrum
γ_r	rate effect factor
γ_m	soil material coefficient
$\Gamma()$	Gamma function
ϕ	velocity potential
η	vertical motion of lifted object
$\tilde{\eta}$	wave induced motion of object
$\dot{\eta}$	vertical velocity of lifted object
η_a	vertical single amplitude crane tip motion
η_L	motion of lifted object

κ	moonpool correction factor
κ	amplification factor
μ	discharge coefficient
ν	fluid kinematic viscosity
ν_j	natural wave numbers of cable
ν_{ij}	wave number
λ	wave length
θ	wave direction
θ	adjustment factor for mass of hoisting line
ψ	wave amplification factor
ρ	mass density of water
ρ_s	mass density of cable
ρ_w	mass density of water
σ	spectral width parameter
σ	linear damping coefficient for cable motion
σ_η	standard deviation of vertical crane tip motion
σ_v	standard deviation of water particle velocity
σ_r	standard deviation of dynamic load
Σ	linear damping coefficient for motion of lifted object
$\bar{\tau}_c$	average duration of “calm” periods
$\bar{\tau}_s$	average duration of “storm” periods
ω	wave angular frequency
ω_j	natural frequencies of cable
ω_0	resonance wave angular frequency
ω'	non-dimensional frequency
ω_η	angular frequency of vertical motion of lifted object
ω_p	angular spectral peak frequency
ξ_j	rigid body motion
ξ_L	horizontal offset at end of cable
$\xi(z)$	horizontal offset of lifted object
$\zeta(t)$	wave surface elevation
ζ_a	wave amplitude
ζ_b	motion of body in moonpool
ζ_s	heave motion of ship
ζ_w	sea surface elevation outside moonpool

2 General Methods of Analysis

2.1 Introduction

This chapter is a selective extract of the description of wave load analysis given in *DNV-RP-C205, ref./1/*. The most recent valid version of DNV-RP-C205 should be consulted. For more thorough discussion of this topic and other metocean issues, see *refs /2/, /3/, /4/ and /5/*.

2.2 Description of waves

2.2.1 General

2.2.1.1 Ocean waves are irregular and random in shape, height, length and speed of propagation. A real sea state is best described by a random wave model.

2.2.1.2 A linear random wave model is a sum of many small linear wave components with different amplitude, frequency and direction. The phases are random with respect to each other.

2.2.1.3 A non-linear random wave model allows for sum- and difference frequency wave component caused by non-linear interaction between the individual wave components.

2.2.1.4 Wave conditions which are to be considered for structural design purposes, may be described either by deterministic design wave methods or by stochastic methods applying wave spectra.

2.2.1.5 For quasi-static response of structures, it is sufficient to use deterministic regular waves characterized

by wave length and corresponding wave period, wave height, crest height and wave. The deterministic wave parameters may be predicted by statistical methods.

2.2.1.6 Structures with significant dynamic response require stochastic modelling of the sea surface and its kinematics by time series. A sea state is specified by a wave frequency spectrum with a given significant wave height, a representative frequency, a mean propagation direction and a spreading function. A sea state is also described in terms of its duration of stationarity, usually taken to be 3 hours.

2.2.1.7 The wave conditions in a sea state can be divided into two classes: *wind seas* and *swell*. Wind seas are generated by local wind, while swell have no relationship to the local wind. Swells are waves that have travelled out of the areas where they were generated. Moderate and low sea states in open sea areas are often composed of both wind sea and swell.

2.2.1.8 In certain areas internal solitary waves can occur at a water depth where there is a rapid change in water density due to changes in temperature or salinity. Such waves may have an effect on deepwater lowering operations, *ref. Section 5*.

2.2.2 Regular waves

2.2.2.1 A *regular* travelling wave is propagating with permanent form. It has a distinct wave length, wave period, wave height.

2.2.2.2 A regular wave is described by the following main characteristics;

- *Wave length*: The wave length λ is the distance between successive crests.
- *Wave period*: The wave period T is the time interval between successive crests passing a particular point.
- *Phase velocity*: The propagation velocity of the wave form is called phase velocity, wave speed or wave celerity and is denoted by $c = \lambda / T = \omega / k$
- *Wave frequency* is the inverse of wave period: $f = 1/T$
- *Wave angular frequency*: $\omega = 2\pi / T$
- *Wave number*: $k = 2\pi / \lambda$
- *Surface elevation*: The surface elevation $z = \eta(x, y, t)$ is the distance between the still water level and the wave surface.
- *Wave crest height* A_C is the distance from the still water level to the crest.
- *Wave trough depth* A_H is the distance from the still water level to the trough.
- *Wave height*: The wave height H is the vertical distance from trough to crest. $H = A_C + A_T$.
- *Water depth*: d

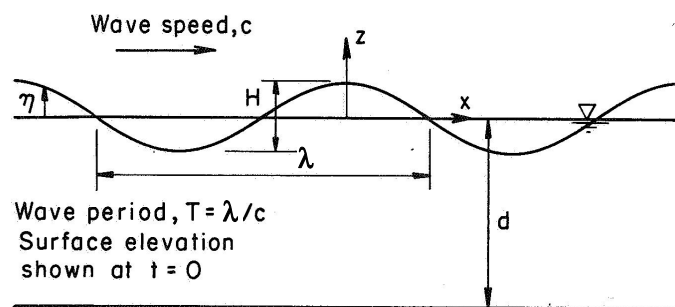


Figure 2-1
Regular travelling wave properties

2.2.2.3 Nonlinear regular waves are asymmetric, $A_C > A_T$ and the phase velocity depends on wave height.

2.2.2.4 For a specified regular wave with period T , wave height H and water depth d , two-dimensional regular wave kinematics can be calculated using a relevant wave theory valid for the given wave parameters.

2.2.2.5 Table 3-1 in DNV-RP-C205, *ref./1/*, gives expressions for horizontal fluid velocity u and vertical fluid velocity w in a linear Airy wave and in a second-order Stokes wave.

2.2.3 Modelling of irregular waves

2.2.3.1 Irregular random waves, representing a real sea state, can be modelled as a summation of sinusoidal

wave components. The simplest random wave model is the linear long-crested wave model given by;

$$\eta_1(t) = \sum_{k=1}^N A_k \cos(\omega_k t + \varepsilon_k)$$

where ε_k are random phases uniformly distributed between 0 and 2π , mutually independent of each other and of the random amplitudes which are taken to be Rayleigh distributed with mean square value

$$E[A_k^2] = 2S(\omega_k)\Delta\omega_k$$

$S(\omega)$ is the wave spectrum and $\Delta\omega_k = (\omega_{k+1} - \omega_{k-1})/2$. Use of deterministic amplitudes $A_k = \sigma_k$ can give non-conservative estimates.

2.2.3.2 The lowest frequency interval $\Delta\omega$ is governed by the total duration of the simulation t , $\Delta\omega = 2\pi/t$. The number of frequencies to simulate a typical short term sea state is governed by the length of the simulation, but should be at least 1000 in order to capture the properties of extreme waves. For simulations of floater motions randomness is usually assured by using on the order of 100 frequencies. The influence of the maximum frequency ω_{max} should be investigated. This is particularly important when simulating irregular fluid velocities.

2.2.4 Breaking wave limit

2.2.4.1 The wave height is limited by breaking. The maximum wave height H_b is given by;

$$\frac{H_b}{\lambda} = 0.142 \tanh \frac{2\pi d}{\lambda}$$

where λ is the wave length corresponding to water depth d .

2.2.4.2 In deep water the breaking wave limit corresponds to a maximum steepness $S_{max} = H_b/\lambda = 1/7$. In shallow water the limit of the wave height can be taken as 0.78 times the local water depth.

2.2.5 Short term wave conditions

2.2.5.1 Short term stationary irregular sea states may be described by a wave spectrum; that is, the power spectral density function of the vertical sea surface displacement.

2.2.5.2 It is common to assume that the sea surface is stationary for a duration of 20 minutes to 3-6 hours. A stationary sea state can be characterised by a set of environmental parameters such as the *significant wave height* H_s and the *spectral peak period* T_p . The wave spectrum is often defined in terms of H_s and T_p .

2.2.5.3 The significant wave height H_s is approximately equal to the average height (trough to crest) of the highest one-third waves in the indicated time period.

2.2.5.4 The spectral peak period T_p is the wave period determined by the inverse of the frequency at which a wave energy spectrum has its maximum value.

2.2.5.5 The zero-up-crossing period T_z is the average time interval between two successive up-crossings of the mean sea level.

2.2.5.6 Wave spectra can be given in table form, as measured spectra, or by a parameterized analytic formula. The most appropriate wave spectrum depends on the geographical area with local bathymetry and the severity of the sea state.

2.2.5.7 The Pierson-Moskowitz (PM) spectrum and JONSWAP spectrum are frequently applied for wind seas. The PM-spectrum was originally proposed for fully-developed sea. The JONSWAP spectrum extends PM to include fetch limited seas. Both spectra describe wind sea conditions that often occur for the most severe sea-states.

2.2.5.8 Moderate and low sea states in open sea areas are often composed of both wind sea and swell. A two peak spectrum may be used to account for both wind sea and swell. The Ochi-Hubble spectrum and the Torsethaugen spectrum are two-peak spectra (*ref. /1/*).

2.2.6 Pierson-Moskowitz and JONSWAP spectra

2.2.6.1 The *Pierson-Moskowitz* (PM) spectrum $S_{PM}(\omega)$ is given by;

$$S_{PM}(\omega) = \frac{5}{16} \cdot H_s^2 \omega_p^4 \cdot \omega^{-5} \exp\left(-\frac{5}{4} \left(\frac{\omega}{\omega_p}\right)^4\right)$$

where $\omega_p = 2\pi/T_p$ is the angular spectral peak frequency.

2.2.6.2 The *JONSWAP* spectrum $S_J(\omega)$ is formulated as a modification of the Pierson-Moskowitz spectrum for a developing sea state in a fetch limited situation:

$$S_J(\omega) = A_\gamma S_{PM}(\omega) \gamma^{\exp\left(-0.5\left(\frac{\omega - \omega_p}{\sigma \omega_p}\right)^2\right)}$$

where

$S_{PM}(\omega)$ = Pierson-Moskowitz spectrum
 γ = non-dimensional peak shape parameter
 σ = spectral width parameter

$$\sigma = \sigma_a \text{ for } \omega \leq \omega_p$$

$$\sigma = \sigma_b \text{ for } \omega > \omega_p$$

$A_\gamma = 1 - 0.287 \ln(\gamma)$ is a normalizing factor

2.2.6.3 The corresponding spectral moment M_n , of the wave spectra is;

$$M_n = \int_0^\infty \omega^n S(\omega) d\omega_n$$

2.2.6.4 For the *JONSWAP* spectrum the spectral moments are given approximately as;

$$M_0 = \frac{1}{16} H_s^2$$

$$M_1 = \frac{1}{16} H_s^2 \omega_p \frac{6.8 + \gamma}{5 + \gamma}$$

$$M_2 = \frac{1}{16} H_s^2 \omega_p^2 \frac{11 + \gamma}{5 + \gamma}$$

2.2.6.5 The following sea state parameters can be defined in terms of spectral moments:

The significant wave height H_s is defined by

$$H_s = H_{m0} = 4\sqrt{M_0}$$

The zero-up-crossing period T_z can be estimated by:

$$T_{m02} = 2\pi \sqrt{\frac{M_0}{M_2}}$$

The mean wave period T_1 can be estimated by:

$$T_{m01} = 2\pi \frac{M_0}{M_1}$$

2.2.6.6 Average values for the *JONSWAP* experiment data are $\gamma = 3.3$, $\sigma_a = 0.07$, $\sigma_b = 0.09$. For $\gamma = 1$ the *JONSWAP* spectrum reduces to the Pierson-Moskowitz spectrum.

2.2.6.7 The *JONSWAP* spectrum is expected to be a reasonable model for

$$3.6 < T_p / \sqrt{H_s} < 5$$

and should be used with caution outside this interval. The effect of the peak shape parameter γ is shown in Figure 2-2.

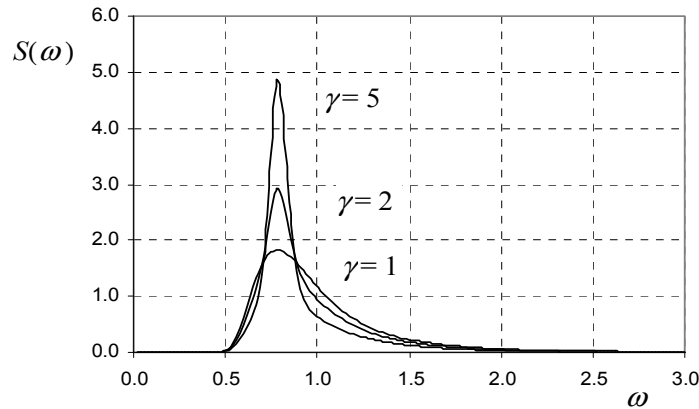


Figure 2-2
JONSWAP spectrum for $H_s = 4.0$ m, $T_p = 8.0$ s for $\gamma = 1$, $\gamma = 2$ and $\gamma = 5$

2.2.6.8 The zero-up-crossing wave period T_z and the mean wave period T_l may be related to the peak period by the following approximate relations ($1 \leq \gamma < 7$).

$$\frac{T_z}{T_p} = 0.6673 + 0.05037\gamma - 0.006230\gamma^2 + 0.0003341\gamma^3$$

$$\frac{T_l}{T_p} = 0.7303 + 0.04936\gamma - 0.006556\gamma^2 + 0.0003610\gamma^3$$

For $\gamma = 3.3$; $T_p = 1.2859T_z$ and $T_l = 1.0734T_z$

For $\gamma = 1.0$ (PM spectrum); $T_p = 1.4049T_z$ and $T_l = 1.0867T_z$

2.2.6.9 If no particular values are given for the peak shape parameter γ , the following value may be applied:

$$\gamma = 5 \quad \text{for} \quad T_p / \sqrt{H_s} \leq 3.6$$

$$\gamma = \exp(5.75 - 1.15T_p / \sqrt{H_s}) \quad \text{for} \quad 3.6 < T_p / \sqrt{H_s} < 5$$

$$\gamma = 1 \quad \text{for} \quad 5 \leq T_p / \sqrt{H_s}$$

where T_p is in seconds and H_s is in metres.

2.2.7 Directional distribution of wind sea and swell

2.2.7.1 Directional short-crested wave spectra $S(\omega, \theta)$ may be expressed in terms of the uni-directional wave spectra,

$$S(\omega, \theta) = S(\omega)D(\theta, \omega) = S(\omega)D(\theta)$$

where the latter equality represents a simplification often used in practice. Here $D(\theta, \omega)$ and $D(\theta)$ are directionality functions. θ is the angle between the direction of elementary wave trains and the main wave direction of the short crested wave system.

2.2.7.2 The directionality function fulfils the requirement;

$$\int D(\theta, \omega) d\theta = 1$$

2.2.7.3 For a two-peak spectrum expressed as a sum of a swell component and a wind-sea component, the total directional frequency spectrum $S(\omega, \theta)$ can be expressed as

$$S(\omega, \theta) = S_{wind\ sea}(\omega)D_{wind\ sea}(\theta) + S_{swell}(\omega)D_{swell}(\theta)$$

2.2.7.4 A common directional function often used for wind sea is;

$$D(\theta) = \frac{\Gamma(1 + n/2)}{\sqrt{\pi}\Gamma(1/2 + n/2)} \cos^n(\theta - \theta_p)$$

where Γ is the Gamma function and $|\theta - \theta_p| \leq \frac{\pi}{2}$.

2.2.7.5 The main direction θ_p may be set equal to the prevailing wind direction if directional wave data are not available.

2.2.7.6 Due consideration should be taken to reflect an accurate correlation between the actual sea-state and the constant n . Typical values for wind sea are $n = 2$ to $n = 4$. If used for swell, $n \geq 6$ is more appropriate.

2.2.8 Maximum wave height in a stationary sea state

2.2.8.1 For a stationary narrow banded sea state with N independent local maximum wave heights, the extreme maxima in the sea state can be taken as:

Quantity	H_{max}/H_s (N is large)
Most probable largest	$\sqrt{\frac{1}{2} \ln N}$
Median value	$\sqrt{\frac{1}{2} \ln N} \cdot \left(1 + \frac{0.367}{\ln N}\right)^{1/2}$
Expected extreme value	$\sqrt{\frac{1}{2} \ln N} \left(1 + \frac{0.577}{\ln N}\right)^{1/2}$
p-fractile extreme value	$\sqrt{\frac{1}{2} \ln N} \left(1 - \frac{\ln(-\ln p)}{\ln N}\right)^{1/2}$

For a narrow banded sea state, the number of maxima can be taken as $N = t/T_z$ where t is the sea state duration.

2.3 Wave loads on large volume structures

2.3.1 Introduction

2.3.1.1 Offshore structures are normally characterized as either large volume structures or small volume structures. For a large volume structure the structure's ability to create waves is important in the force calculations while for small volume structures this is negligible.

2.3.1.2 Small volume structures may be divided into structures dominated by drag force and structures dominated by inertia (mass) force. Figure 2-3 shows the different regimes where area I, III, V and VI covers small volume structures.

2.3.1.3 The term large volume structure is used for structures with dimensions D on the same order of magnitude as typical wave lengths λ of ocean waves exciting the structure, usually $D > \lambda/6$. This corresponds to the *diffraction* wave force regimes II and IV shown in Figure 2-3 below where this boundary is equivalently defined as $\pi D/\lambda > 0.5$.

2.3.2 Motion time scales

2.3.2.1 A floating, moored structure may respond to wind, waves and current with motions on three different time scales,

- high frequency (HF) motions
- wave frequency (WF) motions
- low frequency (LF) motions.

2.3.2.2 The largest wave loads on offshore structures take place at the same frequencies as the waves, causing wave frequency (WF) motions of the structure. To avoid large resonant effects, offshore structures and their mooring systems are often designed in such a way that the resonant frequencies are shifted well outside the wave frequency range.

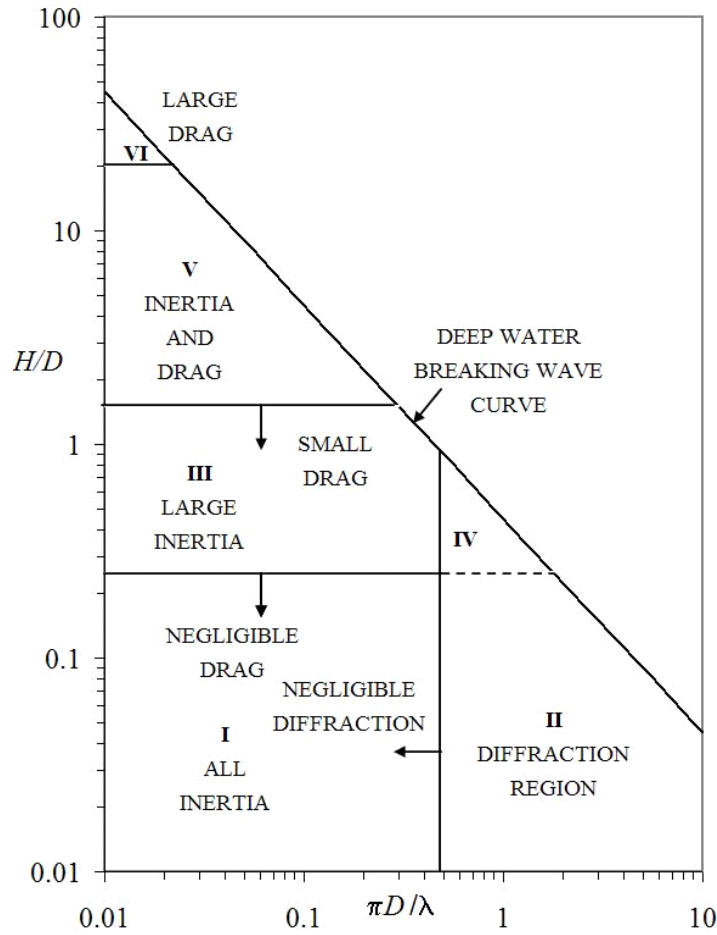


Figure 2-3
Different wave force regimes (Chakrabarti, 1987).
 D = characteristic dimension, H = wave height, λ = wave length.

2.3.2.3 A floating structure responds mainly in its six rigid modes of motions including translational modes, surge, sway, heave, and rotational modes, roll, pitch, yaw. In addition, wave induced loads can cause high frequency (HF) elastic response, i.e. spring-ing and whipping of ships. Current may induce high frequency (HF) vortex induced vibrations (VIV) on slender structural elements.

2.3.2.4 Due to non-linear load effects, some responses always appear at the natural frequencies. Slowly varying wave and wind loads give rise to low frequency (LF) resonant horizontal motions, also named slow-drift motions.

2.3.2.5 The WF motions are mainly governed by inviscid fluid effects, while viscous fluid effects are relatively important for LF mo-tions. Viscous fluid effects may be important for WF motions close to resonance. A typical example is resonant roll motion. Different hydrodynamic effects are important for each floater type, and must be taken into account in the analysis and design.

2.3.3 Natural periods

2.3.3.1 Natural periods for a large moored offshore structure in surge, sway and yaw are typically more than 100 seconds. Natural periods in heave, roll and pitch of semi-submersibles are usually above 20 seconds.

2.3.3.2 The uncoupled natural periods $T_j, j = 1, 2, \dots, 6$ of a moored offshore structure are approximately given by

$$T_j = 2\pi \left(\frac{M_{jj} + A_{jj}}{C_{jj} + K_{jj}} \right)^{\frac{1}{2}}$$

where M_{jj} , A_{jj} , C_{jj} and K_{jj} are the diagonal elements of the mass, added mass, hydrostatic and mooring stiffness matrices.

2.3.3.3 Natural periods depend on coupling between different modes and the amount of damping.

2.3.3.4 The uncoupled natural period in heave for a freely floating offshore vessel is

$$T_3 = 2\pi \left(\frac{M + A_{33}}{\rho g S} \right)^{\frac{1}{2}}$$

where M is the mass, A_{33} the heave added mass and S is the water plane area.

2.3.3.5 The uncoupled natural period in pitch for a freely floating offshore vessel is;

$$T_5 = 2\pi \left(\frac{Mr_{55}^2 + A_{55}}{\rho g V GM_L} \right)^{\frac{1}{2}}$$

where r_{55} is the pitch radius of gyration, A_{55} is the pitch added moment and GM_L is the longitudinal metacentric height. The uncoupled natural period in roll is

$$T_4 = 2\pi \left(\frac{Mr_{44}^2 + A_{44}}{\rho g V GM_T} \right)^{\frac{1}{2}}$$

where r_{44} is the roll radius of gyration, A_{44} is the roll added moment and GM_T is the transversal metacentric height.

2.3.4 Frequency domain analysis

2.3.4.1 The wave induced loads in an irregular sea can be obtained by linearly superposing loads due to regular wave components. Analysing a large volume structure in regular incident waves is called a *frequency domain analysis*.

2.3.4.2 Assuming steady state, with all transient effects neglected, the loads and dynamic response of the structure is oscillating harmonically with the same frequency as the incident waves, or with the frequency of encounter in the case of a forward speed.

2.3.4.3 Within a linear analysis, the hydrodynamic problem is usually divided into two sub-problems:

- *Radiation problem* where the structure is forced to oscillate with the wave frequency in a rigid body motion mode with no incident waves. The resulting loads are usually formulated in terms of *added mass*, *damping* and *restoring* loads

$$F_k^{(r)} = -A_{kj} \frac{d^2 \xi_j}{dt^2} - B_{kj} \frac{d \xi_j}{dt} - C_{kj} \xi_j$$

where A_{kj} and B_{kj} are added mass and damping, and C_{kj} are the hydrostatic restoring coefficients, $j, k = 1, 6$, for the six degrees of rigid body modes. A_{kj} and B_{kj} are functions of wave frequency ω .

- *Diffraction problem* where the structure is restrained from motions and is excited by incident waves. The resulting loads are *wave excitation* loads

$$F_k^{(d)} = f_k(\omega) e^{-i\alpha x}; k = 1, 6$$

2.3.4.4 The part of the wave excitation loads that is given by the undisturbed pressure in the incoming wave is called the *Froude-Krylov* forces/moments. The remaining part is called *diffraction* forces/moments.

2.3.4.5 Large volume structures are inertia-dominated, which means that the global loads due to wave diffraction are significantly larger than the drag induced global loads. To avoid an excessive increase in the number of elements/panels on slender members/braces of the structure in the numerical diffraction analysis, a Morison load model with predefined added mass coefficients can be added to the radiation/diffraction model, *ref. Section 2.4*.

Guidance note:

For some large volume floater types, like semisubmersibles with rectangular shaped pontoons and columns, edges may lead to flow separation and introduce considerable viscous damping. For such floaters a dual hydrodynamic model may be applied, adding Morison type viscous loads and radiation/diffraction loads on the same structural element.

---e-n-d---of---G-u-i-d-a-n-c-e---n-o-t-e---

2.3.4.6 A linear analysis will usually be sufficiently accurate for prediction of global wave frequency loads. Hence, this section focuses on first order wave loads. The term *linear* means that the fluid dynamic pressure and the resulting loads are proportional to the wave amplitude. This means that the loads from individual waves in an arbitrary sea state can be simply superimposed.

2.3.4.7 Only the wetted area of the floater up to the mean water line is considered. The analysis gives first order

excitation forces, hydrostatics, potential wave damping, added mass, first order motions in rigid body degrees of freedom and the mean drift forces/moments. The mean wave drift force and moments are of second order, but depends on first order quantities only.

2.3.4.8 The output from a frequency domain analysis will be transfer functions of the variables in question, e.g. exciting forces/moments and platform motions per unit wave amplitude. The first order or linear force/moment transfer function (LTF) is usually denoted $H^{(1)}(\omega)$. The linear motion transfer function, $\xi^{(1)}(\omega)$ is also denoted the response transfer function. These quantities are usually taken as complex numbers. The linear motion transfer function gives the response per unit amplitude of excitation, as a function of the wave frequency,

$$\xi^{(1)}(\omega) = H^{(1)}(\omega)L^{-1}(\omega)$$

where $L(\omega)$ is the linear structural operator characterizing the equations of motion,

$$L(\omega) = -\omega^2[M + A(\omega)] + i\omega B(\omega) + C$$

M is the structure mass and inertia, A the added mass, B the wave damping and C the stiffness, including both hydrostatic and structural stiffness. The equations of rigid body motion are, in general, six coupled equations for three translations (surge, sway and heave) and three rotations (roll, pitch and yaw). The module of the motion transfer function is denoted the Response Amplitude Operator (RAO).

2.3.4.9 The concept of RAOs may also be used for global forces and moments derived from rigid body motions and for diffracted wave surface elevation, fluid pressure and fluid kinematics.

2.3.4.10 The frequency domain method is well suited for systems exposed to random wave environments, since the random response spectrum can be computed directly from the transfer function and the wave spectrum in the following way:

$$S_R(\omega) = |\xi^{(1)}(\omega)|^2 S(\omega)$$

where

ω	= angular frequency ($= 2\pi/T$)
$\xi^{(1)}(\omega)$	= transfer function of the response
$S(\omega)$	= wave spectrum
$S_R(\omega)$	= response spectrum

2.3.4.11 Based on the response spectrum, the short-term response statistics can be estimated. The method limitations are that the equations of motion are linear and the excitation is linear.

2.3.4.12 A linear assumption is also employed in the random process theory used to interpret the solution. This is inconvenient for nonlinear effects like drag loads, damping and excitation, time varying geometry, horizontal restoring forces and variable surface elevation. However, in many cases these non-linearities can be satisfactorily linearised, *ref. //*.

2.3.4.13 Frequency domain analysis is used extensively for floating units, including analysis of both motions and forces. It is usually applied in fatigue analyses, and analyses of more moderate environmental conditions where linearization gives satisfactory results. The main advantage of this method is that the computations are relatively simple and efficient compared to time domain analysis methods.

2.3.4.14 Low frequency motions of a moored floating structure are caused by slowly varying wave, wind and current forces. The wave-induced drift force can be modelled as a sum of an inviscid force and a viscous force. The inviscid wave drift force is a second-order wave force, proportional to the square of the wave amplitude. In a random sea-state represented by a sum of N wave components ω_i , $i = 1, N$ the wave drift force oscillates at difference frequencies $\omega_i - \omega_j$ and is given by the expression

$$F_{wd}(t) = \text{Re} \sum_{i,j}^N A_i A_j H^{(2-)}(\omega_i, \omega_j) e^{i(\omega_i - \omega_j)t}$$

where A_i, A_j are the individual wave amplitudes and $H^{(2-)}$ is the difference frequency quadratic transfer function (QTF). The QTF is usually represented as a complex quantity to account for the proper phase relative to the wave components. Re denotes the real part. The mean drift force is obtained by keeping only diagonal terms ($\omega_i = \omega_j$) in the sum above

2.3.4.15 If the natural frequency of the horizontal floater motion is much lower than the characteristic frequencies of the sea state, the so called Newman's approximation can be used to approximate the wave drift force. In this approximation the QTF matrix can be approximated by the diagonal elements,

$$H^{(2-)}(\omega_i, \omega_j) \cong \frac{1}{2} [H^{(2-)}(\omega_i, \omega_i) + H^{(2-)}(\omega_j, \omega_j)]$$

More detailed information on drift forces and Newman's approximation is given in *Ref. /1/*.

2.3.5 Multi-body hydrodynamic interaction

2.3.5.1 Hydrodynamic interactions between multiple floaters in close proximity and between a floater and a large fixed structure in the vicinity of the floater, may be analysed using radiation/diffraction software through the so-called multi-body options. The N floaters are solved in an integrated system with motions in $6 \cdot N$ degrees of freedom.

2.3.5.2 An example of a two-body system is a crane vessel and a side-by-side positioned transport barge during lifting operations where there may be strong hydrodynamic interaction between the two floaters. The interaction may be of concern due to undesirable large relative motion response between the two floaters.

2.3.5.3 An important interaction effect is a near resonance trapped wave between the floaters that can excite sway and roll motions. This trapped wave is undamped within potential theory. Some radiation-diffraction codes have means to damp such trapped waves. The discretisation of the wetted surfaces in the area between the floaters must be fine enough to capture the variations in the trapped wave. Additional resonance peaks also appear in coupled heave, pitch and roll motions.

Guidance note:

In the case of a narrow gap between near wall sided structures in the splash zone a near resonant piston mode motion may be excited at a certain wave frequency. The eigenfrequency ω_0 of the piston mode is within a frequency range given by

$$1 + \frac{2}{\pi} \cdot \frac{G}{D} < \frac{\omega_0^2 D}{g} < 1 + \frac{\pi}{2} \cdot \frac{G}{D}$$

where

D = draft of structure (barge) [m]
 G = width of gap [m]
 g = acceleration of gravity [m/s²]

In addition transverse and longitudinal sloshing mode motions in the gap may occur. Formulas for the eigenfrequencies of such sloshing mode motions are given in *ref /8/*.

---e-n-d---of---G-u-i-d-a-n-c-e---n-o-t-e---

2.3.5.4 When analyzing hydrodynamic interactions between multiple floater using a radiation/diffraction panel method one should take care to distinguish between the eigenfrequencies of near resonant trapped modes and possible irregular frequencies inherent in the numerical method (*ref. 2.3.9*).

2.3.5.5 Another interaction effect is the sheltering effect which leads to smaller motions on the leeside than on the weather side. Hydrodynamic interaction effects between multiple surface piercing structures should be included if the excitation loads on each structure is considerably influenced by the presence of the other structures.

2.3.5.6 When calculating individual drift forces on multiple floaters, direct pressure integration of second-order fluid pressure on each body is required. The momentum approach usually applied for one single floater gives only the total drift force on the global system. Care should be taken when calculating drift force in vicinity of the frequencies of the trapped modes (2.3.5.3) since undamped free surface motion may lead to erroneous drift force predictions.

2.3.6 Time domain analysis

2.3.6.1 Some hydrodynamic load effects can be linearised and included in a frequency domain approach, while others are highly non-linear and can only be handled in time-domain.

2.3.6.2 The advantage of a time domain analysis is that it can capture non-linear hydrodynamic load effects and non-linear interaction effects between objects, including fenders with non-linear force-displacement relationships. In addition, a time domain analysis gives the response statistics without making assumptions regarding the response distribution.

2.3.6.3 A time-domain analysis involves numerical integration of the equations of motion and should be used when nonlinear effects are important. Examples are

- transient slamming response
- simulation of low-frequency motions (slow drift)
- coupled floater, riser and mooring response.

2.3.6.4 Time-domain analysis methods are usually used for prediction of extreme load effects. In cases where time-domain analyses are time-consuming, critical events can be analysed by a refined model for a time duration defined by a simplified model.

2.3.6.5 Time-domain analyses of structural response due to random load effects must be carried far enough to obtain stationary statistics.

2.3.7 Numerical methods

2.3.7.1 Wave-induced loads on large volume structures can be predicted based on potential theory which means that the loads are deduced from a velocity potential of the irrotational motion of an incompressible and inviscid fluid.

2.3.7.2 The most common numerical method for solution of the potential flow is the boundary element method (BEM) where the velocity potential in the fluid domain is represented by a distribution of sources over the mean wetted body surface. The source function satisfies the free surface condition and is called a *free surface Green function*. Satisfying the boundary condition on the body surface gives an integral equation for the source strength.

2.3.7.3 An alternative is to use elementary *Rankine sources* ($1/R$) distributed over both the mean wetted surface and the mean free surface. A Rankine source method is preferred for forward speed problems.

2.3.7.4 Another representation is to use a mixed distribution of both sources and normal dipoles and solve directly for the velocity potential on the boundary.

2.3.7.5 The mean wetted surface is discretised into flat or curved panels, hence these methods are also called panel methods. A *low-order* panel method uses flat panels, while a *higher order* panel method uses curved panels. A higher order method obtains the same accuracy with less number of panels. Requirements to discretisation are given in *ref./1/*.

2.3.7.6 The potential flow problem can also be solved by the finite element method (FEM), discretising the volume of the fluid domain by elements. For infinite domains, an analytic representation must be used a distance away from the body to reduce the number of elements. An alternative is to use so-called infinite finite element.

2.3.7.7 For fixed or floating structures with simple geometries like sphere, cylinder, spheroid, ellipsoid, torus, etc. semi-analytic expressions can be derived for the solution of the potential flow problem. For certain offshore structures, such solutions can be useful approximations.

2.3.7.8 Wave-induced loads on slender ship-like large volume structures can be predicted by *strip theory* where the load is approximated by the sum of loads on two-dimensional strips. One should be aware that the numerical implementation of the strip theory must include a proper treatment of head sea ($\beta = 180^\circ$) wave excitation loads.

2.3.7.9 Motion damping of large volume structures is due to wave radiation damping, hull skin friction damping, hull eddy making damping, viscous damping from bilge keels and other appendices, and viscous damping from risers and mooring. Wave radiation damping is calculated from potential theory. Viscous damping effects are usually estimated from simplified hydrodynamic models or from experiments. For simple geometries Computational Fluid Dynamics (CFD) can be used to assess viscous damping.

2.3.8 Frequency and panel mesh requirements

2.3.8.1 Several wave periods and headings need to be selected such that the motions and forces/moments can be described as correctly as possible. Cancellation, amplification and resonance effects must be properly captured.

2.3.8.2 Modelling principles related to the fineness of the panel mesh must be adhered to. For a low-order panel method (BEM) with constant value of the potential over the panel the following principles apply:

- Diagonal length of panel mesh should be less than $1/6$ of smallest wave length analysed.
- Fine mesh should be applied in areas with abrupt changes in geometry (edges, corners).
- When modelling thin walled structures with water on both sides, the panel size should not exceed 3-4 times the modelled wall thickness.
- Finer panel mesh should be used towards water-line when calculating wave drift excitation forces.
- The water plane area and volume of the discretised model should match closely to the real structure.

2.3.8.3 Convergence tests by increasing number of panels should be carried out to ensure accuracy of computed loads. Comparing drift forces calculated by the pressure integration method and momentum method provides a useful check on numerical convergence for a given discretisation.

2.3.8.4 Calculating wave surface elevation and fluid particle velocities require an even finer mesh as compared to a global response analysis. The diagonal of a typical panel is recommended to be less than $1/10$ of the shortest wave length analysed. For low-order BEM, fluid kinematics and surface elevation should be calculated at least one panel mesh length away from the body boundary, preferably close to centre of panels.

2.3.8.5 For a motion analysis of a floater in the frequency domain, computations are normally performed for at least 30 frequencies. Special cases may require a higher number. This applies in particular in cases where a narrow-band resonance peak lies within the wave spectral frequency range. The frequency spacing should be less than $\zeta\omega_0$ to achieve less than about 5% of variation in the standard deviation of response. ζ is the damping ratio and ω_0 the frequency.

2.3.9 Irregular frequencies

2.3.9.1 For radiation/diffraction analyses, using free surface Green function solvers, of large volume structures with large water plane area like ships and barges, attention should be paid to the existence of so-called *irregular frequencies*.

2.3.9.2 Irregular frequencies correspond to fictitious eigenmodes of an internal problem (inside the numerical model of the structure) and do not have any direct physical meaning. It is a deficiency of the integral equation method used to solve for the velocity potential.

2.3.9.3 In the vicinity of irregular frequencies a standard BEM method may give unreliable values for added mass and damping and hence for predicted RAOs and drift forces. Methods are available in some commercial software tools to remove the unwanted effects of the irregular frequencies. The Rankine source method avoids irregular frequencies.

2.3.9.4 Irregular wave numbers ν of a rectangular barge with length L , beam B and draft T are given by the relations

$$\nu = \nu_{ij} = k_{ij} \coth(k_{ij}T)$$

where

$$k_{ij} = \pi \sqrt{(i/L)^2 + (j/B)^2}; i, j = 0, 1, 2, \dots; i + j \geq 1$$

2.3.9.5 Irregular wave numbers ν of a vertical cylinder with radius R and draft T are given by the relations

$$\nu = \nu_{ms} = k_{ms} \coth(k_{ms}T)$$

where $k_{ms} = j_{ms}/R$ are given by the zeros of the m^{th} order Bessel function $J_m(j_{ms}) = 0$; $m = 0, 1, 2, \dots$, $s = 1, 2, \dots$. The lowest zeros are $j_{01} = 2.405$, $j_{11} = 3.832$, $j_{21} = 5.136$, $j_{02} = 5.520$. The corresponding irregular frequencies are then given by the dispersion relation

$$\omega^2 = g\nu \tanh(\nu d)$$

where

ν = irregular wave number
 g = acceleration of gravity
 d = water depth.

2.4 Wave Loads on small volume structures

2.4.1 Small volume 3D objects

2.4.1.1 The term *small volume structure* is used for structures with dimensions D that are smaller than the typical wave lengths λ of ocean waves exciting the structure, usually $D < \lambda/5$, see Figure 2-3.

2.4.1.2 A Morison type formulation may be used to estimate drag and inertia loads on three dimensional objects in waves and current. For a fixed structure the load is given by,

$$F(t) = \rho V(1 + C_A)\ddot{v} + \frac{1}{2}\rho C_D S v |v|$$

where

v = fluid particle (waves and/or current) velocity [m/s]
 \ddot{v} = fluid particle acceleration [m/s²]
 V = displaced volume [m³]
 S = projected area normal to the force direction [m²]
 ρ = mass density of fluid [kg/m³]
 C_A = added mass coefficient [-]
 C_D = drag coefficient [-]

Added mass coefficients for some 3D objects are given in *Table A2 in Appendix A*. Drag coefficients are given in *Appendix B*.

2.4.1.3 For some typical subsea structures which are perforated with openings (holes), the added mass may depend on motion amplitude or equivalently, the KC -number (*ref. Section 3.3.3*). A summary of force coefficients for various 3D and 2D objects can be found in *ref. [7]*.

2.4.2 Sectional force on slender structures

2.4.2.1 The hydrodynamic force exerted on a slender structure in a general fluid flow can be estimated by summing up sectional forces acting on each strip of the structure. In general the force vector acting on a strip can be decomposed in a normal force f_N , an axial force f_T and a lift force f_L being normal to both f_N and f_T , see Figure 2-4. In addition a torsion moment m_T will act on non-circular cross-sections.

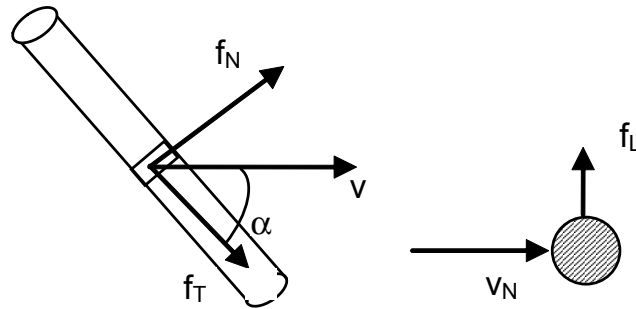


Figure 2-4
Definition of normal force, axial force and lift force on slender structure

2.4.2.2 For slender structural members (cylinders) having cross-sectional dimensions sufficiently small to allow the gradients of fluid particle velocities and accelerations in the direction normal to the member to be neglected, wave loads may be calculated using the Morison's load formula. The sectional force f_N on a *fixed* slender structure in two-dimensional flow normal to the member axis is then given by

$$f_N(t) = \rho(1 + C_A)A\dot{v} + \frac{1}{2}\rho C_D D v |v|$$

where

- v = fluid particle (waves and/or current) velocity [m/s]
- \dot{v} = fluid particle acceleration [m/s²]
- A = cross sectional area [m²]
- D = diameter or typical cross-sectional dimension [m]
- ρ = mass density of fluid [kg/m³]
- C_A = added mass coefficient (with cross-sectional area as reference area) [-]
- C_D = drag coefficient [-]

2.4.2.3 Normally, Morison's load formula is applicable when the following condition is satisfied:

$$\lambda > 5 D$$

where λ is the wave length and D is the diameter or other projected cross-sectional dimension of the member.

2.4.2.4 For combined wave and current flow conditions, wave and current induced particle velocities should be added as vector quantities. If available, computations of the total particle velocities and accelerations based on more exact theories of wave/current interaction are preferred.

2.4.3 Definition of force coefficients

2.4.3.1 The drag coefficient C_D is the non-dimensional drag-force;

$$C_D = \frac{f_{\text{drag}}}{\frac{1}{2}\rho D v^2}$$

where

- f_{drag} = sectional drag force [N/m]
- ρ = fluid density [kg/m³]
- D = diameter (or typical dimension) [m]
- v = velocity [m/s]

2.4.3.2 In general the fluid velocity vector will be in a direction α relative to the axis of the slender member (Figure 2-4). The drag force f_{drag} is decomposed in a normal force f_N and an axial force f_T .

2.4.3.3 The added mass coefficient C_A is the non-dimensional added mass

$$C_A = \frac{m_a}{\rho A}$$

where

m_a = the added mass per unit length [kg/m]

A = cross-sectional area [m²]

2.4.3.4 The mass coefficient is defined as

$$C_M = 1 + C_A$$

2.4.3.5 The lift coefficient is defined as the non-dimensional lift force

$$C_L = \frac{f_{lift}}{\frac{1}{2} \rho D v^2}$$

where

f_{lift} = sectional lift force [N/m]

2.4.4 Moving structure in still water

2.4.4.1 The sectional force f_N on a *moving* slender structure in still water can be written as

$$f_N(t) = -\rho C_A A \ddot{r} - \frac{1}{2} \rho C_d D \dot{r} |\dot{r}|$$

where

\dot{r} = velocity of member normal to axis [m/s]

\ddot{r} = acceleration of member normal to axis [m/s²]

C_d = hydrodynamic damping coefficient [-]

2.4.5 Moving structure in waves and current

2.4.5.1 The sectional force f_N on a *moving* slender structure in two-dimensional non-uniform (waves and current) flow normal to the member axis can be obtained by summing the force contributions in 2.4.2.2 and 2.4.4.1.

$$f_N(t) = -\rho C_A A \ddot{r} + \rho(1 + C_A) A \dot{v} + \frac{1}{2} \rho C_D D v |v| - \frac{1}{2} \rho C_d D \dot{r} |\dot{r}|$$

2.4.5.2 This form is known as the *independent flow field model*. In a response analysis, solving for $r = r(t)$, the added mass force $\rho C_A A \ddot{r} = m_a \ddot{r}$ adds to the structural mass m_s times acceleration on the left hand side of the equation of motion.

Guidance note:

The drag coefficient C_D may be derived experimentally from tests with wave excitation on fixed cylinder while the damping coefficient C_d may be derived by cylinder decay tests in otherwise calm water. For most applications there is no need to differentiate between these two coefficients.

---e-n-d---of---G-u-i-d-a-n-c-e---n-o-t-e---

2.4.6 Relative velocity formulation

2.4.6.1 When the drag force is expressed in terms of the relative velocity, a single drag coefficient is sufficient. Hence, the relative velocity formulation is most often applied. The sectional force can then be written in terms of relative velocity;

$$f_N(t) = -\rho C_A A \ddot{r} + \rho(1 + C_A) A \dot{v} + \frac{1}{2} \rho C_D D v_r |v_r|$$

or in an equivalent form when relative acceleration is also introduced;

$$f_N(t) = \rho A a + \rho C_A A a_r + \frac{1}{2} \rho C_D D v_r |v_r|$$

where

$a = \dot{v}$ is the fluid acceleration [m/s]

$v_r = \dot{v} - \dot{r}$ is the relative velocity [m/s]

$a_r = \ddot{v} - \ddot{r}$ is the relative acceleration [m/s²]

2.4.6.2 When using the relative velocity formulation for the drag forces, additional hydrodynamic damping should normally not be included.

2.4.7 Applicability of relative velocity formulation

2.4.7.1 The use of relative velocity formulation for the drag force is valid if

$$r/D > 1$$

where r is the member displacement amplitude and D is the member diameter.

2.4.7.2 When $r/D < 1$ the validity is depending on the value of the parameter $V_R = vT_n/D$ as follows:

$20 \leq V_R$ Relative velocity recommended

$10 \leq V_R < 20$ Relative velocity may lead to an over-estimation of damping if the displacement is less than the member diameter. The independent flow field model (2.4.5.1) may then be applied with equal drag C_D and damping C_d coefficients.

$V_R < 10$ It is recommended to discard the velocity of the structure when the displacement is less than one diameter, and use the drag formulation in 2.4.2.2.

2.4.7.3 For a vertical surface piercing member in combined wave and current field, the parameter V_R can be calculated as

$$V_R = \left[v_c + \pi \frac{H_s}{T_z} \right] \frac{T_n}{D}$$

where

v_c = current velocity [m/s]

T_n = period of structural oscillations [s]

H_s = significant wave height [m]

T_z = zero-up-crossing period [s]

2.4.8 Drag force on inclined cylinder

2.4.8.1 For incoming flow with an angle of attack of 45-90 degrees, the cross flow principle is assumed to hold. The normal force on the cylinder can be calculated using the normal component of the water particle velocity

$$v_n = v \sin \alpha$$

where α is the angle between the axis of the cylinder and the velocity vector. The drag force normal to the cylinder is then given by

$$f_{dN} = \frac{1}{2} \rho C_{Dn} D v_n |v_n|$$

In general C_{Dn} depends on the Reynolds number and the angle of incidence. For sub-critical and super-critical flow C_{Dn} can be taken as independent of α . (Ref. /1/).

2.4.9 Hydrodynamic coefficients for normal flow

2.4.9.1 When using Morison's load formula to calculate the hydrodynamic loads on a structure, one should take into account the variation of C_D and C_A as function of Reynolds number, the Keulegan-Carpenter number and the roughness.

$$C_D = C_D(Re, KC, \Delta)$$

$$C_A = C_A(Re, KC, \Delta)$$

The parameters are defined as:

— Reynolds number: $Re = vD/\nu$

— Keulegan-Carpenter number: $KC = v_m T/D$

— Non-dimensional roughness: $\Delta = k/D$

where

D = Diameter [m]

T = wave period or period of oscillation [s]

k = roughness height [m]

- v = total flow velocity [m/s]
 ν = fluid kinematic viscosity [m²/s]. See *Appendix C*.
 v_m = maximum orbital particle velocity [m/s]

The effect of Re , KC and Δ on the force coefficients is described in detail in *refs. /4/ and /6/*.

2.4.9.2 For wave loading in random waves the velocity used in the definition of Reynolds number and Keulegan-Carpenter number should be taken as $\sqrt{2}\sigma_v$, where σ_v is the standard deviation of the fluid velocity. The wave period should be taken as the zero-up-crossing period T_z .

2.4.9.3 For oscillatory fluid flow a *viscous frequency parameter* is often used instead of the Reynolds number. This parameter is defined as the ratio between the Reynolds number and the Keulegan-Carpenter number,

$$\beta = Re/KC = D^2/\nu T = \omega D^2/(2\pi\nu)$$

where

- D = diameter [m]
 T = wave period or period of structural oscillation [s]
 ω = $2\pi/T$ = angular frequency [rad/s]
 ν = fluid kinematic viscosity [m²/s]

Experimental data for C_D and C_M obtained in U-tube tests are often given as function of KC and β since the period of oscillation T is constant and hence β is a constant for each model.

2.4.9.4 For a circular cylinder, the ratio of maximum drag force $f_{D,max}$ to the maximum inertia force $f_{I,max}$ is given by

$$\frac{f_{D,max}}{f_{I,max}} = \frac{C_D}{\pi^2(1+C_A)} KC$$

The formula can be used as an indicator on whether the force is drag or inertia dominated. When $f_{I,max} > 2 \cdot f_{D,max}$ the drag force will not influence the maximum total force.

2.4.9.5 For combined wave and current conditions, the governing parameters are Reynolds number based on maximum velocity, $v = v_c + v_m$, Keulegan-Carpenter number based on maximum orbital velocity v_m and the *current flow velocity ratio*, defined as

$$\alpha_c = v_c/(v_c + v_m)$$

where v_c is the current velocity.

2.4.9.6 For sinusoidal (harmonic) flow the Keulegan-Carpenter number can also be written as

$$KC = 2\pi\eta_0 / D$$

where η_0 is the oscillatory flow amplitude. Hence, the KC-number is a measure of the distance traversed by a fluid particle during half a period relative to the member diameter.

2.4.9.7 For fluid flow in the wave zone η_0 in the formula above can be taken as the wave amplitude so that the KC-number becomes

$$KC = \frac{\pi H}{D}$$

where H is the wave height.

2.4.9.8 For an oscillating structure in still water, which for example is applicable for the lower part of the riser in deep water, the KC-number is given by

$$KC = \frac{\dot{x}_m T}{D}$$

where \dot{x}_m is the maximum velocity of the structure, T is the period of oscillation and D is the cylinder diameter.

2.5 References

- /1/ DNV Recommended Practice DNV-RP-C205 "Environmental Conditions and Environmental Loads", April 2007
- /2/ Faltinsen, O.M. (1990) "Sea loads on ships and offshore structures". Cambridge University Press.
- /3/ Newman, J.N. (1977) "Marine Hydrodynamics". MIT Press, Cambridge, MA, USA.
- /4/ Sarpkaya, T. and Isaacson, M. (1981), "Mechanics of Wave Forces on Offshore Structures", Van Nostrand, Reinhold Company, New York, 1981.

- /5/ Chakrabarti, S.K. (1987): “Hydrodynamics of Offshore Structures”. Springer Verlag.
- /6/ Sumer, B.M and Fredsøe, J. (1997) “Hydrodynamics around cylindrical structures”. World Scientific.
- /7/ Øritsland, O. (1989) “A summary of subsea module hydrodynamic data”. Marine Operations Part III.2. Report No. 70. Marintek Report MT51 89-0045.
- /8/ Molin, B. (2001) “On the piston and sloshing modes in moonpools”. J. Fluid. Mech., vol. 430, pp. 27-50.

3 Lifting through Wave Zone – General

3.1 Introduction

3.1.1 Objective

3.1.1.1 Design loads need to be established when lowering subsea structures through the wave zone. Accurate prediction of these design loads may reduce the risk of expensive waiting on weather, increase the number of suitable installation vessels and also increase the safety level of the operation.

3.1.1.2 The objective of this section is to give guidance on how to improve the modelling and analysis methods in order to obtain more accurate prediction of the design loads.

3.1.2 Phases of a subsea lift

3.1.2.1 A typical subsea lift consists of the following main phases:

- lift off from deck and manoeuvring object clear of transportation vessel
- lowering through the wave zone
- further lowering down to sea bed
- positioning and landing.

All phases of a subsea lift operation should be evaluated. Lift off is covered in Section 9. Loads and response on object when deeply submerged is covered in Section 5. Landing of object on seabed is covered in Section 6.

3.1.3 Application

3.1.3.1 This section gives general guidance for modelling and analysis of the lifting through the wave zone phase.

3.1.3.2 Only typical subsea lifts are covered. Other installation methods as e.g. free fall pendulum installation are not covered.

3.1.3.3 A simplified method for estimating the hydrodynamic forces is given in Section 4. Topics related to the lowering phase beneath the wave influenced zone are covered in Section 5 while landing on seabed is dealt with in Section 6.

3.2 Loads and load effects

3.2.1 General

3.2.1.1 An object lowered into or lifted out of water will be exposed to a number of different forces acting on the structure. In general the following forces should be taken into account when assessing the response of the object;

- F_{line} = force in hoisting line/cable
- W_0 = weight of object (in air)
- F_B = buoyancy force
- F_c = steady force due to current
- F_I = inertia force
- F_{wd} = wave damping force
- F_d = drag force
- F_w = wave excitation force
- F_s = slamming force
- F_e = water exit force

3.2.1.2 The force $F_{line}(t)$ in the hoisting line is the sum of a mean force F_0 and a dynamic force $F_{dyn}(t)$ due to motion of crane tip and wave excitation on object. The mean force is actually a slowly varying force, partly due to the lowering velocity and partly due to water ingress into the object after submergence.

3.2.2 Weight of object

3.2.2.1 The weight of the object in air is taken as;

$$W_0 = Mg \quad [\text{N}]$$

where

M = mass of object including pre-filled water within object [kg]
 g = acceleration of gravity [m/s^2]

Guidance note:

The interpretation of the terms weight and structural mass is sometimes misunderstood. Weight is a static force on an object due to gravity. The resulting static force on a submerged object is the sum of the weight of the object acting downwards and the buoyancy force acting upwards. Structural mass is a dynamic property of an object and is unchanged regardless of where the object is situated. The inertia force is the product of mass (including added mass) and acceleration required to accelerate the mass.

---e-n-d---of---G-u-i-d-a-n-c-e---n-o-t-e---

3.2.2.2 Additional water flowing into the (partly or fully) submerged object shall be taken into account as described in 4.6.3.4.

3.2.3 Buoyancy force

3.2.3.1 The buoyancy force for a submerged object is equal to the weight of the displaced water,

$$F_B(t) = \rho g V(t) \quad [\text{N}]$$

where

ρ = mass density of water [kg/m^3]
 g = acceleration of gravity [m/s^2]
 $V(t)$ = displaced volume of water [m^3]

Guidance note:

The mass density of water varies with salinity and temperature as shown in Table C1 in Appendix C.

---e-n-d---of---G-u-i-d-a-n-c-e---n-o-t-e---

3.2.3.2 During water entry of an object lowered through the free surface, the buoyancy force is given by the weight of the instantaneous displaced water.

3.2.3.3 For a totally submerged object the buoyancy force may vary with time in the case of continued water ingress into the object.

3.2.3.4 The direction of the buoyancy force is opposite to gravity. If the centre of buoyancy is not vertically above the centre of gravity, the buoyancy force will exert a rotational moment on the lifted object.

Guidance note:

The centre of buoyancy x_B is defined as the geometrical centre of the displaced volume of water.

---e-n-d---of---G-u-i-d-a-n-c-e---n-o-t-e---

3.2.3.5 For a partly submerged object in long waves (compared to characteristic horizontal dimension) the buoyancy force varies with wave elevation according to 3.2.5.2. The time varying part of the buoyancy force due to waves can then be taken as a wave excitation force.

3.2.3.6 For a submerged object, the *submerged weight* W of the object is defined as;

$$W(t) = W_0 - F_B(t) = [M - \rho V(t)] \cdot g \quad [\text{N}]$$

3.2.4 Steady force due to current

3.2.4.1 The steady force due to ocean current can be taken as a quadratic drag force

$$F_c = \frac{1}{2} \rho C_{DSi} A_{pi} U_c(z_0)^2 \quad [\text{N}]$$

where

C_{DSi} = the steady state drag coefficient in the current direction i [-]
 A_{pi} = projected area in direction i [m^2]

$U_c(z_0)$ = current velocity at depth z_0 of object [m/s]

3.2.4.2 The steady current force is opposed by the horizontal component of the hoisting line force.

3.2.5 Inertia force due to moving object

3.2.5.1 The inertia force in direction i ($i = 1, 2, 3$) on an object moving in pure translation can be calculated from

$$F_{I,i} = -(M\delta_{ij} + A_{ij})\ddot{x}_j \quad [\text{N}]$$

where summation over j is assumed and

M = structural mass [kg]

$\delta_{ij} = 1$ if $i = j$
 $= 0$ if $i \neq j$

A_{ij} = added mass in direction i due to acceleration in direction j [kg]

\ddot{x}_j = acceleration of object in direction j ($x_1=x$, $x_2=y$, and $x_3=z$) [m/s^2]

The added mass is usually expressed in terms of an added mass coefficient C_A^{ij} defined by;

$$A_{ij} = \rho C_A^{ij} V_R \quad [\text{kg}]$$

where

ρ = mass density of water [kg/m^3]

V_R = reference volume of the object [m^3]

C_A^{ij} = added mass coefficient [-]

Guidance note:

In the absence of body symmetry, the cross-coupling added mass coefficients A_{12} , A_{13} and A_{23} are non-zero, so that the hydrodynamic inertia force may differ in direction from the acceleration. Added-mass coefficients are symmetric, $A_{ij} = A_{ji}$. Hence, for a three-dimensional object of arbitrary shape there are in general 21 different added mass coefficients for the 3 translational and 3 rotational modes. Added mass coefficients for general compact non-perforated structures may be determined by potential flow theory using a sink-source technique.

---e-n-d---of---G-u-i-d-a-n-c-e---n-o-t-e---

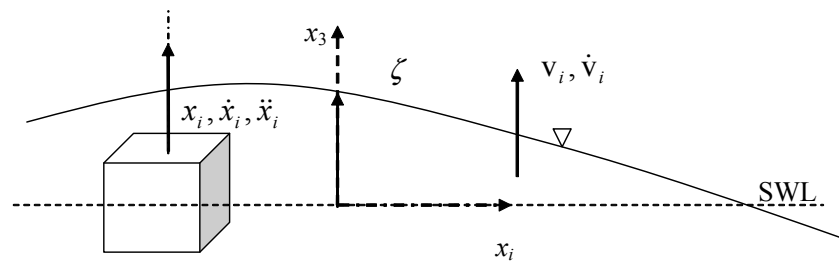


Figure 3-1
Submerged object lifted through wave zone

3.2.5.2 For objects crossing the water surface, the submerged volume V and the vertical added mass A_{33} shall be taken to the still water level, $z = 0$.

3.2.5.3 For rotational motion (typically yaw motion) of a lifted object the inertia effects are given by the mass moments of inertia M_{ij} and the added moments of inertia A_{ij} where $i, j = 4, 5, 6$ as well as coupling coefficients with dimension mass multiplied by length. Reference is made to /6/.

Guidance note:

For perforated structures viscous effects may be important and the added mass will depend on the amplitude of motion defined by the KC-number. The added mass will also be affected by a large volume structure in its close proximity.

---e-n-d---of---G-u-i-d-a-n-c-e---n-o-t-e---

3.2.5.4 A general object in pure translational motion may be destabilized due to the Munk moment which can be expressed in terms of the translational added mass coefficients, ref. /6/.

3.2.6 Wave damping force

3.2.6.1 In general when an object moves in vicinity of a free surface, outgoing surface waves will be created.

The energy of these waves comes from the work done to dampen the motion of the object. The resulting force on the object is the *wave damping force*.

3.2.6.2 The wave damping force F_{wd} is proportional to the velocity of the object;

$$F_{wd} = B_{ij} \dot{x}_j \quad [\text{N}]$$

where

B_{ij} = wave generation damping coefficient [kg/s]

\dot{x}_j = velocity of lifted object [m/s]

3.2.6.3 For oscillatory motion of the object, the wave damping force vanishes for high frequencies and for low frequencies. Wave damping can be neglected if;

$$T \gg \sqrt{2\pi D / g} \quad [\text{s}]$$

where T is the period of the oscillatory motion, D is a characteristic dimension of the object normal to the direction of motion and g is the acceleration of gravity. For transparent structures composed of several slender elements, the characteristic dimension is the cross-sectional dimension of the slender elements.

3.2.7 Wave excitation force

3.2.7.1 The wave exciting forces and moments are the loads on the structure when it is restrained from any motion response and there are incident waves.

3.2.7.2 When the characteristic dimensions of the object is considerably smaller than the wave length, the wave excitation force in direction i on a *fully submerged object* is found from

$$F_{wi} = \rho V (\delta_{ij} + C_A^{ij}) \dot{v}_j + F_{Di} \quad [\text{N}]$$

where

ρ = mass density of water [kg/m³]

V = submerged volume of object (taken to still water level $z = 0$) [m³]

$\delta_{ij} = 1$ if $i = j$
 $\delta_{ij} = 0$ if $i \neq j$

C_A^{ij} = added mass coefficient [-]

\dot{v}_j = water particle acceleration in direction j [m/s²]

F_{Di} = viscous drag excitation force [N] (see 3.2.8)

3.2.7.3 For a *partly submerged object* the excitation force in direction i is found from

$$F_{wi} = \rho g A_w \zeta(t) \delta_{i3} + \rho V (\delta_{ij} + C_A^{ij}) \dot{v}_j + F_{Di} \quad [\text{N}]$$

where the first term is a hydrostatic force (see Guidance Note) associated with the elevation of the incident wave at the location of the object and where

g = acceleration of gravity [m/s²]

A_w = water plane area [m²]

$\zeta(t)$ = wave surface elevation [m]

$\delta_{i3} = 1$ if $i = 3$ (vertically)
 $\delta_{i3} = 0$ if $i = 1$ or $i = 2$ (horizontally)

Guidance note:

The hydrostatic contribution in the excitation force for a partly submerged object can also be viewed as part of a time dependent buoyancy force (acting upwards) since in long waves the increase in submerged volume for the object can be approximated by $A_w \zeta(t)$. Note that this is strictly valid for vertical wall sided objects only.

---e-n-d---of---G-u-i-d-a-n-c-e---n-o-t-e---

3.2.8 Viscous drag force

3.2.8.1 The viscous drag force in direction i can be expressed by the equation

$$F_{di} = \frac{1}{2} \rho C_D A_p |\mathbf{v}_r| v_{ri} \quad [\text{N}]$$

where

ρ = mass density of water [kg/m³]
 C_D = drag coefficient in oscillatory fluid [-]
 A_p = projected area normal to motion/flow direction [m²]
 v_r = total relative velocity [m/s]
 v_{ri} = $v_i - \dot{x}_i$ = relative velocity component in dir. i [m/s]

Guidance note:

Note that the viscous drag force can either be an excitation force or a damping force depending on the relative magnitude and direction of velocity of object and fluid particle velocity.

---e-n-d---of---G-u-i-d-a-n-c-e---n-o-t-e---

3.2.8.2 If the damping of an oscillating object is calculated by a quadratic drag formulation as given by 3.2.8.1, the drag coefficient C_D depends on the oscillation amplitude. The oscillation amplitude is usually expressed in terms of the non-dimensional Keulegan-Carpenter number defined as

$$KC = 2\pi \frac{z_m}{D} \quad [-]$$

where

z_m = oscillation amplitude [m]
 D = characteristic length of object, normally the smallest dimension transverse to the direction of oscillation [m]

Guidance note:

For sinusoidal motion the KC-number can also be defined as $KC = v_m T / D$ where $v_m = 2\pi z_m / T$ and T is the period of oscillation. The KC-number is a measure of the distance traversed by a fluid particle during half a period relative to the dimension of the object.

---e-n-d---of---G-u-i-d-a-n-c-e---n-o-t-e---

3.2.8.3 The dependence of KC-number for force coefficients (inertia and damping) also applies to objects exposed to oscillatory water particle motion in the wave zone. For regular waves, the KC-number can be taken as

$$KC = \frac{\pi H}{D} \quad [-]$$

where H is the regular wave height. For irregular wave conditions the KC-number can be taken as

$$KC = \frac{(\sqrt{2}\sigma_v)T_z}{D} \quad [-]$$

where

σ_v = standard deviation of water particle velocity [m/s]
 T_z = zero up-crossing period [s]

3.2.8.4 For small KC-numbers (typically less than 10) it may be convenient to express the drag and damping force as a sum of linear and quadratic damping;

$$F_{Di} = B_1 v_{ri} + B_2 v_{ri} |v_r|$$

3.2.8.5 The upper graph in Figure 3-2 shows a typical variation of C_D with KC-number. The drag coefficient for steady flow is denoted C_{DS} . This corresponds to the value of C_D for large KC-number.

Guidance note:

Damping coefficients obtained from oscillatory flow tests of typical subsea modules for KC-number in the range $0 < KC < 10$ can be several times larger than the drag coefficient obtained from steady flow data. Hence, using steady-flow drag coefficients C_{DS} in place of KC-dependent drag coefficients C_D may underestimate the damping force and overestimate resonant motions of the object. The variation of drag coefficients with KC-number is described in 3.3.5.2.

---e-n-d---of---G-u-i-d-a-n-c-e---n-o-t-e---

3.2.8.6 When estimating damping coefficient and its dependence on KC-number from oscillatory flow tests, the product $C_D KC$ is plotted against KC-number. A straight line can then often be drawn through a considerable part of the experimental values in this representation. See lower graph in Figure 3-2.

Guidance note:

The effect of KC -number on damping coefficients can also be determined by numerical simulation using Computational Fluid Dynamics (CFD) of the fluid flow past objects in forced oscillation. Guidance on use of CFD is given in 3.4.4.

---e-n-d---of---G-u-i-d-a-n-c-e---n-o-t-e---

3.2.8.7 The intersection with the vertical axis is given by b_1/ω' where b_1 represents a linear damping term, and the quadratic damping term, b_2 , is equal to the slope of the straight line. The parameter ω' is the non-dimensional frequency of oscillation;

$$\omega' = \omega \sqrt{D/2g} \quad [\text{rad/s}]$$

where D is the same characteristic length of the object as used in the KC -number.

The damping coefficient can then be written as;

$$C_D KC = \frac{b_1}{\omega'} + b_2 KC \quad [-]$$

These constant parameters can replace the amplitude dependent C_D for a realistic range of amplitudes, which is necessary for dynamic analysis of irregular motion.

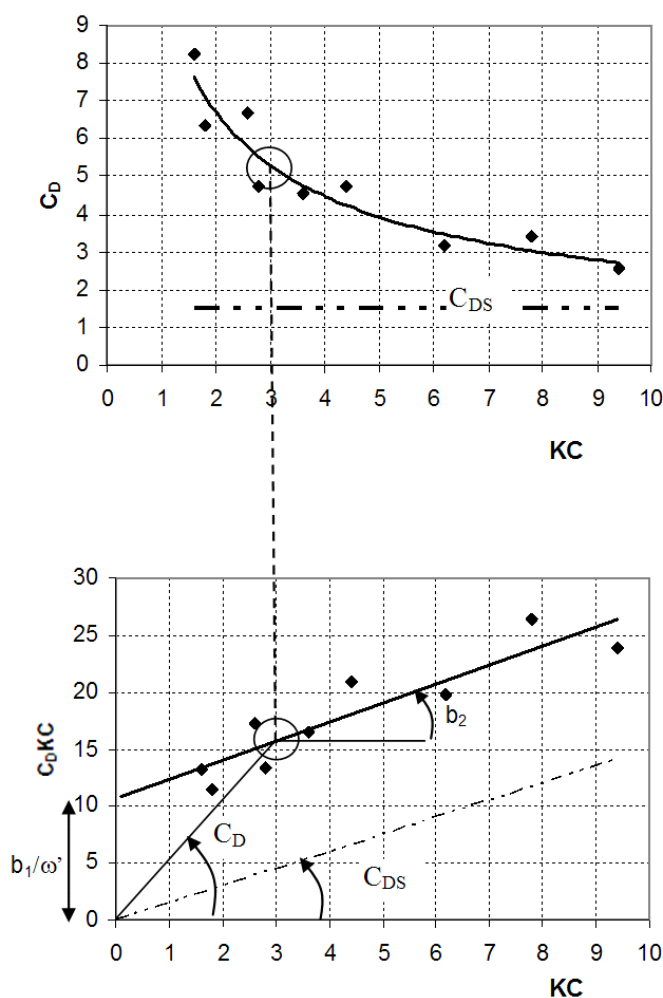


Figure 3-2
Estimation of damping coefficients from experimental values.
In this example $C_D KC = 10.62 + 1.67 KC$.

3.2.8.8 When b_1 and b_2 are determined, the coefficients B_1 and B_2 in the expression in 3.2.8.4 can be calculated from the formulas;

$$B_1 = \frac{2\rho A_p \sqrt{2gD}}{3\pi^2} \cdot b_1 \quad [\text{kg/s}]$$

$$B_2 = \frac{1}{2} \rho A_p \cdot b_2 \quad [\text{kg/m}]$$

where

A_p = projected area normal to motion/flow direction [m^2]
 g = acceleration of gravity [m/s^2]

Guidance note:

The linear damping can be associated physically with skin friction and the quadratic damping with form drag.

---e-n-d---of---G-u-i-d-a-n-c-e---n-o-t-e---

3.2.9 Slamming force

3.2.9.1 The slamming force on an object lowered through the free surface with a *constant* slamming velocity v_s (assumed positive) in *still water* can be expressed as the rate of change of fluid momentum;

$$F_s(t) = \frac{d(A_{33}^\infty v_s)}{dt} = v_s \frac{dA_{33}^\infty(t)}{dt} \quad [\text{N}]$$

where $A_{33}^\infty(t)$ is the instantaneous *high-frequency* limit heave added mass, ref. /4/.

Guidance note:

Using the high-frequency limit of the added mass is based on the assumption that the local fluid accelerations due to water entry of the object are much larger than the acceleration of gravity g . This corresponds to the high frequency limit for a body oscillating with a free surface.

---e-n-d---of---G-u-i-d-a-n-c-e---n-o-t-e---

3.2.9.2 The slamming force can be written in terms of a *slamming coefficient* C_s as

$$F_s(t) = \frac{1}{2} \rho C_s A_p v_s^2 \quad [\text{N}]$$

where C_s is defined by

$$C_s = \frac{2}{\rho A_p v_s} \frac{dA_{33}^\infty}{dt} = \frac{2}{\rho A_p} \frac{dA_{33}^\infty}{dh} \quad [-]$$

and dA_{33}^∞ / dh is the rate of change of added mass with submergence.

ρ = mass density of water [kg/m^3]
 A_p = horizontal projected area of object [m^2]
 h = submergence relative to surface elevation [m]

Guidance note:

The rate of change of added mass with submergence can be derived from position dependent added mass data calculated by a sink-source technique or estimated from model tests. The high frequency limit heave added mass for a partly submerged object is half of the added mass of the corresponding “double body” in infinite fluid where the submerged part of the object is mirrored above the free surface, ref. /6/.

---e-n-d---of---G-u-i-d-a-n-c-e---n-o-t-e---

3.2.9.3 For water entry in waves the relative velocity between lowered object and sea surface must be applied, so that the slamming force can be taken as

$$F_s(t) = \frac{1}{2} \rho C_s A_p (\dot{\zeta} - \dot{\eta})^2 \quad [\text{N}]$$

where

$\dot{\zeta}$ = vertical velocity of sea surface [m/s]
 $\dot{\eta}$ = the vertical motion of the object [m/s]

3.2.9.4 It should be noted that when measuring the vertical force on an object during water entry, the buoyancy force and a viscous drag force will be part of the measured force. However, during the initial water entry, the slamming force may dominate.

3.2.10 Equation of vertical motion of lifted object when lowered into wave zone.

3.2.10.1 Combining the expressions for buoyancy, inertia, wave excitation, slamming and drag damping forces valid for wave lengths much longer than the dimensions of the object, the equation of vertical motion

$\eta(t)$ for the lowered object can be taken as;

$$(M + A_{33})\ddot{\eta} = B_{33}^{(1)}(v_3 - \dot{\eta}) + B_{33}^{(2)}(v_3 - \dot{\eta})|(v_3 - \dot{\eta})| \\ + (\rho V + A_{33})\dot{v}_3 + \frac{dA_{33}^\infty}{dh}(\dot{\zeta} - \dot{\eta})^2 + \rho g V(t) - Mg + F_{line}(t)$$

where

- $B_{33}^{(1)}$ = the linear damping coefficient [kg/s]
 $B_{33}^{(2)}$ = the quadratic damping coefficient [kg/m]
 v_3 = water particle velocity [m/s]
 \dot{v}_3 = water particle acceleration [m/s²]
 $F_{line}(t)$ = force in hoisting line [N]

3.2.10.2 The force in the hoisting line is given by

$$F_{line}(t) = Mg - \rho g V(t) + K(z_{ct} - \eta)$$

where

- K = hoisting line stiffness [N/m]
 z_{ct} = motion of crane tip [m]
 η = motion of object [m]

3.2.10.3 The velocity and acceleration of the lowered object are

$$\dot{\eta} = \dot{\tilde{\eta}} + v_c \quad [\text{m/s}] \\ \ddot{\eta} = \ddot{\tilde{\eta}} \quad [\text{m/s}^2]$$

where

- $\tilde{\eta}(t)$ = the wave-induced motion of the object [m/s]
 v_c = a constant lowering velocity (v_c is negative during lowering as positive direction is upwards) [m/s]

3.2.10.4 For an object with vertical sidewalls at the mean water level, the instantaneous buoyancy force $\rho g \Omega$ can be split into a slowly varying (mean) component, a wave excitation part, and a hydrostatic restoring part due to the wave induced motion of the object;

$$\rho g V(t) = \rho g [V_0 + A_w \zeta(t) - A_w \tilde{\eta}(t)] \quad [\text{N}]$$

where

- V_0 = displaced volume of object in still water [m³]
 A_w = instantaneous water plane area [m²]

The instantaneous water plane area A_w is a slowly varying function of time, depending on lowering velocity v_c .

3.2.10.5 Assuming a constant vertical velocity v_c of the lowered object and neglecting the motion of the crane tip, the force in the hoisting line can be taken as;

$$F_{line}(t) = Mg - \rho g V(t) - (\rho V + A_{33})\dot{v}_3 - \frac{dA_{33}^\infty}{dh}(\dot{\zeta} - v_c)^2 \\ - B_1(v_3 - v_c) - B_2(v_3 - v_c)|(v_3 - v_c)| \quad [\text{N}]$$

Slamming and wave excitation forces can cause slack ($F = 0$) in the hoisting wire followed by high snatch loads.

3.2.10.6 Slamming on the top plate of a suction anchor will lead to a change in velocity of the anchor. The change in velocity is given by

$$\Delta v_c = \frac{2A_{33}}{M + A_{33}}(\dot{\zeta} - v_{c,0})$$

where

- M = mass of suction anchor [kg]
 A_{33} = mass of water plug (added mass) inside suction anchor [kg]

$\dot{\zeta}$ = vertical velocity of water surface inside suction anchor before slamming event [m/s]

$v_{c,0}$ = vertical velocity of suction anchor before slamming event [m/s]

Both $\dot{\zeta}$ and $v_{c,0}$ are defined to be positive upwards.

3.2.10.7 The reduction in the force in the hoisting line due to slamming can be taken as

$$\Delta F_{line} = K \frac{\Delta v_c}{\omega_0}$$

where

K = stiffness of hoisting system [N/m]

ω_0 = natural frequency of anchor motion [rad/s]

3.2.11 Water exit force

3.2.11.1 The water exit force $F_e(t)$ on a fully submerged object lifted up beneath the free surface with *constant* lifting velocity v_e (positive upwards) in *still water* can be expressed by the rate of change of fluid kinetic energy by the relation

$$v_e F_e(t) = - \frac{dE_k}{dt} \quad [\text{Nm/s}]$$

where

$$E_k = \frac{1}{2} A_{33}^0 v_e^2 \quad [\text{Nm}]$$

$A_{33}^0(t)$ = instantaneous *low-frequency* limit heave added mass, *ref./9/*.

3.2.11.2 The water exit force can then be written as

$$F_e(t) = - \frac{1}{v_e} \frac{d}{dt} \left(\frac{1}{2} A_{33}^0 v_e^2 \right) = - \frac{1}{2} \frac{dA_{33}^0}{dt} v_e \quad [\text{N}]$$

Guidance note:

Using the low-frequency limit of the added mass is based on the assumption that the local fluid accelerations during water exit are much smaller than the acceleration of gravity g . This corresponds to the low frequency limit for a body oscillating beneath a free surface. The exit velocity can be expressed in terms of exit Froude number $F_n = v_e / \sqrt{gD}$ where D is a characteristic horizontal dimension of the object. Hence the formulation is valid for low Froude number $F_n \ll 1$. See *ref./9/*.

---e-n-d---of---G-u-i-d-a-n-c-e---n-o-t-e---

3.2.11.3 The heave added mass increases as the fully submerged object approaches the free surface. Hence, the water exit force acts downwards, in the opposite direction to the exit velocity.



Figure 3-3
Water exit of ROV (Courtesy of Statoil)

3.2.11.4 The water exit force can usually be neglected on a partly submerged object being lifted out of the water. However, large horizontal surfaces beneath the object may contribute to the water exit force.

3.2.11.5 The water exit force can be written in terms of a *water exit coefficient* C_e as;

$$F_e(t) = - \frac{1}{2} \rho C_e A_p v_e^2 \quad [\text{N}]$$

where C_e is defined by;

$$C_e = \frac{1}{\rho A_p v_e} \frac{dA_{33}^0}{dt} = - \frac{1}{\rho A_p} \frac{dA_{33}^0}{dh} \quad [-]$$

and

dA_{33}^0 / dh = rate of change of added mass with submergence [kg/m]
 ρ = mass density of water [kg/m³]
 A_p = horizontal projected area of object [m²]
 h = submergence relative to surface elevation [m]

Note that the rate of change of added mass is negative.

3.2.11.6 Enclosed water within the object and drainage of water during the exit phase must be taken into account. Drainage of water may alter the weight distribution during exit.

3.2.11.7 For water exit in waves the relative velocity between lifted object and sea surface must be applied, so that the exit force can be taken as;

$$F_e(t) = -\frac{1}{2} \rho C_e A_p (\dot{\zeta} - \dot{\eta})^2 \quad [\text{N}]$$

where

$\dot{\zeta}$ = vertical velocity of sea surface [m/s]
 $\dot{\eta}$ = vertical motion of the object (positive upwards) [m/s]

3.2.12 Equation of vertical motion of lifted object when hoisted out of wave zone.

Combining the expressions for buoyancy, inertia, wave excitation and water exit forces the equation of vertical motion $\eta(t)$ for the lifted object can be taken as;

$$(M + A_{33})\ddot{\eta} = B_{33}^{(1)}(v_3 - \dot{\eta}) + B_{33}^{(2)}(v_3 - \dot{\eta})|(v_3 - \dot{\eta})| \\ + (\rho V + A_{33})\dot{v}_3 - \frac{1}{2} \frac{dA_{33}^0}{dh} (\dot{\zeta} - \dot{\eta})^2 + \rho g V(t) - Mg + F_{line}(t)$$

The velocity of the lifted object is

$$\dot{\eta} = \dot{\tilde{\eta}} + v_e \quad [\text{N}]$$

The force in the hoisting line is given by 3.2.10.2.

3.2.13 Hydrodynamic loads on slender elements

3.2.13.1 The hydrodynamic force exerted on a slender object can be estimated by summing up sectional forces acting on each strip of the structure. For slender structural members having cross-sectional dimensions considerably smaller than the wave length, wave loads may be calculated using Morison's load formula being a sum of an inertia force proportional to acceleration and a drag force proportional to the square of the velocity.

3.2.13.2 Normally, Morison's load formula is applicable when the wave length is more than 5 times the characteristic cross-sectional dimension.

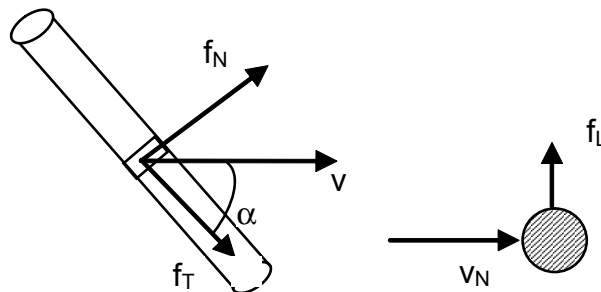


Figure 3-4
Normal force f_N , tangential force f_T and lift force f_L on slender structure

3.2.13.3 The sectional normal force on a slender structure is given by;

$$f_N = -\rho C_A A \ddot{x}_N + \rho (I + C_A) A \dot{v}_N + \frac{1}{2} \rho C_D D v_{rN} |v_{rN}| \quad [\text{N/m}]$$

where

- ρ = mass density of water [kg/m³]
 A = cross-sectional area [m²]
 C_A = added mass coefficient [-]
 C_D = drag coefficient in oscillatory flow [-]
 D = diameter or characteristic cross-sectional dimension [m]
 \ddot{x}_N = acceleration of element normal to element [m/s²]
 v_{rN} = relative velocity normal to element [m/s]
 \dot{v}_N = water particle acceleration in normal dir. [m/s²]

Guidance note:

The relative velocity formulation for the drag force is valid when the motion x_N of the element in the normal direction is larger than the characteristic cross-sectional dimension D . The use of normal velocity in the force formulation is valid if the angle of attack α (Figure 3-4) is in the range 45-90 deg. The drag coefficient can be taken as independent of angle of attack. Ref. DNV-RP-C205 sec.6.2.5.

---e-n-d---of---G-u-i-d-a-n-c-e---n-o-t-e---

3.2.13.4 The sectional (2D) added mass for a slender element is $a_{ij} = \rho C_A A_R$, $i, j = 1, 2$ where A_R is a reference area, usually taken as the cross-sectional area.

3.2.13.5 For bare cylinders the tangential drag force f_t is mainly due to skin friction and is small compared to the normal drag force. However for long slender elements with a predominantly tangential velocity component, the tangential drag force may be important. More information on tangential drag is given in DNV-RP-C205.

3.2.13.6 The lift force f_L , in the normal direction to the direction of the relative velocity vector may be due to unsymmetrical cross-section, wake effects, close proximity to a large structure (wall effects) and vortex shedding. For more information on lift forces for slender cylindrical elements, see *ref. /8/*.

3.2.13.7 The sectional slamming force on a horizontal cylinder can be written in terms of a slamming coefficient C_s as

$$f_s(t) = \frac{1}{2} \rho C_s D v_s^2 \quad [\text{N/m}]$$

C_s is defined by;

$$C_s = \frac{2}{\rho D} \frac{da_{33}^{\infty}}{dh} \quad [-]$$

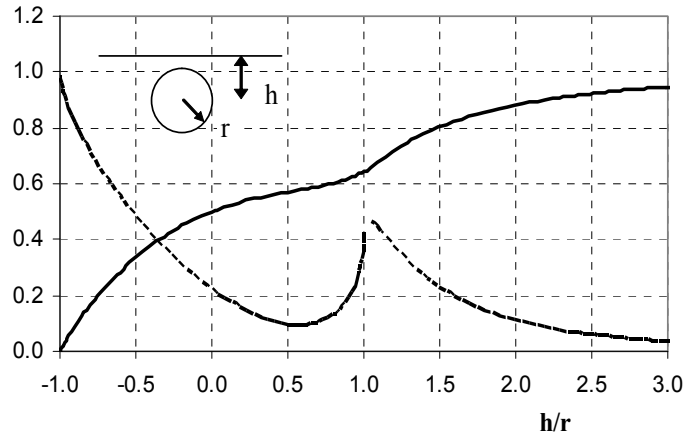
where

- ρ = mass density of water [kg/m³]
 D = diameter of cylinder [m]
 h = submergence [m]
 da_{33}^{∞}/dh = rate of change of sectional added mass with submergence [kg/m²]

Guidance note:

h is the distance from centre of cylinder to free surface so that $h = -r$ at the initial time instant when the cylinder impacts the water surface.

---e-n-d---of---G-u-i-d-a-n-c-e---n-o-t-e---

**Figure 3-5**

High frequency limit of vertical added mass coefficient and its derivative close to a free surface as function of water depth. Solid line: $a_{33}/\rho\pi r^2$. Dotted line: $(da_{33}/dh)/\rho\pi r$.

3.2.13.8 The high frequency vertical added mass coefficient as function of submergence is shown in Figure 3-5. The added mass coefficient is defined by;

$$C_A = a_{33} / \rho \pi r^2 \quad [-]$$

3.2.13.9 The sectional water exit force on a horizontal cylinder can be written in terms of a *water exit coefficient* C_e as

$$F_e(t) = -\frac{1}{2} \rho C_e D v_e^2 \quad [\text{N/m}]$$

where C_e is defined by

$$C_e = -\frac{1}{\rho D} \frac{da_{33}^0}{dh} \quad [-]$$

da_{33}^0/dh = rate of change of sectional low frequency added mass with submergence $[\text{kg/m}^2]$

A discussion of water exit for circular cylinders is presented in *ref. /9/*.

Guidance note:

Note that the exit coefficient may depend strongly on the exit Froude number $F_n = v_e/\sqrt{gD}$ and the formulation in terms of rate of change of added mass is valid only for $F_n \ll 1$ (See also 3.2.11.2)

---e-n-d---of---G-u-i-d-a-n-c-e---n-o-t-e---

3.2.13.10 The slamming coefficient for a circular cylinder can be taken from experimental values by Campbell & Weinberg, *ref. /10/* for a smooth cylinder,

$$C_s(s) = 5.15 \left[\frac{D}{D+19s} + \frac{0.107s}{D} \right] \quad [-]$$

where

$s = h + D/2$ = submergence of cylinder [m]

D = diameter of cylinder [m]

h = distance from centre of cylinder to SWL [m] as shown in Figure 3-5.

It should be noted that buoyancy effects are included in this formula so that it should only be used for $s/D < 0.5$ or $h/r < 0$.

Guidance note:

The initial value of this empirical slamming coefficient $C_s(0) = 5.15$ lies between the theoretical values obtained by two classical water entry solutions, π (von Karman) and 2π (Wagner).

---e-n-d---of---G-u-i-d-a-n-c-e---n-o-t-e---

3.3 Hydrodynamic coefficients

3.3.1 General

3.3.1.1 In general the hydrodynamic force coefficients (added mass coefficient, drag and damping coefficient, lift coefficient) depend on the following,

- geometry
- Reynolds number ($Re = v_m D / \nu$) based on the maximum velocity v_m
- Keulegan-Carpenter number ($KC = v_m T / D$).

where

- D = diameter [m]
- ν = fluid kinematic viscosity [m^2/s]
- T = wave period or period of oscillation.

In addition, aspect ratio, angle of inclination to the flow, surface roughness, perforation ratio, frequency of oscillation, proximity to free surface and proximity to solid boundary may have an influence.

Guidance note:

Close to the free surface the added mass and damping vary with frequency and distance to the free surface. Close to the seabed the coefficients depend upon the proximity, but not frequency.

---e-n-d---of---G-u-i-d-a-n-c-e---n-o-t-e---

3.3.2 Added mass and drag coefficients for simple bodies

3.3.2.1 Added mass and drag coefficients for 2- and 3-dimensional bodies with simple geometry are given in Appendix A & B.

3.3.2.2 Notice that the added mass coefficient given in Appendix A & B are exclusive of water inside the body. Water inside the body may either be included in the added mass or in the body mass. In case it is included in the body mass, the buoyancy should include the internal volume.

Guidance note:

A simple guideline is as follows; water that is contained within the structure when object is lifted out of water should be taken as a part of the body mass, otherwise the water should be included in the added mass. For example; water inside tubular frames flooded through small holes may typically be taken as part of the body mass, while water inside suction anchors most often is included in the added mass.

---e-n-d---of---G-u-i-d-a-n-c-e---n-o-t-e---

3.3.3 Added mass and damping for typical subsea structures

3.3.3.1 Most subsea structures such as remotely operated tools, templates and protection structures, have a complex geometry. It is therefore difficult to determine the hydrodynamic coefficients by analytical methods or by use of sink-source programs.

3.3.3.2 The presently most accurate method to determine hydrodynamic coefficient for complex 3-dimensional subsea structures, is by model tests. Two test methods are used; either free motion decay test or forced oscillation test (See 3.3.6).

3.3.3.3 The added mass and damping of an open subsea structure may be estimated as the sum of contributions from its individual structural members. However, interaction effects between members caused by flow restrictions can cause a significant increase in the added mass and damping.

Guidance note:

Interaction effects can be neglected if the solid projected area normal to the direction of motion (within a typical amplitude of either body motion or wave particle motion) is less than 50% of the silhouette area.

---e-n-d---of---G-u-i-d-a-n-c-e---n-o-t-e---

3.3.4 Added mass and damping for ventilated structures

3.3.4.1 In the present context *ventilated structures* comprise structures where a plane normal to the oscillation direction is either arranged with holes or slots or consists of parallel slender elements. Examples are the horizontal top plate of a suction anchor with ventilation holes and the top area of a protection structure (Figure 3-6). Also other parts of a 3-dimensional structure with significant flow restriction are here defined as ventilated structures.



Figure 3-6
Example of ventilated structure, a protection cover used to shelter subsea modules on seabed
(Courtesy of Marintek)

3.3.4.2 For assessment of the effect of oscillation amplitude on the force coefficients for a ventilated structures, a “porous Keulegan-Carpenter number” may be defined as

$$KC_{\text{por}} = \frac{z_m}{D} \cdot \frac{(1-p)}{2\mu p^2} \quad [-]$$

where

z_m = oscillation amplitude [m]
 D = characteristic horizontal dimension [m]
 p = perforation ratio $0 < p < 1$
 μ = discharge coefficient [-]

The perforation ratio p is defined as the open area divided by the total area. The discharge coefficient μ is usually between 0.5 and 1.0, see *ref./2/* and */3/*.

3.3.4.3 Figure 3-7 shows model test results for added mass of 5 ventilated structures representing typical protection structures, with perforation ratio varying from 0.15 to 0.47. The added mass A_{33} is normalized with the added mass of a solid structure, $A_{33,0}$ (with same dimensions perpendicular to the motion direction). The variation of added mass with amplitude of oscillation is considerable (by a factor of 2-3) for all the objects.

3.3.4.4 The asymptotic value for A_{33} in the limit of zero amplitudes ($KC = 0$) can be found from potential theory and calculated by a sink-source panel program. The following approximated formula has been found by curve fitting through results for plates with circular holes, and has been found applicable for plates with ventilation openings;

$$\left. \frac{A_{33}}{A_{33,0}} \right|_{KC=0} = e^{-\frac{p}{0.28}} \quad [-]$$

However, as seen in figure 3-7, this asymptotic value at $KC = 0$ may give inaccurate values for structures in oscillatory fluid flow.

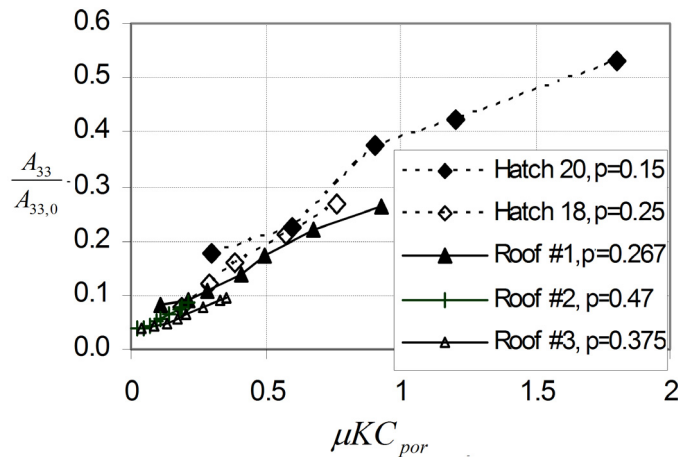


Figure 3-7
Added mass of 5 perforated objects compared, *ref. /7/*

3.3.5 Drag coefficients for circular cylinders

3.3.5.1 The drag coefficient for circular cylinders depends strongly on the roughness k of the cylinder. For high Reynolds number ($Re > 10^6$) and large KC number, the steady drag-coefficient C_{DS} may be taken as

$$C_{DS}(\Delta) = \begin{cases} 0.65 & ; \Delta < 10^{-4} \text{ (smooth)} \\ (29 + 4 \cdot \log_{10}(\Delta)) / 20 & ; 10^{-4} < \Delta < 10^{-2} \\ 1.05 & ; \Delta > 10^{-2} \text{ (rough)} \end{cases}$$

where

$\Delta = k/D$ is the non-dimensional roughness. The above values apply for both irregular and regular wave analysis.

3.3.5.2 The variation of the drag coefficient with *Keulegan-Carpenter number* KC for circular cylinders can be approximated by;

$$C_D = C_{DS} \cdot \psi(KC) \quad [-]$$

where C_{DS} is the drag coefficient for steady flow past a cylinder and;

$$\psi(KC) \quad [-]$$

is an *amplification factor*. The shaded area in Figure 3-8 shows the variation in ψ from various experimental results. Note that surface roughness varies.

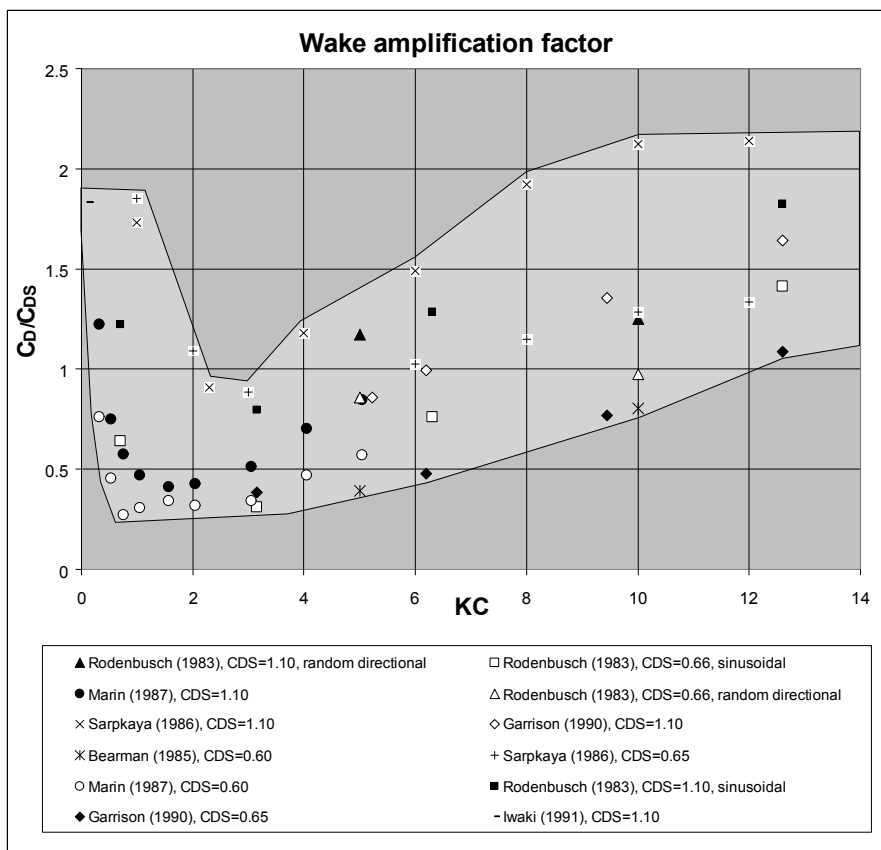


Figure 3-8
Wake amplification factor, *ref. /11/*

3.3.6 Estimating added mass and damping coefficients from model tests or CFD analyses

3.3.6.1 In forced oscillation tests the structure is forced to oscillate sinusoidally at a frequency ω .

3.3.6.2 Time series for motion $z(t)$ and force $F(t)$ are analyzed and the total oscillating mass ($M+A_{33}$) and the linearised damping B can be estimated by a least-squares method, using the equation;

$$F = -(M + A)\ddot{z} - B\dot{z} \quad [\text{N}]$$

3.3.6.3 The added mass, A , is found by subtracting the structural mass of the structure and the suspension elements from the total oscillating mass. The added mass coefficient is extracted from the added mass by;

$$C_A = \frac{A}{\rho V_R} \quad [-]$$

where

ρ = mass density of water [kg/m^3]
 V_R = reference volume of the object [m^3]
 C_A = added mass coefficient [-]

3.3.6.4 The derived linearised damping, B , may be plotted as function of the oscillation amplitude, z . If a fairly straight line can be fitted, the damping may be split into a linear and quadratic term by:

$$B_1 = B \quad \text{at } z = 0 \quad [\text{kg/s}]$$

$$B_2 = (B - B_1) \cdot \frac{3T}{16z} \quad [\text{kg/m}]$$

where

T = oscillation period [s]
 z = oscillation amplitude [m]
 B_1 = linear damping, ref. 3.2.8.4 [kg/s]
 B_2 = quadratic damping, ref. 3.2.8.4 [kg/m]

3.3.6.5 Alternatively, a better fit may be obtained by applying;

$$F = -(M + A)\ddot{z} - B\dot{z}|\dot{z}| \quad [\text{N}]$$

3.3.6.6 The drag coefficient is then extracted from the damping factor B by;

$$C_D = \frac{2B}{\rho A_p} \quad [-]$$

where

A_p = projected area of object normal to the direction of oscillation $[\text{m}^2]$

3.3.6.7 Having established drag coefficients for a number of oscillation amplitudes, the linear and quadratic damping terms, B_1 and B_2 , may be derived as described in 3.2.8.7 (if a straight line is obtained).

3.3.6.8 These methods are more robust than estimating the two damping coefficients in one single step. A similar approach is applied for estimating added mass and damping from CFD analyses.

3.3.6.9 In a free motion decay test the total mass is found from the period of each oscillation cycle, and the damping is derived from the decaying amplitudes of oscillation.

3.3.6.10 Test models used for estimating force coefficients are scaled by use of Froude's scaling law defined by the Froude number. Scales are typically chosen between 1:30 and 1:100. When viscous forces are significant, the Reynolds number is also relevant due to vortex shedding, and corrections to the Froude scaling may be needed. Such corrections are normally referred to as "scaling effects". One should be aware that scaling effects may be important for perforated structures. General recommendations for model testing are given in DNV-RP-C205, *ref. /1/*.

3.4 Calculation methods for estimation of hydrodynamic forces

3.4.1 The Simplified Method

3.4.1.1 The Simplified Method as described in *Section 4* may be used for estimating characteristic hydrodynamic forces on objects lowered through the water surface and down to the sea bottom.

3.4.1.2 The Simplified Method may also be applied on retrieval of an object from sea bottom back to the installation vessel.

3.4.1.3 The intention of the Simplified Method is to give simple conservative estimates of the forces acting on the object.

3.4.1.4 The Simplified Method assumes that the horizontal extent of the lifted object is small compared to the wave length. A regular design wave approach or a time domain analysis should be performed if the object extension is found to be important.

3.4.1.5 The Simplified Method assumes that the vertical motion of the structure is equal to the vertical motion of the crane tip. A time domain analysis is recommended if amplification due to vertical resonance is present.

3.4.2 Regular design wave approach

3.4.2.1 Lifting and lowering operations may be analysed by applying a regular design wave to the structure using a spreadsheet, or a programming language, as described in this section.

3.4.2.2 Documentation based upon this method should be thoroughly described in every detail to such extent that the calculations are reproducible.

3.4.2.3 Shallow water effects are for simplicity not included in this section.

Guidance note:

A finite water depth, d , may be taken into account by deriving the water particle velocity $\mathbf{v} = \text{grad } \phi$ and acceleration $\mathbf{a} = \partial \mathbf{v} / \partial t$ from the velocity potential for linear Airy waves;

$$\phi = \frac{g \zeta_a}{\omega} \frac{\cosh k(z+d)}{\cosh kd} \cos(\omega t - kx \cos \beta - ky \sin \beta) \quad [\text{m}^2/\text{s}]$$

Detailed expressions for water particle velocity and acceleration are given in DNV-RP-C205.

---e-n-d---of---G-u-i-d-a-n-c-e---n-o-t-e---

3.4.2.4 The global structure geometry should be divided into individual main elements both horizontally and

vertically, each of which contributes to the hydrodynamic forces, see Figure 3-9.

3.4.2.5 Separate calculations are made for each defined wave direction and for each defined load case where the still water level is positioned either beneath a slamming area or just above the top of a main item.

3.4.2.6 A regular wave is applied. Calculations are made to obtain acceptance limits for both significant wave height and zero-up-crossing wave period.

3.4.2.7 The regular wave height should not be less than the most probable largest wave height. If the lowering through the wave zone are to be performed within 30 minutes, the largest characteristic wave height may be assumed equal to 1.80 times the significant wave height, see 3.4.2.11.

3.4.2.8 The applied regular wave height should be 2.0 times the significant wave height in cases where the planned operation time (including contingency time) exceeds 30 minutes.

3.4.2.9 The regular wave period should be assumed equal to the zero-up-crossing period, T_z , of the associated sea state.

3.4.2.10 Figure 3-9 shows the definition of the coordinate system for the wave description given in 3.4.2.11. The waves propagate in a direction β relative to the x-axis. The origin of the coordinate system is in the still water level.

Guidance note:

The structure may in this case roughly be divided into four suction anchors (A, B, C and D) and two manifold halves (Left Side and Right Side).

---e-n-d---of---G-u-i-d-a-n-c-e---n-o-t-e---

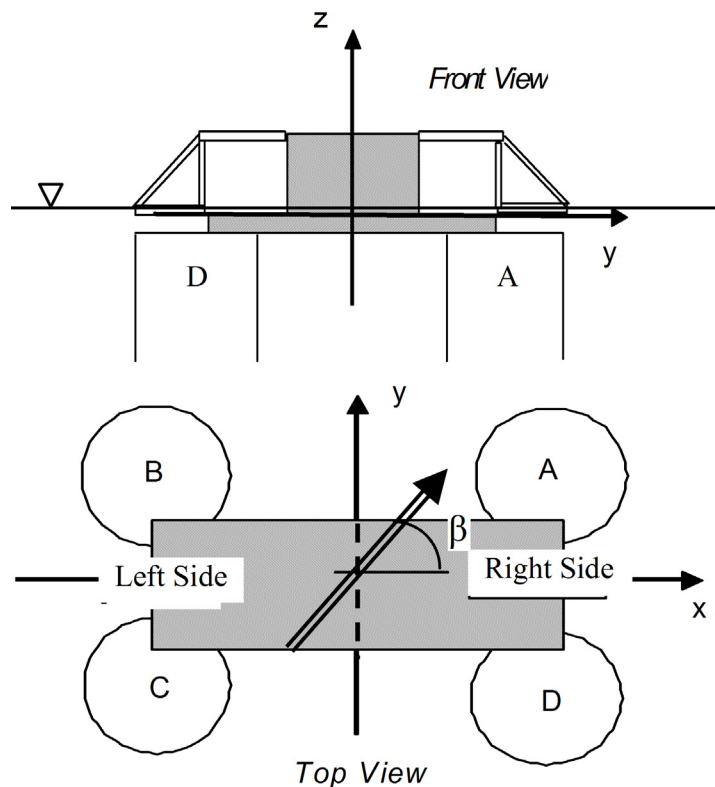


Figure 3-9
Example of subsea module. Main elements, coordinate system and wave direction.

3.4.2.11 The regular wave is given by:

$$\zeta = \zeta_a \sin(\omega t - kx \cos \beta - ky \sin \beta) \quad [\text{m}]$$

where

ζ_a = wave amplitude, i.e. $\zeta_a = 0.9H_s$ for operations less than 30 minutes and $\zeta_a = H_s$ for operations exceeding

30 minutes [m]

- ω = wave angular frequency, i.e. $\omega = 2\pi/T$ where the regular wave period, T , should be assumed equal to the applied zero-up-crossing period $T = T_z$ [rad/s]
 t = time varying from 0 to T with typical increments of 0.1 [s]
 k = wave number, i.e. $k = \omega^2/g$ for deep water, where g is the acceleration of gravity [m^{-1}]
 x, y = horizontal CoG coordinates for the individual main items of the lifted object [m]
 β = wave propagation direction measured from the x-axis and positive counter-clockwise [rad]

Guidance note:

In shallow water the wave number is given by the general dispersion relation

$$\omega^2 = gk \tanh(kd)$$

---e-n-d---of---G-u-i-d-a-n-c-e---n-o-t-e---

3.4.2.12 The vertical wave particle velocity and acceleration can be taken as:

$$v = \omega \zeta_a e^{kz} \cos(\omega t - kx \cos \beta - ky \sin \beta) \quad [\text{m/s}]$$

and

$$\dot{v} = -\omega^2 \zeta_a e^{kz} \sin(\omega t - kx \cos \beta - ky \sin \beta) \quad [\text{m/s}^2]$$

where

- v = vertical water particle velocity [m/s]
 \dot{v} = vertical water particle acceleration [m/s²]
 z = vertical CoG coordinate for the individual main items of the lifted object (negative downwards) [m]

3.4.2.13 The vertical motion of the lifted object is in this calculation method assumed to follow the motion of the crane tip. The vertical crane tip motion is assumed to oscillate harmonically with an amplitude, η_a , and a regular period T_{ct} .

Guidance note:

A time domain analysis is recommended in cases where this assumption is not valid.

---e-n-d---of---G-u-i-d-a-n-c-e---n-o-t-e---

3.4.2.14 The most probable largest vertical single amplitude crane tip motion, η_a , for the applied T_z wave period can be taken as:

$\eta_a = 3.6\sigma_\eta$ [m] for operation durations less than 30 min.

$\eta_a = 4.0\sigma_\eta$ [m] for operation durations above 30 min.

where σ_η is the standard deviation of the vertical crane tip motion response spectrum.

3.4.2.15 The vertical motion, velocity and acceleration of the lifted object is then given by:

$$\eta = \eta_a \sin(\omega_\eta t + \varepsilon) \quad [\text{m}]$$

$$\dot{\eta} = \omega_\eta \eta_a \cos(\omega_\eta t + \varepsilon) \quad [\text{m/s}]$$

and

$$\ddot{\eta} = -\omega_\eta^2 \eta_a \sin(\omega_\eta t + \varepsilon) \quad [\text{m/s}^2]$$

where

- η = vertical motion of lifted object [m]
 $\dot{\eta}$ = vertical velocity of lifted object [m/s]
 $\ddot{\eta}$ = vertical acceleration of lifted object [m/s²]
 η_a = vertical single amplitude motion of lifted object, assumed equal the most probable largest crane tip single amplitude, see 3.4.2.14 [m]
 ω_η = circular frequency of the vertical motion of the lifted object, i.e. $\omega_\eta = 2\pi/T_{ct}$ where T_{ct} is the peak period of the crane tip motion response spectrum for the applied T_z wave period [rad/s]
 t = time varying from 0 to T with typical increments of 0.1 [s]
 ε = phase angle between wave and crane tip motion, see 3.4.2.16 [rad]

3.4.2.16 The phase angle that results in the largest dynamic tension amplitudes in the lifting slings and hoisting line should be applied.

Guidance note:

This can be found by applying a set of phase angles in a range from $\varepsilon = 0$ to $\varepsilon = 2\pi$ with increments of e.g. 0.1π . The phase angles that result in the highest risk of slack sling or the largest DAF_{conv} should be applied, ref. 4.4.3.3 and 4.4.4.3.

---e-n-d---of---G-u-i-d-a-n-c-e---n-o-t-e---

3.4.2.17 The characteristic vertical hydrodynamic force acting on each of the structure main items can be found by:

$$F_{hyd} = F_{\rho} + F_m + F_s + F_d \quad [N]$$

where

F_{ρ} = varying buoyancy force [N]
 F_m = hydrodynamic mass force [N]
 F_s = slamming impact force [N]
 F_d = hydrodynamic drag force [N]

3.4.2.18 The varying buoyancy force for items intersecting the water surface can be found by:

$$F_{\rho} = \rho g \delta V(\zeta - \eta) \quad [N]$$

where

$\delta V(\zeta - \eta)$ = change in displacement due to relative vertical motion, $\zeta - \eta$, (see 3.2.10.2 and Figure 3-10) [m³]
 ζ = water surface elevation in the applied regular wave as defined in 3.4.2.11 [m]
 η = vertical motion of lifted object, see 3.4.2.15 [m]
 ρ = density of sea water, normally = 1025 [kg/m³]
 g = acceleration of gravity = 9.81 [m/s²]

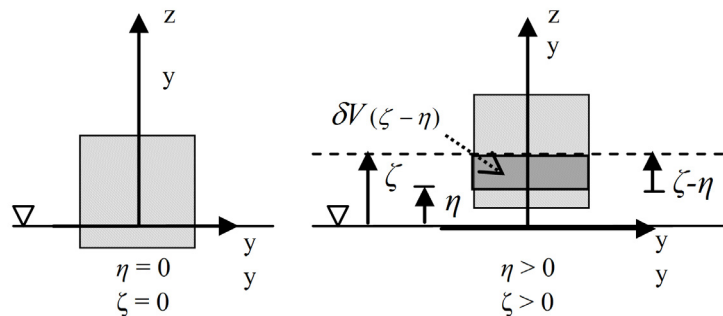


Figure 3-10
The displacement change $\delta V(\zeta - \eta)$

3.4.2.19 The mass force is in this simplified regular design wave approach estimated by:

$$F_m = \rho V \dot{v} + A_{33}(\dot{v} - \ddot{\eta}) - M \ddot{\eta} \quad [N]$$

where

M = mass of object item in air [kg]
 A_{33} = added mass of object item [kg]
 ρ = density of sea water, normally = 1025 [kg/m³]
 V = volume of displaced water of object item [m³]
 \dot{v} = vertical water particle acceleration as found in 3.4.2.12 [m/s²]
 $\ddot{\eta}$ = vertical acceleration of lifted object, see 3.4.2.15 [m/s²]

The mass force as defined above is the sum of the inertia force (3.2.5.1) and the wave excitation force (3.2.7.2).

Guidance note:

For items intersecting the water surface, the volume of displaced water should be taken as the volume at still water level.

---e-n-d---of---G-u-i-d-a-n-c-e---n-o-t-e---

3.4.2.20 The slamming impact force on object items that penetrate the water surface may be taken as:

$$F_s = 0.5 \rho C_s A_s (v - \dot{\eta})^2 \quad [N]$$

where

ρ = density of sea water [kg/m³]

C_s = slamming coefficient which may be determined by theoretical and/or experimental methods. For smooth circular cylinders C_s should not be taken less than 3.0. Otherwise, C_s should not be taken less than 5.0. See also *DNV-RP-C205*.

A_s = slamming area projected on a horizontal plane [m²]

v = vertical water particle velocity at slamming area, $z = 0$ if slamming area is situated in the still water level, see 3.4.2.12 [m/s]

$\dot{\eta}$ = vertical velocity of lifted object [m/s]

3.4.2.21 The drag force may be taken as:

$$F_d = 0.5 \rho C_D A_p (v - \dot{\eta}) |v - \dot{\eta}| \quad [\text{N}]$$

where

C_D = drag coefficient of object item [-]

A_p = area of object item projected on a horizontal plane [m²]

and otherwise as defined in 3.4.2.20.

Guidance note:

Alternatively, the drag force can be estimated by:

$$F_d = B_1 (v - \dot{\eta}) + B_2 (v - \dot{\eta}) |v - \dot{\eta}| \quad [\text{N}]$$

where

B_1 is the linear damping of the object [kg/s]

B_2 is the quadratic damping of the object [kg/m]

---e-n-d---of---G-u-i-d-a-n-c-e---n-o-t-e---

3.4.2.22 The performed analyses should cover the following zero-up-crossing wave period range for a given significant wave height H_s :

$$8.9 \cdot \sqrt{\frac{H_s}{g}} \leq T_z \leq 13 \quad [\text{s}]$$

3.4.2.23 A more limited T_z range may be applied if this is reflected in the installation criteria in the operation procedures.

3.4.2.24 The vertical crane tip motion is found according to *Section 4.3.3*.

3.4.2.25 The motions, velocities and accelerations are calculated for each time step at each defined main item.

3.4.2.26 Some motion response analysis computer programs are able to define off-body points on the wave surface and generate relative motion directly. In such case, these values may be applied.

3.4.2.27 The varying buoyancy force, mass force, slamming force and drag force are calculated for each time step at each defined main item.

3.4.2.28 The forces are then summed up. The static weight is applied as a minimum and maximum value according to *Section 4.2.2*. Reaction forces in slings and crane hooks are found applying the force and moment equilibrium. The slack sling criterion as described in *Section 4.4.3* should be fulfilled. The structure and the lifting equipment should be checked according to *Section 4.4.4*.

3.4.3 Time domain analyses

3.4.3.1 Computer programs applying non-linear time domain simulations of multi-body systems may be used for more accurate calculations.

3.4.3.2 If applicable, a full 3 hour simulation period for each load case is recommended in the analyses.

3.4.3.3 In sensitivity analyses a number of shorter simulations may be performed, e.g. 30 minutes.

3.4.3.4 The largest and smallest observed loads in e.g. slings and fall during simulation time should be stated.

3.4.3.5 Assuming that the dynamic loads can be Rayleigh distributed, the most probable largest maximum load, R_{\max} , may be found applying the following relation:

$$R_{\max} = \sigma_r \sqrt{2 \ln \left(\frac{t}{T_z} \right)} \quad [\text{N}]$$

where

σ_r = standard deviation of the dynamic load [N]

t = duration of operation including contingency time, minimum 30 minutes [s]

T_z = zero up-crossing period of the dynamic load [s]

The zero up-crossing period of the dynamic load is defined by

$$T_z = 2\pi \sqrt{\frac{M_0}{M_2}} \quad [\text{s}]$$

where M_0 and M_2 are the zero and second moments of the load spectrum (2.2.6.4)

Guidance note:

In most dynamic non-linear cases the response does not adequately fit the Rayleigh distribution. The estimated maximum load should therefore always be compared with the largest observed load in the simulation.

---e-n-d---of---G-u-i-d-a-n-c-e---n-o-t-e---

3.4.3.6 If analyses are based upon selected wave trains of short durations, the selections should preferably be based upon maximum vertical relative motion between crane tip and water surface. Both relative motion amplitude, velocity and acceleration should be decision parameters in the selection of wave trains.

3.4.3.7 For lowering operations it is generally recommended to keep the object fixed in selected positions for minimum 30 min. If a continuous lowering of the object is simulated a large number of realizations is required in order to obtain a proper statistical confidence.

3.4.3.8 Damping and added mass values should be carefully chosen in the analyses, ensuring that also the moment of inertia values are correctly modelled.

3.4.4 CFD analyses

3.4.4.1 Wave load analyses based on Computational Fluid Dynamics (CFD) may be performed on subsea lifts. The fluid motion is then described by the Navier-Stokes equations.

3.4.4.2 Examples of numerical methods applicable for simulation of wave-structure interaction including water entry (slamming) and water exit are:

- Volume-of-Fluid (VOF) method
- Level Set (LS) method
- Constrained Interpolation Profile (CIP) method
- Smooth Particle Hydrodynamics (SPH) method.

3.4.4.3 The first three methods (VOF, LS, CIP) are grid methods while SPH is a particle method where a grid is not needed.

3.4.4.4 The applied boundary conditions and the size of the computational domain should ensure that reflections from the boundaries of the domain do not influence the hydrodynamic forces on the object.

3.4.4.5 Convergence tests should be performed verifying adequacy of applied number of cells or particles (for particle methods) in the model.

3.4.4.6 Stretching of cells may influence the incoming wave. Hence, this should be thoroughly tested.

3.4.4.7 The distance from inflow boundary to the structure may in some cases influence the wave action on the structure.

3.4.4.8 For simulations where generated waves start from rest, a sufficient number of subsequent waves should be generated in order to avoid transient effects.

3.4.4.9 Approximations of actual structure geometry due to limitations in available computer capacities should be performed applying correct total areas. Holes and penetrations may be summed into fewer and larger openings.

Guidance note:

Geometry approximations may give an inadequate representation of local forces and pressures. Convergence tests should always be performed.

---e-n-d---of---G-u-i-d-a-n-c-e---n-o-t-e---

3.4.4.10 Additional buoyancy due to model approximations should be taken into account when evaluating

computed total vertical forces.

3.4.4.11 The computed slamming loads may be overestimated when single phase modelling is applied. For wave impact problems it is recommended to use two-phase modelling.

3.4.4.12 Computed forces, pressures and velocities should be checked and compared with approximate hand-calculations.

3.4.4.13 If model test results are available, numerical simulation results should be compared and validated with the model test.

3.4.4.14 Figure 3-11 shows an example of prediction of added mass and damping coefficients for model mud mat geometries with 3 different perforation ratios (0%, 15% and 25%). Calculations are carried out using 2 different CFD models and are validated with experimental results.

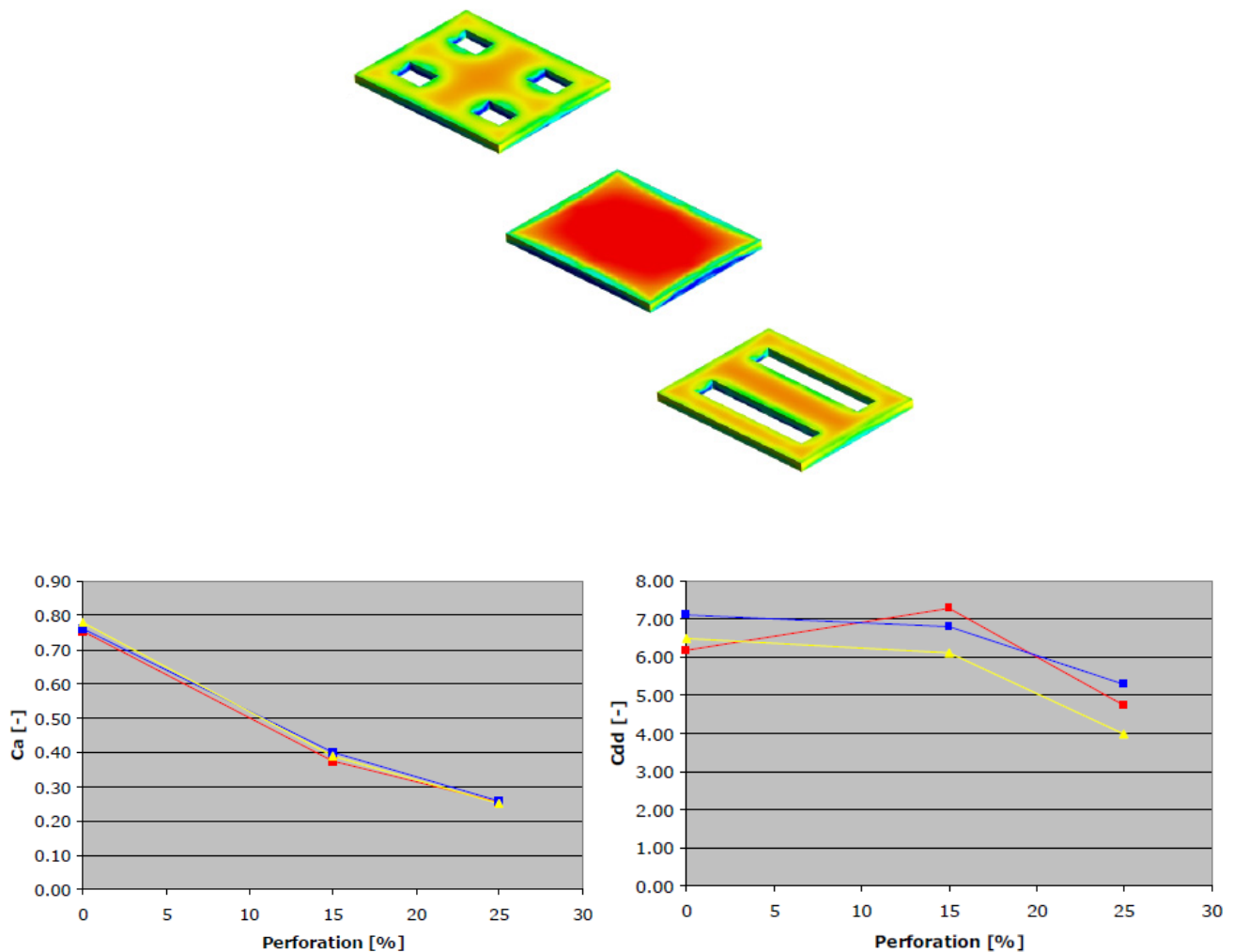


Figure 3-11
Example of use of CFD for prediction of added mass and drag coefficients for model mud mat geometries
(Courtesy of Acergy)

3.5 Moonpool operations

3.5.1 General

For small subsea modules and tools, installation through the moonpool of the vessel is often preferred. This may reduce the dynamic forces, increase the limiting seastate and thus reduce the costs of installation and intervention operations. A typical application area is maintenance and repair operations of subsea production plants.

3.5.2 Simplified analysis of lift through moonpool

3.5.2.1 The simplified analysis described in this subsection is based on the following limiting assumptions,

- The moonpool dimensions are small compared to the breadth of the ship.
- Only motion of the water and object in vertical direction is considered.
- The blocking effect of the lifted object on the water in the moonpool is moderate.
- Cursors prevent impact into the moonpool walls. Only vertical forces parallel to the moonpool axis are considered.

3.5.3 Equation of motion

3.5.3.1 A body object suspended inside a moonpool is considered, see Figure 3-12. The moonpool may have varying cross-sectional area $A(z)$. The draught of the ship is D . The vertical motion of the lifted body may differ from the vertical ship motion due to the winch operation and/or dynamic amplification in the hoisting system.

3.5.3.2 The equation of motion for the water plug can be written as

$$(M + A_{33})\ddot{\zeta} + C_s|\dot{\zeta} - \dot{\zeta}_s|(\dot{\zeta} - \dot{\zeta}_s) + C_b|\dot{\zeta} - \dot{\zeta}_b|(\dot{\zeta} - \dot{\zeta}_b) + K\zeta = F(t)$$

where

- M = mass of water plug [kg]
 A_{33} = added mass of water plug (see 3.5.4.3) [kg]
 ζ = motion of water plug [m]
 ζ_s = heave motion of the ship [m]
 ζ_b = motion of body in moonpool [m]
 ζ_w = sea surface elevation outside moonpool [m]
 C_s = damping coefficient for relative motion between water plug and ship [kg/m]
 C_b = damping coefficient for relative motion between water plug and body [kg/m]
 K = $\rho g A$ water plane stiffness [kg/s²]
 $F(t)$ = wave excitation force on water plug [N]

The ship heave motion is related to the sea surface elevation by a transfer function G_s (amplitude and phase),

$$\zeta_s = G_s \zeta_w \quad [\text{m}]$$

The hydrodynamic pressure force acting on the water plug can also be related to the sea surface elevation by a transfer function G_w (amplitude and phase),

$$F(t) = G_w \zeta_w \quad [\text{N}]$$

3.5.3.3 Both G_s and G_w can be found by integrating the pressure p obtained by a sink-source diffraction program over the cross-section of the moonpool at $z = -D$. G_s and G_w are functions of wave frequency and wave direction.

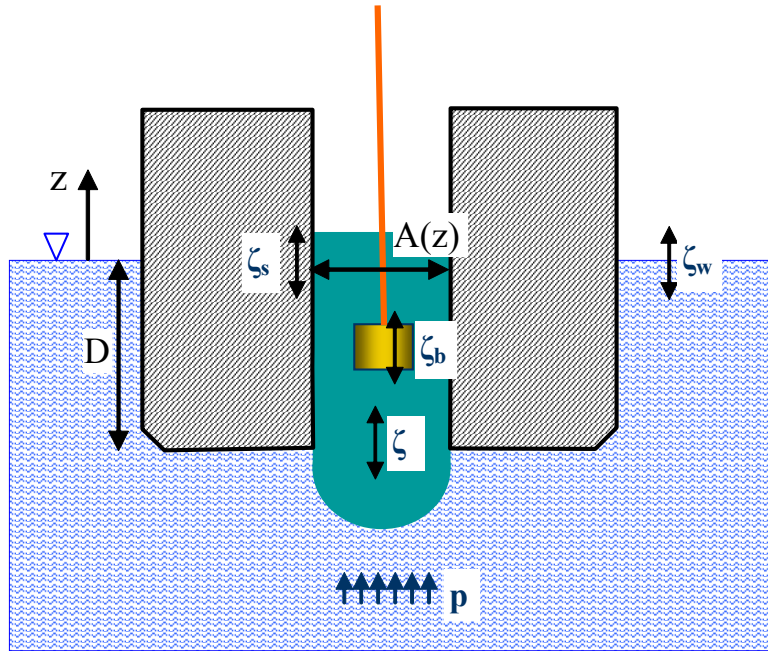


Figure 3-12
Suspended body in a moonpool

3.5.4 Resonance period

3.5.4.1 The natural period of vertical oscillations of the water plug and the damping conditions given by the moonpool design are important for the dynamic forces on an object inside the moonpool.

3.5.4.2 In general the cross-sectional area of the moonpool is a function of the vertical position z . Assuming the moonpool walls do not move, the requirement of continuity yields

$$A(z) \cdot \dot{\zeta}(z) = A(0) \cdot \dot{\zeta}(0) \quad [\text{m}^3/\text{s}]$$

3.5.4.3 The requirement of energy conservation gives,

$$\frac{d}{dt}(E_k + E_p) = 0 \quad [\text{Nm/s}]$$

where

$$\begin{aligned} E_k &= \frac{1}{2} \rho \int_{-D}^0 A(z) \cdot \dot{\zeta}^2(z) dz + \frac{1}{2} A_{33} \cdot \dot{\zeta}^2(-D) \\ &= \frac{1}{2} \rho A(0) \cdot \dot{\zeta}^2(0) \left\{ \int_{-D}^0 \frac{A(0)}{A(z)} dz + \frac{A(0)}{A(-D)} \cdot \frac{A_{33}}{\rho A(-D)} \right\} \quad [\text{Nm}] \end{aligned}$$

and

$$E_p = \frac{1}{2} \rho g A(0) \cdot \zeta^2(0) \quad [\text{Nm}]$$

3.5.4.4 A_{33} is the added mass for vertical oscillation of the water plug, which can be expressed as

$$A_{33} = \rho \kappa A(-D) \sqrt{A(-D)} \quad [\text{kg}]$$

3.5.4.5 The parameter κ has been found to be within 0.45 and 0.47 for rectangular moonpools with aspect ratios between 0.4 and 1.0. Thus $\kappa = 0.46$ can be used for all realistic rectangular moonpools. For a circular moonpool $\kappa = 0.48$.

3.5.4.6 The resonance period is found from the energy conservation expression,

$$\omega_0^2 \left\{ \int_{-D}^0 \frac{A(0)}{A(z)} dz + \frac{A(0)}{A(-D)} \cdot \kappa \sqrt{A(-D)} \right\} - g = 0 \quad [\text{m/s}^2]$$

or

$$T_0 = \frac{2\pi}{\sqrt{g}} \sqrt{\int_{-D}^0 \frac{A(0)}{A(z)} dz + \frac{A(0)}{A(-D)} \cdot \kappa \sqrt{A(-D)}} \quad [\text{s}]$$

3.5.4.7 The energy-equivalent mass (mass plus added mass) moving with the surface velocity $\dot{\zeta}(0)$ is;

$$M_{eq} = \frac{E_k}{\frac{1}{2} \dot{\zeta}^2(0)} = \rho A(0) \left\{ \int_0^D \frac{A(0)}{A(z)} dz + \frac{A(0)}{A(-D)} \cdot \kappa \sqrt{A(-D)} \right\} \quad [\text{kg}]$$

3.5.4.8 If the moonpool has a constant cross-sectional area $A(z) = A$, the above expressions simplify to the following;

$$T_0 = \frac{2\pi}{\sqrt{g}} \sqrt{D + \kappa \sqrt{A}} \quad [\text{s}]$$

$$M_{eq} = \rho A (D + \kappa \sqrt{A}) \quad [\text{kg}]$$

3.5.5 Damping of water motion in moonpool

3.5.5.1 The amplitude of the water motion in the moonpool, in particular for wave excitation close to the resonance period T_0 , depends on the level of damping. In addition to inviscid damping due to wave generation, damping is provided by viscous drag damping caused by various structures like guidance structures, fittings, cofferdam or a bottom plate.

3.5.5.2 In model tests of several offshore diving support vessels and work vessels with different damping devices, the water motion inside a moonpool has been investigated. In these tests the relative motion between the water plug and the ship at the moonpool centre axis has been measured. An amplitude RAO for the relative motion is defined as;

$$RAO = \left| \frac{\zeta - \zeta_s}{\zeta_w} \right| \quad [\text{m/m}]$$

where

ζ = motion of water plug [m]

ζ_s = heave motion of the ship [m]

ζ_w = sea surface elevation outside moonpool [m]

3.5.5.3 Figure 3-13 shows the measured RAO for different structures causing damping of water motion in moonpool.

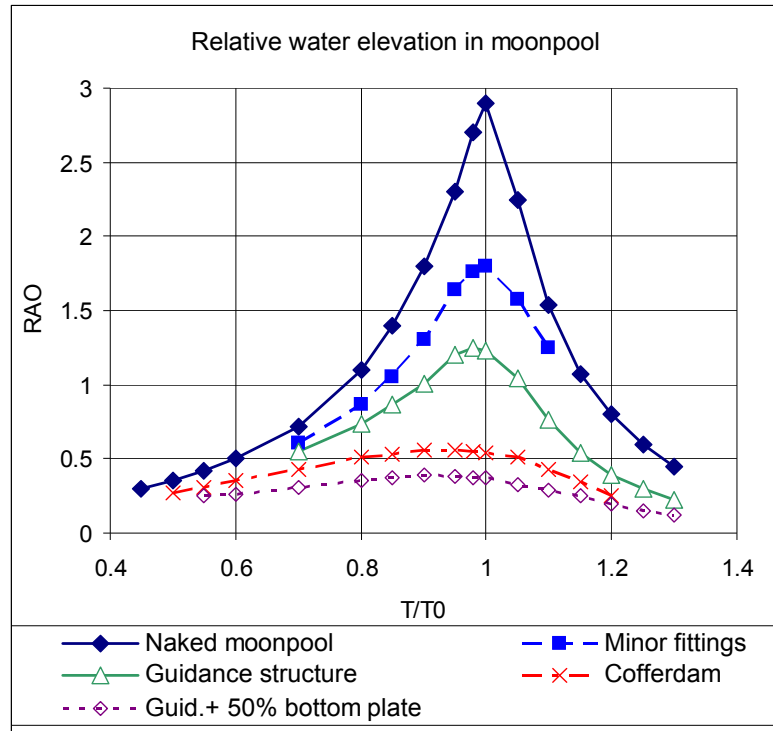


Figure 3-13
Measured relative water elevation in a moonpool per unit incoming wave amplitude (Courtesy of Marintek)

3.5.5.4 The water plug is excited both by the incoming waves and by the vertical ship motion. Hence it is not straightforward to derive damping data directly from such curves. An approximated approach has been used in order to estimate the damping given by the various damping arrangements. An approximate linearised complex equation of motion of the water plug in an empty moonpool (without a lifted object) is;

$$M \ddot{\zeta} + C_{s1}(\dot{\zeta} - \dot{\zeta}_s) + K\zeta = F(t) \quad [\text{N}]$$

⇓

$$-\omega^2 M \zeta + i\omega C_{s1}(\zeta - G_s \zeta_w) + K\zeta = G_w \zeta_w \quad [\text{N}]$$

where

- M = $\rho A(D + \kappa\sqrt{A})$ = total mass of water plug, including added mass [kg]
- K = $\rho g A$ = water plane stiffness [kg/s²]
- C_{s1} = $2\eta\sqrt{KM}$ = linearised damping [kg/s]
- η = damping ratio (relative to critical damping) [-]
- G_s = transfer function for vertical moonpool motion [m/m]
- G_w = transfer function from wave elevation to excitation force [N/m]

3.5.5.5 The ratio between the motion of the water plug and the sea surface elevation outside the moonpool is;

$$\frac{\zeta}{\zeta_w} = \frac{i\omega C_{s1}G_s + G_w}{-\omega^2 M + i\omega C_{s1} + K} = \frac{\frac{G_w}{\rho g A} + 2iG_s\eta\frac{\omega}{\omega_0}}{1 - \left(\frac{\omega}{\omega_0}\right)^2 + 2i\eta\frac{\omega}{\omega_0}} \quad [-]$$

3.5.5.6 To obtain a relationship between transfer functions G_w and G_s , some simplifying assumptions are made,

— The moonpool dimensions are small compared to the ship breadth.

- Excitation force due to incoming waves, F_1 , and due to ship motion, F_2 , can be assessed as for a ship without moonpool.
- The fluid pressure expressions valid for long waves can be used.
- Deep water is assumed.

The following approximate expressions for the excitation force can then be used;

$$\begin{aligned}
 F(t) &= F_1(t) + F_2(t) \\
 &= p_{FK} \cdot A + A_{33} \cdot \ddot{\zeta}_s \\
 &= \rho A g \zeta_w e^{-kD} + \kappa \rho \sqrt{A} A \ddot{\zeta}_s \\
 &= \rho A \zeta_w \left(g e^{-kD} - \omega^2 \kappa \sqrt{A} G_s \right) \quad [\text{N}]
 \end{aligned}$$

where

p_{FK} = the undisturbed (Froude-Krylov) dynamic fluid pressure $[\text{N/m}^2]$

A_{33} = the added mass of the water plug as given in 3.5.4.4 $[\text{kg}]$

Hence,

$$G_w = \frac{F(t)}{\zeta_w} = \rho A \left(g e^{-kD} - \omega^2 \kappa \sqrt{A} G_s \right) \quad [\text{N/m}]$$

where $k = \omega^2 / g$.

3.5.5.7 The amplitude ratio of relative water plug elevation to incoming wave elevation is then given by

$$RAO = \left| \frac{\zeta - \zeta_s}{\zeta_w} \right| = \left| \frac{\zeta}{\zeta_w} - G_s \right|$$

3.5.5.8 In Figure 3-14 an example case of the relative water elevation inside the moonpool is plotted. The motion transfer functions of a typical 80 m long diving support vessel have been used. G_s for vertical moonpool motion has been inserted in the above expressions, and the RAO curves have been computed for varying relative damping, η .

3.5.5.9 The results are uncertain for the shortest wave periods ($T/T_0 < 0.8$), where the curve shapes differ from the model test results.

3.5.5.10 The maximum RAO values, found at resonance, are shown as a function of the relative damping, for the cases without bottom plate, in Figures 3-14 and 3-15.

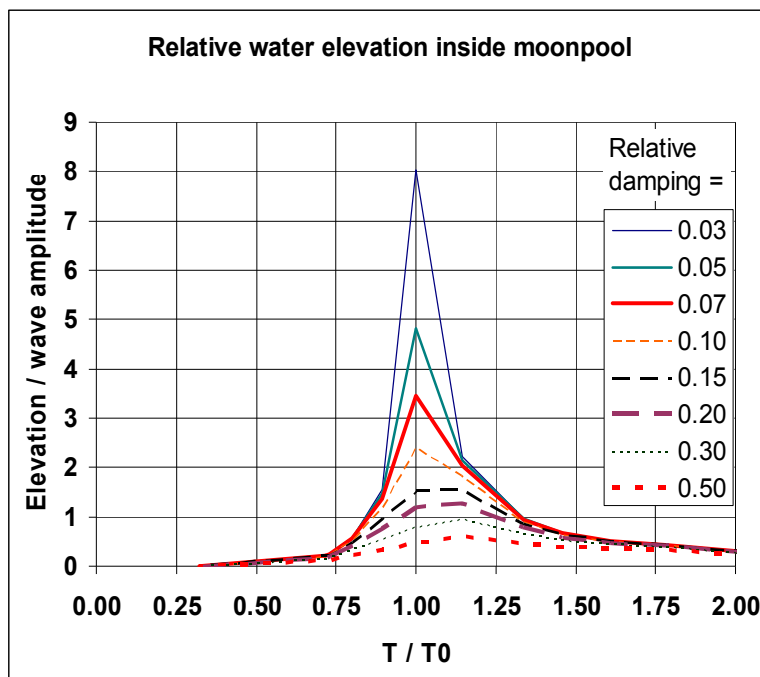


Figure 3-14
Calculated relative water elevation, no bottom plate ($\beta = 1$)

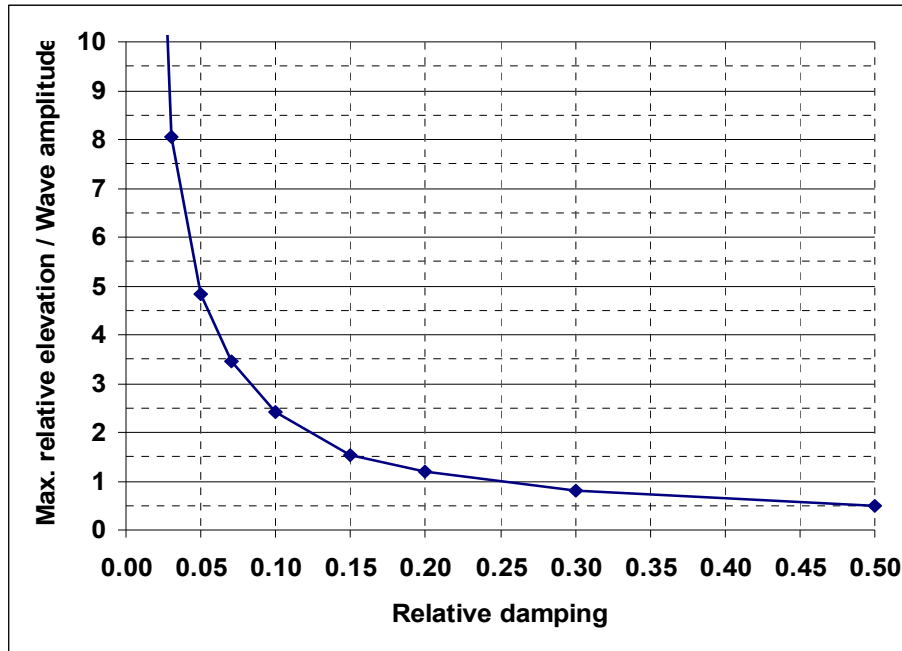


Figure 3-15
Calculated relative water elevation at resonance

3.5.5.11 Approximate relative damping values for the cases without bottom plate have been found by a comparison between Figure 3-13 and Figure 3-14. The following approximate relative damping values have been assessed,

Naked moonpool:	$\eta = 8 - 9\%$
Minor fittings:	$\eta = 13 - 14\%$
Guidance structure:	$\eta = 18 - 19\%$
Guidance structure + 50% bottom plate:	$\eta = 40 - 45\%$
Cofferdam:	$\eta \approx 45\%$

3.5.5.12 The quadratic damping coefficient C_s can be estimated from the relative damping and the motion. The following approximation may be used,

$$C_s = \frac{3\pi}{8} \cdot \omega \zeta_0 \cdot 2\eta \sqrt{KM} \quad [-]$$

where ζ_0 is the amplitude of relative motion.

3.5.6 Force coefficients in moonpool

3.5.6.1 Restricted flow around the object inside a moonpool leads to increased hydrodynamic forces. Increased drag coefficient C_D and added mass coefficient C_A to be used in the calculation can be taken as

$$\frac{C_D}{C_{D0}} = \frac{1 - 0.5A_b/A}{(1 - A_b/A)^2} \quad \text{for } A_b/A < 0.8$$

$$\frac{C_A}{C_{A0}} = 1 + 1.9 \left(\frac{A_b}{A} \right)^{\frac{9}{4}} \quad \text{for } A_b/A < 0.8$$

where

C_{D0} = drag coefficient for unrestricted flow [-]

C_{A0} = added mass coefficient for unrestricted flow [-]

A_b = solid projected area of the object [m²]

A = cross-sectional area of the moonpool (at the vertical level of the object) [m²]

For $A_b/A > 0.8$ a more comprehensive calculation method should be used.

3.5.6.2 The dynamic behaviour of the lifted object when leaving the lower moonpool end during lowering or

prior to entry at lifting, should be analysed by a time domain calculation method, in irregular waves.

3.5.6.3 For an object close to the lower end of the moonpool, a conservative approach is to analyse the dynamics, using hydrodynamic forces based on the wave kinematics of undisturbed waves and hydrodynamic coefficients for unrestricted flow condition.

3.5.6.4 Realistic impact forces between lifted body and moonpool walls require accurate stiffness data for the cursor system.

3.5.7 Comprehensive calculation method

A more comprehensive calculation method should be used, either if the solid projected area covers more than 80% of the moonpool section area, or if the vertical motion of the lifted object differs from the vertical motion of the vessel at moonpool, i.e.:

- if a motion control system is applied when the lifted object is inside the moonpool, or
- if the object is suspended in soft spring, such as a pneumatic cylinder.

3.5.7.1 The following calculation steps are defined,

- 1) Calculate the first order wave pressure transfer functions at the moonpool mouth, using a diffraction theory program with a panel model of the ship with moonpool. Emphasis should be put on obtaining numerical stability for the moonpool oscillation mode.
- 2) Carry out a non-linear time domain analysis of the system, with a model as described below. The analysis should be made for relevant irregular wave sea states. Calculate motion of the lifted object and forces in lifting gear.

3.5.7.2 The following analysis model is proposed,

- a) The lifted object is modelled, with mass and hydrodynamic mass and damping.
- b) The lifting system is modelled, with motion compensator or soft spring, if applicable.
- c) The water plug inside the moonpool is modelled as a fluid body moving only in vertical direction, with mass equal to the energy-equivalent mass given in 3.5.4.7.
- d) The water body should be excited by the water pressure multiplied by the section area of the moonpool opening.
- e) The interaction between the water plug and the moonpool walls should be modelled as a quadratic damping coupling in vertical direction.
- f) The interaction force between the water plug and the lifted object is found as:

$$F = \frac{1}{2} \rho C_D A_b v_r |v_r| + (\rho V + A_{33}) \ddot{\zeta}_w - A_{33} \ddot{\zeta}_b \quad [\text{N}]$$

where

- v_r = relative velocity between lifted object and water plug [m/s]
- A_b = solid projected area of the lifted object [m²]
- V = volume of lifted body [m³]
- A_{33} = added mass of lifted body [kg]
- $\ddot{\zeta}_w$ = vertical acceleration of the water plug [m/s²]
- $\ddot{\zeta}_b$ = vertical acceleration of lifted object [m/s²]

3.5.7.3 The use of Computational Fluid Dynamics (CFD) may not be recommended for moonpool dynamics. Even though CFD can analyse the fluid dynamic interaction between the lifted object and the water plug inside the moonpool, it is difficult to couple with the dynamic characteristics of ship in waves and the response of the lifting system. Force predictions may hence be uncertain.

3.6 Stability of lifting operations

3.6.1 Introduction

Situations where stability during lifting operations is particularly relevant include,

- tilting of partly air-filled objects during lowering
- effects of free water surface inside the object.

3.6.2 Partly air-filled objects

3.6.2.1 This case is also relevant for lifting of objects where the buoyancy is distributed differently from the mass. Figure 3-16 shows a submerged body where the centre of gravity C_G and the centre of buoyancy C_B do not coincide.

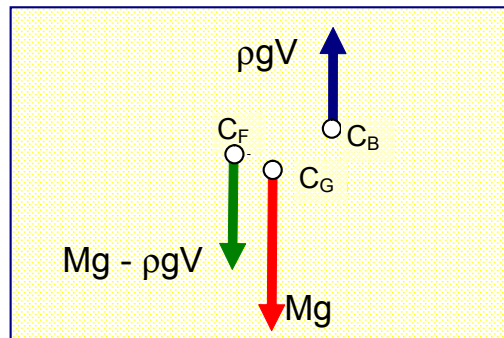


Figure 3-16
Definition of C_G , C_B and C_F

3.6.2.2 The force centre is found from moment equilibrium;

$$C_F = \frac{Mg \cdot C_G - \rho g V \cdot C_B}{Mg - \rho g V} = \frac{C_G - \alpha \cdot C_B}{1 - \alpha} \quad [\text{m}]$$

where

$$\alpha = \frac{\rho g V}{Mg} \quad [-]$$

3.6.2.3 If no other forces are acting on the object, it will rotate until C_B is vertically above C_G . If the object is suspended, the lift wire must be attached vertically above C_F in order to avoid tilting.

3.6.2.4 The adjustments of sling lengths required for a horizontal landing on seabed may thus give a tilt angle when the object is in air (due to the horizontal distance $C_F - C_G$).

3.6.3 Effects of free water surface inside the object

3.6.3.1 In case of a free water surface inside the body, the vertical distance GB between C_G and C_B must be large enough to give an up-righting moment larger than the overturning moment provided by the free water surface. Figure 3-17 illustrates this.

$$Mg \cdot GB > \rho g I \quad [\text{Nm}]$$

where

M = object mass [kg]

I = area moment of inertia of the free surface [m^4]

The area moment of inertia I varies with filling, geometry and tilt angle.

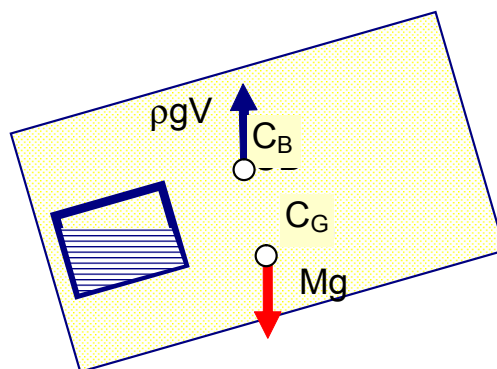


Figure 3-17
Lifting with free surface inside the object

3.7 References

- /1/ DNV Recommended Practice DNV-RP-C205 "Environmental Conditions and Environmental Loads", April 2007
- /2/ Molin B. (2001) "On the added mass and damping of periodic arrays of fully or partially porous disks". *J. Fluids & Structures*, 15, 275-290.

- /3/ Molin, B. and Nielsen, F.G. (2004) “Heave added mass and damping of a perforated disk below the free surface”, 19th Int. Workshop on Water Waves and Floating Bodies, Cortona, Italy, 28-31 March 2004.
- /4/ Faltinsen, O.M.; “Sea Loads on Ships and Offshore Structures”, Cambridge University Press, 1990.
- /5/ Greenhow, M. and Li, Y. (1987) “Added masses for circular cylinders near or penetrating fluid boundaries – Review, Extension and application to water entry, exit and slamming.”. *Ocean Engineering*. 14 (4) 325-348.
- /6/ Newman, J.N. (1977) “Marine Hydrodynamics”. MIT Press.
- /7/ Sandvik, P.C., Solaas, F. and Nielsen, F.G. (2006) “Hydrodynamic Forces on ventilated Structures” ISOPE Paper no. 2006-JSC-322, San Francisco, May 2006.
- /8/ Sumer, B.M. and Fredsøe, J. (1997) “Hydrodynamics around cylindrical structures”. World Scientific.
- /9/ Zhu, X.Y., Faltinsen, O.M. and Hu, C.H. (2005) “Water entry and exit of a circular cylinder”. Proc. 24th OMAE Conference, Halkidiki, Greece.
- /10/ Campbell, I.M.C. and Weynberg, P.A. (1980) “Measurement of parameters affecting slamming”. Final Report, Rep. No. 440, *Technology Reports Centre No. OT-R-8042*. Southampton University: Wolfson Unit for Marine Technology.
- /11/ ISO 19902 (2001), “Petroleum and Natural Gas Industries – Fixed Steel Offshore Structures”, Annex A9.6.2.3.

4 Lifting through Wave Zone – Simplified Method

4.1 Introduction

4.1.1 Objective

4.1.1.1 This section describes the Simplified Method for estimating characteristic hydrodynamic forces on objects lowered through the water surface and down to the sea bottom.

4.1.1.2 The intention of the Simplified Method is to give simple conservative estimates of the forces acting on the object.

4.1.2 Application

4.1.2.1 Calculation results based upon the Simplified Method may be used as input in *DNV-OS-H205, Lifting*, ref./3/.

4.1.2.2 The Simplified Method supersedes the recommendations for determination of environmental load effects given in *DNV Rules for Marine Operations, 1996, Pt.2 Ch.6, ref./5/*.

4.1.2.3 The sign of the motion, velocity, acceleration and force terms in the Simplified Method should always be applied as positive unless denoted otherwise.

4.1.2.4 In general, the Simplified Method describes forces acting during lowering from air down through the wave zone. The method is however also applicable for the retrieval case.

4.1.3 Main assumptions

4.1.3.1 The Simplified Method is based upon the following main assumptions;

- The horizontal extent of the lifted object (in the wave propagation direction) is relatively small compared to the wave length.
- The vertical motion of the object follows the crane tip motion.
- The load case is dominated by the vertical relative motion between object and water – other modes of motions can be disregarded.

4.1.3.2 More accurate estimations are recommended if the main assumptions are not fulfilled, see, *Section 3*.

4.1.3.3 Increased heave motion of the lifted object due to resonance effects is not covered by the Simplified Method, see 4.3.3.3.

4.2 Static weight

4.2.1 General

4.2.1.1 The static weight of the submerged object is given by:

$$F_{static} = Mg - \rho Vg \text{ [N]}$$

where

M = mass of object in air [kg]

g = acceleration due to gravity = 9.81 [m/s²]
 ρ = density of sea water, normally = 1025 [kg/m³]
 V = volume of displaced water during different stages when passing through the water surface [m³]

4.2.1.2 The static weight is to be calculated with respect to the still water surface.

4.2.1.3 A weight inaccuracy factor should be applied on the mass of the object in air according to *DNV-OS-H102 Section 3, C200*.

4.2.2 Minimum and Maximum Static weight

4.2.2.1 Flooding of subsea structures after submergence may take some time. In such cases, the static weight should be calculated applying both a minimum value and a maximum value.

4.2.2.2 The minimum and maximum static weight for objects being flooded after submergence should be taken as:

$$F_{static-min} = M_{min}g - \rho Vg \text{ [N]}$$

$$F_{static-max} = M_{max}g - \rho Vg \text{ [N]}$$

where

M_{min} = the minimum mass is equal the mass of object in air (i.e. the structure is submerged but the flooding has not yet started) [kg]

M_{max} = the maximum mass is equal the mass of object in air including the full weight of the water that floods the structure (i.e. the structure is fully flooded after submergence) [kg]

Guidance note:

The volume of displaced water, V , is the same for both cases.

---e-n-d---of---G-u-i-d-a-n-c-e---n-o-t-e---

4.2.2.3 The weight inaccuracy factor should be applied as a reduction of the minimum mass and as an increase in the maximum mass.

4.2.2.4 Water that is pre-filled before lifting should be taken as part of the mass of object in air.

4.2.2.5 Water that is retained within the lifted object during recovery should be taken as part of the mass of object in air.

4.2.2.6 The possibility of entrapped air should be evaluated and included in calculations when relevant. Both loss of stability, risk of implosion and risk of slack slings should be investigated.

4.3 Hydrodynamic forces

4.3.1 General

4.3.1.1 This section describes the Simplified Method for estimation of the environmental loads and load effects.

4.3.1.2 Only characteristic values are included. Implementation of safety factors in the capacity check of structure and lifting equipment should be performed as described in *DNV-OS-H102, ref./2/* and *DNV-OS-H205, ref./3/*.

4.3.1.3 For further explanation of the term “characteristic”, see *DNV-OS-H102 Section 1, C100*.

4.3.2 Wave periods

4.3.2.1 The influence of the wave period may be taken into account. The performed analyses should then cover the following zero-up-crossing wave period range for a given significant wave height H_s :

$$8.9 \cdot \sqrt{\frac{H_s}{g}} \leq T_z \leq 13 \quad [\text{s}]$$

where

g = acceleration of gravity = 9.81 [m/s²]
 H_s = significant wave height of design sea state [m]
 T_z = zero-up-crossing wave periods [s]

Guidance note:

T_z values with increments of 1.0 s are in most cases sufficient.

---e-n-d---of---G-u-i-d-a-n-c-e---n-o-t-e---

Guidance note:

A lower limit of $H_{max} = 1.8 \cdot H_s = \lambda/7$ with wavelength $\lambda = g \cdot T_z^2 / 2\pi$ is here used.

---e-n-d---of---G-u-i-d-a-n-c-e---n-o-t-e---

Guidance note:

The relation between the zero-up-crossing wave period, T_z , and the peak wave period, T_p , may be taken according to DNV-RP-C205, ref./6/, Section 3.5.5, applying a JONSWAP spectrum. For a PM spectrum the relation can be taken as $T_p = 1.4 \cdot T_z$.

---e-n-d---of---G-u-i-d-a-n-c-e---n-o-t-e---

4.3.2.2 Applied T_z -ranges or concluded allowable T_z -ranges deviating from 4.3.2.1 should be reflected in the weather criteria in the operation procedures.

4.3.2.3 Alternatively, one may apply the wave kinematic equations that are independent of the wave period. The operation procedures should then reflect that the calculations are only valid for waves longer than the following acceptance limit, i.e. :

$$T_z \geq 10.6 \cdot \sqrt{\frac{H_s}{g}} \quad [\text{s}]$$

Guidance note:

As zero-up-crossing wave periods less than the above acceptance limit very rarely occur, this operation restriction will for most cases not imply any practical reduction of the operability.

---e-n-d---of---G-u-i-d-a-n-c-e---n-o-t-e---

Guidance note:

A lower limit of $H_{max} = 1.8 \cdot H_s = \lambda/10$ with wavelength $\lambda = g \cdot T_z^2 / 2\pi$ is here used.

---e-n-d---of---G-u-i-d-a-n-c-e---n-o-t-e---

4.3.3 Crane tip motions

4.3.3.1 In order to establish the relative motion between the waves and the lifted structure, it is necessary to find the motions of the vessel's crane tip.

4.3.3.2 The Simplified Method assumes that the vertical motion of the structure is equal to the vertical motion of the crane tip. More accurate calculations should be made if amplification due to vertical resonance is present.

4.3.3.3 Resonance amplification may be present if the crane tip oscillation period or the wave period is close to the resonance period, T_0 , of the hoisting system:

$$T_0 = 2\pi \sqrt{\frac{M + A_{33} + \theta \cdot mL}{K}} \quad [\text{s}]$$

where

m = mass of hoisting line per unit length [kg/m]

L = length of hoisting line [m]

M = mass of object in air [kg]

A_{33} = heave added mass of object [kg]

K = stiffness of hoisting system, see 4.7.6.1 [N/m]

θ = adjustment factor taking into account the effect of mass of hoisting line and possible soft springs (e.g. crane master), see 5.3.5.2.

Guidance note:

In most cases, T_0 is less than the relevant wave periods. Wave induced resonance amplification of an object located in the wave zone may in such cases be disregarded if the peak wave period, T_p , is significantly larger than the resonance period of the hoisting system, typically:

$$T_p > 1.6 \cdot T_0$$

---e-n-d---of---G-u-i-d-a-n-c-e---n-o-t-e---

Guidance note:

Resonance amplification due to the crane tip motion may be disregarded if the peak period of the response spectrum for the vertical motion of the crane tip, T_{p-ct} , is larger than the resonance period of the hoisting system, typically:

$$T_{p-ct} > 1.3 \cdot T_0$$

where T_{p-ct} is calculated for a T_z range as described in 4.3.2.1.

---e-n-d---of---G-u-i-d-a-n-c-e---n-o-t-e---

Guidance note:

The resonance period of the hoisting system, T_0 , increases with the length of the hoist line. Resonance amplification due to crane tip motion may therefore occur during deployment of objects down to very deep water. This should be given special attention, see *Section 4.7.7* and *Section 5*.

---e-n-d---of---G-u-i-d-a-n-c-e---n-o-t-e---

4.3.3.4 Active or passive heave compensation systems should normally not be taken into account in the Simplified Method when calculating hydrodynamic loads, see, *Section 3* for more accurate time-domain simulations.

Guidance note:

The effect of passive heave compensation systems may be implemented as soft springs in the stiffness of the hoisting system when performing snap load calculations and when checking risk of resonance amplification.

---e-n-d---of---G-u-i-d-a-n-c-e---n-o-t-e---

4.3.3.5 The characteristic vertical crane tip motions on the installation vessel should be calculated for the environmental design conditions, either by a refined analysis, or by acceptable documented simplified calculations.

4.3.3.6 For subsea lift operations dependent on a fixed vessel heading, vessel responses for all wave directions should be analysed.

4.3.3.7 For subsea lift operations that may be performed independent of vessel headings, vessel response should be analysed for wave directions at least $\pm 15^\circ$ off the vessel heading stated in the procedure.

4.3.3.8 Long-crested sea may be applied in the analysis. See however the guidance note below.

Guidance note:

In some cases it may be appropriate to apply short crested sea in order to find the most critical condition. Vertical crane tip motion may e.g. be dominated by the roll motion in head sea $\pm 15^\circ$. Roll motion may then be larger for short crested sea than for long crested sea. It is hence recommended to investigate the effect of short crested sea in such cases, see also *DNV-OS-H101 Section 3, C800*.

---e-n-d---of---G-u-i-d-a-n-c-e---n-o-t-e---

Guidance note:

If long-crested sea is applied for simplicity, a heading angle of $\pm 20^\circ$ is recommended in order to account for the additional effect from short-crested sea. A heading angle of $\pm 15^\circ$ combined with long-crested sea should only be applied if the vertical crane tip motion is not dominated by the roll motion, or if the vessel can document that it is able to keep within $\pm 10^\circ$ in the design sea state.

---e-n-d---of---G-u-i-d-a-n-c-e---n-o-t-e---

4.3.3.9 The computed heave, pitch and roll RAOs for the vessel should be combined with crane tip position in the vessel's global coordinate system in order to find the vertical motion of the crane tip.

4.3.3.10 The applied values for the crane tip velocity and acceleration should represent the most probable largest characteristic single amplitude responses.

4.3.3.11 If the lowering through the wave zone (including contingency time) is expected to be performed within 30 minutes, the most probable largest characteristic responses may be taken as 1.80 times the significant responses.

4.3.3.12 The performed motion response analyses should cover a zero-up-crossing wave period range as described in *Section 4.3.2*.

4.3.4 Wave kinematics

4.3.4.1 The lowering through the wave zone (including contingency time) is in this subsection assumed to be performed within 30 minutes.

4.3.4.2 If the duration of the lifting operation is expected to exceed the 30 minutes limit, the significant wave height, H_s , in the below equations for wave amplitude, wave particle velocity and wave particle accelerations

should be multiplied with a factor of 1.10.

4.3.4.3 The characteristic wave amplitude can be taken as:

$$\zeta_a = 0.9 \cdot H_s \quad [\text{m}]$$

4.3.4.4 In this Simplified Method the following characteristic wave particle velocity and acceleration can be applied:

$$v_w = \zeta_a \cdot \left(\frac{2\pi}{T_z} \right) \cdot e^{-\frac{4\pi^2 d}{T_z^2 g}} \quad [\text{m/s}]$$

and

$$a_w = \zeta_a \cdot \left(\frac{2\pi}{T_z} \right)^2 \cdot e^{-\frac{4\pi^2 d}{T_z^2 g}} \quad [\text{m/s}^2]$$

where

- v_w = characteristic vertical water particle velocity [m/s]
- a_w = characteristic vertical water particle acceleration [m/s²]
- ζ_a = characteristic wave amplitude according to 4.3.4.3 [m]
- g = acceleration of gravity = 9.81 [m/s²]
- d = distance from water plane to centre of gravity of submerged part of object [m]
- H_s = Significant wave height of design sea state [m]
- T_z = Zero-up-crossing wave periods, see 4.3.2.1 [s]

4.3.4.5 Alternatively, one may apply the following wave kinematic equations that are independent of the wave period;

$$v_w = 0.30 \sqrt{\pi g H_s} \cdot e^{-\frac{0.35 d}{H_s}} \quad [\text{m/s}]$$

$$a_w = 0.10 \pi g \cdot e^{-\frac{0.35 d}{H_s}} \quad [\text{m/s}^2]$$

with definition of parameters as given in 4.3.4.4 and a T_z application limit as described in 4.3.2.3.

Guidance note:

A lower limit of $H_{max} = 1.8 \cdot H_s = \lambda/10$ with wavelength
 $\lambda = g \cdot T_z^2 / 2\pi$ is here used.

---e-n-d---of---G-u-i-d-a-n-c-e---n-o-t-e---

4.3.4.6 It should be clearly stated in the analyses documentation whether or not the influence of the wave period is included. The two alternatives for the Simplified Method should not be interchanged within the analyses.

4.3.5 Slamming impact force

4.3.5.1 The characteristic slamming impact force on the parts of the object that penetrate the water surface may be taken as:

$$F_{slam} = 0.5 \rho C_s A_s v_s^2 \quad [\text{N}]$$

where

- ρ = density of sea water [kg/m³]
- C_s = slamming coefficient which may be determined by theoretical and/or experimental methods. For smooth circular cylinders C_s should not be taken less than 3.0. Otherwise, C_s should not be taken less than 5.0. See also *DNV-RP-C205*.
- A_s = slamming area, i.e. part of structure projected on a horizontal plane that will be subject to slamming loads during crossing of water surface [m²]
- v_s = slamming impact velocity [m/s]

4.3.5.2 The slamming impact velocity may be calculated by:

$$v_s = v_c + \sqrt{v_{ct}^2 + v_w^2} \quad [\text{m/s}]$$

where

v_c = hook lowering velocity, typically 0.50 [m/s]

v_{ct} = characteristic single amplitude vertical velocity of the crane tip [m/s]

v_w = characteristic vertical water particle velocity as found in 4.3.4.4 or 4.3.4.5 applying a distance, d , equal zero [m/s]

4.3.5.3 Increased slamming impact velocity due to excitation of the water column inside suction anchors can be specially considered.

Guidance note:

A simplified estimation of the local slamming impact velocity inside a suction anchor may be to apply:

$$v_s = v_c + \sqrt{v_{ct}^2 + v_w^2 \cdot \kappa^2} \quad [\text{m/s}]$$

where

v_c = hook lowering velocity, typically 0.50 [m/s]

v_{ct} = characteristic single amplitude vertical velocity of the crane tip [m/s]

v_w = characteristic vertical water particle velocity [m/s]

κ = amplification factor, typically $1.0 \leq \kappa \leq 2.0$ [-]

---e-n-d---of---G-u-i-d-a-n-c-e---n-o-t-e---

Guidance note:

Compression and collapse of air cushions are disregarded in this simplified estimation. The air cushion effect due to limited evacuation of air through ventilation holes may contribute to reduced slamming force.

---e-n-d---of---G-u-i-d-a-n-c-e---n-o-t-e---



Figure 4-1
Top-plate of suction anchor crossing the water surface.
Water spray from ventilation hole.

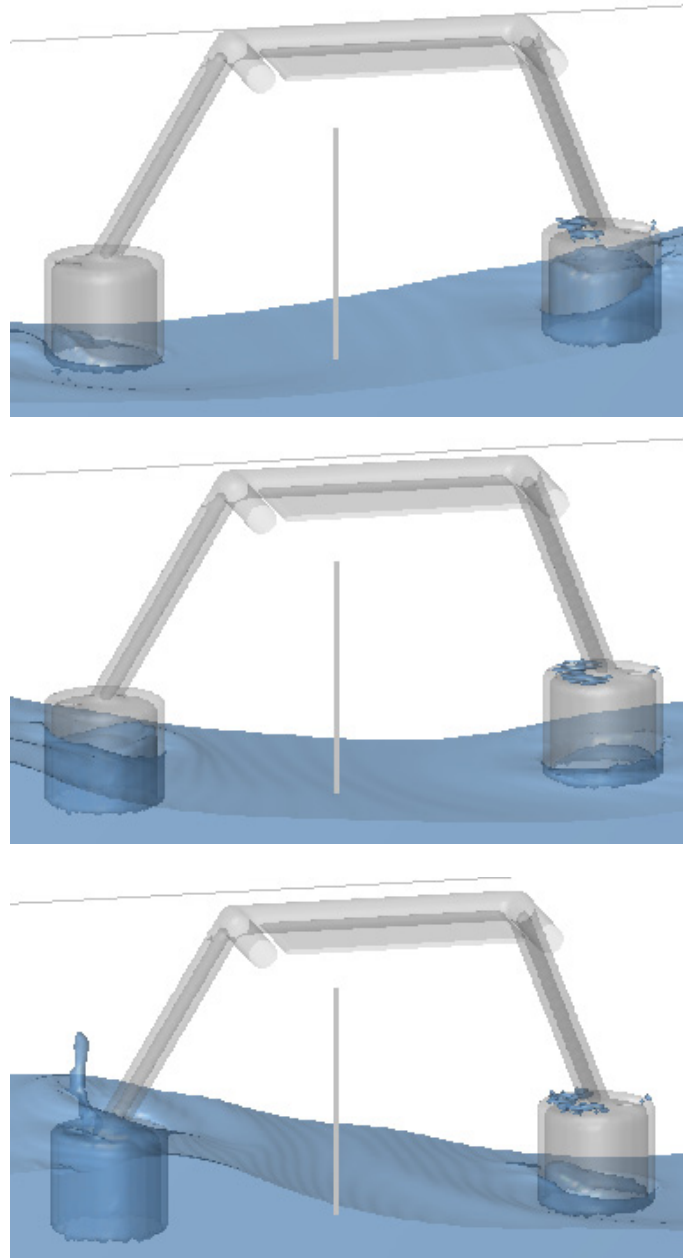


Figure 4-2
Internal slamming on top-plate of foundation bucket. From CFD analysis. Bucket dim. $3.5 \times \text{Ø}4.0$ m. Ventilation holes $\text{Ø}0.8$ m. Regular wave $H = 3.5$ m, $T = 5.5$ s. Lowering speed 0.25 m/s. One second between snapshots.

4.3.6 Varying buoyancy force

4.3.6.1 The static weight of the object is related to the still water surface. The change in buoyancy due to the wave surface elevation may be taken as:

$$F_p = \rho \cdot \delta V \cdot g \quad [\text{N}]$$

where

ρ = density of sea water, normally = 1025 $[\text{kg/m}^3]$

δV = change in volume of displaced water from still water surface to wave crest or wave trough $[\text{m}^3]$

g = acceleration of gravity $[\text{m/s}^2]$

4.3.6.2 The change in volume of displaced water may be estimated by:

$$\delta V = \tilde{A}_w \cdot \sqrt{\zeta_a^2 + \eta_{ct}^2} \quad [\text{m}^3]$$

where

\tilde{A}_w = mean water line area in the wave surface zone [m²]
 ζ_a = characteristic wave amplitude, see 4.3.4.3 [m]
 η_{ct} = characteristic single amplitude vertical motion of the crane tip [m]

4.3.6.3 The change in volume of displaced water may be asymmetric about the still water surface.

Guidance note:

If the change in displacement is highly nonlinear, a direct calculation of the volume from still water surface to wave crest or to wave trough may be performed applying a water surface range of:

$$\delta\zeta = \pm \sqrt{\zeta_a^2 + \eta_{ct}^2} \quad [\text{m}]$$

---e-n-d---of---G-u-i-d-a-n-c-e---n-o-t-e---

4.3.7 Mass force

4.3.7.1 The characteristic mass force on an object item due to combined acceleration of object and water particles may be taken as:

$$F_{Mi} = \sqrt{[(M_i + A_{33i}) \cdot a_{ct}]^2 + [\rho V_i + A_{33i}) \cdot a_w]^2} \quad [\text{N}]$$

where

M_i = mass of object item in air [kg]
 A_{33i} = heave added mass of object item [kg]
 a_{ct} = characteristic single amplitude vertical acceleration of crane tip [m/s²]
 ρ = density of sea water, normally = 1025 [kg/m³]
 V_i = volume of displaced water of object item relative to the still water level [m³]
 a_w = characteristic vertical water particle acceleration as found in 4.3.4.4 or 4.3.4.5 [m/s²]

Guidance note:

The structure may be divided into main items. The mass, added mass, displaced volume and projected area for each individual main item are then applied in 4.3.7.1 and 4.3.8.1. Mass forces and drag forces are thereafter summarized as described in 4.3.9.6.

---e-n-d---of---G-u-i-d-a-n-c-e---n-o-t-e---

Guidance note:

The term “mass force” is here to be understood as a combination of the inertia force and the hydrodynamic force contributions from Froude Kriloff forces and diffraction forces (related to relative acceleration). The crane tip acceleration and the water particle accelerations are assumed statistically independent.

---e-n-d---of---G-u-i-d-a-n-c-e---n-o-t-e---

4.3.7.2 Estimation of added mass may be performed according to 4.6.3 – 4.6.5.

4.3.8 Drag force

4.3.8.1 The characteristic drag force on an object item may be taken as:

$$F_{Di} = 0.5 \rho C_D A_{pi} v_r^2 \quad [\text{N}]$$

where

ρ = density of sea water, normally = 1025 [kg/m³]
 C_D = drag coefficient in oscillatory flow of submerged part of object [-]
 A_{pi} = area of submerged part of object item projected on a horizontal plane [m²]
 v_r = characteristic vertical relative velocity between object and water particles, see 4.3.8.3 [m/s]

4.3.8.2 Estimation of drag coefficients may be performed according to 4.6.2.

4.3.8.3 The characteristic vertical relative velocity between object and water particles may be taken as:

$$v_r = v_c + \sqrt{v_{ct}^2 + v_w^2} \quad [\text{m/s}]$$

where

v_c = hook hoisting/lowering velocity, typically 0.50 [m/s]
 v_{ct} = characteristic single amplitude vertical velocity of the crane tip [m/s]
 v_w = characteristic vertical water particle velocity as found in 4.3.4.4 or 4.3.4.5 [m/s]

4.3.9 Hydrodynamic force

4.3.9.1 The characteristic hydrodynamic force on an object when lowered through water surface is a time dependent function of slamming impact force, varying buoyancy, hydrodynamic mass forces and drag forces.

4.3.9.2 The following combination of the various load components is acceptable in this Simplified Method:

$$F_{hyd} = \sqrt{(F_D + F_{slam})^2 + (F_M - F_\rho)^2} \quad [\text{N}]$$

where

F_D = characteristic hydrodynamic drag force [N]
 F_{slam} = characteristic slamming impact force [N]
 F_M = characteristic hydrodynamic mass force [N]
 F_ρ = characteristic varying buoyancy force [N]

Guidance note:

During lowering through the water surface, the structure may have both fully submerged parts and items in the splash zone. The slamming force acting on the surface crossing item is then in phase with the drag force acting on the fully submerged part. Likewise, the mass and varying buoyancy forces are 180° out of phase.

---e-n-d---of---G-u-i-d-a-n-c-e---n-o-t-e---

4.3.9.3 The slamming impact force on a structure part that is hit by the wave surface may be taken as the only load component acting on that structure part, see 4.5.2.

4.3.9.4 This method assumes that the horizontal extent of the lifted object is small compared to the wave length. A more accurate estimation should be performed if the object extension is found to be important, see Section 3.

4.3.9.5 The structure may be divided into main items and surfaces contributing to the hydrodynamic force.

4.3.9.6 The water particle velocity and acceleration should be related to the vertical centre of gravity for each main item when calculating mass and drag forces. These force contributions should then be found by:

$$F_M = \sum_i F_{Mi} \quad \text{and} \quad F_D = \sum_i F_{Di} \quad [\text{N}]$$

where

F_{Mi} and F_{Di} are the individual force contributions from each main item, see 4.5.2.

4.4 Accept criteria

4.4.1 General

4.4.1.1 This section describes the accept criteria for the calculated hydrodynamic forces.

4.4.2 Characteristic total force

4.4.2.1 The characteristic total force on an object lowered through water surface should be taken as:

$$F_{total} = F_{static} + F_{hyd} \quad [\text{N}]$$

where

F_{static} = static weight of object, ref. 4.2.2 [N]
 F_{hyd} = characteristic hydrodynamic force, ref. 4.3.9 [N]

4.4.2.2 In cases where snap loads occur the characteristic total force on object should be taken as:

$$F_{total} = F_{static} + F_{snap} \quad [\text{N}]$$

where

F_{static} = static weight of object, ref. 4.2.2 [N]
 F_{snap} = characteristic snap force, ref. 4.7.2 [N]

4.4.3 The slack sling criterion

4.4.3.1 Snap forces shall as far as possible be avoided. Weather criteria should be adjusted to ensure this.

4.4.3.2 Snap forces in slings or hoist line may occur if the hydrodynamic force exceeds the static weight of the object.

4.4.3.3 The following criterion should be fulfilled in order to ensure that snap loads are avoided in slings and

hoist line:

$$F_{hyd} \leq 0.9 \cdot F_{static-min} \quad [N]$$

Guidance note:

A 10% margin to the start of slack slings is here assumed to be an adequate safety level with respect to the load factors and load combinations stated in the ULS criteria.

---e-n-d---of---G-u-i-d-a-n-c-e---n-o-t-e---

Guidance note:

Hydrodynamic forces acting upwards are to be applied in 4.4.3.3.

---e-n-d---of---G-u-i-d-a-n-c-e---n-o-t-e---

Guidance note:

In cases involving objects with large horizontal extent, e.g. long slender structures like spool pieces, more refined analyses are needed in order to establish loads in individual slings. In general, time domain analyses are recommended for this purpose. A simpler and more conservative approach may be to apply the Regular Design Wave Approach as described in Section 3.4.2. In this method the wave induced motion response of the lifted object is assumed negligible.

---e-n-d---of---G-u-i-d-a-n-c-e---n-o-t-e---

4.4.3.4 The minimum static weight of the object should be applied as described in 4.2.2.

4.4.4 Capacity checks

4.4.4.1 In addition to the slack sling criterion, the capacity of lifted structure and lifting equipment should be checked according to *DNV-OS-H205, Lifting, ref./3/*.

4.4.4.2 The characteristic total force on the object should be calculated applying the maximum static weight.

4.4.4.3 The capacity checks described in *DNV-OS-H205, Lifting* relates to the weight of the object in air. Hence, a converted dynamic amplification factor (*DAF*) should be applied equivalent to a factor valid in air. The following relation should be applied in the equations given in *DNV-OS-H205*:

$$DAF_{conv} = \frac{F_{total}}{Mg} \quad [-]$$

where

DAF_{conv} = is the converted dynamic amplification factor

M = mass of object in air [kg]

g = acceleration of gravity = 9.81 [m/s²]

F_{total} = is the largest of: $F_{total} = F_{static-max} + F_{hyd}$ or $F_{total} = F_{static-max} + F_{snap}$ [N]

4.4.4.4 The maximum static weight of the object should be applied as described in 4.2.2.

4.5 Typical load cases during lowering through water surface

4.5.1 General

4.5.1.1 There will be different hydrodynamic loads acting on different parts of the structure during lowering through water surface. The operation should therefore be analysed covering a number of different load cases.

4.5.1.2 When establishing load cases one should identify main items on the object contributing to hydrodynamic forces. The still water levels may be positioned according to the following general guidance:

- the still water level is located just beneath the slamming area of the main item
- the still water level is located just above the top of the submerged main item.

4.5.1.3 Examples of typical load cases are given in 4.5.2. These are merely given as general guidance. Typical load cases and load combinations should be established for all structures individually.

4.5.1.4 The total hydrodynamic force on the structure should be calculated as specified in 4.3.9.2.

4.5.2 Load cases for a protection structure

4.5.2.1 The lowering through water surface of a typical protection structure with roof, legs and ventilated buckets may be divided into four load cases as shown in figures 4-3 to 4-6.

4.5.2.2 The first load case is slamming on the mud mats, figure 4-3:

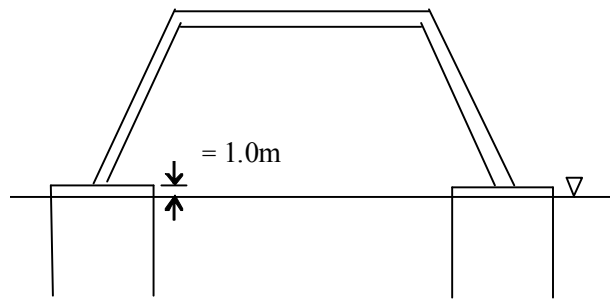


Figure 4-3
Load Case 1 – Still water level beneath top of ventilated bucket

where

- Slamming impact force, F_{slam} , acts upwards on top-plate inside the buckets. Only the mud mat area of buckets simultaneously affected need to be applied. Typically, if the object has four buckets, it may be sufficient to apply two.
- Varying buoyancy force F_{ρ} , mass force F_M and drag force F_D are negligible assuming the horizontal projected area of the skirt walls is small.

4.5.2.3 The second load case is when buckets are fully submerged, figure 4-4:

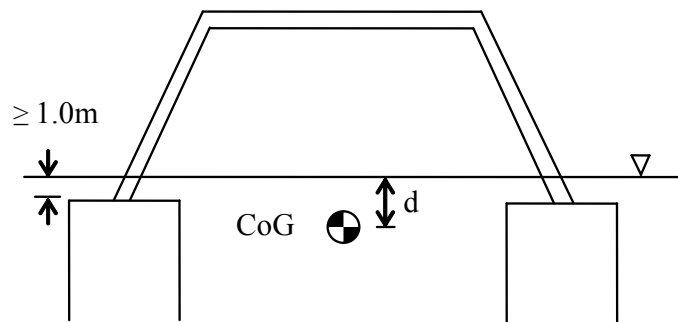


Figure 4-4
Load Case 2 – Still water level above top of buckets

where

- Slamming impact force, F_{slam} , is zero.
- Varying buoyancy force F_{ρ} , mass force F_M and drag force F_D are calculated. The characteristic vertical relative velocity and acceleration are related to CoG of submerged part of structure.

4.5.2.4 The third load case is when the roof cover is just above the still water level, figure 4-5:

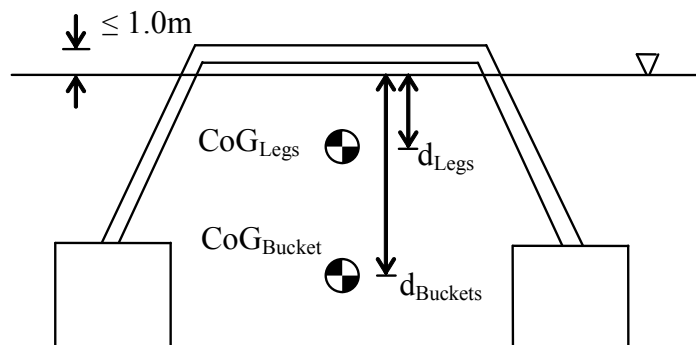


Figure 4-5
Load Case 3 – Still water level beneath roof cover

where

- Slamming impact force, F_{slam} , is calculated on the roof cover.
- Varying buoyancy force, F_{ρ} , in the wave surface zone is calculated.
- Mass forces, F_{Mi} , are calculated separately for buckets and legs, applying the characteristic vertical water particle acceleration for CoG of buckets and legs individually. The total mass force is the sum of the two load components, see 4.3.9.6.
- Drag forces, F_{Di} , are also calculated separately for buckets and legs applying correct CoGs. The total drag force is the sum of the two load components.

4.5.2.5 The fourth load case is when the whole structure is fully submerged, figure 4-6:

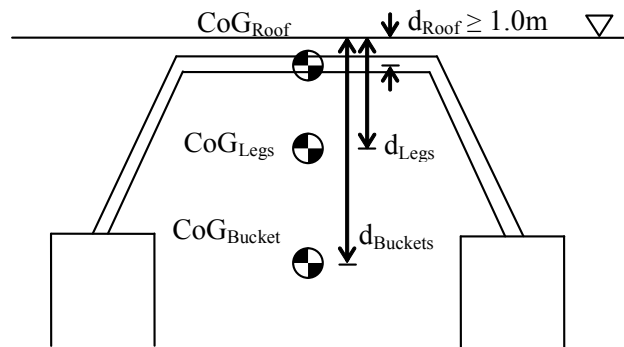


Figure 4-6
Load Case 4 – Still water level above roof cover

where

- Slamming impact force, F_{slam} , is zero.
- Varying buoyancy force F_{ρ} is zero.
- Mass forces, F_{Mi} , are calculated separately for buckets, legs and roof, applying the characteristic vertical water particle acceleration for CoG of buckets, legs and roof individually. The total mass force is the sum of the three load components.
- Drag forces, F_{Di} , are also calculated separately for buckets, legs and roof, applying correct CoGs. The total drag force is the sum of the three load components, see 4.3.9.6.

4.6 Estimation of hydrodynamic parameters

4.6.1 General

4.6.1.1 The hydrodynamic parameters may be determined by theoretical and/or experimental methods.

4.6.1.2 The hydrodynamic parameters may be dependent on a number of factors, as e.g.:

- structure geometry
- perforation
- sharp edges
- proximity to water surface or sea bottom
- wave height and wave period
- oscillation frequency
- oscillation amplitude

4.6.1.3 The drag coefficients and added mass values given in this simplified method do not fully take into account all the above listed parameters.

4.6.1.4 Model tests have shown that the added mass may be highly dependent on the oscillation amplitude of typical subsea structures, see e.g. *Ref./11/*.

4.6.2 Drag coefficients

4.6.2.1 Hydrodynamic drag coefficients in oscillatory flow should be used.

4.6.2.2 The drag coefficient in oscillatory flow, C_D , vary with the KC-number and can be typically two to three times larger than the steady flow drag coefficient, C_{DS} , see e.g. *Ref./6/* and */7/*.

4.6.2.3 Waves, current or vertical fluid flow due to lowering speed may partly wash away some of the wake. This may reduce the oscillatory drag coefficient compared to model test data obtained without this influence.

Guidance note:

Beneath the wave zone, the drag coefficient decreases with increasing lowering speed. The reason for this is that the lowered structure will tend to enter more undisturbed fluid. If the lowering speed exceeds the maximum oscillation velocity, the drag coefficient will tend to approach the value of the steady flow drag coefficient.

---e-n-d---of---G-u-i-d-a-n-c-e---n-o-t-e---

4.6.2.4 Unless specific CFD studies or model tests have been performed, the following guideline for drag coefficients on typical subsea structures in oscillatory flow is given:

$$C_D \geq 2.5 \quad [-]$$

4.6.2.5 For long slender elements a drag coefficient equal to twice the steady state C_{DS} may be applied provided that hydrodynamic interaction effects are not present, see App.B.

4.6.2.6 Sensitivity studies of added mass and damping are in general recommended in order to assess whether or not more accurate methods as CFD studies or model tests should be performed.

Guidance note:

The drag coefficient may be considerable higher than the recommended value given in 4.6.2.4. In model tests and CFD analyses of complex subsea structures at relevant KC numbers, oscillatory flow drag coefficients in the range $C_D \approx 4$ to 8 may be obtained when wake wash-out due to waves, current or lowering speed is disregarded.

---e-n-d---of---G-u-i-d-a-n-c-e---n-o-t-e---

Guidance note:

It should be noted that for extremely low KC numbers the drag coefficient as applied in 4.3.8.1 goes to infinity as the fluid velocity goes to zero.

---e-n-d---of---G-u-i-d-a-n-c-e---n-o-t-e---

4.6.3 Added mass for non-perforated structures

4.6.3.1 Hydrodynamic added mass values for different bodies and cross-sectional shapes may be found in Appendix A-1 and A-2.

4.6.3.2 The heave added mass of a surface piercing structure may be taken as half the heave added mass (in an infinite fluid domain) of an object formed by the submerged part of the structure plus its mirror about the free surface.

Guidance note:

This approximation is based upon the high frequency limit and is hence only applicable in cases where the radiated surface waves are negligible.

---e-n-d---of---G-u-i-d-a-n-c-e---n-o-t-e---

4.6.3.3 The following simplified approximation of the added mass in heave for a three-dimensional body with vertical sides may be applied:

$$A_{33} \approx \left[1 + \sqrt{\frac{1 - \lambda^2}{2(1 + \lambda^2)}} \right] \cdot A_{33o} \quad [\text{kg}]$$

and

$$\lambda = \frac{\sqrt{A_p}}{h + \sqrt{A_p}} \quad [-]$$

where

A_{33o} = added mass for a flat plate with a shape equal to the horizontal projected area of the object [kg]

h = height of the object [m]

A_p = area of submerged part of object projected on a horizontal plane [m²]

4.6.3.4 A structure that contains a partly enclosed volume of water moving together with the structure may be taken as a three-dimensional body where the mass of the partly enclosed water volume is included in the added mass.

Guidance note:

For example, a bucket shaped suction anchor with a diameter equal the height will according to 4.6.3.3 have an added mass equal 1.57 times the added mass of a circular disc plus the mass of the water volume inside the bucket.

---e-n-d---of---G-u-i-d-a-n-c-e---n-o-t-e---

Guidance note:

In this Simplified Method flooded items as e.g. tubular frames or spool pieces should be applied in the static weight calculations according to 4.2.2. The mass of this water volume should not be included in the added mass as it is already included in the body mass.

---e-n-d---of---G-u-i-d-a-n-c-e---n-o-t-e---

4.6.3.5 Added mass calculations based upon panel methods like the sink-source technique should be used with care (when subject to viscous fluid flow). It may give underestimated values due to oscillation amplitude dependency.

4.6.3.6 Added mass calculations based upon summation of contributions from each element is not recommended if the structure is densely compounded. The calculated values may be underestimated due to interaction effects and the oscillation amplitude dependency.

Guidance note:

Interaction effects can be neglected if the solid projected area normal to the direction of motion (within a typical amplitude of either body motion or wave particle motion) is less than 50%.

---e-n-d---of---G-u-i-d-a-n-c-e---n-o-t-e---

4.6.4 Effect of perforation

4.6.4.1 The effect of perforation on the added mass may roughly be estimated by the following guidance:

$$A_{33} = A_{33s} \quad \text{if } p \leq 5$$

$$A_{33} = A_{33s} \cdot \left(0.7 + 0.3 \cdot \cos \left[\frac{\pi \cdot (p - 5)}{34} \right] \right) \quad \text{if } 5 < p < 34$$

and

$$A_{33} = A_{33s} \cdot e^{\frac{10-p}{28}} \quad \text{if } 34 \leq p \leq 50$$

where

A_{33s} = solid added mass (added mass in heave for a non-perforated structure) [kg]

p = perforation rate (percentage) [-]

Guidance note:

For example, a bucket shaped suction anchor with a ventilation hole corresponding to 5% perforation will have an added mass equal the solid added mass, i.e. the added mass is in this case unaffected by the ventilation hole.

---e-n-d---of---G-u-i-d-a-n-c-e---n-o-t-e---

Guidance note:

This guidance is based upon a limited number of model test data and includes hence a safety margin. It is not considered applicable for perforation rates above 50%.

---e-n-d---of---G-u-i-d-a-n-c-e---n-o-t-e---

Guidance note:

The recommended DNV-curve is shown as the upper curve in figure 4-7. The shadowed area represents model test data for different subsea structures at varying KC-numbers. The $\exp(-P/28)$ curve is derived from numerical simulations (based on potential flow theory) of perforated plates and included in the figure for reference. As shown, the $\exp(-P/28)$ curve may give non-conservative values.

---e-n-d---of---G-u-i-d-a-n-c-e---n-o-t-e---

4.6.4.2 The intention of this guidance is to ensure a conservative estimate of the perforation rate influence on the added mass. As seen in figure 4-7 (shaded area) the actual reduction factor may vary a lot depending on geometry and oscillation amplitude. The recommended guidance in 4.6.4.1 will in most cases significantly overestimate the added mass. CFD studies or model tests are recommended if more accurate estimations are needed.

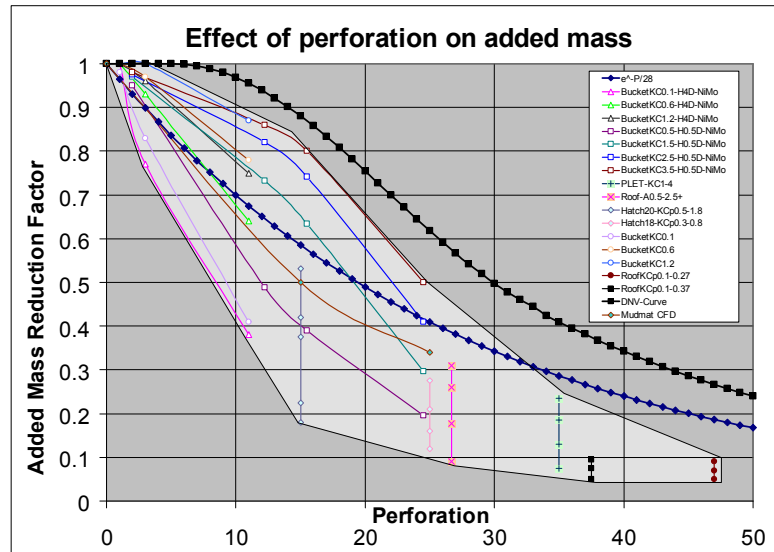


Figure 4-7
Added mass reduction factor A_{33}/A_{33S} as function of the perforation rate (percentage)

4.7 Snap forces in slings or hoisting line

4.7.1 General

4.7.1.1 Snap forces shall as far as possible be avoided. Weather criteria should be adjusted to ensure this.

4.7.1.2 Snap forces may occur if the slack sling criterion is not fulfilled, see 4.4.3.3.

4.7.2 Snap force

4.7.2.1 Characteristic snap load may be taken as:

$$F_{snap} = v_{snap} \sqrt{K \cdot (M + A_{33})} \quad [\text{N}]$$

where

v_{snap} = characteristic snap velocity [m/s]

K = stiffness of hoisting system, see 4.7.6 [N/m]

M = mass of object in air [kg]

A_{33} = heave added mass of object [kg]

4.7.2.2 The characteristic snap load should be applied as described in 4.4.2.2 and 4.4.4.3.

4.7.3 Snap velocity

4.7.3.1 The snap velocity may be taken as:

$$v_{snap} = v_{ff} + C \cdot v_r \quad [\text{m/s}]$$

where

v_{ff} = free fall velocity, see 4.7.3.5 [m/s]

v_r = characteristic vertical relative velocity between object and water particles, see 4.7.3.2, [m/s]

C = Correction factor, see 4.7.3.4 [-]

4.7.3.2 The vertical relative velocity between object and water particles may be taken as:

$$v_r = v_c + \sqrt{v_{ct}^2 + v_w^2} \quad [\text{m/s}]$$

where

v_c = hook hoisting/lowering velocity, see 4.7.3.3 [m/s]

v_{ct} = characteristic single amplitude vertical velocity of the crane tip [m/s]

v_w = characteristic vertical water particle velocity as found in 4.3.4.4 or 4.3.4.5 [m/s]

4.7.3.3 Two values for hook lowering velocity should be applied; $v_c = 0$ m/s and $v_c =$ typical lowering velocity. In addition, a retrieval case should be covered applying a v_c equal to a typical hoisting velocity. The highest snap velocity for the three options should be applied in the snap force calculation.

Guidance note:

If the typical hoisting/lowering velocity is unknown, a value of $v_c = \pm 0.50$ m/s may be applied.

---e-n-d---of---G-u-i-d-a-n-c-e---n-o-t-e---

4.7.3.4 The correction factor should be taken as:

$$C = 1 \quad \text{for} \quad v_{ff} < 0.2v_r$$

$$C = \cos \left[\pi \left(\frac{v_{ff}}{v_r} - 0.2 \right) \right] \quad \text{for} \quad 0.2v_r < v_{ff} < 0.7v_r$$

and

$$C = 0 \quad \text{for} \quad v_{ff} > 0.7v_r$$

4.7.3.5 The free fall velocity of the object may be taken as:

$$v_{ff} = \sqrt{\frac{2F_{static}}{\rho A_p C_D}} \quad [\text{m/s}]$$

where

F_{static} = the minimum and maximum static weight as defined in 4.2.2.2 [N]
 ρ = density of sea water, normally = 1025 [kg/m³]
 A_p = area of submerged part of object projected on a horizontal plane [m²]
 C_D = drag coefficient of submerged part of object

4.7.3.6 If the snap load is caused by a slamming impact force while the object is still in air, the snap velocity may be assumed equal the slamming impact velocity given in 4.3.5.2.

Guidance note:

It is here assumed that the maximum free fall velocity after impact will not exceed the maximum relative velocity between object and water surface.

---e-n-d---of---G-u-i-d-a-n-c-e---n-o-t-e---

4.7.4 Snap force due to start or stop

4.7.4.1 Snap force due to start or stop may be calculated according to 4.7.2.1, applying a characteristic snap velocity equal to:

v_{snap} : maximum lowering velocity, typically $v_{snap} = 1.0$ [m/s]

4.7.5 Snap force due to lift-off

4.7.5.1 Snap forces due to lift off from e.g. a barge should be taken into due considerations. The calculated DAF_{conv} as specified in 4.4.4.3 should be applied in the equations given in DNV-OS-H205, ref./3/, Section 2, D200.

4.7.5.2 Snap loads during lift off may be calculated according to 4.7.2.1, applying a characteristic snap velocity equal to:

$$v_{snap} = v_c + v_{ret} \quad [\text{m/s}]$$

where

v_c = hook hoisting velocity, typically 0.50 [m/s]
 v_{ret} = characteristic vertical relative velocity between object and crane tip [m/s]

4.7.5.3 The characteristic vertical relative velocity between object and crane tip should be calculated applying design sea states according to 4.3.2.1 and using the same guidelines as given in 4.3.3.

4.7.6 Stiffness of hoisting system

4.7.6.1 The stiffness of the hoisting system may be calculated by:

$$\frac{1}{K} = \frac{1}{k_{rigging}} + \frac{1}{k_{line}} + \frac{1}{k_{soft}} + \frac{1}{k_{block}} + \frac{1}{k_{boom}} + \frac{1}{k_{other}}$$

where

K = total stiffness of hoisting system [N/m]

$k_{rigging}$ = stiffness of rigging, spreader bar, etc.

k_{line} = stiffness of hoist line(s)

k_{soft} = stiffness of soft stop or passive heave compensation system if used, see 4.7.7

k_{block} = stiffness of multiple lines in a block if used

k_{boom} = stiffness of crane boom

k_{other} = other stiffness contributions, if any

4.7.6.2 The line stiffness may be calculated by:

$$k_{line} = \frac{EA}{L} \quad [\text{N/m}]$$

where

E = modulus of rope elasticity [N/m²]

A = effective cross section area of line(s), see 4.7.6.3. The areas are summarized if there are multiple parallel lines. [m²]

L = length of line(s). If multiple lines the distance from block to crane tip is normally applied [m]

4.7.6.3 The effective cross section area of one wire line is found by:

$$A_{wire} = \frac{\pi \cdot D^2}{4} \cdot c_F \quad [\text{m}^2]$$

where

c_F = fill-factor of wire rope [-]

D = the rope diameter [m]

Guidance note:

The value of the fill factor c_F needs to be defined in consistence with A_{wire} , D , and E . Typical values for e.g. a 6 × 37 IWRC steel core wire rope could be $c_F = 0.58$ and $E = 85 \cdot 10^9 \text{ N/m}^2$.

---e-n-d---of---G-u-i-d-a-n-c-e---n-o-t-e---

4.7.7 Application of passive heave compensation systems with limited stroke length

4.7.7.1 Passive heave compensation systems may have a certain available stroke length. This stroke length must not be exceeded during the lift.

4.7.7.2 Dynamic motions of lifted object exceeding available stroke length may cause huge peak loads and failure of the hoisting system.

Guidance note:

A more accurate calculation of the lifting operation is recommended if the Simplified Method indicates risk for snap loads.

---e-n-d---of---G-u-i-d-a-n-c-e---n-o-t-e---

4.7.7.3 Estimation of available stroke length should take into account the change in static weight as lifted object is transferred from air to submerged. The smallest available single amplitude stroke length at each load case should be applied.

Guidance note:

The equilibrium position (and thereby the available stroke length) will change during the lifting operation as the static weight of the object change when lowered through the water surface.

---e-n-d---of---G-u-i-d-a-n-c-e---n-o-t-e---

Guidance note:

Also the recovery load cases should be verified.

---e-n-d---of---G-u-i-d-a-n-c-e---n-o-t-e---

4.7.7.4 Entrapped water causing increased weight in air during recovery should be taken into account when checking available stroke length.

4.7.7.5 Changes in equilibrium position of pressurized pistons due to increased water pressure may be taken into account if relevant.

4.7.7.6 A simplified check of the available single amplitude stroke length, δx , may be to apply the following criterion:

$$\delta x > \sqrt{\frac{(M + A_{33}) \cdot v_{stroke}^2}{k_{soft}}} \quad [\text{m}]$$

where

M = mass of object in air [kg]

A_{33} = heave added mass of object [kg]

v_{stroke} = stroke velocity, to be assumed equal the relative velocity, v_r (see 4.7.3.2) unless snap forces occur at which the snap velocity, v_{snap} , should be applied, see e.g. 4.7.3.1 or 4.7.5.2. [m/s]

k_{soft} = stiffness of the passive heave compensation system [N/m]

Guidance note:

A more accurate estimation of available stroke length is recommended if the system characteristics are known, e.g. in pressurized pistons the energy loss due to flow resistance is not included in 4.7.7.6.

---e-n-d---of---G-u-i-d-a-n-c-e---n-o-t-e---

4.8 References

- /1/ DNV Offshore Standard DNV-OS-H101, "Marine Operations, General" (planned issued 2010).
- /2/ DNV Offshore Standard DNV-OS-H102, "Marine Operations, Loads and Design" (planned issued 2010).
- /3/ DNV Offshore Standard DNV-OS-H205, "Marine Operations, Lifting Operations" (planned issued 2010, see ref./12/ until release).
- /4/ DNV Offshore Standard DNV-OS-H206, "Marine Operations, Subsea Operations" (planned issued 2010 see ref./13/ until release).
- /5/ "DNV Rules for Planning and Execution of Marine Operations", 1996.
- /6/ DNV Recommended Practice DNV-RP-C205 "Environmental Conditions and Environmental Loads", April 2007.
- /7/ Øritsland, O., "A Summary of Subsea Module Hydrodynamic Data", Marintek Report No.511110.05, 1989.
- /8/ Faltinsen, O.M.; "Sea Loads on Ships and Offshore Structures", Cambridge University Press, 1990.
- /9/ Molin B. (2001) "On the added mass and damping of periodic arrays of fully or partially porous disks". *J. Fluids & Structures*, 15, 275-290.
- /10/ Molin, B. and Nielsen, F.G. (2004) "Heave added mass and damping of a perforated disk below the free surface", 19th Int. Workshop on Water Waves and Floating Bodies, Cortona, Italy, 28-31 March 2004.
- /11/ Sandvik, P.C., Solaas, F. and Nielsen, F.G. (2006) "Hydrodynamic Forces on ventilated Structures" ISOPE Paper no. 2006-JSC-322, San Francisco, May 2006.
- /12/ DNV Rules for Planning and Execution of Marine Operations (1996). Pt.2 Ch.5 Lifting
- /13/ DNV Rules for Planning and Execution of Marine Operations (1996). Pt.2 Ch.6 Sub Sea Operations.

5 Deepwater Lowering Operations

5.1 Introduction

5.1.1 General

5.1.1.1 For lifting operations in deep water the following effects should be considered,

- stretched length of cable due to cable own weight and weight of lifted object
- horizontal offset due to current where the current velocity may be time-dependent and its magnitude and direction may vary with water depth
- dynamics of lifted object due to wave induced motion of crane tip on vessel
- methods for controlling vertical motion of lifted object.

5.1.1.2 The term “cable” is in the following used to denote the lifting line from crane to lifted object. Cable can consist of steel wire, fibre rope, chain, or a combination of these.

5.1.2 Application

5.1.2.1 Calculation results based upon the method and formulas given in this section may be used as input in *DNV-OS-H205, Lifting, ref./1/*.

5.1.2.2 The sign of the motion, velocity, acceleration and force terms in this section should always be applied as positive unless denoted otherwise.

5.1.2.3 In general, this section describes forces acting on the vertical cable and the lowered object from beneath the wave zone down to the sea bed. The method and formulas are also applicable for the retrieval case. Forces on lifted objects in the wave zone is covered in Sections 3 and 4.

5.1.2.4 Static and dynamic response of lowered or lifted objects in deep water can be predicted by established commercial computer programs. The analytic formulas presented in this section may be used to check or verify predictions from such numerical analyses.

5.2 Static forces on cable and lifted object

5.2.1 Stretched length of a cable

A vertical cable will stretch due to its own weight and the weight of the lifted object at the end of the cable. The stretched length L_s of a cable of length L is;

$$L_s = L \left[1 + \frac{W + \frac{1}{2} wL}{EA} \right] \quad [\text{m}]$$

where

L_s = stretched length of cable [m]

L = original length of cable [m]

$W = Mg - \rho gV$ = fully submerged weight of lifted object [N]

$w = mg - \rho gA$ = fully submerged weight per unit length of cable [N/m]

M = mass of lifted object [kg]

m = mass per unit length of cable [kg/m]

g = acceleration of gravity = 9.81 m/s²

ρ = density of water [kg/m³]

E = modulus of elasticity of cable [N/m²]

A = nominal cross sectional area of cable [m²].

See Guidance Note in 5.2.4

V = displaced volume of lifted object [m³]

5.2.2 Horizontal offset due to current

5.2.2.1 For an axially stiff cable with negligible bending stiffness the offset of a vertical cable with a heavy weight W_0 at the end of the cable in an arbitrary current with unidirectional (in x-direction) velocity profile $U_c(z)$ is given by;

$$\xi(z) = \int_z^0 \left[\frac{F_{D0} + (1/2)\rho \int_{-L}^{z_1} C_{Dn} D_c [U_c(z_2)]^2 dz_2}{W + w(z_1 + L)} \right] dz_1 \quad [\text{m}]$$

where

$$F_{D0} = \frac{1}{2} \rho C_{Dn} A_x [U_c(-L)]^2 \quad [\text{N}]$$

is the hydrodynamic drag force on the lifted object. The parameters are defined as;

$\xi(z)$ = horizontal offset at vertical position z [m]

ξ_L = horizontal offset at end of cable $z = -L$ [m]

L = un-stretched length of cable [m]

C_{Dn} = drag coefficient for normal flow past cable [-]

C_{Dx} = drag coefficient for horizontal flow past lifted object [-]
 D_c = cable diameter [m]
 A_x = x-projected area of lifted object [m²]
 $U_c(z)$ = current velocity at depth z [m/s]
 z_1, z_2 = integration variables [m]

Guidance note:

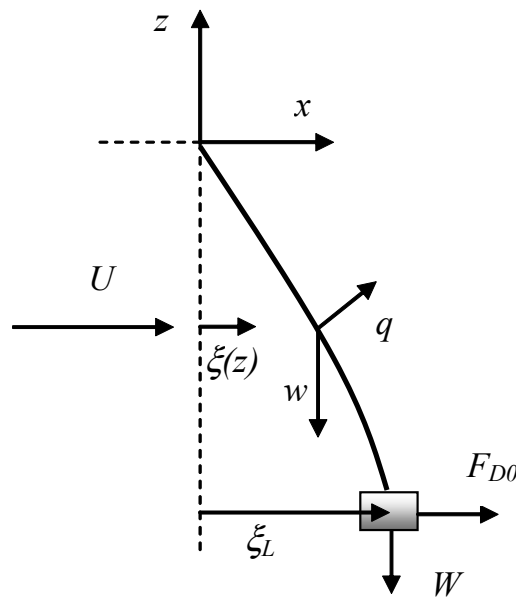
It is assumed that the sum of the weight wL of the cable and the submerged weight W of the lifted object are so large that the angle between cable and a vertical line is small. See Figure 5-1.

---e-n-d---of---G-u-i-d-a-n-c-e---n-o-t-e---

Guidance note:

The cable diameter $D_c(z)$ and drag coefficient for normal flow $C_{Dn}(z)$ may vary with depth. This variation must be taken into account when calculating the offset.

---e-n-d---of---G-u-i-d-a-n-c-e---n-o-t-e---

**Figure 5-1**

Horizontal offset $\xi(z)$ due to uniform current. Parameters are defined in 5.2.2. Curvature of cable determined by $F_{D0}/W < q/w$.

5.2.2.2 For a uniform current U_c and cable properties D_c, C_{Dn} the horizontal offset can be derived by;

$$\xi(z) = L \left(\frac{q}{w} \kappa - \lambda \right) \ln \left[\frac{\kappa + \frac{z}{L} + 1}{\kappa + 1} \right] - \frac{q}{w} z \quad [\text{m}] \quad (1)$$

where the top of the cable is at $z = 0$ and the lifted object is at the end of the cable at $z = -L$. See Figure 5-1. The horizontal offset of the lifted object is obtained by setting $z = -L$ in the expression for $\xi(z)$;

$$\xi_L = L \left(\frac{q}{w} \kappa - \lambda \right) \ln \left[\frac{\kappa}{\kappa + 1} \right] + \frac{qL}{w} \quad [\text{m}] \quad (2)$$

where κ is the ratio between the weight of the lifted object, W , and the weight of the cable;

$$\kappa = \frac{W}{wL} \quad [-] \quad (3)$$

and λ is the ratio between the drag on the lifted object, F_{D0} , and the weight of the cable;

$$\lambda = \frac{F_{D0}}{wL} \quad [-] \quad (4)$$

The hydrodynamic drag force per unit length of cable, q , is given by;

$$q = \frac{1}{2} \rho C_{Dn} D_c U_c^2 \quad [\text{N/m}] \quad (5)$$

Guidance note:

A correction to? account for the vertical component of drag is to replace w by $(w - q\xi_L/L)$ in formula (1) for the horizontal offset, where ξ_L is the uncorrected offset at the end of the cable as calculated by formula (2).

---e-n-d---of---G-u-i-d-a-n-c-e---n-o-t-e---

5.2.2.3 When the current velocity direction and cable properties vary with water depth a static analysis using a Finite Element methodology with full numerical integration is recommended to find the offset.

5.2.3 Vertical displacement

5.2.3.1 For installation of modules on seabed it is important to control the distance from the seabed to the lower part of the lifted object at the end of the cable. The difference Δz of vertical position of the lower end of the cable between the real condition and a vertical un-stretched condition has two contributions

$$\Delta z = \Delta z_G + \Delta z_E$$

where

Δz_G = vertical geometric displacement due to curvature of the cable

Δz_E = vertical elastic displacement due to stretching of cable

The geometric effect increase the clearance to seabed while the stretching decrease the clearance to seabed.

5.2.3.2 For constant unidirectional current and constant cable properties along the length of the cable, the vertical displacement due to curvature of the cable may be taken as;

$$\frac{\Delta z_G}{L} \approx \frac{q}{w} \left(\frac{q}{w} \kappa - \lambda \right) \left\{ \ln \left[\frac{\kappa}{\kappa + 1} \right] + \frac{1}{2} \left[\frac{1 - \frac{\lambda w}{\kappa q}}{1 + \kappa} \right] \right\} + \frac{1}{2} \left(\frac{q}{w} \right)^2 \quad [-]$$

where the parameters q , w , κ and λ are defined in 5.2.2.1 and 5.2.2.2.

5.2.3.3 The vertical displacement due to stretching of the cable may be taken as;

$$\frac{\Delta z_E}{L} \approx -\frac{1}{EA} \left[W + \frac{1}{2} (wL - q\xi_L) \right] \quad [-]$$

5.2.3.4 When the current velocity direction and cable properties varies with water depth a three-dimensional static analysis using a Finite Element methodology is recommended to find the offset.

5.2.4 Vertical cable stiffness

5.2.4.1 The vertical cable stiffness k_V is the vertical force that has to be applied to the lifted object at the lower end of the cable per unit vertical displacement;

$$k_V = \frac{dF_V}{dz} \quad [\text{N/m}]$$

5.2.4.2 The vertical stiffness is the sum of two contributions, the elastic stiffness k_E and the geometric stiffness k_G . The vertical stiffness k_V is given by;

$$\frac{1}{k_V} = \frac{1}{k_E} + \frac{1}{k_G} \quad [\text{m/N}]$$

5.2.4.3 The elastic stiffness k_E is given by;

$$k_E = \frac{EA}{L} \quad [\text{N/m}]$$

where

E = modulus of elasticity $[\text{N/m}^2]$
 A = cross-sectional area of cable $[\text{m}^2]$
 L = length of cable $[\text{m}]$

Guidance note:

A is the nominal cross-sectional area of the cable defined as $A = S \cdot c_F$ where S is the cross-sectional area (of circumscribed circle) and c_F is the fill factor. See also Sections 4 and 7.

---e-n-d---of---G-u-i-d-a-n-c-e---n-o-t-e---

5.2.4.4 The geometric stiffness k_G is given by

$$\frac{1}{k_G} = -\frac{d(\Delta z_G)}{dW_0} = -\frac{q^2}{w^3} \left[\ln \left(\frac{\kappa}{\kappa+1} \right) + \frac{1}{2} \frac{2\kappa+3}{(\kappa+1)^2} \right] \\ + \frac{q}{w^2} \frac{\lambda}{\kappa} \frac{1}{(\kappa+1)^2} + \frac{1}{w} \left(\frac{\lambda}{\kappa} \right)^2 \frac{2\kappa+1}{2(\kappa+1)^2} \quad [\text{m/N}]$$

Guidance note:

The vertical cable stiffness defined above is valid for static loads, and gives the change in position of the lower end of the cable for a unit force applied at the end.

---e-n-d---of---G-u-i-d-a-n-c-e---n-o-t-e---

Guidance note:

The geometric stiffness decreases with increasing current speed at a rate of U_c^{-4} . Hence, the geometric stiffness becomes rapidly more important at higher current speeds.

---e-n-d---of---G-u-i-d-a-n-c-e---n-o-t-e---

5.2.5 Horizontal stiffness

5.2.5.1 The horizontal stiffness k_H of lifted object is the horizontal force that has to be applied to the lower end of the cable per unit horizontal displacement.

$$k_H = \frac{dF_H}{dx} \quad [\text{N/m}]$$

5.2.5.2 The horizontal stiffness k_H is given by

$$\frac{1}{k_H} = \frac{\partial \xi_L}{\partial F_{DO}} = \frac{1}{w} \ln \left[\frac{\kappa+1}{\kappa} \right] \quad [\text{m/N}]$$

Note that the horizontal stiffness is not influenced by the current drag on the cable and the lifted object. It should also be noted that this expression for horizontal stiffness is valid for static loads only.

5.2.5.3 When the lifted object is much heavier than the weight of the cable the horizontal cable stiffness reduces to the stiffness of the mathematical pendulum,

$$\kappa = \frac{W}{wL} \gg 1 \quad \Rightarrow \quad k_H = w\kappa = \frac{W}{L} \quad [\text{N/m}]$$

5.2.6 Cable payout – quasi-static loads

The quasi-static tension $T(s)$ at the top end of the cable during payout for a deepwater lowering operation is given by

$$T(s) = W + ws + \frac{1}{2} \rho C_{Df} \pi D_c s v_c |v_c| + \frac{1}{2} \rho C_{Dz} A_p v_c |v_c| \quad [\text{N}]$$

where

- s = length of cable payout [m]
- ρ = water density [kg/m³]
- C_{Df} = cable longitudinal friction coefficient [-]
- C_{Dz} = drag coefficient for vertical flow past lifted object [-]
- D_c = cable diameter [m]
- A_p = horizontal projected area of lifted object [m²]
- v_c = constant cable payout velocity, hauling being positive and lowering negative [m/s]
- w = submerged weight per unit length of cable [N/m]
- W = submerged weight of lifted object [N]

For a cable payout length s , the necessary payout velocity to produce a slack condition is found by setting $T = 0$ in the equation above. Note that the formula above neglects the effect of current and water particle velocity due to waves and is therefore only valid for still water.

Guidance note:

Data describing friction coefficients for flow tangentially to a cable may be found in e.g. *DNV-RP-C205, ref./6/*.

---e-n-d---of---G-u-i-d-a-n-c-e---n-o-t-e---

5.3 Dynamic forces on cable and lifted object

5.3.1 General

5.3.1.1 For a typical lifting operation from a floating vessel it is normally acceptable to assume that the motion of the vessel is not affected by the motion of the object. This simplification is based on the following assumptions:

- mass and added mass of lifted object is much smaller than the displacement of the vessel
- the objects contribution to moment of inertia around CoG / centre plane of vessel is much smaller than the vessels moment of inertia
- the motion of the crane tip is vertical
- the effect of current can be neglected.

Guidance note:

Typically, applying uncoupled vessel RAOs will give conservative results as the object in most cases tend to reduce the vertical crane tip motion.

---e-n-d---of---G-u-i-d-a-n-c-e---n-o-t-e---

5.3.2 Dynamic drag forces

5.3.2.1 Due to the motion of crane tip and lifted object, dynamic drag forces will act on the cable. The drag forces restrict the change of shape of the cable. As the velocity/accelerations of the crane tip increases, the elastic stiffness becomes increasingly important.

5.3.3 Application

5.3.3.1 For lifting and lowering operations in deep water the dynamic response of the object depends on its vertical position (depth). In order to perform a controlled lowering of the object in a given sea state, an assessment of the dynamic response of the lifted object at all depths should be carried out in the planning of the operation.

5.3.4 Natural frequencies, straight vertical cable

5.3.4.1 The natural frequencies of a straight vertical cable (Figure 5-4) is given by

$$\omega_j = v_j \sqrt{\frac{EA}{m}} \quad [\text{rad/s}] ; j = 0, 1, 2, \dots$$

5.3.4.2 The exact solution for wave numbers v_j are given by the equation (assuming un-damped oscillations);

$$v_j L \tan(v_j L) = \varepsilon = \frac{mL}{M + A_{33}} \quad [-]$$

where

$$\omega_j = 2\pi/T_j = \text{angular natural frequencies} [\text{rad/s}]$$

- T_j = eigenperiods [s]
 ν_j = corresponding wave numbers [1/m]
 L = length of cable [m]
 E = modulus of elasticity [N/m²]
 A = nominal cross-sectional area of cable [m²]
 m = mass per unit length of cable [kg/m]
 M = mass of lifted object in air [kg]
 A_{33} = added mass for motion in vertical direction [kg]
 ε = $mL/(M+A_{33})$ = mass ratio [-]

Guidance note:

The vertical added mass for three-dimensional bodies in infinite fluid is defined as $A_{33} = \rho C_A V_R$ where C_A is the added mass coefficient and V_R is a reference volume, usually the displaced volume. The added mass of the lifted object is affected by proximity to free surface and proximity to sea floor. It should be noted that for complex subsea modules that are partly perforated, the added mass also depends on the oscillation amplitude, which again affects the eigenperiod of the lifted object. Reference is made to sections 3 and 4. Added mass coefficients for certain three-dimensional bodies are given in *Appendix A, Table A2*.

---e-n-d---of---G-u-i-d-a-n-c-e---n-o-t-e---

5.3.4.3 For small mass ratios, ε , the fundamental wave number is given by the approximation

$$\nu_0 L = \left(\frac{\varepsilon}{1 + \varepsilon/3} \right)^{1/2}$$

Guidance note:

The difference between the exact solution and the approximate solution is shown in Figure 5-2. The figure shows that the above approximation is close to the exact solution even for mass ratios, ε , up to 3. Hence, the eigenperiod stated in 5.3.5.1 (derived from 5.3.4.3) should be valid for most practical cases. For mass ratios above 3 it is recommended to use $2\varepsilon/5$ instead of $\varepsilon/3$ in the denominator of the approximate solution above.

---e-n-d---of---G-u-i-d-a-n-c-e---n-o-t-e---

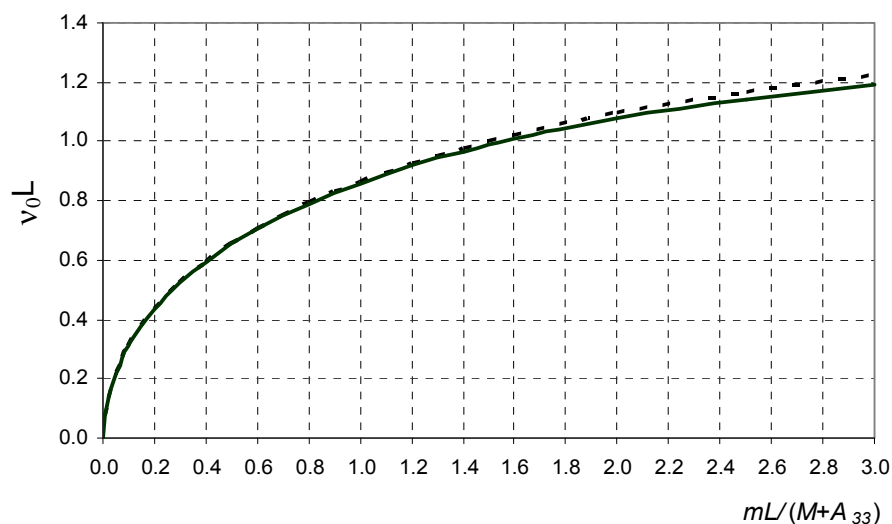


Figure 5-2

Exact solution and approximated solution of the fundamental wave number $\nu_0 L$ as function of mass ratio (corresponding to the first natural frequency of vertical oscillations). Solid line is exact solution while the dotted line is the approximation for small mass ratio ε

5.3.4.4 The higher natural frequencies can for small mass ratios, ε , be estimated by the corresponding wave

numbers, ν_j , given by;

$$\nu_j L \approx j\pi + \frac{mL}{j\pi(M + A_{33})} \quad [-] ; j = 1, 2, \dots$$

Guidance note:

The fundamental frequency is normally related to the oscillation of the lifted object (with modifications due to the mass of the cable), while the higher modes are related to longitudinal pressure waves in the cable (Ref. 5.3.6).

---e-n-d---of---G-u-i-d-a-n-c-e---n-o-t-e---

5.3.5 Eigenperiods

5.3.5.1 The first (fundamental) eigenperiod for un-damped oscillations of the lifted object in the presence of crane master and/or soft slings (Figure 5-3) may be taken as

$$T_0 = \frac{2\pi}{\omega_0} = 2\pi \sqrt{\frac{M + A_{33} + \theta \cdot mL}{K}} \quad [s]$$

where

$$\frac{1}{K} = \left(\frac{1}{k_c} + \frac{1}{k_s} + \frac{L}{EA} \right)$$

K = stiffness of total hoisting system [kg/s²]

k_c = stiffness of crane master at top of cable [kg/s²]

k_s = stiffness of soft sling or crane master at lifted object [kg/s²]

θ = adjustment factor to account for the cable mass

5.3.5.2 The adjustment factor to account for the cable mass is given by the general formula

$$\theta = \frac{1 + c + c^2 / 3}{(1 + c + c/s)^2}$$

where

$$c = \frac{k_c L}{EA} \quad \text{and} \quad s = \frac{k_s L}{EA}$$

5.3.5.3 The following limiting values for the adjustment factor may be applied:

- $\theta \sim 1/3$ if the line stiffness EA/L is the dominant soft stiffness (c and s are both large numbers)
- $\theta \sim 0$ if the dominant soft spring is located just above the lifted object ($s \ll 1$ and $c > 1$)
- $\theta \sim 1$ if the dominant soft spring is located at the crane tip ($c \ll 1$ and $s > 1$)

In the case of soft springs at both ends of the cable ($s \ll 1$ and $c \ll 1$), the adjustment factor can be approximated by

$$\theta = \left(\frac{s}{s + c} \right)^2$$

Guidance note:

For deep water operations where hoisting system consists mainly of one long cable (rope, wire), K may be assumed equal the elastic stiffness of the cable k_E (See 5.2.4). For a given lifted object and hoisting system, the eigenperiod increases then with the square root of the length of the cable.

---e-n-d---of---G-u-i-d-a-n-c-e---n-o-t-e---

Guidance note:

The effect of damping on the eigenperiod can normally be disregarded.

---e-n-d---of---G-u-i-d-a-n-c-e---n-o-t-e---

5.3.5.4 For straight vertical cables, the higher eigenperiods are given by

$$T_j = \frac{2\pi}{\omega_j} \quad [s] ; j = 1, 2, \dots$$

where ω_j is defined in 5.3.4.4.

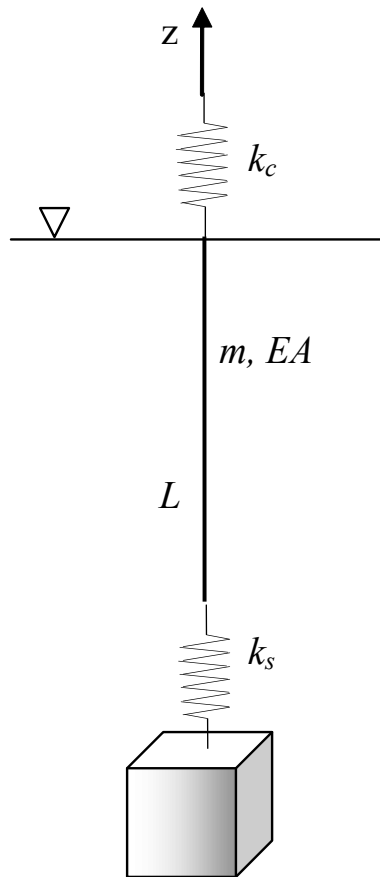


Figure 5-3
Forced oscillation of lifted object in cable with crane master at top of cable and soft sling at top of lifted object.

5.3.6 Longitudinal pressure waves

5.3.6.1 The speed of longitudinal pressure waves in the cable (or the speed of sound) is given by

$$c_L = \sqrt{\frac{EA}{m}} = \sqrt{\frac{E}{\rho_s}} \quad [\text{m/s}]$$

where

c_L = speed of sound [m/s]

$\rho_s = m/A$ = mass density of cable [kg/m³]

5.3.6.2 Dynamic effects due to longitudinal pressure waves must be accounted for when the cable is excited with a characteristic period T which is comparable to or less than;

$$T \leq \tau = \frac{2L}{c_L} \quad [\text{s}]$$

where τ is the time it takes for a pressure signal to travel from the top of the cable, down to the end and back.

Guidance note:

For a steel wire with modulus of elasticity $E = 0.85 \cdot 10^{11}$ N/m² and $\rho_s = 7800$ kg/m³, $c_L = 3300$ m/s. For a polyester rope c_L may be in the order of 1000 m/s which means that for a depth of 3000 m a pressure signal will take 6 sec. to travel from top of the cable, down to the lifted object and back.

---e-n-d---of---G-u-i-d-a-n-c-e---n-o-t-e---

5.3.7 Response of lifted object in a straight vertical cable exposed to forced vertical oscillations

5.3.7.1 When a deeply submerged object is lifted from a vessel in waves, the vertical motion of the object is governed by the motion of the top of the cable, fixed to the oscillating vessel.

Guidance note:

The motion of top of the cable, or motion of crane tip in a given sea state is derived from the motion characteristics of the crane vessel by linear combination of vessel RAOs determined by the location of the crane tip relative to centre of rotation of the vessel. The resulting motion RAOs in x-, y- and z-directions for crane tip may be combined with a wave spectrum to obtain time history of motion of crane tip. For deep water lowering operations only the vertical motion is of interest. See also 5.3.3.1.

---e-n-d---of---G-u-i-d-a-n-c-e---n-o-t-e---

5.3.7.2 The vertical motion of a straight vertical cable with the lifted object at vertical position $z = -L$ caused by a forced oscillation of top of the cable with frequency ω and amplitude η_a is given by;

$$\frac{|\eta(z)|}{\eta_a} = \left| \frac{kEA \cos[k(z+L)] + (-\omega^2 M' + i\omega\Sigma) \sin[k(z+L)]}{kEA \cos(kL) + (-\omega^2 M' + i\omega\Sigma) \sin(kL)} \right| \quad [\text{m/m}]$$

where $||$ means the absolute value (or modulus) of a complex number and the mass $M' = M + A_{33}$ (ref. 5.3.4.2).

5.3.7.3 The complex wave number k is given by

$$k = k_r + ik_i = \sqrt{\frac{m}{EA}} \sqrt{\omega^2 - i\omega \left(\frac{\sigma}{m} \right)} \quad [\text{m}^{-1}]$$

where the positive square root is understood. $i = \sqrt{-1}$ is the imaginary unit and m is the mass per unit length of cable. The functions $\cos(u)$ and $\sin(u)$ are the complex cosine and sine functions of complex numbers $u = u_r + iu_i$ as defined in Abramowitz and Stegun (1965).

σ and Σ are linear damping coefficients for cable motion and motion of lifted object respectively defined by equivalent linearization.

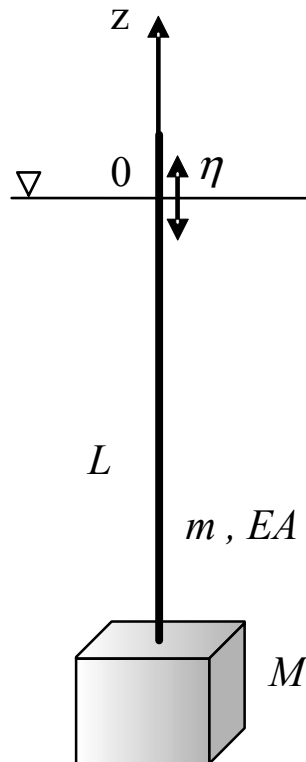


Figure 5-4
Forced oscillation of lifted object in cable

5.3.7.4 The linear damping coefficient for cable motion is defined by;

$$\sigma = \frac{4}{3} \rho C_{Df} D_c \omega \eta_a \quad [\text{kg/ms}]$$

and the longitudinal cable friction force per unit length is given by;

$$f_v = \frac{1}{2} \rho C_{Df} D_c |\dot{\eta}| \dot{\eta} \quad [\text{N/m}]$$

where the vertical motion along the cable is given by;

$$\dot{\eta} = \partial \eta / \partial t \quad [\text{m/s}]$$

Guidance note:

Using the motion amplitude at top of cable in the definition of the linear damping coefficient for cable motion is an approximation. The linearized damping actually varies along the cable.

---e-n-d---of---G-u-i-d-a-n-c-e---n-o-t-e---

5.3.7.5 The linear damping coefficient for motion of lifted object is defined by;

$$\Sigma = \frac{4}{3\pi} \rho C_{Dz} A_p \omega \eta_L \quad [\text{kg/s}]$$

and the vertical drag force for lifted object is given by

$$F_v = \frac{1}{2} \rho C_{Dz} A_p |\dot{\eta}_L| \eta_L \quad [\text{N}]$$

where

- M = structural mass of lifted object [kg]
- A_{33} = added mass of lifted object [kg]
- M' = $M + A_{33}$ = the total mass [kg]
- m = mass per unit length of cable [kg/m]
- L = length of cable [m]
- E = modulus of elasticity [N/m^2]
- A = nominal cross-sectional area of cable [m^2]
- C_{Df} = cable longitudinal friction coefficient [-]
- C_{Dz} = vertical drag coefficient for lifted object [-]
- ρ = mass density of water [kg/m^3]
- D_c = cable diameter [m]
- A_p = z -projected area of lifted object [m^2]
- η_L = $\eta(-L)$ = motion of lifted object [m]

Guidance note:

Since the linearized damping coefficients depend on the amplitude of motion η_L , an iteration is needed to find the actual response. Note that the oscillatory KC effects on C_{Dz} should be taken into account (3.3.5.2). Note that structural damping is not included in this simplified analysis.

---e-n-d---of---G-u-i-d-a-n-c-e---n-o-t-e---

5.3.7.6 The amplitude of the vertical motion of the lifted object caused by a forced oscillation of top of the cable with frequency ω and amplitude η_a is given by

$$\frac{|\eta_L|}{\eta_a} = \left| \frac{kEA}{kEA \cos(kL) + (-\omega^2 M' + i\omega \Sigma) \sin(kL)} \right| \quad [\text{m/m}]$$

5.3.7.7 The ratio between the motion of the lifted object and the motion at the top of the cable, is the motion transfer function

$$H_L(\omega) = \frac{\eta_L}{\eta_a} \quad [\text{m/m}]$$

Guidance note:

An example response curve of a lifted object in deep water is shown in Figure 5-5, plotted with respect to oscillation period $T = 2\pi/\omega$. The following parameters were used in the calculations:

- M' = $M + A_{33} = 190\,000$ kg
- m = 25.0 kg/m
- L = 3 000 m
- EA = 3.00E+08 N
- ρ = 1 025 kg/m^3
- D_c = 0.04 m
- C_{Df} = 0.02

$$\begin{aligned}
C_{Dz} &= 1.0 - 2.0 \\
A_p &= 25 \text{ m}^2 \\
\eta_a &= 1 \text{ m}
\end{aligned}$$

Large response is observed close to eigenperiod $T_0 = 9.2 \text{ s}$ (as given by the formula in 5.3.5.1 for un-damped oscillations). Enhanced response at eigenperiod $T_1 = 1.7 \text{ s}$ can also be observed.

For long oscillation periods, the combined system of cable and lifted object is oscillating like a rigid body where the lifted object follows the motion of the top of the cable, $|\eta_L/\eta_a| \sim 1$.

---e-n-d---of---G-u-i-d-a-n-c-e---n-o-t-e---

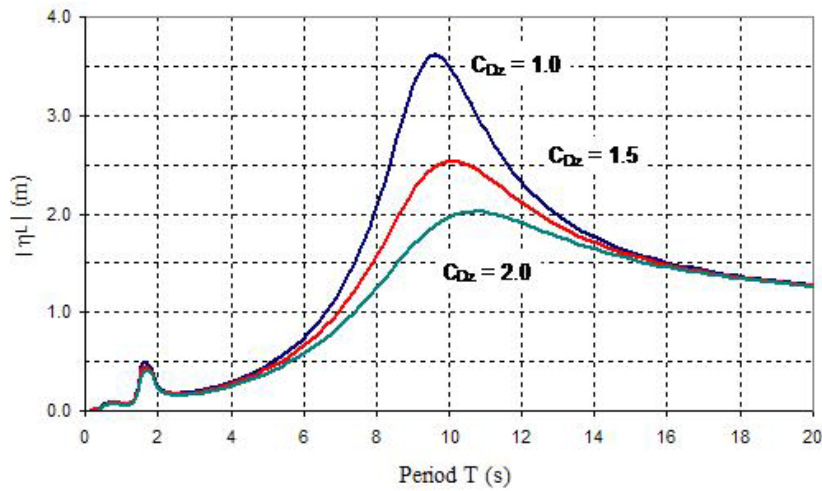


Figure 5-5

Example response amplitude of a lifted object in deep water due to a forced motion $\eta_a = 1 \text{ m}$ at top end of cable for three different drag coefficients $C_{Dz} = 1.0, 1.5, 2.0$.

5.3.7.8 The amplitude of the dynamic force $F_d(z)$ in the cable at position z is given by;

$$\frac{F_d(z)}{\eta_a k_E} = \left| \frac{-(kL)^2 k_E \sin[k(z+L)] + (kL)h(\omega) \cos[k(z+L)]}{(kL)k_E \cos(kL) + h(\omega) \sin(kL)} \right|$$

where

$$\begin{aligned}
h(\omega) &= -\omega^2 M' + i\omega \Sigma \\
k_E &= EA / L
\end{aligned}$$

The amplitude of the dynamic force F_{d0} at the top of the cable is obtained by setting $z = 0$ in the expression above. Likewise, the amplitude of the dynamic force F_{dL} at the lifted object is obtained by setting $z = -L$,

$$\frac{F_{dL}}{\eta_a k_E} = \frac{|h(\omega)|}{|k_E \cos(kL) + h(\omega) \sin(kL) / kL|}$$

5.3.7.9 The dynamic force per unit motion of top of cable is the force transfer function

$$H_F(\omega, z) = \frac{F_d}{\eta_a} \quad [\text{N/m}]$$

5.3.7.10 The motion of the lifted object due to a general irregular wave induced motion of top of the cable is obtained by combining transfer functions for motion of lifted object and motion of top of cable at crane tip position. The response spectrum of the lifted object is given by

$$S_L(\omega) = [H_L(\omega)H_a(\omega)]^2 S(\omega) \quad [\text{m}^2\text{s}]$$

where $H_a(\omega)$ is the transfer function for crane tip motion, $S(\omega)$ is the wave spectrum and $H_L(\omega)$ is defined in 5.3.7.7. Likewise, the dynamic force in the cable due to a general irregular wave induced motion of top of the cable is given by

$$S_F(\omega, z) = [H_F(\omega, z)H_a(\omega)]^2 S(\omega) \quad [\text{N}^2\text{s}]$$

where $H_F(\omega; z)$ is defined in 5.3.7.8.

5.3.8 Slack cable conditions

5.3.8.1 In the general case the dynamic force varies along the length of the cable due to inertia effects in the cable. If the amplitude of the dynamic force exceeds the static tension in the cable, a slack cable condition will occur. Alternatively, a slack wire will occur if the relative motion between lifted object and crane tip is greater than the static stretch of the cable,

$$|\eta_L - \eta_a| \geq \eta_{st}$$

where η_L is given by 5.3.7.6 and the static stretch η_{st} is obtained from 5.2.1,

$$\eta_{st} = L_s - L = \frac{WL + \frac{1}{2}wL^2}{EA}$$

5.3.8.2 Neglecting the damping due to friction along the cable ($\sigma = 0$), the slack cable criterion can be expressed as

$$\frac{\sqrt{(a_1 a_2)^2 + (a_1 b)^2 + (a_2 b)^2 + b^4}}{a_1^2 + b^2} \geq \tau$$

Where the non-dimensional parameters are defined as

$$a_1 = \Lambda_\varepsilon \cos \Lambda_\varepsilon - \Lambda^2 \sin \Lambda_\varepsilon$$

$$a_2 = \Lambda_\varepsilon - a_1$$

$$b = 2\xi\Lambda \sin \Lambda_\varepsilon$$

$$\Lambda = \omega \sqrt{\frac{M'L}{AE}}$$

$$\Lambda_\varepsilon = \Lambda \sqrt{\varepsilon}$$

$$\varepsilon = \frac{mL}{M'}$$

$$\xi = \frac{1}{2} \Sigma \sqrt{\frac{L}{EAM'}}$$

$$\tau = \frac{\eta_{st}}{\eta_a}$$

Λ is the non-dimensional frequency, ξ is the non-dimensional damping (damping ratio), and τ is the displacement ratio. Σ is the linearized damping as given in 5.3.7.5. The other variables are defined in 5.3.7.5. Regions of taut and slack cable conditions are shown in Figure 5-6 for mass ratios ε and damping ratios ξ of 0, 0.4 and 1.0.

Guidance note:

Neglecting the damping due to friction along the cable reduces the region for slack in the (Λ, τ) domain. To account for this, a comparison should be done between the drag force $F_v L$ on the lifted object and the total friction force $f_v L$ along the cable as given in 5.3.7.4 and increase the damping ratio ξ by a factor $1 + f_v L / F_v$ in the criterion 5.3.8.2. A slack cable criterion similar to 5.3.8.2 for the general case, including damping due to friction along the cable may be derived from the general criterion 5.3.8.1 using 5.3.7.3 and 5.3.7.6.

---e-n-d---of---G-u-i-d-a-n-c-e---n-o-t-e---

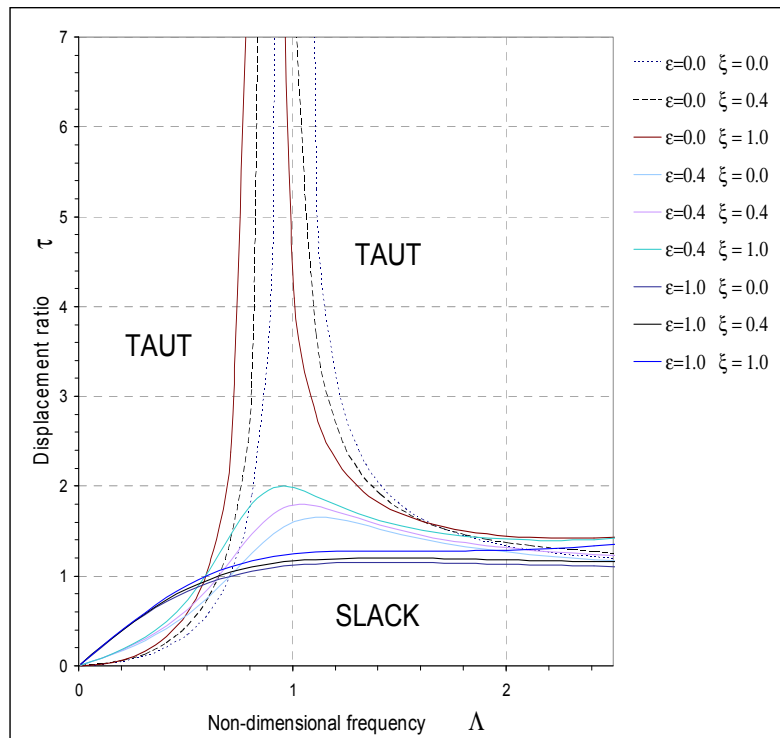


Figure 5-6
Regions for slack and taut cable conditions for given frequency and amplitude of oscillation. Regions depend on mass ratio and damping of lifted object.

5.3.8.3 When the mass of the cable is negligible, the criterion for impending slack in the cable can be expressed as (Ref. /7/)

$$\frac{\Lambda^4 + (2\xi\Lambda)^2}{\sqrt{\Lambda^4 (\Lambda^2 + 4\xi^2 - 1)^2 + (2\xi\Lambda)^2}} \geq \tau$$

Guidance note:

The following approximations can be useful for investigation of slack conditions. For small values of the damping $\xi < 0.01$, the condition can be approximated by

$$\frac{\Lambda^2}{|1 - \Lambda^2|} \geq \tau$$

For small displacement ratios $\tau < 0.04$, the condition can be approximated by

$$\sqrt{\Lambda^4 + (2\xi\Lambda)^2} \geq \tau$$

---e-n-d---of---G-u-i-d-a-n-c-e---n-o-t-e---

5.3.9 Horizontal motion response of lifted object in a straight vertical cable

5.3.9.1 The first (fundamental) eigenperiod for un-damped oscillations of the lifted object may be taken as:

$$T_{0h} \approx 2\pi \sqrt{\frac{\left(M + A_{II} + \frac{mL}{3}\right) \cdot L}{W + 0.45wL}} \quad [\text{s}]$$

where

L = length of cable [m]

$W = Mg - \rho g V$ = submerged weight of lifted object [N]

$w = mg - \rho g A$ = submerged weight per unit length of cable [N/m]

M = mass of lifted object [kg]

m = mass per unit length of cable [kg/m]

A_{II} = surge added mass of lifted object [kg]

5.3.9.2 Applying added mass in sway, A_{22} , in equation 5.3.8.1 will give the eigenperiod for sway motion of lifted object.

5.3.9.3 If the ocean current energy spectrum is non-zero in a range of frequencies close to $f_0 = 1/T_{0h}$ horizontal oscillations of the lifted object can be excited. Likewise, the oscillations may be excited by horizontal motion of crane tip. Such oscillations may be highly damped due to viscous drag on cable and lifted object.

5.4 Heave compensation

5.4.1 General

5.4.1.1 Various motion control devices may be used to compensate for the vertical motion of the vessel. The most commonly used device is a *heave compensator*.

5.4.1.2 A heave compensator may be used to control the motion of the lifted object and tension in cable during a lifting operation.

5.4.1.3 Heave compensators may be divided into three main groups:

- passive heave compensators
- active heave compensators
- combined passive/active systems.

5.4.1.4 A passive heave compensator is in principle a pure spring damper system which does not require input of energy during operation. An active heave compensator may use actively controlled winches and hydraulic pistons. The active system is controlled by a reference signal. In a combined system the active system is working in parallel with the passive.

5.4.1.5 Examples of input reference signals to an active heave compensator are:

- wire tension
- crane top motion
- winch or hydraulic piston motion
- position of lifted object
- vessel motion
- wave height/current velocity.

5.4.2 Dynamic model for heave compensation, example case

5.4.2.1 As an example case, a simplified dynamic model for a passive heave compensator situated at crane tip is shown in Figure 5-6. The equations of motion at top of wire, η_{3P} , and at lifted object, η_3 , can be taken as;

$$m_c \ddot{\eta}_{3P} + c_c \dot{\eta}_{3P} + k_c \eta_{3P} + k_w (\eta_{3P} - \eta_3) = F_{3T}(t)$$

$$(M + A_{33}) \ddot{\eta}_3 + c \dot{\eta}_3 + k_w (\eta_3 - \eta_{3P}) = F_{3M}(t)$$

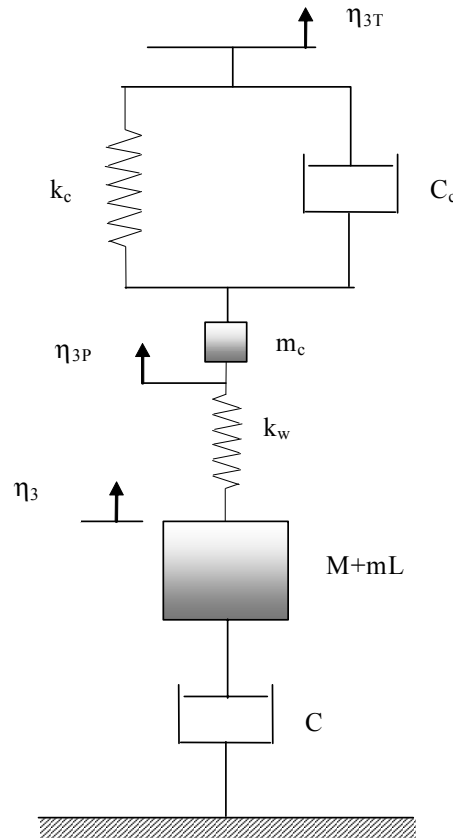


Figure 5-7
Simplified dynamic model of a passive heave compensator

where

- m_c = Mass of heave compensator [kg]
- k_c = Stiffness of heave compensator [N/m]
- c_c = Linear damping of heave compensator [kg/s]
- M = Mass of lifted object [kg]
- A_{33} = Added mass of lifted object [kg]
- k_w = Wire stiffness = EA/L [N/m]
- c = Linear damping of lifted object [kg/s]
- η_{3P} = Vertical motion at top of wire (i.e. below compensator) [m]
- η_3 = Vertical motion of lifted object [m]
- η_{3T} = Vertical motion at crane tip (i.e. at top of compensator) [m]
- $F_{3T}(t)$ = Vertical force at crane tip (i.e. at top of compensator) [N]
- $F_{3M}(t)$ = Vertical force at lifted object [N]

Guidance note:

Note that the damping of compensator and lifted object is in general due to quadratic viscous damping and the compensator stiffness is in general nonlinear. Linear damping estimates can be obtained by equivalent linearization. Compensator stiffness may be due to compression of gas volume in pneumatic cylinders.

---e-n-d---of---G-u-i-d-a-n-c-e---n-o-t-e---

5.4.2.2 For forced motion of top of heave compensator due to vessel motion, the force on compensator is given by

$$F_{3T}(t) = \eta_{3T} k_c + \dot{\eta}_{3T} c_c \quad [\text{N}]$$

5.4.2.3 The vertical force $F_{3M}(t)$ on the lifted object is related to the motion of top of wire $\eta_{3P} = \eta_a$ by the transfer function as given in 5.3.7.2.

5.4.2.4 In a lowering operation the length of the wire changes with time hence the wire stiffness k_w will be a function of time.

5.4.2.5 For given time series of $F_{3T}(t)$ and $F_{3M}(t)$ the equations of motion in 5.4.2.1 can be integrated in time by replacing the two equations by four first order differential equations and using a standard integration scheme, i.e. 4th order Runge-Kutta technique.

5.4.2.6 For harmonic excitation of the top of heave compensator, we have that;

$$F_{3T}(t) = F_{3Ta} \cos(\omega t) \quad [\text{N}]$$

5.4.2.7 The ratio between the response of the lifted object and the excited motion can be expressed through a complex transfer function

$$\frac{\eta_3}{\eta_{3T}} = G(\omega) \quad [\text{m/m}]$$

where the efficiency of the heave compensator is defined as

$$e = 1 - |G(\omega)| \quad [-]$$

5.4.2.8 Active heave compensation systems generally use information from vessel motion reference unit (MRU) to control payout of winch line. The heave motion at crane tip is calculated from the vessel motions in six degrees of freedom and signal sent to compensator unit.

5.4.2.9 Motion measurements and control system inevitably introduces errors and time delays. Hence, a theoretical model of active heave compensation will have to take into account physical imperfections in order to produce realistic results. Such imperfections must be based on operating data for the actual system.

5.4.2.10 Deviations due to imperfect motion measurements and tracking control may result in residual motion of the lifting cable at suspension point on ship. This residual motion may cause low amplitude oscillations of the lifted object at the resonance frequency.

5.4.2.11 An active heave compensator is generally not equally effective in reducing motions at all frequencies. At some frequencies it will be more effective than at others.

5.5 Fibre rope properties

5.5.1 General

Fibre ropes are constructed from materials that display visco-elastic properties. This means that response characteristics differ greatly from the ideal elastic-plastic response for steel. The main differences are:

- Response is nonlinear and inelastic
- Lack of recovery to initial static loading case
- Energy dissipation (hysteresis) associated with dynamic loading. Different load-elongation paths are observed when ascending and descending. The hysteresis depends upon load history.
- Continued elongation with time under static or dynamic load (creep)

Guidance note:

Choice of fibre material depends on the application. For deepwater deployment systems High Modulus Polyethylene (HMPE) has been applied due to its high strength to weight ratio and high stiffness properties. Another alternative is Aramid which possesses greater heat resistance than HMPE. Factors that limit the life of HMPE ropes include hydrolysis, heating (from bend-over-sheave loading) and internal abrasion, tension-tension fatigue, axial-compressive fatigue, and creep rupture.

---e-n-d---of---G-u-i-d-a-n-c-e---n-o-t-e---

5.5.2 Elongation and stiffness

5.5.2.1 The change-in-length characteristics of fibre ropes are more complex than those of steel wire rope. Stiffness can be non-linear since strain may be different for the same load level. Permanent strain can be significant. Both stiffness and strain depend on the loading history and even the load frequency.

5.5.2.2 The stretch $\Delta L = L_s - L$ is defined as the change in length of the rope. The strain ε is defined as the change in length divided by its length L before change in tension,

$$\varepsilon = \Delta L / L \quad [-]$$

The non-dimensional stiffness S is defined as the incremental rope tension $\Delta F / F_0$ (where ΔF is the variation in

the load, and F_0 is the minimum breaking load) divided by the strain ε

$$S = \frac{\Delta F}{F_0} \bigg/ \frac{\Delta L}{L_0} \quad [-]$$

The rope strength F_0 is also denoted MBL (the minimum breaking load).

5.5.2.3 The change-in-length characteristics of polyester ropes can generally be described by six elements (DNV-OS-E303)

- ε_p = polymer creep strain, a function of time under tension
- ε_c = rope construction strain, a function of highest applied tension
- S_o = original stiffness, during loading to a load which is higher than any previous load
- S_s = static stiffness, during subsequent loadings less than or up to the highest previous load
- S_d = dynamic stiffness, after a number of relatively fast load cycles
- ε_{se} = sustained elastic strain, which occurs during cycling and is relaxed after cycling

5.5.2.4 The spring rate K for a fibre rope is defined by

$$K = \frac{\Delta F}{\Delta L} \quad [\text{N/m}]$$

The following notations are used for spring rate,

- K_o = original spring rate
- K_s = static spring rate
- K_d = dynamic spring rate

5.5.2.5 The quantity generally used to report stiffness from test results is the specific modulus of elasticity, E/ρ , which eliminates the influence of change in cross-section area.

$$\frac{E}{\rho_s} = \frac{EA}{m} \quad [\text{m}^2/\text{s}^2]$$

where

- E = Young's modulus of elasticity $[\text{N/m}^2]$
- ρ_s = mass density of fibre rope $[\text{kg/m}^3]$
- A = cross-sectional area $[\text{m}^2]$
- m = mass per unit length of rope $[\text{kg/m}]$

Guidance note:

Note that the speed of longitudinal pressure waves in the fibre rope is equal to the square root of the specific modulus of elasticity (see 5.3.6.1).

---e-n-d---of---G-u-i-d-a-n-c-e---n-o-t-e---

5.5.2.6 For an oscillatory motion of a suspended weight, the specific modulus of elasticity for a fibre rope depends in general on the mean load and the load amplitude as well as the frequency of the oscillatory load (Ref. /8/). It can be expressed as

$$\frac{E}{\rho} = \alpha + \beta F_m - \gamma F_a + \delta \log_{10}(f)$$

where

- F_m = mean load $[\text{N}]$
- F_a = load amplitude $[\text{N}]$
- f = excitation frequency $[\text{Hz}]$
- $\alpha, \beta, \gamma, \delta$ = constants $[-]$

5.5.2.7 Since the dependence on loading frequency is only logarithmic, the frequency term does not contribute significantly, and may be neglected. It should be noted that effects of load amplitude and frequency tend to vanish under complex loading sequences (corresponding to real wave loading).

5.5.2.8 Permanent stretch affects change in length of the fibre rope. It is of concern when determining the fibre rope length for a lowering operation and the amount of line which must be taken up during a lifting operation.

5.5.2.9 The additional elongation associated with initial loading of a new fibre rope is known as bedding-in, when the rope is pulled into a tighter and thus stiffer structure. During the initial installation and tensioning it is difficult to define a general stiffness. Once the initial load is completely taken off for a period of time, the

rope recovers to some extent. After the rope has been tensioned to allow bedding-in, and cyclic load and relaxation has occurred for some time, the stiffness of fibre ropes tends towards a linear function of mean load and load range.

5.5.3 Creep

5.5.3.1 Elongation in fibre ropes results from bedding-in of the rope structure and terminations, and from both initial extension and creep in the yarns. Creep may be a problem with HMPE under high tensions.

5.5.3.2 Creep can be classified into three areas:

- primary creep (recoverable part of extension)
- secondary creep (permanent part of extension)
- creep rupture (the most damaging form of creep).

5.5.3.3 Primary creep is also referred to as delayed elastic elongation and is recoverable. For most fibre ropes, creep rate reduces with time and is approximately the same for equal increments of logarithmic time.

5.5.3.4 Creep of polyester rope can be expressed as (Ref. /10/)

$$u = u_0 + a_c \log_{10} \left(1 + \frac{t - t_0}{t_0} \right)$$

where

- u_0 = elongation at $t = t_0$, measured from start of loading
- t_0 = time origin, i.e. start of load plateau
- a_c = creep per decade
- t_a = length of zeroth decade

5.5.3.5 The secondary creep results in a permanent increase in the length of the fibre rope when under a sustained load over time. This is the part that is normally referred to as creep and which is important for HMPE fibre ropes used for deep water deployment. Secondary creep does not follow the same log function of time as primary creep, but increases linearly with time. Ref. /9/.

5.5.3.6 Protection against creep rupture can be obtained using discard criteria based on rope permanent elongation (10% has been proposed).

5.5.4 Axial damping

5.5.4.1 Axial rope damping is an important parameter for prediction of dynamic response of the payload and cable system, and when evaluating snap loads and resonant response. In such cases fibre rope axial damping determines the peak tension in the rope.

5.5.4.2 The damping coefficient for fibre ropes may depend on the mass of the suspended weight. Relevant data on axial damping of fibre ropes is scarce.

5.5.5 Fatigue life of fibre ropes cycled over sheaves

5.5.5.1 The fatigue life of fibre ropes cycled over sheaves is limited due to the following:

- Low friction of ropes on steel sheaves causing risk of slippage and burning
- Risk of crushing and cutting-in where multiple layers of rope are wound on top of each other
- Internal heating leading to creep or melting of the rope.

5.6 References

- /1/ DNV Offshore Standard DNV-OS-H205, "Marine Operations, Lifting Operations" (planned issued 2010 see ref./4/ until release).
- /2/ Abramowitz, M. and Stegun, I.A. (1965) "Handbook of Mathematical Functions". Dover Publications.
- /3/ Nielsen, F.G. (2007) "Lecture notes in marine operations". Dept. of Marine Hydrodynamics, NTNU.
- /4/ DNV Rules for Planning and Execution of Marine Operations (1996). Pt.2 Ch.5 Lifting – Pt.2 Ch.6 Sub Sea Operations.
- /5/ Sandvik, P.C. (1987) "Methods for specification of heave compensator performance". NTNF Research Programme "Marine Operations". Marintek Report No. 511003.80.01.
- /6/ DNV Recommended Practice DNV-RP-C205 "Environmental Conditions and Environmental Loads", April 2007.
- /7/ Niedzwecki, J.M. & Thampi, S. K. (1991) "Snap loading of marine cable systems". Applied Ocean Research, Vol. 13, No. 1.

- /8/ Chaplin, C.R. and Del Vecchio, C.J.M. (1992) "Appraisal of Lightweight Moorings for Deep Water". Offshore Technology Conference Paper no. OTC 6965, Houston.
- /9/ Davies, P., Huard, G., Grosjean, F., Lyon, I.F.P. and Francois, M. (2000) "Creep and Relaxation of Polyester Mooring Lines". Offshore Technology Conf. paper no. OTC 12176, Houston, Texas, USA.
- /10/ Francois, M. and Davies, P. (2000) "Fibre Rope Deepwater Mooring: A practical model for the analysis of polyester mooring systems". IBP24700, Rio Oil and Gas Conf., Rio de Janeiro, Brazil.
- /11/ BMT Fluid Mechanics Limited (2004) "Deepwater Installation of Subsea Hardware (DISH) Phase 2. Task 3.3 - Fibre Rope Deployment System (FRDS). Simulation Study: State-of-Art Literature Review.
- /12/ DNV-OS-E303 "Certification of fibre ropes for offshore mooring". April 2008.

6 Landing on Seabed and Retrieval

6.1 Introduction

6.1.1 Types of structures and foundation designs

6.1.1.1 This chapter gives recommendations for evaluating seabed landing and retrieval of any subsea structure with permanent or temporary foundation consisting of plate foundations that may or may not be equipped with skirts. This includes the foundation solution of suction anchors, also called bucket foundations. Installation or retrieval of driven piles or drilled and grouted piles is not treated. Structures with piles as permanent pile foundations, however, go through a temporary phase supported on plate foundations or "mud mats".

6.1.2 Geotechnical data

6.1.2.1 Geotechnical data required for these evaluations will normally be covered by the data gathered and established for the foundation design. Reference to requirements for soil investigations are the DNV Classification Note 30.4 "Foundations" and NORSOK G-001 "Soil investigation".

6.2 Landing on seabed

6.2.1 Introduction

6.2.1.1 The aim of evaluating the landing on seabed shall be to assure that

- foundation failure does not take place during the landing
- damage does not occur to acceleration sensitive equipment.

Acceptance criteria should thus be available to compare with the analysed/evaluated responses related to allowable displacements or allowable accelerations (retardations).

6.2.1.2 Whether or not the foundation solution (i.e. size of plate foundations) is equipped with skirts, strongly depends on the type and characteristics of the subsea structure and the soil characteristics. This again has influence on the challenges for the landing and how this shall be considered.

6.2.1.3 Some foundations on hard soils have ample capacity to carry the submerged weights without skirts, whereby the landing evaluation should focus on the dynamic impact force and maximum retardations. Other foundations on soft soil may require a significant penetration of skirts before the soil can resist even the static submerged weight of the structure. In that case the main design issue is to assure sufficient area of holes for evacuation of entrapped water within the skirt as they penetrate in order for the water pressure not to exceed the bearing capacity of the soil.

6.2.1.4 In the following sections a problem definition of the landing impact is given including a description of the physical effects and the parameters involved. Then an 'optimal' solution taking account for the relevant effects is described. Finally, simplified methods are suggested to check out landing impact of a foundation without skirts on hard soil and required water evacuation for skirted foundations on very soft soil.

6.2.2 Landing impact problem definition

6.2.2.1 The following describes a methodology for simulating the landing of a bucket on the seabed. The method considers one degree of freedom only, i.e. vertical motion.

6.2.2.2 This methodology can also be used to solve the vertical impact of structures with several foundations, as long as centre of gravity and centre of reaction for other forces coincides with the geometrical centre of the foundations. In that case masses and forces can be divided equally onto each of the foundations and the impact can be analysed for one foundation.

6.2.2.3 A mud mat foundation without skirts can be considered a special case of the method described for a bucket foundation. The model to be analysed is illustrated on Figure 6-1.

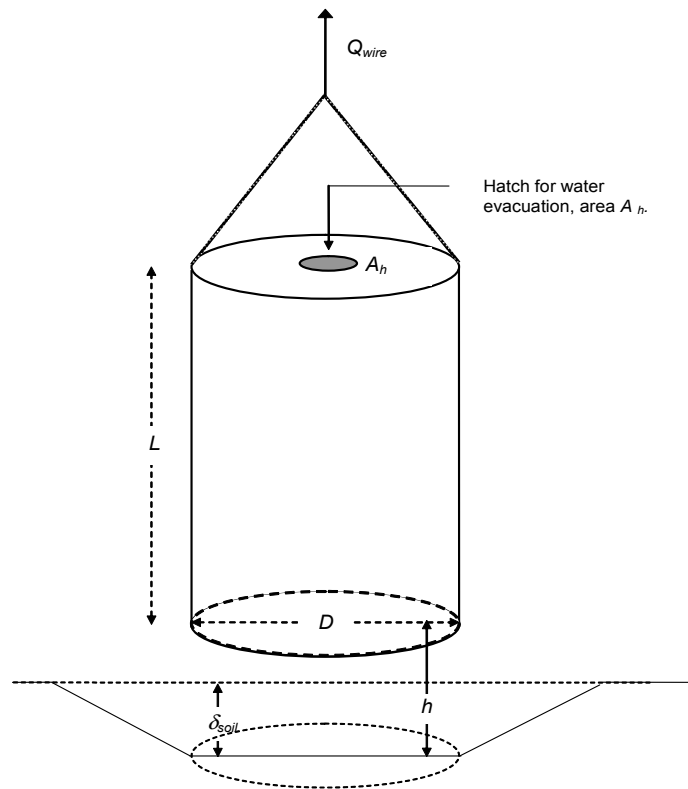


Figure 6-1
Model for impact analysis

6.2.2.4 The anchor is lowered down to seabed in a sling from an installation vessel being exposed to wave action.

6.2.2.5 During lowering the vertical motion of the anchor is given by a constant downwards velocity plus an oscillatory heave motion caused by the wave induced motion of the installation vessel.

6.2.2.6 The geometry of the bucket is simplified to a vertical cylindrical surface of diameter D and height L . A hatch for water evacuation is located on the top of the anchor.

6.2.2.7 The impact is to be solved by time integration of the general equation of motion, which may be performed as time integration assuring energy preservation.

All relevant forces acting upon the foundation shall be considered in the time integration with their instant time dependent values. Such forces are gravity, buoyancy, sling forces, dynamic water pressure from within the bucket and soil resistance acting upon the skirts as they penetrate.

6.2.3 Physical parameters and effects to be considered

6.2.3.1 The following physical parameters are involved in the simulation model

Assuming bucket consists of only steel volume we get a submerged weight W given by,

$$W = M \cdot g \cdot \frac{\rho_s - \rho}{\rho_s} \quad [\text{N}]$$

where

- M = structural mass [kg]
- ρ_s = mass density of steel [kg/m^3]
- ρ = mass density of water [kg/m^3]
- g = acceleration of gravity [m/s^2]

6.2.3.2 The structural mass, M , shall include mass of structural elements and equipment on top of the anchor.

6.2.3.3 The added mass including mass of water entrapped within the skirts may for a typical foundation bucket be taken as;

$$A_{33} = \rho \cdot A_b \cdot L \left(1 + \frac{2}{3} \frac{D}{L} \right) \quad [\text{kg}]$$

where

A_{33} = added mass for vertical motion [kg]

D = diameter of bucket [m]

L = length of bucket [m]

$A_b = \pi D^2/4$ = bucket area [m²]

Additional added mass may have to be added to represent added mass caused by structural elements and equipment on top of the anchor.

Guidance note:

Bucket height and size of ventilation hole may affect the heave added mass. See Section 4.6.3 for more accurate estimation.

---e-n-d---of---G-u-i-d-a-n-c-e---n-o-t-e---

6.2.3.4 The total dynamic mass is:

$$M' = M + A_{33} \quad [\text{kg}]$$

and the initial kinetic energy is:

$$E_{k0} = \frac{1}{2} \cdot M' \cdot v_{c0}^2 \quad [\text{Nm}]$$

where v_{c0} is the initial velocity at start of the calculations.

6.2.3.5 For vertical motion of an object very close to the seabed the added mass will vary with distance to seabed. The effect is an upward force of;

$$0.5(dA_{33} / dh) \dot{\eta}_L^2 \quad [\text{N}]$$

where

$\dot{\eta}_L$ = velocity of the object [m/s]

h = distance to the seabed [m]

dA_{33} / dh = rate of change of added mass vs. h [kg/m]

Guidance note:

This estimation of hydrodynamic force uses the same approach for added mass as for water exit, ref. 3.2.11.2.

---e-n-d---of---G-u-i-d-a-n-c-e---n-o-t-e---

6.2.3.6 The hydrodynamic water pressure increases as the bucket approaches the seabed, and the area for water evacuation decreases. The development of the water pressure also depends on the interaction with the soil (mobilisation of soil bearing capacity). The increase in bearing capacity with skirt penetration must be accounted for, and penetration resistance as skirt starts to penetrate must be included in the calculations.

6.2.3.7 The sum of the penetration resistance and the force from water pressure inside the bucket, shall be limited by the bearing capacity.

6.2.3.8 The hydrodynamic force from the water pressure beneath and within the bucket is calculated using Bernoulli's equation:

$$p_w = \frac{1}{2} k_{flow} \cdot \rho \cdot v_{flow}^2 \quad [\text{N/m}^2]$$

where

p_w = hydrodynamic pressure within the bucket [N/m²]

v_{flow} = velocity of water out of the bucket [m/s]

ρ = mass density of water [kg/m³]

k_{flow} = pressure loss coefficient [-]

6.2.3.9 In the case of valve sleeves with high length to diameter ratio, the pressure loss coefficient can be

determined as;

$$k_{flow} = 1 + 1/2 \left[1 - (d_i / D)^2 \right]^2 + f \cdot n \cdot L_{sleeve} / d_i \quad [-]$$

where

$$\begin{aligned} d_i &= \text{diameter of flow valves [m]} \\ f &= \text{friction coefficient for valve sleeves [-]} \\ n &= \text{number of flow valves} \\ L_{sleeve} &= \text{length of the valve sleeves [m]} \end{aligned}$$

6.2.3.10 Alternatively, k_{flow} for different outlet geometries are given by Blevins (1984), *ref./3/*.

6.2.3.11 The velocity of water out of the bucket can be expressed as

$$v_{flow} = \frac{q_{flow}}{A_{flow}} \quad [\text{m/s}]$$

where

$$\begin{aligned} q_{flow} &= \text{flow of water out of the bucket [m}^3\text{/s]} \\ A_{flow} &= A_h + \pi D \cdot h \quad [\text{m}^2] \\ A_h &= \text{area of available holes in the bucket [m}^2] \\ h &= \text{gap between the soil and the skirt tip, which reduces as the bucket approaches the seabed [m]} \end{aligned}$$

6.2.3.12 Assuming incompressible water, the water flow that escapes at any time from within and beneath the bucket is taken as;

$$q_{flow} = A_b \cdot (v_c - \dot{\delta}_{soil}) \quad [\text{m}^3\text{/s}]$$

v_c is the vertical velocity of the bucket and;

$$\dot{\delta}_{soil} = d\delta_{soil} / dt \quad [\text{m/s}]$$

where $d\delta_{soil}$ is the change in soil displacement due to the change in bearing pressure taking place during time step dt .

6.2.3.13 The total force Q_{soil} transferred to the soil at any time can be written as;

$$Q_{soil} = Q_w + Q_{skirt} \quad [\text{N}]$$

which is the sum of the force $Q_w = p_w A_b$ resulting from the hydrodynamic water pressure and the force Q_{skirt} transferred from the penetrating skirts to the soil.

6.2.3.14 The relation between Q_{soil} and δ_{soil} is illustrated in Figure 6-2. As a simplified solution it is suggested that mobilisation of soil resistance follows a parabolic function. The following relation between Q_{soil} and δ_{soil} can thus be applied,

$$\begin{aligned} Q_{soil} &= Q_{sd} \cdot \sqrt{\delta_{soil} / \delta_{mob}} & \text{for } \delta_{soil} < \delta_{mob} \\ Q_{soil} &= Q_{sd} & \text{for } \delta_{soil} \geq \delta_{mob} \\ \Delta Q &= k_u \cdot \Delta \delta_{soil} & \text{for unloading} \end{aligned}$$

where

$$\begin{aligned} Q_{sd} &= \text{the design bearing capacity for loading within area } A_p \text{ at seabed or at skirt tip level [N]} \\ \delta_{mob} &= \text{the vertical soil displacement to mobilise } Q_{sd} \text{ [m]} \\ k_u &= \text{the unloading stiffness [N/m]} \end{aligned}$$

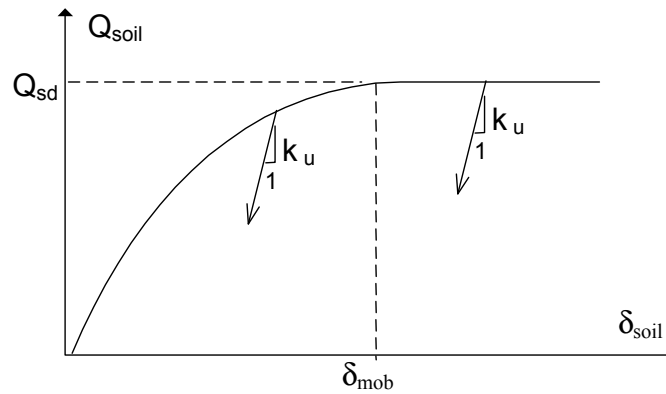


Figure 6-2
Mobilisation of soil bearing capacity

6.2.3.15 The characteristic static soil resistance, Q_{sc} is in the calculations transferred to a ‘design soil resistance’ by the following relation

$$Q_{sd} = Q_{sc} \cdot \gamma_r / \gamma_m \quad [\text{N}]$$

where

γ_r = rate effect factor to account for increased shear strength due to rapid loading [-]

γ_m = soil material coefficient [-]

6.2.3.16 The soil bearing capacity can be determined based on bearing capacity formulae, or computer programs using limit equilibrium or finite element methods, as described in DNV Class Note 30.4 Foundations. The skirt penetration resistance can be calculated as described in 6.2.8.

6.2.3.17 The bucket impact problem can be solved by a time integration with an iterative solution at each time step. The calculations should start at a distance above the seabed where the build-up of hydrodynamic pressure is moderate, with correspondingly moderate soil displacements.

6.2.3.18 The interaction with the string is taken as a prescribed lowering velocity combined with a sinusoidal heave motion given by its amplitude and period. The phase angle for start of calculations is an input. The clearance with the seabed at start of calculations is related to a given minimum clearance and to the heave amplitude and a phase angle of start as illustrated in Figure 6-3.

$$h_{start} = h_{min} + \eta_L \cdot (1 + \sin \varphi) \quad [\text{m}]$$

where

h_{start} = clearance at start of calculations, $t = 0$ [m]

h_{min} = required minimum clearance for start of calculation [m]

η_L = heave amplitude of the foundation (at the end of the crane wire, of length L) [m]

φ = phase angle at $t = 0$ [-]

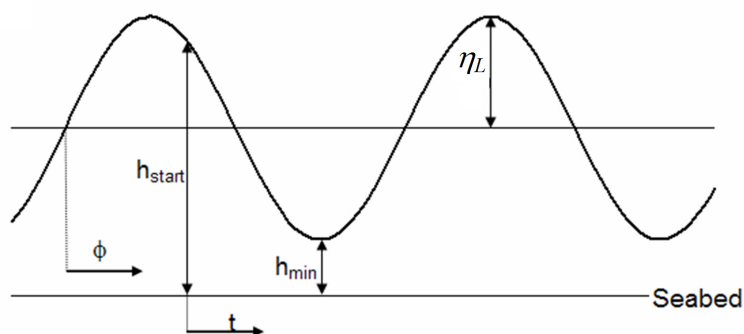


Figure 6-3
Situation for start of analysis

6.2.3.19 Conservatively the heave motions can be taken into account by analysing the impact for a constant lowering velocity, taken as the sum of the crane lowering velocity and the maximum heave velocity of the

foundation. This will represent the worst phasing of the heave motions, which is also relevant to consider, since a beneficial phasing is not likely possible to control.

6.2.3.20 When the impact lasts long, as when skirts penetrate deeply before the peak impact is reached, it may be beneficial and relevant to account explicitly for the combined crane lowering and heave motions. In that case several phase angles of the heave motions should be considered.

6.2.3.21 For the analysis method described it is assumed that the heave motions relates to the motion η_L of the foundation close to seabed, which is to be observed and controlled during installation. In order to include the interaction with the crane wire the motion at the vessel end of the wire η_a can be set considering an un-damped oscillation of the modelled total dynamic mass in the wire.

$$\frac{\eta_L}{\eta_a} = M_f = \frac{1}{\left(1 - \frac{\omega^2}{\omega_0^2}\right)}$$

where

M_f = dynamic amplification factor [-]

ω = angular frequency of the heave motions [rad/s]

ω_0 = angular eigenfrequency [rad/s]

Guidance note:

For resonant conditions, when the characteristic frequency of crane tip motion is close to the eigenfrequency of the hoisting system, the un-damped response given by the formula above may be too conservative. Results from a dynamic analysis including relevant damping effects can then be applied. Dynamic response of a lowered object due to wave action is described in Section 5.

---e-n-d---of---G-u-i-d-a-n-c-e---n-o-t-e---

6.2.4 Iterative analysis procedure

6.2.4.1 For each time step in the suggested time domain analysis the following iteration procedure is suggested in order to account for the non-linear behaviour of the soil resistance.

1) Assume an incremental soil displacement $\Delta\delta_{soil}$ [m]

2) Calculate the clearance h_i between the skirt tip and the seabed as;

$$h_i = h_{i-1} - \Delta z_i + \Delta\delta_{soil} \quad [\text{m}] \quad \text{where} \quad \Delta z_i = v_{c,i} \cdot \Delta t \quad [\text{m}]$$

Note that h_i has negative values when skirt penetrates

3) Calculate area for escape of water;

$$A_{flow,i} = A_h + \max(\pi \cdot D \cdot h_i, 0) \quad [\text{m}^2]$$

4) Calculate corresponding water pressure reaction on the soil and bucket

$$\begin{aligned} Q_{w,i} &= \text{sign}(v_{c,i}) \cdot k_{flow} \cdot \frac{v_{flow,i}^2 \cdot \rho}{2} \cdot A_b \\ &= \text{sign}(v_{c,i}) \cdot k_{flow} \cdot \frac{A_b \cdot \rho}{2} \cdot \left(\left(v_{c,i} - \frac{\Delta\delta_{soil,i}}{\Delta t} \right) \cdot \frac{A_b}{A_{flow}} \right)^2 \quad [\text{N}] \end{aligned}$$

5) Calculate total reaction on soil;

$$Q_{soil,i} = Q_{w,i} + Q_{skirt,i} \quad [\text{N}]$$

6) Calculate soil displacements $\delta_{soil,i}$ and $\Delta\delta_{soil,i}$;

a) For $Q_{soil,i} < Q_{sd}$;

$$\delta_{soil,i} = \delta_{mob} \cdot (Q_i / Q_s)^2 \quad [\text{m}]$$

$$\Delta\delta_{soil,i} = \delta_{soil,i} - \delta_{soil,i-1} \quad [\text{m}]$$

b) For $Q_{soil} \geq Q_{sd}$ or $(Q_{soil} - Q_{sd}) / Q_{sd} \geq -0.0001$;

When $h_i > 0$ (i.e. skirts are not yet penetrated);

$$\Delta\delta_{soil,i} = -h_{i-1} + \Delta z_i + h_i \quad [\text{m}]$$

$$h_i = \frac{A_{flow,i} - A_h}{\pi \cdot D} \quad [\text{m}]$$

$$A_{flow,i} = \left(v_{c,i} - \frac{\Delta\delta_{soil,i}}{\Delta t} \right) \cdot A_b \cdot \sqrt{\frac{k_{flow} \cdot A_b \cdot \rho}{2 \cdot Q_{sd}}} \quad [\text{m}^2]$$

Note that iteration on $\Delta\delta_{soil,i}$ is required to solve for the unknown $A_{flow,i}$;

$$\delta_{soil,i} = \delta_{soil,i-1} + \Delta\delta_{soil,i} \quad [\text{m}]$$

When $h_i \leq 0$ (i.e. skirts are penetrating);

$$\Delta\delta_{soil,i} = \left(v_{c,i} - \frac{A_{flow,i}}{A_b} \cdot \sqrt{\frac{2 \cdot (Q_{sd} - Q_{skirt,i})}{k_{flow} \cdot A_b \cdot \rho}} \right) \cdot \Delta t \quad [\text{m}]$$

c) For unloading;

$$\Delta\delta_{soil,i} = (Q_{soil,i} - Q_{soil,i-1}) / k_u \quad [\text{m}]$$

7) Repeat steps 1. – 6. until convergence

8) Calculate total change in crane wire length;

$$\delta_{wire,i} = \sum \Delta z_i - \left[v_c \cdot t + d_0 \cdot \frac{1}{M_f} \cdot (\sin(\omega t + \varphi) - \sin \varphi) \right] \quad [\text{m}]$$

where v_c is the crane lowering velocity

9) Calculate new wire force;

$$Q_{wire,i} = Q_{wire,0} + k_{wire} \cdot \delta_{wire,i} \geq 0 \quad [\text{N}]$$

where k_{wire} is the crane wire stiffness as defined in Sec.5.

10) Calculate loss in kinetic energy;

$$\Delta E_i = \left(Q_{w,i} \cdot \frac{A_b - A_h}{A_b} + Q_{skirt,i} + Q_{sling,i} - W \right) \cdot \Delta z_i \quad [\text{Nm}]$$

It is assumed that the retardation from dynamic water pressure within the bucket does not act on the evacuation holes in the top plate, A_h .

$$E_{k,i} = E_{k,i-1} - \Delta E_{k,i} \quad [\text{Nm}]$$

11) Calculate new velocity;

$$v_{c,i+1} = \sqrt{2 \cdot E_{k,i} / m_d} \quad [\text{m/s}]$$

6.2.4.2 As the skirts penetrate, the penetration resistance and the global soil resistance should be updated to account for the increased resistance with increased penetration.

6.2.4.3 It should be noticed that a requirement for using the above method is that the crane lowering velocity is kept constant until the foundation comes to rest and is not increased when skirts start to penetrate.

6.2.5 Simplified method for foundations without skirts

6.2.5.1 In a simplified approach to check the foundation capacity for the seabed landing situation for a foundation without skirts one may neglect the beneficial effects of water cushion underneath the mud mat and the beneficial effect of the work performed by the crane wire.

6.2.5.2 Applied boundary conditions for the problem are then a structure with a given dynamic mass and submerged weight, a velocity at the impact with the seabed and a non-linear mobilisation of the bearing

capacity. A simplified equation to solve landing impact problem then becomes;

$$\frac{1}{2} M' v_{imp}^2 + W \cdot \delta_{soil} = \int_0^{\delta_{soil}} Q_{soil}(\delta) d\delta \quad [\text{Nm}]$$

6.2.5.3 Assuming the non-linear soil resistance being described as in Figure 6-2, the right side of equation 6.2.5.2 becomes;

$$\frac{2}{3} Q_{sd} \cdot \sqrt{\frac{\delta_{soil}^3}{\delta_{mob}}} \quad [\text{Nm}] \quad \text{for} \quad \delta_{soil} \leq \delta_{mob} \quad [\text{m}]$$

and

$$Q_{sd} \cdot (\delta_{soil} - \frac{\delta_{mob}}{3}) \quad [\text{Nm}] \quad \text{for} \quad \delta_{soil} > \delta_{mob} \quad [\text{m}]$$

6.2.5.4 Load coefficients should be included in the design dynamic mass and submerged weight, and material coefficients in the soil resistance as relevant. Normally the acceptance criteria would be;

$$\delta_{soil} \leq \delta_{mob} \quad [\text{m}]$$

in which case the requirements to the landing impact velocity becomes;

$$v_{imp} \leq \sqrt{\frac{(\frac{4}{3} Q_{sd} - 2W) \cdot \delta_{mob}}{M'}} \quad [\text{m/s}]$$

6.2.5.5 Other criteria may however be used based on an evaluation of consequences.

6.2.6 Simplified method for foundations with skirts on soft soil

6.2.6.1 For skirted foundations on soft soil where it is required that the skirts penetrate before the soil can resist the dynamic landing impact (or even the submerged weight of the installed subsea structure with foundation), it is necessary that sufficient areas for escape of water are provided so that the hydrodynamic pressure never exceeds the bearing capacity.

6.2.6.2 A conservative design can be performed by neglecting the beneficial effects on the impact from flexibility of crane wire and soil. The boundary conditions for the problem then becomes the impact velocity as the skirts start to penetrate, the gross foundation area, the area for escape of water, and the soil bearing capacity for a surface loading on the gross foundation area. The relation between impact velocity and required area for escape of water is then given by the following equation;

$$\frac{Q_{sd}}{A_b} \geq p_w = \frac{1}{2} k_{flow} \cdot \rho \cdot v_{imp}^2 \cdot (A_b / A_h)^2 \quad [\text{N/m}^2]$$

6.2.6.3 The requirements to area for escape of water for a desired landing velocity becomes;

$$A_h \geq \sqrt{\frac{k_{flow} \cdot \rho \cdot v_{imp}^2 \cdot A_b^3}{2 \cdot Q_{sd}}} \quad [\text{m}^2]$$

or if the area for escape of water is set, requirements to landing velocities becomes;

$$v_{imp} \leq \sqrt{\frac{2 \cdot Q_{sd} \cdot A_h^2}{k_{flow} \cdot \rho \cdot A_b^3}} \quad [\text{m/s}]$$

6.2.7 Application of safety factors

6.2.7.1 Application of safety factors should be evaluated in relation to the consequences of exceeding selected limits. Load coefficients may be applied to masses and corresponding submerged weights, and material coefficients should be applied to the soil resistance. When consequences are considered serious a load coefficient $\gamma_f = 1.3$ and a material coefficient $\gamma_m = 1.25$ should be applied.

6.2.8 Calculation of skirt penetration resistance

6.2.8.1 Calculation of skirt penetration resistance is required as input to seabed landing analyses, but is also required in order to evaluate the need for suction aided penetration and in order to determine the suction required.

6.2.8.2 The skirt penetration resistance shall be calculated as the sum of the vertical shear resistance, often noted as skin friction, along both sides of the skirts and the resistance against the skirt tip;

$$Q_{skirt} = A_s \cdot \int_0^d f(z) dz + A_t \cdot q_t(d) \quad [\text{N}]$$

where

Q_{skirt} = skirt penetration resistance [N]
 d = depth of penetration [m]
 A_s = friction area per meter depth [m²/m]
 A_t = skirt tip area [m²]
 $f(z)$ = skin friction at depth z [N/m²]
 $q_t(d)$ = tip resistance at the depth of penetration [N/m²]

6.2.8.3 In sand and over-consolidated clays the skin friction and tip resistances may most reliably be predicted by correlations to cone penetration resistance as;

$$f(z) = k_f \cdot q_c(z) \quad [\text{N}]$$

$$q_t(z) = k_t \cdot q_c(z) \quad [\text{N}]$$

where

$q_c(z)$ = cone penetration resistance as measured in a cone penetration test (CPT) [N]
 k_f = skin friction correlation coefficient [-]
 k_t = tip resistance correlation coefficients [-]

6.2.8.4 The most probable and highest expected values for the skin friction correlation coefficient k_f and tip resistance correlation coefficient k_t for clay and sand (North Sea condition) are given in Table 6-1.

6.2.8.5 Alternatively in less over consolidated clays the skin friction may be taken equal to the remoulded shear strength. The uncertainties should be accounted for by defining a range for the remoulded shear strength. The tip resistance may in clays be taken as 7.5 times the intact un-drained shear strength of the clay.

Table 6-1 Correlation coefficients for skin friction and tip resistance in sand and over-consolidated clay				
Correlation coefficient	Clay		Sand	
	Most probable	Highest expected	Most probable	Highest expected
Skin friction, k_f	0.03	0.05	0.001	0.003
Tip resistance, k_t	0.4	0.6	0.3	0.6

6.3 Installation by suction and levelling

6.3.1 Installation by suction

6.3.1.1 When suction is required to install skirted foundations it is important that the range for expected necessary suction is calculated in order to provide adequate equipment and to design the skirted foundation to resist the suction.

6.3.1.2 The skirt penetration resistance may be calculated as prescribed in 6.2.8 and may be applied in the estimation of required suction in order to provide the necessary penetrating force (in excess of the submerged weight).

6.3.1.3 The skirts as well as the mud mat shall be designed with respect to buckling for the upper estimate of the required suction.

6.3.1.4 As part of the foundation design it shall be checked that when applying suction, a soil plug failure is not achieved. Such failure will take place when the total skin friction on the outside of the skirts exceeds the reversed bearing capacity at the skirt tip level. This may be the case for suction anchors with high length to diameter ratio, also often called 'suction piles'.

6.3.1.5 The actual suction applied during installation should be continuously monitored and logged as a documentation of the installation performance.

6.3.2 Levelling by application of suction or overpressure

6.3.2.1 A subsea structure supported by three or more (typically four) individual skirted foundations may be levelled by applying pressure into the void between the mud mat and the soil at low corners, or by applying suction at high corners.

6.3.2.2 The procedures should be well planned, and the necessary suction and or overpressure to accomplish the levelling should be calculated.

6.3.2.3 When levelling a subsea structure with four foundations application of suction or overpressure should be performed at two neighbouring foundations at a time to avoid restraining of the structure.

6.3.2.4 The righting moment to achieve the levelling comes from differential pressures within the skirt foundation. The resistance to overcome is;

- The vertical soil skin friction and tip resistance due to penetration or rising of skirts.
- The resistance to rotate the skirts within the soil.
- The structural weight that contributes to increased overpressure or reduction in suction.

6.3.2.5 The vertical soil skin friction and tip resistance can be calculated, as described in 6.2.8. Skin friction may be taken equal in both directions. In clay a suction contribution below the tip should be considered when the skirts are moved upwards.

6.3.2.6 The resistance to rotate a skirt foundation within the soil will be the least of a '*local*' mode where soil resistance is mobilised on each side of the skirt walls and a '*global*' mode where the skirt foundation is rotated as a pile with the soil plug following the motions of the pile. Both modes can be studied using a simple pile model where at any level above skirt tip the maximum horizontal resistance equals the integrated resistance around the skirt periphery of passive and active pressures and horizontal shear resistance.

6.3.2.7 For the local mode resistance to both sides of the skirt wall should be included, whereas for the global mode resistance only to the outside should be included. For the global mode a horizontal resistance at the skirt tip reflecting shear off of the soil plug at skirt tip level should be included. The resistance can be implemented as p/γ -curves. The boundary condition for the analysis should be applied moment with no horizontal force at the 'pile top'.

6.3.2.8 Alternatively the resistance to rotate the skirts within the soil could be analysed with finite element analyses.

6.3.2.9 The skirt foundation including the mud mat should be checked structurally for the maximum foreseen suction or overpressure. Likewise the possible soil plug failure mode of a reversed bearing failure for high suction or a downward bearing failure for high overpressure should be checked.

6.3.2.10 For foundations with long skirts requiring suction to penetrate, levelling should normally be performed following the stage of self penetration, with a subsequent frequent adjustment of the level during the further penetration.

6.3.2.11 The levelling process should be carefully monitored and logged as a documentation of the installation performance.

6.4 Retrieval of foundations

6.4.1 Retrieval of skirted foundations

6.4.1.1 Retrieval of skirted foundation may be achieved by a combination of lifting and application of pressure underneath the mud mat. The total force to be overcome is the sum of submerged weights and soil resistance.

6.4.1.2 Skirted foundations intended to be removed should be equipped with a filter mat attached to the underside of the mud mat in order to prevent adhesion to the soil and to assure a distribution of applied pressure on the total area between the mud mat and the soil. The soil resistance will then only be vertical resistance towards the skirts.

6.4.1.3 The initial outside and inside skin friction may be calculated using methods developed for calculation of axial capacity of driven piles. In clay also a downwards tip resistance should be included. After the motion is initiated, the soil resistance may drop towards that used for calculation of skirt penetration.

6.4.2 Retrieval of non-skirted foundations

6.4.2.1 When retrieving non-skirted foundations the suction from the soil will have to be considered. Even on sandy soils suction will occur for a rapid lifting. Depending on the size of the area and the permeability of the sand, some seconds or minutes may be required to release the suction. This should be considered when establishing lifting procedures.

6.4.2.2 When lifting non-skirted foundations off clayey seabed, the suction will last so long that it will normally be unrealistic to rely on suction release. In addition to lifting the submerged weight of the structure, one will then have to overcome a reversed bearing failure in the soil. The magnitude of this additional soil resistance will be at least equal to the submerged weight of the structure.

6.4.2.3 If the structure has been installed with a high set down velocity, the resistance to overcome may be close to the dynamic impact load onto the soil during installation. This impact load may e.g. be evaluated by the method suggested in 6.2.5. If e.g. the impact load is twice the submerged weight of the structure, the required lifting load to free the structure will be three times the submerged weight. This should be taken into account when choosing and designing lifting equipment. The required lifting force may be reduced by lifting at one end of the structure or by use jetting in combination with the lifting.

6.5 References

- /1/ DNV Classification Note CN-30.4 (1992) "Foundations"
- /2/ NORSOK G-001 (2004) "Marine soil investigation"
- /3/ Blevins, R.D. (1984) "Applied Fluid Dynamics Handbook". Krieger publishing Company.

7 Towing Operations

7.1 Introduction

7.1.1 General

7.1.1.1 Towing is one of the most common marine operations. Most offshore development projects involve towing in one or several of its phases. Examples of tows are:

- rig move
- transport to site and positioning of large floating structure
- transport of objects on barge
- wet tow of subsea modules
- wet tow of long slender elements.

7.1.1.2 Classical surface tow of large volume structures is covered in section 7.2. Tow of submerged small volume structures or long slender structures is covered in Section 7.3.

7.1.2 Environmental restrictions

7.1.2.1 A tow operation may take several days due to the low transit speed, and the operation may either be classified as weather restricted or as unrestricted. Reference is given to *DNV-OS-H101, ref./I/*. A short description is however given in the following paragraphs.

7.1.2.2 For operation reference period, T_R , less than 72 hours a weather window can be established (weather restricted operation). Start of the operation is conditional to an acceptable weather forecast.

Guidance note:

The operation reference period should include both the planned operation period and an estimated contingency time;

$$T_R = T_{POP} + T_C$$

where

- T_R = Operation reference period
- T_{POP} = Planned operation period
- T_C = Estimated contingency time

---e-n-d---of---G-u-i-d-a-n-c-e---n-o-t-e---

7.1.2.3 For $T_R > 72$ hours the operation can be defined as weather restricted provided that:

- Continuous surveillance of actual and forecasted weather is specified in the operation procedures.
- Safe conditions for the towed object is established along the route (e.g. set down at seabed).
- The system satisfies ALS requirements for unrestricted weather conditions.

7.1.2.4 For operations with $T_R > 72$ hours, the operation normally needs to be defined as an unrestricted operation. Environmental criteria for these operations shall be based on extreme value statistics (see *DNV-OS-H101 ref./I/*).

7.2 Surface tows of large floating structures

7.2.1 System definition

7.2.1.1 Dynamic analysis of a tow requires information on geometry and mass properties of towed object and tug, towline data (weight, diameter, stiffness, bridle etc) and operational data including information on environmental conditions (wave, wind and current).

7.2.1.2 Figure 7-1 shows local and global co-ordinate systems and definition of angles for orientation of tug, towed object and towline to be used for static and dynamic analysis of towline in waves propagating in direction β .

7.2.1.3 The wave induced response of tug and towed object (and hence the dynamic tension in the towline) is a function of wave direction relative to the objects.

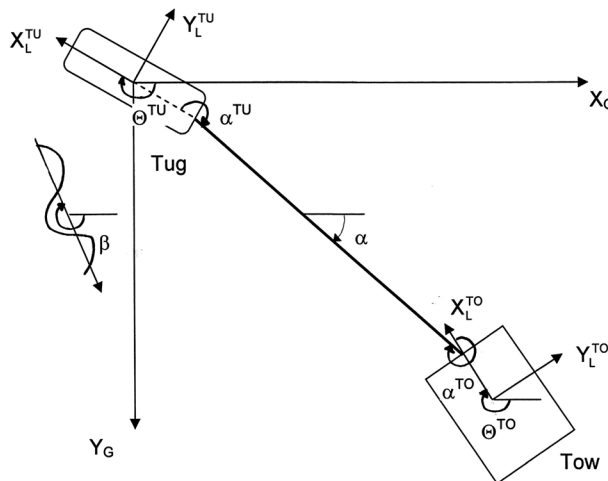


Figure 7-1
Definition of angles for orientation of tug, towed object and towline relative to global axes (X_G, Y_G)

7.2.2 Data for modelling and analysis of tows

7.2.2.1 Input data for analysis of surface tows are classified as tug and tow data, towline data and operational data as given below.

Tug and towed object data:

$H_j^{tug}(\omega, \theta)$	= motion transfer function in six degrees of freedom ($j = 1, 6$) for tug [-]
$H_j^{tow}(\omega, \theta)$	= motion transfer function in six degrees of freedom ($j = 1, 6$) for towed object [-]
\mathbf{r}_0^{tug}	= local position of towline end on tug [m]
\mathbf{r}_0^{tow}	= local position of towline end on tow [m]
B	= breadth of towed object [m]
L_b	= length of towed object [m]
T_b	= draft of towed object [m]

7.2.2.2 Towline data:

D	= hydrodynamic diameter of towline [m]
C_D	= hydrodynamic drag coefficient [-]
C_M	= hydrodynamic inertia coefficient [-]
A	= nominal area of towline (area of steel) [m ²]
S	= area of circumscribed circle = $\pi D^2/4$ [m ²]
c_F	= A/S = Fill factor [-]
E	= modulus of elasticity of towline [N/m ²]
ρ_s	= density of steel [kg/m ³]
m	= mass per unit length of towline [kg/m]
m_a	= added mass per unit length of towline [kg/m]
w	= submerged weight per unit length of towline [N/m]
W	= total submerged weight of towline [N]

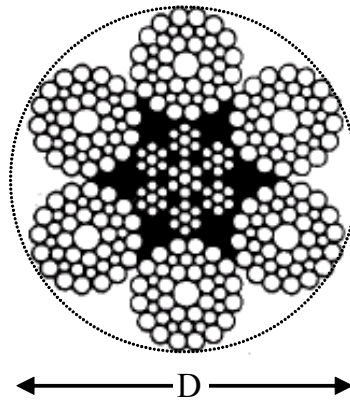


Figure 7-2
Example cross-section of steel wire towline with fill factor $c_F = 0.58$

Guidance note:

Note that modulus of elasticity of a steel wire towline is typically on the order of 40% of the modulus of elasticity of solid steel.

---e-n-d---of---G-u-i-d-a-n-c-e---n-o-t-e---

7.2.2.3 The submerged weight per unit length of the towline is given by

$$w = (m - c_F S \rho_w) g \quad [\text{N/m}]$$

where m is the structural mass per unit length in air, ρ_w is the water density and g is the acceleration of gravity. The total submerged weight of the towline is denoted $W = wL$.

7.2.2.4 Operational input data for tow analysis are:

U	= towing speed [m/s]
T_0	= towline tension [N]
L	= length of towline [m]
α	= towline direction [deg]
H_s	= significant wave height [m]
T_p	= spectrum peak period [s]
$S(\omega, \theta)$	= wave spectrum
β	= mean wave direction [deg]
V_c	= current velocity [m/s]
V_w	= wind velocity [m/s]

7.2.3 Static towline configuration

7.2.3.1 For a towing cable where the towline tension is much larger than the weight of the cable, $T_0/W > 1$, the horizontal $x(s)$ and vertical $z(s)$ coordinates along the towline can be approximated by the following parametric equations

$$x(s) = \left(1 + \frac{T_0}{EA}\right)s - \frac{1}{6} \left(\frac{w}{T_0}\right)^2 s^3 \quad [\text{m}]$$

$$z(s) = -z_m + \frac{1}{2} \frac{ws^2}{T_0} \left(1 + \frac{T_0}{EA}\right) \quad [\text{m}]$$

where s is the coordinate along the towline ($-L/2 < s < L/2$) and z_m is the sag of the towline,

$$z_m = \frac{L}{8} \left(\frac{wL}{T_0}\right) \left(1 + \frac{T_0}{EA}\right) \quad [\text{m}]$$

7.2.3.2 The approximate formulas in 7.2.3.1 give good estimates even when T_0 is comparable to the weight W of the towline. Usually $T_0 \ll EA$ so that the term T_0/EA can be neglected in the expressions above. A typical static geometry of a towline is shown in Figure 7-3.

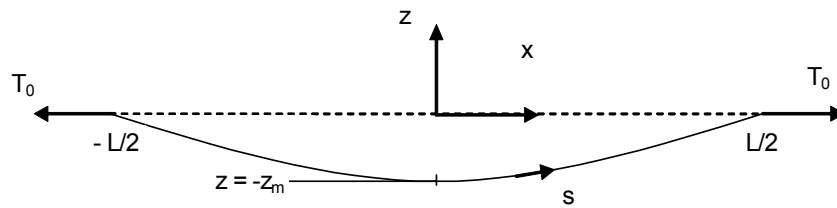


Figure 7-3
Geometry of towline

7.2.3.3 For towing in shallow water the towline length and towline tension should be controlled so that there is sufficient clearance between towline and sea bed;

$$z_m < d \text{ [m]}$$

where d is the water depth. Sliding contact between towline and sea bed may cause severe deterioration of towline strength.

7.2.4 Towline stiffness

7.2.4.1 The towline stiffness can be split into two components, one due to elastic elongation of the line and one due to the change of geometry of the towline catenary.

7.2.4.2 The stiffness due to elastic elongation of the towline is given by;

$$k_E = \frac{EA}{L} \text{ [N/m]}$$

where

A = nominal cross-sectional area of towline [m²]

E = modulus of elasticity of towline [N/m²]

L = length of towline [m]

7.2.4.3 The stiffness due to change of geometry is given by;

$$k_G = \frac{12T_0^3}{(wL)^2 L} \text{ [N/m]}$$

where

T_0 = towline tension [N]

w = submerged weight per unit length of towline [N/m]

L = length of towline [m]

7.2.4.4 The total stiffness k is given by the formula;

$$\frac{1}{k} = \frac{1}{k_E} + \frac{1}{k_G} \text{ [m/N]}$$

or

$$k = \frac{k_G k_E}{k_G + k_E} = \frac{k_E}{1 + k_E/k_G} \text{ [N/m]}$$

For very high towline tension, $k_G \gg k_E$, and the total stiffness can be approximated by the elastic stiffness $k \approx k_E$.

7.2.4.5 It should be noted that the force – displacement ratio given by the combined stiffness above is only valid for slow motion of the end points of the towline. For typical towlines this means motions with periods above 30 sec. For wave frequency motions, dynamic effects due to inertia and damping will be important.

7.2.5 Drag locking

7.2.5.1 When towing in waves the resulting oscillatory vertical motion of the towline may be partly restricted due to drag forces on the line, as if the towline was restricted to move within a narrow bent pipe. Hence, the geometric elasticity is “locked”. This phenomenon is called “drag-locking”. Drag-locking causes the apparent stiffness of the line to increase and the dynamic force is approximately the force which is obtained considering the elastic stiffness only.

7.2.6 Mean towing force

7.2.6.1 At zero velocity and in the absence of wind, waves and current, the tug will have maximum towing force equal to the continuous bollard pull. When the tug has a forward velocity some of the thrust is used to overcome the still water resistance of the tug. This resistance is partly due to viscous skin friction drag, pressure form drag and wave making drag. The available towing force decreases with forward velocity. Also, if the tug is heading into waves, wind or current, the net available towing force is reduced due to increased forces on the tug itself.

7.2.6.2 The towed object is in addition to wind forces and calm water resistance subject to wave drift forces F_{WD} , which may give an important contribution to the towing resistance. Wave drift force on a floating structure can be calculated by a wave diffraction program using a panel discretisation of the wetted surface.

7.2.6.3 The effect of waves can be taken into account by multiplying the continuous bollard pull by an efficiency factor (see *DNV-OS-H202, ref./2/*) depending on length of tug and significant wave height.

7.2.6.4 The wave drift force at zero towing speed can be approximated by the following simplified expression;

$$F_{wd} = \frac{1}{8} \rho_w g R^2 B \cdot H_s^2 \quad [\text{N}]$$

where typical reflection coefficients, R , are;

Table 7-1 Typical reflection coefficients.	
Square face	$R = 1.00$
Condeep base	$R = 0.97$
Vertical cylinder	$R = 0.88$
Barge with raked bow	$R = 0.67$
Barge with spoon bow	$R = 0.55$
Ship bow	$R = 0.45$

and

ρ_w = density of sea water, typically 1025 [kg/m³]
 g = acceleration of gravity, 9.81 [m/s²]
 H_s = the significant wave height [m]
 B = breadth of towed object [m]

Guidance note:

This simplified expression for wave drift force will in most cases give conservative results. Calculation by a wave diffraction program is recommended if more accurate results are needed.

---e-n-d---of---G-u-i-d-a-n-c-e---n-o-t-e---

7.2.6.5 The wave drift force increases linearly with the towing speed according to the formula

$$F_{WD}(U) = F_{WD}(0) + U \cdot B_{11} \quad [\text{N}]$$

where B_{11} is the wave drift damping. For more information on wave drift damping reference is made to *DNV-RP-C205, ref./4/*.

7.2.7 Low frequency motions

7.2.7.1 The tug and the towed object may experience low frequency (slow drift) motions due to slowly varying wave and wind forces. For the low frequency motions the towline will behave as a spring.

7.2.7.2 The eigenperiod of the slow drift motion is given by

$$T_0 = 2\pi \sqrt{\frac{M_s^{tug} + A_{11}^{tug}}{k \left(1 + \frac{M_s^{tug} + A_{11}^{tug}}{M_s^{tow} + A_{11}^{tow}} \right)}} \quad [\text{s}]$$

where

- k = towline stiffness defined in 7.2.4.4 [kg s⁻²]
 M_s^{tow} = structural mass of towed object [kg]
 A_{11}^{tow} = added mass of towed object in towline direction [kg]
 M_s^{tug} = structural mass of tug [kg]
 A_{11}^{tug} = added mass of tug in direction of towline [kg]

7.2.7.3 In most cases, for surface tows, the mass and added mass of the towed object is much larger than the mass and added mass of the tug so that the eigenperiod can be approximated by

$$T_0 = 2\pi \sqrt{\frac{M_s^{tug} + A_{11}^{tug}}{k}} \quad [\text{s}]$$

Guidance note:

The formulas for the eigenperiod of slow drift motion assume that the mass of the towline is much smaller than the mass of the tug and towed object.

---e-n-d---of---G-u-i-d-a-n-c-e---n-o-t-e---

Guidance note:

Guidelines for estimation of the actual slow-drift motion may be found in e.g. *DNV-RP-C205, ref./4/* and *DNV-RP-F205, ref./5/*.

---e-n-d---of---G-u-i-d-a-n-c-e---n-o-t-e---

7.2.8 Short towlines / propeller race

7.2.8.1 When short towlines are applied the tug propeller may induce flow velocities at the towed structure which increases the towing resistance significantly.

7.2.8.2 When the towed structure is small compared to the propeller race the force on each structural member of the towed structure can be estimated from the local flow velocity taking into account the increased velocity in the propeller race and drag force coefficients for normal flow.

7.2.8.3 For deeply submerged thrusters the propeller race can be approximated by an axi-symmetric turbulent jet with a radial velocity distribution

$$U(r; x) = U_m(x) \left[1 + 0.4142(r / r_{0.5}(x))^2 \right]^{-2} \quad [\text{m/s}]$$

where

$$U_m(x) = U_0 [0.89 + 0.149x / D]^{-1} \quad [\text{m/s}]$$

and

$$r_{0.5}(x) = 0.39D + 0.0875x \quad [\text{m}]$$

r is the radial distance from the centre of the jet at $x = -4.46D$ where D is the diameter of the propeller disk and U_0 is the flow velocity through the propeller disk, considered to be uniform. See Figure 7-4. Reference is made to /11/ and /15/ for details.

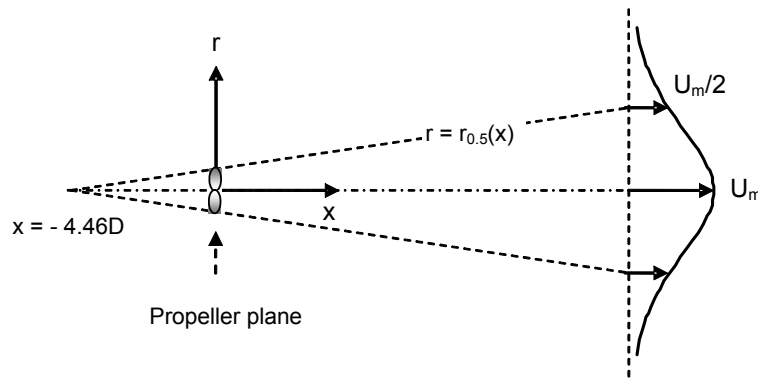


Figure 7-4
Propeller race modelled as an axis-symmetric jet

7.2.8.4 For towlines longer than 30 m, the effect of the propeller race is taken into account by reducing the available bollard pull by an interaction efficiency factor (ref. *DNV-OS-H202*);

$$\alpha_{int} = [1 + 0.015 A_{exp} / L]^{-\eta} \quad [-]$$

where

α_{int} = interaction efficiency factor
 A_{exp} = projected cross sectional area of towed object [m²]
 L = length of towline in metres [m]
 η = 2.1 for typical barge shapes

7.2.8.5 When the towed object is large compared to the dimensions of the propeller on the tug, a large part of the propeller race may be reversed by the towed object, hence reducing the net forward thrust on the system. Actually, the net forward thrust can become negative by this effect, so that the system of tug and tow move backward. Detailed calculation of this effect can be done by use of CFD.

7.2.9 Force distribution in a towing bridle

7.2.9.1 When the towed structure is rotated an angle α , the forces in each of the bridle lines will be different. See Figure 7-4. Assuming each bridle line forms an angle β with the towing line, and the towing force is T_0 , the distribution of forces in each bridle line for *small* rotation angles, is given by;

$$\frac{T_1}{T_0} = \frac{\sin(\beta + \alpha + \gamma)}{\sin 2\beta} \quad [\text{N/N}]$$

$$\frac{T_2}{T_0} = \frac{\sin(\beta - \alpha - \gamma)}{\sin 2\beta} \quad [\text{N/N}]$$

where

T_0 = towing force [N]
 T_1 = force in port bridle [N] (for rotation of towed object towards port. See figure 7-5)
 T_2 = force in starboard bridle [N] (for rotation of towed object towards port. See figure 7-5)
 L = length of towline, measured from bridle [m]
 R = distance from centre of gravity of towed structure to end of bridle lines [m]
 α = angle of rotation of towed structure [rad]
 β = angle between each of the bridle lines and the vessel centreline [rad]
 $\gamma = \frac{R}{L} \alpha$ [rad]

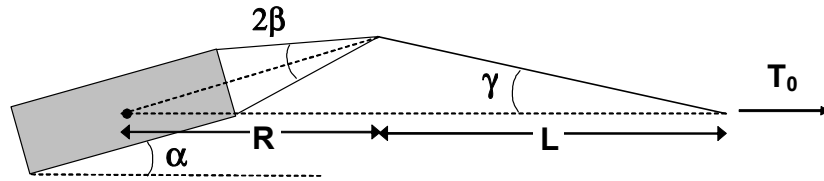


Figure 7-5
Layout of towline and bridle lines

7.2.9.2 The force in starboard bridle line becomes zero when

$$\alpha = \frac{L\beta}{L + R} \quad [\text{rad}]$$

7.2.9.3 For rotation angles greater than this value, one bridle line goes slack and only the other bridle line will take load.

7.2.9.4 The moment of the towing force around the rotation centre of the towed structure is given as;

$$M_G = T_0 R \left(1 + \frac{R}{L}\right) \alpha \quad [\text{Nm}]$$

and the rotational stiffness due to the towing force is given by;

$$C_{66} = T_0 R \left(1 + \frac{R}{L}\right) \quad [\text{Nm/rad}]$$

Hence, the bridle contributes with a substantial increase in the rotational stiffness, improving the directional stability of the tow.

7.2.10 Shallow water effects

7.2.10.1 The towed object will be subject to a set down effect (sinkage) because of the increased velocity past the object causing the pressure on the wetted surface to be decreased. This effect may be greatly increased in shallow, restricted water, such as a canal- or trench-type channel. The trim of the object will also be modified. This combined effect of sinkage and trim in shallow water is called the *squat*-effect. A semi-empirical relation for squat of a ship-like towed object is

$$\frac{z_{\max}}{T} = 2.4 \frac{C_b}{L/B} \frac{F_h^2}{\sqrt{1 - F_h^2}} \quad [\text{m/m}]$$

where

z_{\max} = squat (combined sinkage and trim) at bow or stern [m]

L = length of object [m]

B = beam of object at the maximum area [m]

T = draught of object [m]

C_b = ∇ / LBT [-], where ∇ is the displaced water volume.

F_h = the depth Froude number: $F_h = V / \sqrt{gh}$ [-]

V = $U - U_c$ is the relative speed [m/s]

g = gravitational acceleration [m/s²]

h = water depth [m]

U = towing speed [m/s]

U_c = current velocity (in e.g. a river) being positive in the direction of the tow route [m/s]

7.2.11 Dynamics of towlines

7.2.11.1 Analysis of towline dynamics involves independent motion analysis of tug and towed object in a given sea state and the resulting towline response. A winch can be used on the tug to reduce tension in the towline. The response of the winch and the towline is strongly non-linear and coupled (ref. 7.2.13).

7.2.11.2 Analysis of towline dynamics can be done in the frequency domain or time domain. A frequency domain method is computational efficient, but requires a linearised model of the system. A time-domain method can account for nonlinearities in the system, nonlinear wave induced response as well as nonlinear

towline dynamics.

7.2.11.3 Wave induced response of towed object and tug is well described by linear equations. Neither tug nor towed object is significantly influenced by the towline with respect to first order wave induced response. A frequency domain analysis can be used to obtain relative motion between tug and tow.

7.2.11.4 The following frequency domain solution method can be applied:

- First the static towline configuration is calculated. Static configuration is the basis for calculation of dynamic towline dynamics. Maximum sag depth is obtained from static analysis.
- The motion transfer functions for the line attachment points are calculated on tug and towed object respectively and the transfer function for the relative motion of the towline attachment points can be established. If the towed object is much larger than the tug, the relative motion will be dominated by the tug response, and the towed object transfer functions may be omitted.

7.2.11.5 The transfer function for relative motion η between tug and towed object in the towline secant direction is obtained by a linear transformation. See Figure 7-1.

$$H_{\eta}(\omega, \beta) = H_{\text{sec}}^{TU}(\omega, \beta^{TU}) - H_{\text{sec}}^{TO}(\omega, \beta^{TO}) \quad [\text{m/m}]$$

7.2.11.6 The relative towline motion transfer function is combined with the wave spectrum characterizing the actual sea state. The response spectrum for relative motion in the secant direction of the towline is obtained from;

$$S_{\eta}(\omega) = |H_{\eta}(\omega, \beta)|^2 S(\omega) \quad [\text{m}^2\text{s}]$$

where $S(\omega)$ is the wave spectrum.

Guidance note:

Assuming small wave induced rotations (roll, pitch and yaw) of tug and towed object, the motion transfer function for end point of towline is given by a linear combination of the rigid body motion transfer functions. The transfer function for motion in the secant (towline) direction is the component of the motion vector in this direction.

---e-n-d---of---G-u-i-d-a-n-c-e---n-o-t-e---

7.2.11.7 From the response spectrum an extreme representation of the relative motion can be generated. The most probable extreme value for the relative motion in a time interval T , usually taken as 3 hours, is;

$$\eta_{\max} \approx \sigma_{\eta} \sqrt{2 \ln(T/T_z)} \quad [\text{m}]$$

where

$\sigma_{\eta} = \sqrt{M_0}$ = standard deviation of the relative motion [m]

$T_z = 2\pi \sqrt{\frac{M_0}{M_2}}$ = zero up-crossing period [s]

$M_n = \int \omega^n S(\omega) d\omega$ = spectral moments [m^2/s^n]

7.2.11.8 An estimate of the extreme towline tension when towing in waves can be obtained by assuming drag locking (7.2.5) so that the effective stiffness is the elastic stiffness,

$$T_{\max} = T_0 + \eta_{\max} k_E \quad [\text{N}]$$

where T_0 is the mean towing force and k_E is the towline stiffness as given in 7.2.4.2. Hence, the extreme towline elastic tension decreases with increasing towline length.

7.2.12 Nonlinear time domain analysis

7.2.12.1 An alternative approach to the frequency domain method described above is to model the towline in a non-linear FEM analysis program and prescribe forced motions of the towline end points on tug and towed object respectively.

7.2.12.2 Time histories for the motions of the towline end points $x_p(t)$, $y_p(t)$, $z_p(t)$ are obtained by proper transformation of the rigid body motion transfer function for each of the tug and towed object and combining with a wave spectrum. For example, the time history of the motion in the x-direction of end point p is given by;

$$x_p(t) = \sum_k A_k |H_x^p(\omega_k)| \cos(\omega_k t + \varepsilon_k) \quad [\text{m}]$$

where A_k and ε_k are random amplitudes and phases as given in 2.2.3.1

$$A_k = \sqrt{2S(\omega_k)\Delta\omega_k} \quad [\text{m}]$$

and $H_x^p(\omega)$ is the transfer function for motion in x-direction of end point p . Examples of simulated motions of towline end points at tug and towed object for head waves and no current are shown in Figures 7-6 and 7-7. Resulting towline tension at tug and towed object are shown in Figure 7-8. Minor differences between the two curves at peaks are due to dynamic effects in towline.

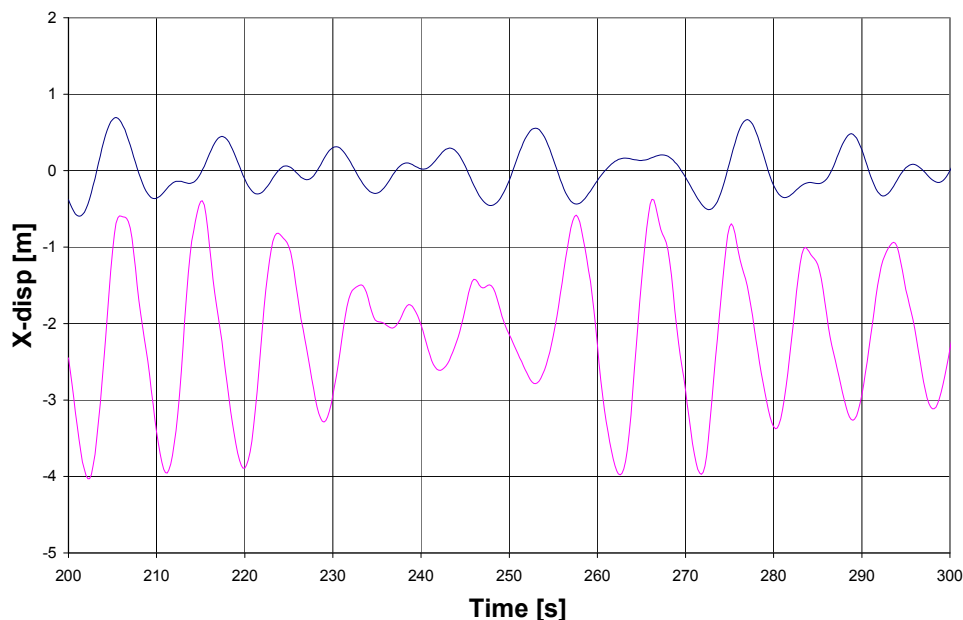


Figure 7-6
Example of simulated horizontal motion of towed object (upper curve) and tug (lower curve) in a given sea state

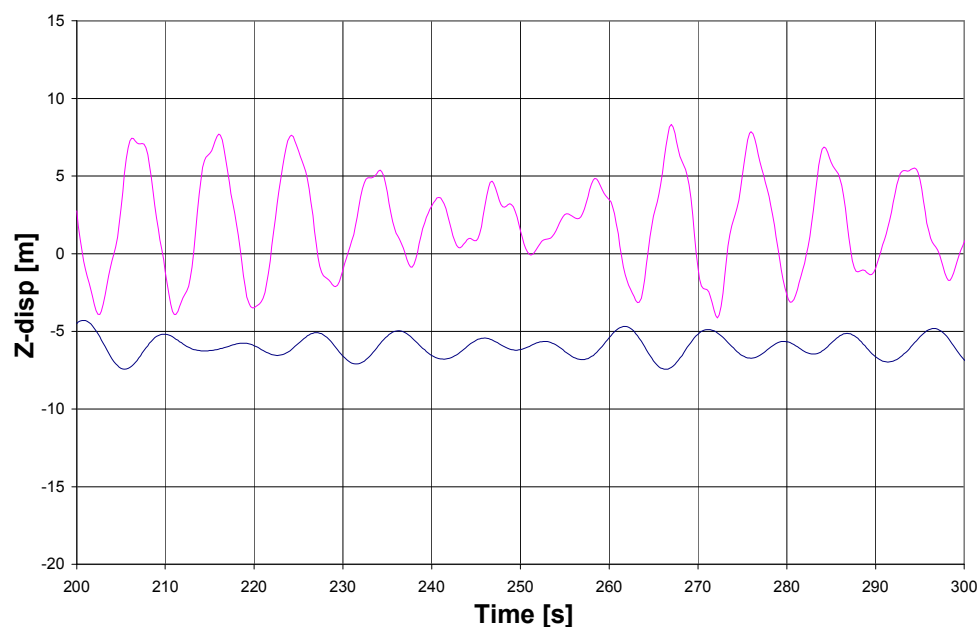


Figure 7-7
Example of simulated vertical motion of towed object (lower curve) and tug (upper curve) in a given sea state

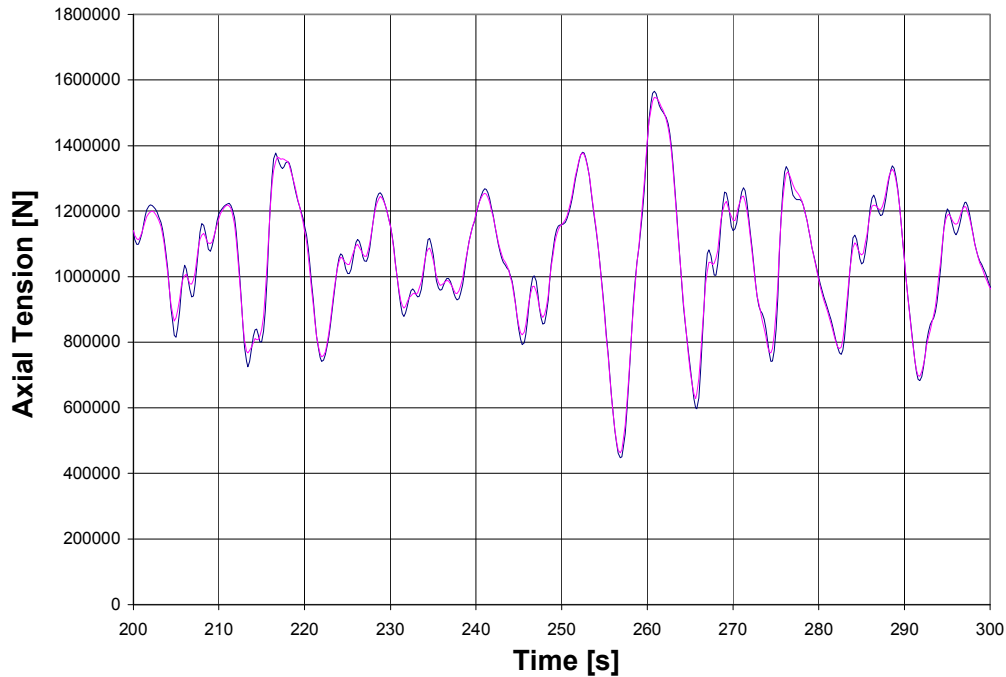


Figure 7-8
Example of simulated axial towline tension at endpoints. Mean tension is $T_0 = 1.0$ MN
(i.e. ≈ 100 tonnes bollard pull).

7.2.13 Rendering winch

7.2.13.1 An automatic rendering winch (Figure 7-9) can be designed to reduce extreme towline tension. The winch is designed to start rendering when the towline tension exceeds a specified limit. A detailed analysis of a coupled towline-winch system during forced excitation was presented in *Ref. /13/*.

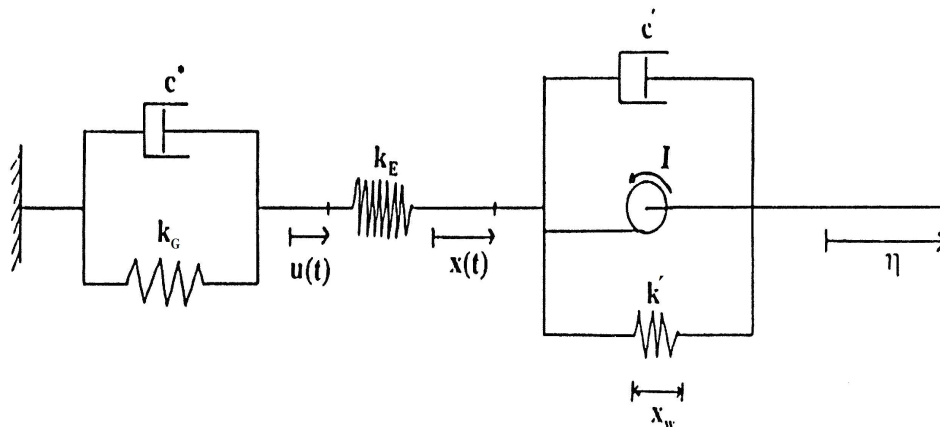


Figure 7-9
Coupled towline – winch model (from *Ref. /13/*).

7.2.13.2 A simplified towline model is based on the assumption that the shape of the dynamic motion is equal to the change in the static towline geometry. Mass forces are neglected. This leads to the following equation for the line motion;

$$c^* \dot{u} + k^* u = k_E x \quad [\text{N}]$$

where

u = displacement of the towline [m]

c^* = generalised line damping [kg/m]

k^* = $k_E + k_G$ = generalised towline stiffness [N/m]

k_E = elastic stiffness [N/m] (7.2.4.2)

k_G = geometric stiffness [N/m] (7.2.4.3)

x = tangential motion excitation at end of towline [m]

7.2.13.3 The rendering winch is modelled by an equivalent mass, damping and stiffness with the equation of motion;

$$m' \ddot{x}_w + c' \dot{x}_w + k' x_w = T_0 + T_d(t) \quad [\text{N}]$$

when the winch is rendering, and where

T_0 = static tension [N]

$T_d(t)$ = dynamic tension [N]

x_w = winch pay-out coordinate [m]

m' = equivalent winch mass ($= I/r^2$ where I is the winch mass moment of inertia and r is the radius of the winch) [kg]

c' = equivalent velocity dependent winch damping coefficient ($= c_w/r^2$ where c_w is the winch damping coefficient) [kg/s]

k' = equivalent position dependent winch stiffness coefficient ($= k_w/r^2$ where k_w is the winch stiffness coefficient) [N/m]

When the winch is stopped

$$\dot{x}_w = 0 \quad [\text{m/s}]$$

7.2.13.4 The winch starts rendering when the total tension $T_0 + T_d(t)$ exceeds the winch rendering limit F .

7.2.13.5 Assuming the towline leaves the winch horizontally, the tangential motion of the towline end is given by;

$$x = \eta - x_w \quad [\text{m}]$$

where η is the relative motion between tug and tow. The towline dynamic tension can be expressed as;

$$T_d = k_E(x - u) \quad [\text{N}]$$

7.2.13.6 Combining the equations in 7.2.13.2 and 7.2.13.3 yields the equations of motion for the coupled towline-winch model

$$m' \ddot{x} + c' \dot{x} + (k' + k)x = f(t) \quad [\text{N}]$$

where

$$f(t) = k_E u(t) + m' \ddot{\eta}(t) + c' \dot{\eta}(t) + k' \eta(t) - T_0 \quad [\text{N}]$$

This equation is coupled with the towline response model in 7.2.12 giving the towline response u as a function of the end point displacement x .

7.3 Submerged tow of 3D objects and long slender elements

7.3.1 General

7.3.1.1 Three different tow configurations will be covered in this chapter;

- 1) Submerged tow of objects attached to Vessel
- 2) Submerged tow of objects attached to Towed Buoy
- 3) Surface or sub-surface tow of long slender elements, e.g. pipe bundles.

7.3.1.2 Submerged tow of objects is an alternative to offshore lift installation. Reasons for selecting such installation method may be;

- to utilise installation vessels with limited deck space or insufficient crane capacity
- to increase operational up-time by avoiding offshore operations with low limiting criteria such as lifting off barges and/or lowering through the splash zone

7.3.1.3 Surface or sub-surface tow of long slender elements are established methods for transportation to field. Acceptably low risk for damage during the transportation phase must be ensured.

7.3.1.4 The following steps are involved in the tow operation:

- inshore transfer to towing configuration
- tow to offshore installation site

— offshore transfer to installation configuration.

This chapter covers the tow to offshore installation site.

7.3.2 Critical parameters

7.3.2.1 Examples of critical parameters to be considered in modelling and analysis of a submerged tow could be:

- vessel motion characteristics
- wire properties
- towing speed
- routing of tow operation (limited space for manoeuvring, varying current condition)
- directional stability of towed object as function of heading
- forces in hang-off wire, slings and towing bridle
- clearance between object and tow vessel
- clearance between rigging and vessel
- VIV of pipe bundles and slender structures (e.g. spools, structure/piping)
- lift effects on sub-surface towed structures
- wave loads on surface towed bundles (extreme and fatigue loading).

In order to calculate/simulate these effects a time domain analysis is necessary.

7.3.3 Objects attached to Vessel

7.3.3.1 Objects attached to vessel in e.g. a hang-off frame (Figure 7-10) are mainly influenced by forward speed and the vertical wave frequency motion (heave, roll and pitch) of the installation vessel.

7.3.3.2 Initially one should determine whether long crested or short crested sea is conservative for the analysis in question. For head sea short crested sea will give increased roll motion compared to long crested sea, while long crested sea will give increased pitch motion compared to short crested sea (*ref. DNV-OS-H102*).

7.3.3.3 From simulations it is seen that coupling effects may be important even for small objects. The object tends to dampen the vessel motions with reduced force in hoist wire as a result. An uncoupled analysis will therefore be conservative.

7.3.3.4 With increased size of object (mass, added mass etc.) the discrepancies can be large and a coupled analysis will thus describe the vessel behaviour more correctly.

7.3.3.5 If the object is located in e.g. a hang-off frame on the side of the vessel the weight of the object will make the vessel heel. This heeling can be counteracted by including a righting moment in the analyses. In effect this models the ballasting that will be performed to keep the vessel on even keel.

7.3.3.6 If the object is hanging in a rigging arrangement through the moon pool of the vessel, particular attention should be given to check clearance between rigging and moon pool edges.

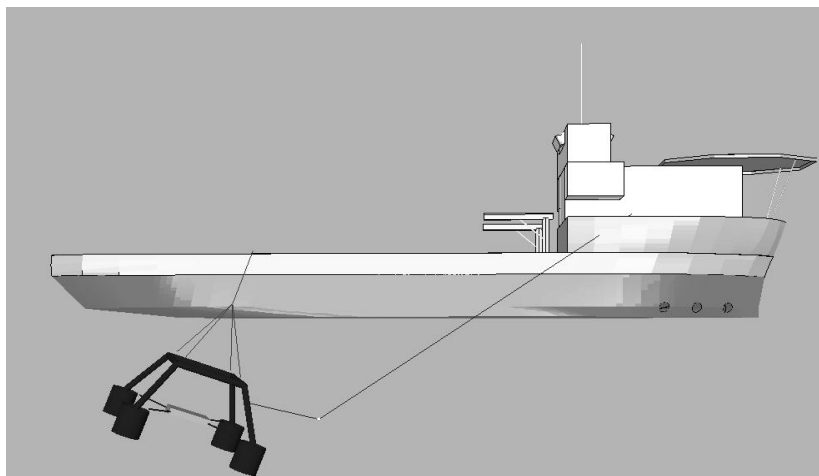


Figure 7-10
Submerged object attached to vessel

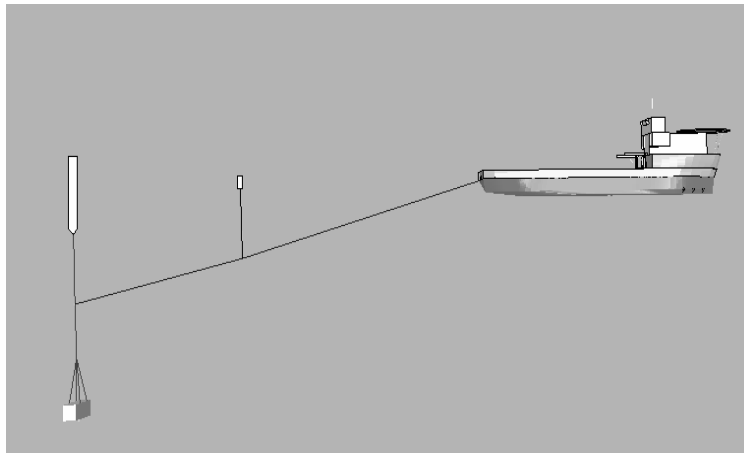


Figure 7-11
Submerged object attached to towed buoy (not to scale)

7.3.4 Objects attached to Towed Buoy

7.3.4.1 For objects attached to Towed Buoy (Figure 7-11) the dynamic forces on object and rigging is not affected by wave induced vertical vessel motions.

7.3.4.2 The buoy itself can be designed with a small water plane area relative to its displacement reducing the vertical wave induced motion of the buoy.

7.3.4.3 Since vessel roll motions do not influence the behaviour of the buoy, long crested sea will be conservative for this analysis.

7.3.5 Tow of long slender elements

7.3.5.1 Examples of slender objects that may be towed to field are;

- pipelines, bundles, spools
- TLP tethers
- riser towers / hybrid risers.

Several slender objects may be towed together as a bundle (strapped together or within a protective casing).

7.3.5.2 Tow of long slender elements are normally performed by one of the following methods:

- 1) Off-bottom tow uses a combination of buoyancy and ballast chains so that the towed object is elevated above the seabed. Ballast chains are used to keep the tow near the seabed and provide sufficient submerged weight and stability.
- 2) Deeply submerged, or Controlled Depth Tow (CDT) method is a further development of the off-bottom tow method. By careful design of towline length, holdback tension, buoyancy, ballast and drag chains with their specific hydrodynamic properties, the towed object will be lifted off the seabed at a critical tow speed to be towed at a 'controlled depth' above obstructions on sea bed, but below the area with strong wave influence.
- 3) Surface or near-surface towing methods for transport of long slender elements over short or long distances. For surface tows the towed object will be influenced by wave loads. Buoyancy elements are often used. See Figure 7-12.

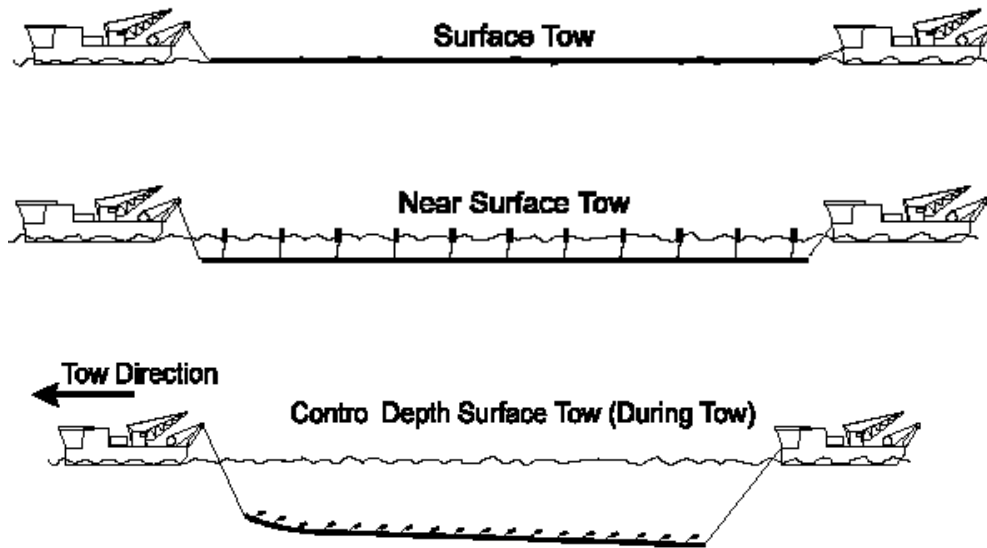


Figure 7-12
Different methods for tow of long slender objects

7.3.5.3 The tow configuration is dependent on:

- Submerged weight in water
- Use of temporary buoyancy/weight
- Tow speed and towline length
- Back tension provided by trailing tug
- Drag loading due to current.

7.3.5.4 Lift effects and stability may impede the control of a sub-surface towed bundle. Particular attention should be given to non axi-symmetrical cross section, tow-heads or other structures attached to the bundle

7.3.5.5 It is important to minimize fatigue loading on the pipe due to tug motions and direct wave action. In order to minimize direct wave action the tow depth of the towed object should be deeper when towing in sea-states with high peak periods since long waves have an effect further down in the water column.

Guidance note:

The wave induced velocity is reduced with a factor e^{kz} downwards in the water column, where $k = 2\pi/\lambda$ is the wave number and λ is the wave length. Hence, at tow depth equal to $\lambda/2$ the energy is only 4% of the value at the surface.

---e-n-d---of---G-u-i-d-a-n-c-e---n-o-t-e---

7.3.6 System data

7.3.6.1 The following system data is necessary in order to perform a time domain analysis for a submerged tow concept:

- *Vessel data*: Mass properties (mass, buoyancy, COG, radius of inertia, draught, trim) and hull geometry. These data will be input to 3D diffraction analysis.
- *Buoy data*: Mass properties (mass, buoyancy, COG, radius of inertia, draught) and hull geometry.
- *Towed object data*: Mass properties (mass, buoyancy, COG, radius of inertia) and General Arrangement (GA) drawing (incl. size of structural members) for establishment of analysis model, stiffness properties, drag and lift effects.
- *Rigging data*: Mass properties (mass, buoyancy) of any lumped masses such as crane hook. Geometry and stiffness.
- *Tow line/bridle data*: Mass properties (mass, buoyancy), any lumped masses, geometry and stiffness.
- *Operational data*: Towing speed, vessel heading, current speed/heading, wave heading and sea states.

7.3.7 System modelling

7.3.7.1 Vessel force transfer functions and hydrodynamic coefficients for all 6 degrees of freedom should be calculated by 3D wave diffraction analysis.

7.3.7.2 For the buoy, in the towed-buoy concept, it is important to apply a model that describes the combined

surge/pitch motion correctly. Further, the effect of trim on the heave motion should also be included. In order to capture these effects a Morison model may be suitable. This is valid for long and slender buoys. Possible forward speed effects should be included.

7.3.7.3 For towed objects attached to vessel or towed buoy, a Finite Element (FE) model of the rigging (slings and hoist wire) and/or the tow line and bridle is normally not necessary. In such cases it may be sufficient to model the lines using springs.

7.3.7.4 In most cases it is recommended that the towed object is modelled by Morison elements with added mass and drag properties for the different basic elements such as cylinders, plates etc. It is important to assure that correct mass and buoyancy distribution is obtained. The towed object should be modelled as a 6DOF body with the Morison elements distributed over the structure to capture the correct dynamic load distribution between the slings.

7.3.7.5 For tow of long slender objects like bundles, the structure should be modelled in a finite element (FE) program. In this case, fatigue loading can be decisive, and the global behaviour of the structure under dynamic loading has to be assessed.

7.3.8 Vortex induced vibrations

7.3.8.1 For slender structures such as bundles, spools, piping etc. special consideration should be given to identify whether vortex induced vibrations (VIV) will be a problem.

7.3.8.2 Eigenmodes for the slender structures can be calculated in a FE program. The eigenmodes are the “wet” eigenmodes including the effect of added mass from surrounding water. If one of the eigenfrequencies f_n of the structure is close to the vortex shedding frequency, vortex induced vibrations may occur and possible fatigue due to VIV during the tow-out operation should be further evaluated.

Guidance note:

For long slender structures submerged in water, vortex induced vibrations may occur if the $3 < V_R < 16$, where

$V_R = U/(f_n D)$ is the reduced velocity
 U = Relative velocity between tow speed and current [m/s]
 f_n = natural frequency [Hz]
 D = Slender element diameter [m]

Further guidance on calculating VIV response is given in *DNV-RP-C205*.

---e-n-d---of---G-u-i-d-a-n-c-e---n-o-t-e---

Guidance note:

The first natural frequency of a simply supported beam may be taken as;

$$f_1 = 1.57 \sqrt{\frac{EI}{m' L^4} \left[1 + 0.8 \left(\frac{\delta}{D} \right)^2 \right]} \quad [\text{s}^{-1}]$$

where EI is the bending stiffness, m' is the total mass per unit length (including added mass), L is the span length, δ is the static deflection (sag) and D is a characteristic cross-sectional dimension (diameter). The static deflection δ due to a uniform current can be estimated as

$$\delta = \frac{5}{384} \frac{q L^4}{EI}$$

where q is the sectional current drag force.

---e-n-d---of---G-u-i-d-a-n-c-e---n-o-t-e---

7.3.8.3 If it is found that the towed object is susceptible to VIV, one should either document that the resulting damage is acceptable, or alter the configuration in such a way that the eigenperiods are reduced to avoid VIV. This can be done by supporting the structure or part of it which is susceptible to VIV to make it stiffer.

Guidance note:

Unless otherwise documented, it is recommended that no more than 10% of the allowable fatigue damage is used in the installation phase, irrespective of safety class. This is according to industry practice.

---e-n-d---of---G-u-i-d-a-n-c-e---n-o-t-e---

7.3.9 Recommendations on analysis

7.3.9.1 It is recommended to use a time domain analysis in order to capture the important physical effects (ref. 7.3.2.1). Frequency domain analysis may be used in planning phase for parameter studies and to obtain quick estimates of the response for various towing configurations. Frequency domain analysis may also be used for

fatigue analysis of long duration tows encountering different sea states during the tow.

7.3.9.2 The duration of the time simulation should be sufficient to provide adequate statistics. It is recommended to perform 3 hour simulations in irregular sea states.

7.3.9.3 Some analysis programs may require very long simulation time for a full 3 hour simulation, and full time simulations for a wide range of sea states and wave headings may therefore not be practical. For these programs a method with selection of characteristic wave trains can be applied.

7.3.9.4 A consistent selection is to compute time series of the vertical motion at the suspension point (e.g. the hang off frame) and then select wave trains that coincide with the occurrence of maximum vertical velocity and maximum vertical acceleration.

7.3.9.5 Special considerations should also be given to the selection of wave trains for calculation of minimum clearance to vessel side and moon pool edges.

7.3.9.6 It is recommended to perform one 3 hour check for the worst limiting cases in order to verify that the selection method give results with approximately correct magnitude.

7.3.9.7 It is important to establish the design limitations for each weather direction.

7.3.9.8 A heading controlled vessel will not be able to keep the exact same direction continuously. It is therefore important that the analyses are performed for the intended direction ± 15 degrees.

Guidance note:

If long crested sea is applied, a heading angle of $\pm 20^\circ$ is recommended in order to account for the additional effect from short crested sea.

---e-n-d---of---G-u-i-d-a-n-c-e---n-o-t-e---

7.3.9.9 It is important to check the results versus established acceptance criteria, such as:

- minimum and maximum sling forces
- clearance between object and vessel
- stability during tow
- VIV of slender structures. For bundles VIV may cause significant fatigue damage.

7.3.9.10 For long slender elements an important result from the analyses will be to determine the optimal tow configuration (tow depth, use of temporary buoyancy/weight, tension in the bundle etc.).

7.3.9.11 Visualisation of results is beneficial. In this way unphysical behaviour, such as large deflections from initial position and large rotations, can be detected.

7.3.10 Wet anchoring

7.3.10.1 Off-bottom tows of long slender objects over long distances may be aborted due to adverse weather conditions and the bundle left in anchored position close to sea bed. See Figure 7-13. Anchors are usually attached to the end of the bundle. In anchored position the bundle will be exposed to current forces. The bundle is stabilized by the friction forces between ballast chains and the sea bed. Typical friction coefficients for anchor chain is given in Table 7-2.

Table 7-2 Friction coefficients between chain and sea bed		
Sea bed condition	Friction coefficient	
	Static	Sliding
Sand	0.98	0.74
Mud with sand	0.92	0.69
Firm mud	1.01	0.62
Soft mud	0.90	0.56
Clay	1.25	0.81

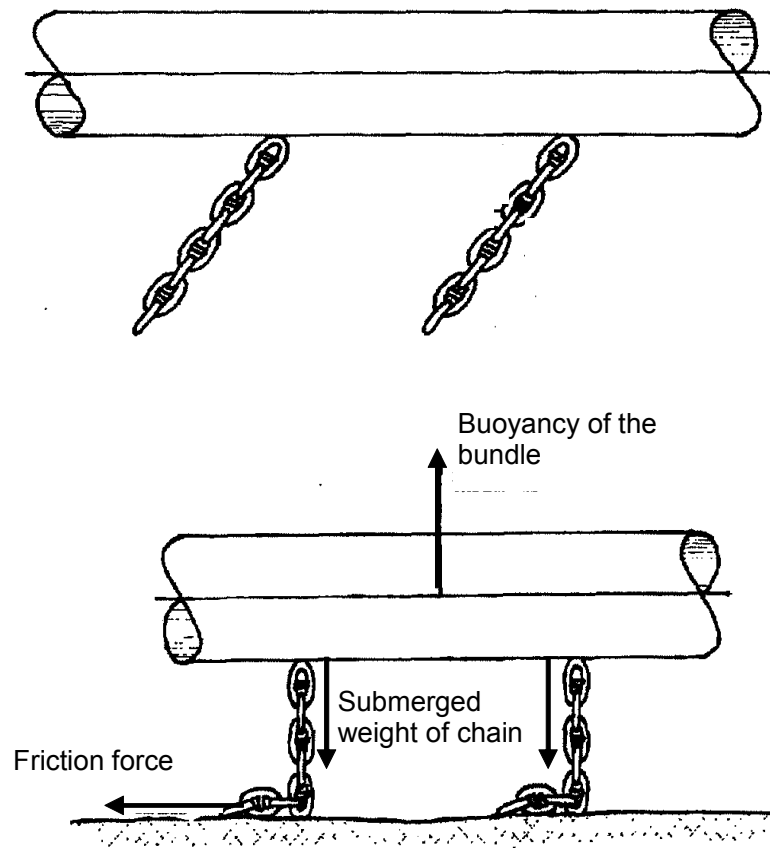


Figure 7-13
chains during tow (upper) and in off-bottom mode (lower)

7.4 References

- /1/ DNV Offshore Standard DNV-OS-H101, "Marine Operations, General" (planned issued 2010, see ref./3/ until release).
- /2/ DNV Offshore Standard DNV-OS-H202, "Marine Operations, Sea Transports" (planned issued 2010, see ref./3/ until release).
- /3/ DNV Rules for Planning and Execution of Marine Operations (1996).
- /4/ DNV Recommended Practice DNV-RP-C205 "Environmental Conditions and Environmental Loads", April 2007.
- /5/ DNV Recommended Practice DNV-RP-F205 "Global Performance Analysis of Deepwater Floating Structures", October 2004.
- /6/ Binns, J.R., Marcollo, H., Hinwood, J. and Doctors, L. J. (1995) "Dynamics of a Near-Surface Pipeline Tow". OTC 7818, Houston, Texas, USA.
- /7/ Dercksen A. (1993) "Recent developments in the towing of very long pipeline bundles using the CDTM method". OTC 7297, Houston, Texas, USA.
- /8/ Fernandez, M.L. (1981) "Tow techniques for offshore pipe laying examined for advantages, limitations". Oil & Gas Journal, June 22, 1981.
- /9/ Headworth, C., Aywin, E. and Smith, M. (1992) "Enhanced Flexible Riser Installation – Extending Towed Production System Technologies". Marine Structures 5, pp. 455-464.
- /10/ Knudsen, C. (2000) "Combined Riser-Bundle-Template Installed by Controlled Depth Tow Method". Proc. 10th Int. Offshore and Polar Eng. Conf., Seattle, May 28-June 2, 1990.
- /11/ Lehn, E. (1985) "On the propeller race interaction effects". Marintek Report P-01, 85. Trondheim, 1985.
- /12/ Ley, T. and Reynolds, D. (2006) "Pulling and towing of pipelines and bundles". OTC 18233. Offshore Technology Conference, Houston, Texas, USA, 1-4 May 2006.
- /13/ Moxnes, S. and Fylling, I. J. (1993) "Dynamics of Offshore Towing Line Systems". Offshore 93 – Installation of Major Offshore Structures and Equipment.
- /14/ Moxnes, S. (1993) "Dynamikk i slepelinor under slep av offshore konstruksjoner". Norske Sivilingeniørers Forening. (In Norwegian)
- /15/ Nielsen, F.G (2007) "Lecture notes in marine operations". NTNU, Trondheim.
- /16/ Risøy, T., Mork, H., Johnsgard, H. and Gramnæs, J. (2007) "The Pencil Buoy Method – A Subsurface Transportation and Installation Method". OTC 19040, Houston, Texas, USA, 30 April – 3 May 2007, 2007.

- /17/Rooduyn, E. (1991) “Towed Production Systems – Further developments in design and installation”. Subsea International’91, 23 April 1991, London, UK.
- /18/Song, R., Clausen, T. and Struijk, P. (2001) “Design and Installation of a Banded Riser System for a North Sea Development”. OTC 12975. Houston, Texas, USA.
- /19/Watters, A. J., Smith, I. C. and Garrett, D. L. (1998) “The lifetime dynamics of a deep water riser design”. Applied Ocean Research Vol. 20., pp. 69-81.

8 Weather Criteria and Availability Analysis

8.1 Introduction

8.1.1 Weather conditions

8.1.1.1 Information about weather conditions required for carrying out marine operations depends on the type of operation, e.g. drilling, pipeline installation, offshore offloading, installation of a platform, crane operations or subsea installation.

8.1.1.2 Relevant environmental parameters for carrying out marine operations as well as recommendations and requirements for description of environmental conditions are given in *DNV-OS-H101*.

8.1.2 Planning and execution

8.1.2.1 Marine operations consist of two phases:

- design and planning
- execution of the operations.

8.1.2.2 The design and planning phase shall select seasons when the marine operations can be carried out and provide weather criteria for starting and interrupting the operations (the availability analysis). The analysis shall be based on historical data covering a time period of at least 5-10 years.

8.1.2.3 Execution of marine operations shall be based on the weather forecast, the Near Real Time (NRT) data (data with a time history 1-5 hours) and, if justified, on Real Time (RT) data (data with a time history 0-1 hours).

8.2 Environmental parameters

8.2.1 General

8.2.1.1 For marine operations the time history of weather conditions and duration of weather events are the key parameters. Weather criteria and availability analysis shall include identified environmental parameters critical for an operation and provide duration of the events for exceeding and not exceeding the threshold limits of these parameters.

8.2.1.2 Threshold limits of environmental parameters critical for carrying out an operation and its sub-operations, time for preparing the operation as well as the duration of each sub-operation need to be specified prior to the start of an operation. These values will depend upon the type of operation and on critical responses.

Guidance note:

If a maximum response limit (X_{max}) is defined for an operation, the corresponding significant wave height limits (threshold values) must be found, for varying wave period and wave direction. Assuming the Pierson-Moskowitz spectrum, a linear response and a constant zero-up-crossing wave period, T_z , and wave direction, the response will be proportional to the significant wave height H_s . Then the response can be calculated for $H_s = 1$ m for all zero-up-crossing wave periods observed in the statistical data. The maximum H_s for each T_z is then scaled according to:

$$H_{s,max}(T_z) = \frac{X_{max}}{X(T_z)_{H_s=1}} H_s(T_z) \quad [\text{m}]$$

---e-n-d---of---G-u-i-d-a-n-c-e---n-o-t-e---

8.2.2 Primary characteristics

8.2.2.1 Often the significant wave height exceeding a given threshold level, as shown in Figure 8-1, will be the primary parameter. Threshold limits for other environmental parameters (e.g. corresponding wave periods) relevant for carrying out a marine operation may be established based on joint probabilities.

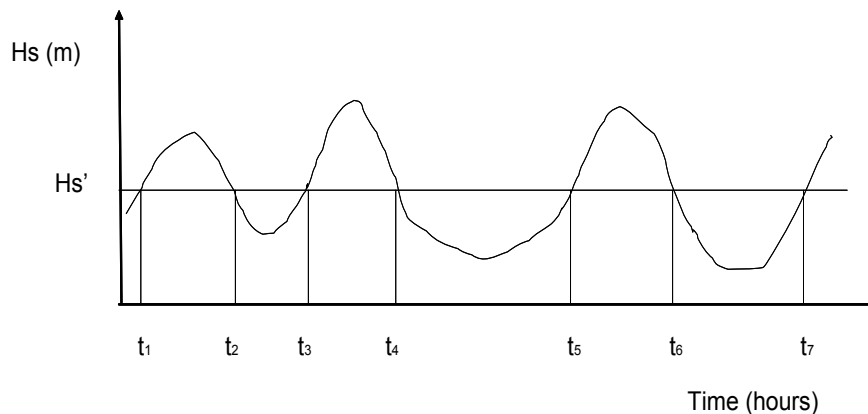


Figure 8-1
Example of significant wave height variation in time

8.2.2.2 The duration of a weather event is defined as the time between a crossing of a level for that parameter and the next crossing of the same level. See Figure 8-1. The event can be defined as above the level (from t_1 to t_2 , $H_S > H_S'$) or below the level (from t_2 to t_3 , $H_S < H_S'$). The events below the threshold level are often called “calm” periods and above the threshold level “storm” periods. Events going to the end of the data series shall not be included in the statistics.

Guidance note:

The duration of the first “calm” period is $\tau_{c1} = t_3 - t_2$ and the corresponding first “storm” period $\tau_{s1} = t_2 - t_1$. The total period considered is $T_{tot} = \sum (\tau_{ci} + \tau_{si})$. Prior to starting marine operations a number of days necessary for operations without interruption shall be approximated.

---e-n-d---of---G-u-i-d-a-n-c-e---n-o-t-e---

8.2.2.3 General weather related requirements for marine operations are given in *DNV-OS-H101, ref/7/*.

8.2.3 Weather routing for unrestricted operations

8.2.3.1 For marine operations involving transportation, e.g. towing, an optimal route is recommended to be decided. Environmental conditions necessary for evaluating critical responses along different alternative routes shall be provided and used in the analysis. Usually they will represent scatter diagrams of significant wave height and zero-up-crossing wave (or spectral peak) period.

8.2.3.2 In the design and planning phase an optimal route is recommended to be selected based on evaluation of responses and fatigue damage along different alternative routes, /2/. Global environmental databases may be utilized for this purpose.

8.2.3.3 Weather routing may also be performed during the execution of the transportation itself on the basis of weather forecasting. Bad weather areas or critical weather directions may then be avoided by altering speed and direction of the vessel. Due to the implicit possibilities of human errors or forecast errors, there is however a certain risk of making wrong decisions, /22/. On-route weather routing should therefore be used with care.

8.3 Data accuracy

8.3.1 General requirements

8.3.1.1 The weather criteria and availability analysis shall be based on reliable data and accuracy of the data shall be indicated. The data applied shall be given for a location or an ocean area where an operation takes place. It is recommended to use reliable instrumental data, if available, or data generated by recognized weather prediction models. Further, it is recommended that the data are sampled at least each 3rd hour and interpolated between the sampling intervals. General requirements to collection of metocean data are given in ref. /23/.

8.3.2 Instrumental data

8.3.2.1 Accuracy of environmental data may vary widely and is very much related to the observation mode.

8.3.2.2 The common wind observations include mean wind speed, mean wind direction and maximum wind speed within the observation interval. The standard wind data represent measured or calibrated 10-minute average speed at 10 m above ground or mean sea level. Wind instruments on buoys are usually mounted approximately 4 m above sea level. The systematic instrumental error in estimating mean wind speed and direction can be regarded as negligible, /1/. Satellite scatter-meters data may be utilized.

8.3.2.3 The instrumental accuracy of wave observations depends on the type of instrument used. Wave buoys are regarded as being highly accurate instruments, and error in the estimated significant wave height and zero-up-crossing wave period may be considered as negligible for most sea states, /1/. During severe sea conditions, the presence of strong surface current or external forces on the buoy (e.g., breaking waves, mooring) may cause the buoy measurements to be biased.

8.3.2.4 Several investigations carried out in the last years indicate very promising results that support use of the satellite data. Ref./6/ demonstrate that over the range of significant wave heights 1 m - 8 m satellite altimeter derived significant wave heights were nearly as accurate as the ones obtained from surface buoy measurements, /19/.

8.3.2.5 In steep waves, the differences between sea surface oscillations recorded by a fixed (Eulerian) probe or laser, and those obtained by a free-floating (Lagrangian) buoy can be very marked, see e.g. /10/ and /18/. The wave buoy data shall not be used for estimation of wave profiles in steep waves. For monitoring a wave profile a laser is recommended to be used.

8.3.2.6 Platform mounted wave gauges and other wave sensing devices have the advantage that they measure directly sea surface displacement rather than the acceleration as the buoys do. A position of a wave gauge may affect accuracy of data, /5/.

8.3.2.7 Ship Borne Wave Recorder (SBWR) makes direct wave height measurements but provides no directional information. The main uncertainty is the response of a ship to the waves. Comparison with the wave buoy data suggests wave height accuracy on average of about 8-10%. The SBWR significant wave height are on average higher than the buoy wave heights, with a greater percentage difference at low wave heights and less at high wave heights, /9/. The zero-up-crossing periods from the two instruments are approximately the same.

8.3.2.8 Marine radars (e.g. WAVEX, WAMOS) provide directional wave spectra but infer wave height indirectly. Initial analysis of WAVEX data shows that the WAVEX may significantly over-estimate wave heights for swell-dominated conditions, /21/. Technology use by marine radars for recording the sea surface is under continuous development and accuracy is continuously improved. Accuracy of a marine radar shall be indicated prior to using it in a marine operation.

8.3.2.9 For instrumentally recorded wave data sampling variability due to a limited registration, time constitutes a significant part of the random errors. For the JONSWAP and Pierson-Moskowitz spectrum the sampling variability coefficient of variation of the significant wave height and zero-up-crossing wave period are approximately 4-6% and 1.5-2.5% respectively for a 20-minute measurement interval, /1/.

8.3.2.10 A current instrumental data set may be erroneous due to instrument failure, such as loss of rotor or marine growth. Before application of a data set in planning and execution of marine operations, it is important to make sure that a data quality check has been carried out. Current data uncertainty is specified e.g. in ref./1/.

8.3.2.11 Water level data are collected either by using mechanical instruments or by using pressure gauges, wave buoys, wave radars, and lasers. The accuracy of these recordings is 2-3 cm. For use of the computed water level data it is necessary to know the assumptions and limitations of the models. The data are usually given as residual sea water levels, i.e., the total sea water level reduced by the tide.

8.3.3 Numerically generated data

8.3.3.1 Numerically generated wave data are produced on routine basis by major national meteorological services and are filed by the data centres. The accuracy of these data may vary and depends on the accuracy of a wave prediction model applied as well as the adopted wind field. The hind-cast data can be used, when the underlying hind-cast is calibrated with measured data and accuracy of the data is documented.

8.3.3.2 The *Global Wave Statistics (GWS)* visual observations (BMT (1986)) collected from ships in normal service all over the world since 1949 are often applied. The data represent average wind and wave climate for 104 ocean wave areas. They have a sufficiently long observation history to give reliable global wind and wave climatic statistics. Accuracy of these data is, however, still questioned, especially concerning wave period, confer e.g. /15/ or /2/. It is recommended to use the data with care, and if possible to compare with other data sources.

8.3.3.3 Recently several global environmental databases have been developed. They include numerical wind and wave data (some provide also current and/or sea water level) calibrated by measurements (in-situ data, satellite data), a mixture of numerical and instrumental data or pure instrumental (satellite) data. Accuracy of a data basis shall be documented before applying the data.

8.3.4 Climatic uncertainty

8.3.4.1 Historical data used for specification of operational weather criteria may be affected by climatic uncertainty. Climatic uncertainty appears when the data are obtained from a time interval that is not fully representative for the long-term variations of the environmental conditions. This may result in overestimation or

underestimation of the operational weather criteria. The database needs to cover at least 20 years of preferably 30 years or more in order to account for climatic variability.

8.3.4.2 If data from 20 to 30 years are available, it is recommended to establish environmental description, e.g. a distribution of significant wave height, for return periods of 1, 3, 5, 10 and 25 years.

8.3.5 Sources of data

8.3.5.1 Because of data inaccuracy it is recommended to use several data sources in analysis (if available), specifying weather criteria for comparison. Particular attention shall be given to ocean areas where data coverage is poor.

8.4 Weather forecasting

8.4.1 Weather restricted operations

8.4.1.1 Marine operations with a reference period less than 72 hours may be defined as weather restricted. These operations may be planned with weather conditions selected independent of statistical data, i.e. set by an owner, an operator, etc. Starts of weather restricted operations are conditional on a reliable weather forecast as given in *DNV-OS-H101*, ref./7/.

8.4.2 Uncertainty of weather forecasts

8.4.2.1 For weather restricted operations uncertainties in weather forecasts shall be considered. Operational limits of environmental parameters (e.g. significant wave height, wind speed) shall be lower than the design values. This is accounted for by the alpha factors as specified in /7/. The *DNV-OS-H101* requirements are location specific and shall be used with care for other ocean locations. It is recommended to apply location and, if justified, model specific corrections when used outside the areas provided in /7/.

Guidance note:

At present, the given alpha-factors in *DNV-OS-H101* are derived from North Sea and Norwegian Sea data only.

---e-n-d---of---G-u-i-d-a-n-c-e---n-o-t-e---

8.5 Persistence statistics

8.5.1 Weather unrestricted operations

8.5.1.1 Marine operations with a reference period exceeding 72 hours are normally defined as unrestricted operations, see ref./7/. These operations shall be planned based on extreme value statistics established from historical data or time domain simulations.

8.5.1.2 Persistence statistics shall be established according to specified a priori operational design criteria.

8.5.1.3 A non-stationary stochastic modelling, suitable for the analysis and simulation of multivariate time series of environmental data may be used as a supporting tool for generating the long-term data, /17/.

8.5.1.4 For limited time periods like months the statistics shall follow the *DNV-OS-H101* requirements and be based on events that start within the period and are followed to the next crossing. The average duration of events will depend on the averaging period and sampling interval of the data.

Guidance note:

Note that certain operations require a start criterion although designed for unrestricted conditions.

---e-n-d---of---G-u-i-d-a-n-c-e---n-o-t-e---

8.5.2 Statistics from historical data

8.5.2.1 It is recommended that duration statistics includes the following parameters (ref./16/):

T_{tot} = total time period of an environmental time series under consideration

N_c = number of “calm” periods

N_s = number of “storm” periods

$\bar{\tau}_c$ = average duration of “calm” periods

$\bar{\tau}_s$ = average duration of “storm” periods

T_c = total duration of all “calm” periods

T_s = total duration of all “storm” periods

Hence;

$$T_c = \sum_{i=1}^{N_c} \tau_{ci} \quad [\text{hours}]$$

$$T_s = \sum_{i=1}^{N_c} \tau_{si} \quad [\text{hours}]$$

$$T_{tot} = T_c + T_s \quad [\text{hours}]$$

8.5.2.2 Unless data indicate otherwise, a 2-parameter Weibull distribution can be assumed for the marginal distribution of “calm” period t (ref./9/ and /14/);

$$F_T(t) = 1 - \exp\left[-\left(\frac{t}{t_c}\right)^\beta\right] \quad [-]$$

where t_c is the scale parameter and β is the shape parameter. The distribution parameters are determined from site specific data by some fitting technique.

8.5.2.3 The average duration is expressed as

$$\bar{\tau}_c = \int_0^\infty t \frac{dF_T}{dt} dt \quad [\text{hours}]$$

For the 2-parameter Weibull distribution it reads;

$$\bar{\tau}_c = t_c \cdot \Gamma\left(\frac{1}{\beta} + 1\right) \quad [\text{hours}]$$

where $\Gamma(\)$ is the Gamma function.

8.5.2.4 If the cumulative distribution of H_s is known then the average duration of periods with significant wave height lower than h can be approximated by

$$\bar{\tau}_c = F_{H_s}(h) \frac{T_{tot}}{N_c} \quad [\text{hours}]$$

alternatively, ref/9/;

$$\bar{\tau}_c = A \left[-\ln(F_{H_s}(h)) \right]^{-\frac{1}{\beta}} \quad [\text{hours}]$$

where A and β are established based on location specific data, and $F_{H_s}(h)$ is a cumulative distribution of significant wave height. For the North Sea, $A = 20$ hours and $\beta = 1.3$ maybe adopted, /9/.

8.5.2.5 The distribution for $h < H_s$ and duration $t < t'$ is;

$$F_{H_s|T}(h < H_s' | t > t') = F_{H_s}(h < H_s') \cdot (1 - \lambda) \quad [-]$$

where

$$\lambda = \frac{\int_0^{t'} t dF_T(t)}{\int_0^\infty t dF_T(t)} \quad [-]$$

8.5.2.6 The number of periods when $h < H_s'$ and $t < t'$ can be expressed as;

$$N_c'(h < H_s' | t < t') = F_T(t < t') \cdot N_c \quad [-]$$

The average duration for $h < H_s'$ and $t < t'$ is;

$$\bar{\tau}_c(h < H_s' | t < t') = \frac{1}{F_T(t < t')} \int_0^{t'} t F_T(t) \quad [\text{hours}]$$

Guidance note:

As an example, assume that the operability shall be studied for a moonpool vessel. Three motion-sensitive operations are considered, with the maximum significant vertical amplitude in the moonpool area equal to 0.5 m, 0.75 m and 1.0 m. Calculated significant amplitudes of vertical motion for the vessel have given the limiting H_s for these three operations, as shown in Figure 8-2.

These sea state limitations have been combined with the scatter diagram in Table 8-1 to show operable and non-operable sea states. The operability for each of the different work tasks is shown in Table 8-2. Calculated operational limits should of course be combined with operational limits based on practical considerations and requirements from personnel that shall carry out the operation.

---e-n-d---of---G-u-i-d-a-n-c-e---n-o-t-e---

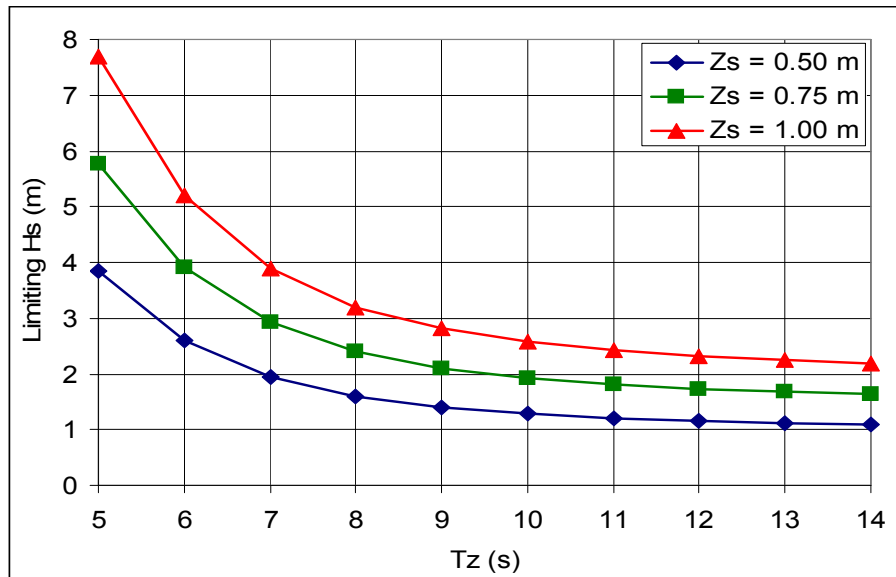


Figure 8-2
Limiting H_s for operations with $Z_s = 0.5$ m, 0.75 m and 1.0 m

Table 8-1 Joint probability of sea states, with operation limitations

Hs (m)	Tz (s)										Sum Tz
	5	6	7	8	9	10	11	12	13	14	
Calm											6.8
0.5	4.9	1.6	1.3	1.1	0.2	1.6	0.9	1.6	1.6	1.1	16.1
1.0	10.4	4.8	2.2	1.1	0.9	1.5	0.5	2.0	1.6	2.6	27.7
1.5	4.6	2.4	1.8	2.0	0.4	0.7	0.7	0.2	1.3	0.7	14.8
2.0	3.3	3.1	1.8	2.0	0.4	0.7	0.7	0.5	-	1.8	14.5
2.5	2.2	2.4	1.5	2.2	0.4	0.9	-	0.2	0.2	0.4	10.3
3.0	0.5	0.2	1.1	1.8	0.5	0.2	0.2	-	-	0.2	4.8
3.5	0.4	-	-	1.3	-	0.2	-	-	-	-	1.8
4.0	0.5	0.2	0.4	0.2	-	0.5	0.2	-	-	-	2.0
4.5	0.4	-	0.2	0.4	0.2	0.2	-	-	-	-	1.3
Sum Hs	27.3	14.7	10.3	12.1	2.9	6.6	3.3	4.6	4.8	6.8	100.

Table 8-2 Calculated operability

Criterion	Down-time: $P(Z_s > Z_{s0})$ %	Operability: $P(Z_s < Z_{s0})$ %
$Z_{s0} = 0.5$ m	35.0	65.0
$Z_{s0} = 0.75$ m	19.4	80.6
$Z_{s0} = 1.0$ m	6.6	93.4

8.5.3 Time domain simulations

8.5.3.1 Alternatively to the statistics described in 8.5.2 the weather criteria and availability analysis can be studied by use of time domain simulations of operation performance. Recognized marine operation performance software shall be used for this purpose. Weather conditions in a form of measured or numerically generated time series are an input to the analysis. Any given number of environmental parameters can usually be handled in the time series.

8.5.3.2 The marine operation performance simulation programs should include specification of durations, weather limits and sequence of activities. They may be used for operation planning in advance and during execution of operations.

8.5.3.3 Given an activity network and the weather time series, the operation performance software scans the weather time series and finds the performance of the given network, assuming the given start date of the year.

8.5.3.4 Advantages of using the time series and not statistical data are:

- It is simpler to deduce the statistical variability than from the statistics.
- The operational limits are more easily checked on the time series than from statistics.
- The activity networks are easy to check against the time series.
- It is easy to combine limits of several weather parameters.
- It allows establishing of statistics for weather parameters of interest. A sufficiently long historical time series shall be analysed to obtain reliable results.
- Duration of operations is taken directly into account.

8.5.3.5 It is recommended to split each operation into a sequence of small and, to the extent possible, independent sub-operations.

8.5.3.6 To avoid a critical sub-operation to be started up but not finalised until unacceptable weather conditions occur an extra duration of the forecasted weather window may be required. The maximum limits for a longer time will depend upon the accuracy of the duration estimates. Alternatively, uncertainty in forecast simulations can be accounted for by introducing a random error (and/or bias) in a real environmental record, e.g. a wave record, /11/.

8.5.4 Seasonality

8.5.4.1 It is recommended that the persistence statistics includes information about seasonal variations of the weather climate. Design and planning of marine operations shall be based on the established average weather conditions for one year, three months and a shorter period of time according to the requirements given in *DNV-OS-H101*. Several return periods are recommended to be considered.

8.6 Monitoring of weather conditions and responses

8.6.1 Monitoring of environmental phenomena

8.6.1.1 For marine operations particularly sensitive for certain environmental conditions such as waves, swell, current, tide, etc., systematic monitoring of these conditions prior to and during the operation shall be arranged.

8.6.1.2 Monitoring shall be systematic and follow the requirements given in *DNV-OS-H101*. Responsibilities, monitoring methods and intervals shall be described in a procedure. Essential monitoring systems shall have back up systems. Any unforeseen monitoring results shall be reported without delay.

8.6.1.3 Carrying out marine operations can be helped by a Decision Support System installed on board of marine structures if reliability of the system is described and approved by an authority or by a Classification Society. The Decision Support System may be based on the Near Real Time (NRT) and/or Real Time (RT) data which can be provided by met-offices, private company or research institutes. The NRT and RT data may represent numerically generated data, a mixture of numerical and instrumental data (in-situ measurements, marine radar and satellite data) or pure instrumental data if sampling frequency of the latter is sufficient for an operation under consideration. Vessel motions may be utilized by a Decision Support System and environmental conditions can be evaluated from measured vessel motions, /16/. Attention shall be given to accuracy of prediction of combined seas (wind sea and swell).

8.6.1.4 A required sampling interval for time monitoring will depend upon the type of operation and its duration, and is recommended to be considered carefully.

8.6.2 Tidal variations

8.6.2.1 Tidal variations shall additionally be monitored a period with the same lunar phase as for the planned operation.

Guidance note:

Tidal variations shall be plotted against established astronomical tide curves. Any discrepancies shall be evaluated, duly considering barometric pressure and other weather effects.

---e-n-d---of---G-u-i-d-a-n-c-e---n-o-t-e---

8.6.3 Monitoring of responses

8.6.3.1 Monitoring of responses shall be carried out by documented reliable instruments.

8.6.4 Alpha factor related monitoring

8.6.4.1 Uncertainties related to monitoring of weather conditions shall be taken into considerations according to the requirements given in *DNV-OS-H101*.

8.7 References

- /1/ Bitner-Gregersen, E. M. and Hagen, Ø (1990), "Uncertainties in Data for the Offshore Environment", *Structural Safety*, Vol. 7., pp. 11-34.
- /2/ Bitner-Gregersen, E. M., Cramer, E., and Løseth, R., (1995), "Uncertainties of Load Characteristics and Fatigue Damage of Ship Structures", *J. Marine Structures*, Vol. 8, pp. 97-117.
- /3/ Bitner-Gregersen, E. M., Cramer, E. H., and Korbijn, F., 1995. "Environmental Description for Long-term Load Response of Ship Structures". *Proceed. ISOPE-95 Conference*, The Hague, The Netherlands, June 11-16.
- /4/ British Maritime Technology (Hogben, N. , Da Cunha, L. F., and Oliver , H. N.) (1986), *Global Wave Statistics*, Unwin Brothers Limited, London, England.
- /5/ Cardone, C. J. Shaw and V. R. Swail (1995), "Uncertainties in Metocean Data", *Proceedings of the E&P Forum Workshop*.
- /6/ Carter, D. J. T., Challenor, P. G. and M. A. Srokosz, (1992), "An Assessment of GEOSAT Wave Height and Wind Speed Measurements", *J. Geophys. Res.* Vol.97 (C7).
- /7/ DNV Offshore Standard "Marine Operations General", DNV-OS-H101., (planned issued 2010).
- /8/ Graham, C. G., Verboom, G. and Shaw, C. J. (1978) "Comparison of Ship Born Wave Recorder and Waverider Buoy Data used to Generate Design and Operational Planning Criteria". *Proc. Coastal Engineering*, Elsevier, Amsterdam, pp. 97-113.
- /9/ Graham, C., (1982), "The Parametrisation and Prediction of Wave height and Wind Speed persistence Statistics for Oil Industry Operational Planning Purposes". *Coastal Engineering*, Vol. 6, pp. 303-329.
- /10/ Marthinsen, T. and S. R. Winterstein (1992), On the skewness of random surface waves, *Proc. of the 2nd International Offshore and Polar Engineering Conference*, San Francisco, pp 472-478, ISOPE.
- /11/ Nielsen, F. G., (2007) , "Lecture Notes in Marine Operations". Department of Marine Hydrodynamics, Faculty of Marine Technology, Norwegian University of Science and Technology, Trondheim/Bergen January 2007.
- /12/ Nielsen, U. D. (2006), Estimations of On-site Directional Wave Spectra from Measured Ship Responses, *Marine Structures*, Vol. 19, no 1.
- /13/ Kleiven, G. and Vik, I. (1984) "Transformation of Cumulative Probability of Significant Wave height into Estimates of Effective Operation Time". Norsk Hydro Research Centre, Bergen July.
- /14/ Houmb, O. G. and Vik, I. (1977), "On the Duration of Sea State". NSFI/NTH Division of port and ocean Eng. Report.
- /15/ Guedes Soares, C. and Moan, T., (1991). "Model Uncertainty in a Long Term Distribution of Wave-induced Bending Moments for Fatigue Design of Ship Structures, *Marine Structures*, Vol. 4.
- /16/ Nielsen, U. D. (2006), Estimations of On-site Directional Wave Spectra from Measured Ship Responses, *Marine Structures*, Vol. 19, no 1.
- /17/ Stefanakos, Ch. N. and Belibassakis, K. A. ,(2005), "Non-stationary Stochastic Modelling of Multivariate Long-term Wind and Wave data", *Proc. OMAE'2005 Conf.*, Halkidiki, Greece, 2005.
- /18/ Vartdal, L., Krogstad, H. and S. F. Barstow (1989), "Measurements of Wave Properties in Extreme Seas During the WADIC Experiment", *Proc. 21st Annual Offshore technology Conference*, Houston, Texas.
- /19/ deValk, C., Groenewoud, P., Hulst S. and Kolpman G. (2004), "Building a Global Resource for Rapid Assessment of the Wave Climate", *Proc. 23rd OMAE Conference*, Vancouver, Canada, June 20-25, 2004.
- /20/ Vik, I. and Kleiven, G., (1985) "Wave Statistics for Offshore Operation". 8th Inter. Conference on Port and Ocean Engineering under Arctic Conditions (POAC 85), Narssarssuaq, Greenland, Sept. 6-13.
- /21/ Yelland, M. J., Bjrheim, K., Gommenginger, C., Pascal R. W. and Moat, B. I. (2007) "Future Exploitation of In-situ Wave Measurements at Station Mike". Poster at the GLOBWAVE Workshops, Brest, September 19-21.
- /22/ Aalbers, A. B. and van Dongen, C. J. G., (2008) "Weather Routing: Uncertainties and the Effect of Decision Support Systems". *Marine Operations Specialty Symposium – MOSS2008*, pp.411-423.
- /23/ NORSOK N-002, "Collection of Metocean Data". Rev. 1. Sept, 1997.

9 Lifting Operations

9.1 Introduction

9.1.1 General

9.1.1.1 A lifting operation usually involves a crane, crane vessel, transport vessel/barge and the lifted object.

9.1.1.2 The following operational aspects should be considered during a lifting operation,

- clearance between lifted object and crane boom
- clearance between crane boom and any other object/structure
- clearance between the lifted object and any other object/structure
- clearance between the underside of the lifted object and grillage or seafastening structure on the transport vessel/barge
- bottom clearance between crane vessel and sea bed for lifting operations at small water depths.

9.1.1.3 The clearances listed in 9.1.1.2 should be decided on the basis of expected duration of the operation, the operational procedures and the environmental conditions.

9.1.1.4 Requirements to clearances are given in DNV-OS-H205 “Marine Operations, Lifting Operations” (Ref. /7/).

9.1.1.5 Clearance between lifted object or transport vessel/barge and the crane vessel or crane boom should be calculated. The calculated clearance should consider motions of the crane vessel and transport vessel/barge. The motion calculations should be based on the environmental design conditions and maximum values should be estimated.

9.1.1.6 Usually, crane lifting operations are divided into two categories:

- *Light lifts* where the lifted object is very small compared to the crane vessel. The weight of the lifted object is less than 1-2% of the displacement of the crane vessel, typically less than a few hundred tons. In this case the motion characteristics of the vessel (at the crane tip) is not affected by the lifted object.
- *Heavy lifts* where the weight of the lifted object is more than 1-2% of the vessel displacement and typically more than 1000 tons. For such lifts the coupled dynamics of the vessel and the lifted object must be considered.

9.1.1.7 Heave compensation is frequently used during light lifts. For heavy lifts, use of heave compensation is generally not possible. Modelling of heave compensation systems is given in Section 5.

9.2 Light lifts

9.2.1 Crane tip motion

9.2.1.1 For light lifts the crane boom can be treated as a stiff structure, hence the motion of the crane tip can be determined directly from the wave induced rigid body motion of the crane vessel.

9.2.1.2 The wave induced translational motions (surge, sway and heave) of the crane tip x_{ct} , y_{ct} and z_{ct} are given from the vessel RAOs for six degrees of freedom motion usually defined for the centre of gravity for the vessel.

Guidance note:

The horizontal surge motion of the crane tip is given by the surge, pitch and yaw RAOs of the vessel. The horizontal sway motion of the crane tip is given by the sway, roll and yaw RAOs of the vessel. The vertical heave motion of the crane tip is given by the heave, roll and pitch RAOs of the vessel. The motion RAOs should be combined with crane tip position in the vessel's global coordinate system. The characteristic values for crane tip motions (x_{ct} , y_{ct} , z_{ct}) in a sea state with given H_s can be taken as the largest motion response when all possible wave periods T_z are considered.

---e-n-d---of---G-u-i-d-a-n-c-e---n-o-t-e---

9.2.1.3 The crane tip's characteristic vertical motion in a given sea state and wave heading can be taken as

$$\eta_{ct} = \sqrt{\eta_3^2 + (b \sin \eta_4)^2 + (l \sin \eta_5)^2}$$

where

- η_{ct} = characteristic single amplitude vertical motion of crane tip [m]
- η_3 = characteristic single amplitude heave motion of vessel [m]
- η_4 = characteristic single amplitude roll angle of vessel [deg]
- η_5 = characteristic single amplitude pitch angle of vessel [deg]

- b = horizontal distance from the vessel's centre line to the crane tip [m]
 l = horizontal distance from midship to the crane tip [m]

The values for characteristic single amplitudes in heave, roll and pitch are to be taken as absolute values.

9.2.1.4 The crane tip's characteristic vertical velocity in a given sea state and wave heading can be taken as

$$v_{ct} = 2\pi \sqrt{\left(\frac{\eta_3}{T_3}\right)^2 + \left(\frac{b \sin \eta_4}{T_4}\right)^2 + \left(\frac{l \sin \eta_5}{T_5}\right)^2}$$

where

- v_{ct} = characteristic single amplitude vertical velocity of crane tip [m/s]
 T_3 = heave natural period [s]
 T_4 = roll natural period [s]
 T_5 = pitch natural period [s]

9.2.1.5 For a given motion of the crane tip, the motion of the lifted object in air can be solved as a forced pendulum problem. Prior to water entry an unsteady wind force may affect the motion of the object. When guide wires are used to control the horizontal motion of the lifted object, these should be modelled as constraints or horizontal springs in the equations of motion for the lifted object.

9.2.1.6 The eigenperiod for horizontal motion of a lifted object in air is given by

$$T_{0h} = 2\pi \sqrt{\left(\frac{L}{g}\right) \left(\frac{M + 0.33mL}{M + 0.45mL}\right)}$$

where

- M = mass of lifted object [kg]
 m = mass per unit length of hoisting line [kg/m]
 L = length of hoisting line [m]
 g = acceleration of gravity [m/s²]

Guidance note:

For most applications the effect of the mass of hoisting line can be neglected when the mass of the hoisting line is less than the lifted object. The effect on the natural period is a factor varying from 1.00 for a mass ratio of 0 to 0.96 for a mass ratio of 1.

---e-n-d---of---G-u-i-d-a-n-c-e---n-o-t-e---

9.2.1.7 The eigenperiod for rotational motion (yaw) of an object lifted by two parallel wires (tandem lift system, see Figure 9-1) is given by

$$T_{0r} = 2\pi \frac{r_g}{a} \sqrt{\frac{L}{g}}$$

where

- L = length of hoisting line [m]
 g = acceleration of gravity [m/s²]
 r_g = yaw radius of gyration of lifted object [m]
 $2a$ = distance between wires [m]

Resonant yaw motion of the lifted object can be excited by either wave action or by fluctuating wind.

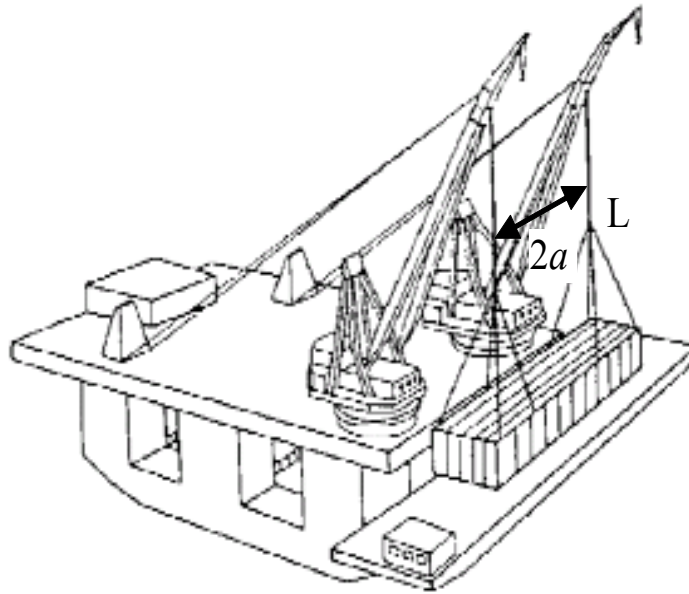


Figure 9-1
Tandem lift system

9.2.2 Hydrodynamic interaction

9.2.2.1 The crane vessel RAOs may be influenced by other fixed or floating structures in close proximity. RAOs calculated for the crane vessel in unrestricted water can in general not be applied for lifting operations without correcting for hydrodynamic interaction between crane vessel and other nearby structures.

9.2.2.2 For lifting from or to a transport vessel/barge in close proximity, RAOs for both vessels should be calculated. The coupled hydrodynamic problem should be solved as a 12 degrees-of-freedom system. Computer program applied for wave induced response of the crane and transport vessels should have an option for analysis of multi-body systems.

9.2.2.3 For lifting operations in very shallow water, the motion of the crane vessel and hence the crane tip motion may be strongly influenced by hydrodynamic interaction with sea bed.

9.2.2.4 Guidance on numerical modelling of hydro-dynamic interaction between floating bodies are given in Section 2.3.5.

9.3 Heavy lifts

9.3.1 General

9.3.1.1 Heavy lifts are usually carried out by semi-submersible crane vessels (SSCV). Heavy lift crane vessels are usually equipped with a computer controlled ballast system to counteract trim and heel moments induced during lifting and setting of the load.

9.3.1.2 For a lift-off operation the crane vessel with bow-mounted cranes is pre-trimmed to a stern-up position. In a pre-hoist operation the hook is hauled up, transferring about 80% of the heavy load from the barge to the SSCV. In this condition with tensioned slings, the barge and SSCV oscillate as a system almost rigidly connected in the vertical direction. By adjusting the ballast water in the ballast tanks the vessel's trim is reversed and the load is lifted 4-5 meters during a period of 90 seconds, corresponding to a lifting velocity of about 5 cm/s.

9.3.2 Degrees of freedom

9.3.2.1 Before lift-off from the transport barge the system of crane vessel and transport barge can be modelled as a 12 DOF system to account for hydrodynamic interaction between semi-submersible and barge. After lift-off the heavy lifted object will influence the motion of the semi-submersible so the total system should be modelled as a 18 DOF system.

9.3.2.2 In the pendulum condition when the load has been lifted off the barge, the dynamic behavior of the

system is rather complicated since the load and the crane vessel perform coupled oscillations. Horizontal relative motions between the load and the crane vessel may be critical. Such motions can be reduced by means of tensioned lines. The vertical motions will then also be reduced due to reduced coupling effects.

9.3.2.3 Hydrodynamic interaction between the SSCV and the transport barge vessel may be important since the columns and characteristic wave lengths in operating conditions are comparable to the vessel dimensions.

9.3.3 Coupled dynamic motion

9.3.3.1 A crane vessel with a heavy load hanging in a vertical hoisting line from the crane tip is in general a 12 DOF system. Rotations of the lifted object are usually controlled by guide wires or tugger lines running from the load to the vessel. In a fully numerical simulations of the coupled system such guide wires must be modelled as springs. In a simplified analysis rotations of the lifted object may be ignored and the number of DOFs is reduced from 12 to 9.

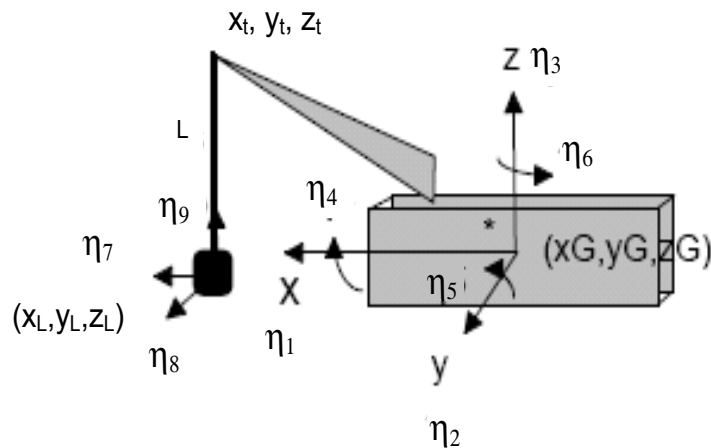


Figure 9-2
Model of crane vessel with lifted object

9.3.3.2 The nine DOF motions are denoted η_i , $i = 1, 2, \dots, 9$ where $i = 1, 2, \dots, 6$ are the rigid body motions of the crane vessel with 3 translatory and 3 rotational motions (see Figure 9-2). η_7 is the motion of the lifted object in the x-direction, η_8 is the motion of the lifted object in the y-direction and η_9 is the motion in the z-direction.

9.3.3.3 The lifted object may be modelled as a point mass with mass m . The lifted object may be submerged. In that case, added mass of the lifted object must be included. The lifted object will in general have different added mass a_{ii} for surge motion ($i = 1$), sway ($i = 2$) and heave motion ($i = 3$).

9.3.3.4 The 9×9 mass matrix M can be written as

$$M = \begin{pmatrix} M_v + A & 0 \\ 0 & m_o + a \end{pmatrix}$$

where

M_v = 6×6 body mass matrix for crane vessel [kg]

A = 6×6 added mass matrix for crane vessel [kg]

m_o = 3×3 mass matrix for lifted object [kg]

a = 3×3 added mass matrix for lifted object [kg]

The mass matrix M and the added mass matrix A are both symmetric. There are no inertia coupling terms between the vessel and the lifted object. Body mass and added mass matrix for a floating body is given in Ref. [2]. Neglecting off-diagonal ($i \neq j$) added mass terms, the mass matrix for the lifted object is taken as

$$m_o + a = (m + a_{ii})\delta_{ij}$$

9.3.3.5 In general there is hydrodynamic interaction between a submerged lifted object and the crane vessel. Such interaction would give non-zero coupled added mass terms (between A and a), but is usually small and

can be ignored in the coupled analysis.

9.3.3.6 The stiffness matrix C for the coupled system can be split into three contributions:

$$C = C_h + C_m + C_c$$

where

C_h = hydrostatic stiffness matrix

C_m = mooring stiffness matrix

C_c = coupling stiffness matrix

Mooring stiffness only contributes to the horizontal motions of the crane vessel. Vertical mooring forces may normally be ignored compared to hydrostatic effects.

9.3.3.7 The 9×9 hydrostatic stiffness matrix can be written as

$$C_h = \begin{pmatrix} C_{vh} & \mathbf{0} \\ \mathbf{0} & \mathbf{0} \end{pmatrix}$$

where the 6×6 hydrostatic matrix for the crane vessel is given by

$$C_{vh} = \begin{pmatrix} 0 & 0 & 0 & 0 & 0 & 0 \\ 0 & 0 & 0 & 0 & 0 & 0 \\ 0 & 0 & C_{h,33} & C_{h,34} & C_{h,35} & 0 \\ 0 & 0 & C_{h,34} & C_{h,44} & 0 & C_{h,46} \\ 0 & 0 & C_{h,35} & 0 & C_{h,55} & C_{h,56} \\ 0 & 0 & 0 & C_{h,46} & C_{h,56} & 0 \end{pmatrix}$$

Expressions for the non-zero $C_{h,ij}$ are given in DNV-RP-C205, *ref. /2/*. When the crane vessel is symmetric about $y = 0$ and when vertical mooring forces are ignored, $C_{h,34}$, $C_{h,45}$ and $C_{h,56}$ may all be set to zero.

9.3.3.8 The 9×9 mooring stiffness matrix can be written as

$$C_m = \begin{pmatrix} C_{vm} & \mathbf{0} \\ \mathbf{0} & \mathbf{0} \end{pmatrix}$$

where C_{vm} is the 6×6 mooring stiffness matrix for the crane vessel. The mooring stiffness matrix is symmetric and the only non-zero elements are

$$C_{vm11}, C_{vm12}, C_{vm22}, C_{vm16}, C_{vm26}, C_{vm66}$$

These elements may be estimated by a mooring analysis program. If the mooring system is symmetric, only the diagonal elements are non-zero. If the crane vessel is not moored but is using dynamic positioning (DP), the DP system may be approximated by a linear spring damper system with a restoring matrix similar to the one above.

9.3.3.9 The symmetric 9×9 coupling stiffness matrix is given by (see Ref. /1/)

$$C_c = \begin{pmatrix} k_s & 0 & 0 & 0 & k_s z_t & -k_s y_t & -k_s & 0 & 0 \\ & k_s & 0 & -k_s z_t & 0 & k_s x_t & 0 & -k_s & 0 \\ & & k_e & k_e y_t & -k_e x_t & 0 & 0 & 0 & -k_e \\ & & & C_{c44} & -k_e x_t y_t & k_s z_t x_t & 0 & k_s z_t & k_e y_t \\ & & & & C_{c55} & -k_s z_t y_t & -k_s z_t & 0 & k_e x_t \\ & & & & & C_{c66} & k_s y_t & -k_s x_t & 0 \\ & & & & & & k_s & 0 & 0 \\ & & & & & & & k_s & 0 \\ & & & & & & & & k_e \end{pmatrix}$$

where

$$k_s = w/L_s \text{ [N/m]}$$

$$k_e = AE/L_e \text{ [N/m]}$$

$$L_s = \text{length of hoisting wire from crane tip to centre of load [m]}$$

- L_e = effective length of hoisting wire including flexibility of total length from load to winch as well as crane flexibility [m]
 AE = stiffness of wire per unit length [N]
 w = submerged weight of load [N]
 $C_{c44} = k_s z_t^2 + k_e y_t^2$ [Nm]
 $C_{c55} = k_s z_t^2 + k_e x_t^2$ [Nm]
 $C_{c66} = k_s y_t^2 + k_e y_t^2$
 x_t = x-position of crane tip [m]
 y_t = y-position of crane tip [m]
 z_t = z-position of crane tip [m]

9.3.3.10 The undamped eigenfrequencies and eigenvectors of the coupled system can be computed from

$$\omega_i, i = 1, 2, \dots, 9$$

$$(-\omega^2 \mathbf{M} + \mathbf{C})\mathbf{x} = 0$$

Due to coupling between modes of motion, the eigenvectors have contributions from the different degrees of freedom.

9.3.3.11 For harmonic wave induced excitation of the vessel, the load vector can be written on complex form

$$\mathbf{F} = \text{Re}\{\mathbf{F}_a e^{i\omega t}\}$$

where

$$\mathbf{F}_a = (F_1, \dots, F_6, 0, 0, 0)^T$$

is the complex excitation force vector, ω is the frequency of oscillation and Re denotes the real part of the expression. Procedures for simplified calculation of linear wave loads on barges and semisubmersibles are given in Ref. /3/.

9.3.3.12 The motion response of the coupled vessel – load system is obtained from

$$\boldsymbol{\eta} = (-\omega^2 \mathbf{M} + i\omega \mathbf{B} + \mathbf{C})^{-1} \mathbf{F}$$

where $\boldsymbol{\eta} = \{\eta_i\}, i = 1, 2, \dots, 9$ and \mathbf{B} is a linear damping matrix.

9.3.4 Time domain simulation of heavy lifts

9.3.4.1 Heavy lift operations can be analysed by time-domain simulations based on pre-generated frequency dependent wave excitation force transfer function, added mass and wave damping for crane vessel, transport barge and lifted object (in submerged position). The wave damping is represented in the time domain by a convolution integral where previous values of the velocities are multiplied by retardation functions.

9.3.4.2 For a given sea state the pre-generated frequency dependent wave forces on crane vessel, transport barge and lifted object (when submerged), are converted to force time histories applied in the coupled equations of motion for the system.

9.3.4.3 When the structural elements of the lifted object are small compared to characteristic wave lengths, the exciting force and damping for the submerged object can be approximated by Morison's load formula in terms of the wave particle kinematics (fluid velocity and acceleration).

9.3.4.4 For transient response simulations where the lifted object undergoes large changes in draft during the operation, care should be taken to ensure that the hydrostatic forces, added mass and wave damping are correctly modelled. Several stationary steps with different hydrodynamic models for each steps may be used instead.

9.3.4.5 The time varying wind drag force on the lifted object in air is given by a wind force coefficient and the instantaneous relative velocity between wind and lifted object. Usually, the velocity of the lifted object can be neglected when calculating relative velocity.

9.4 Hydrodynamic coupling

9.4.1 Vessels situated side-by-side

9.4.1.1 When two vessels are situated closely side-by-side hydrodynamic resonance may occur in the gap between the two vessels. There are three types of resonant motions to be considered

- piston mode motion
- longitudinal sloshing
- transverse sloshing.

9.4.1.2 The eigenfrequencies ω_n corresponding to the hydrodynamic resonances in the gap are given by (Ref. /5/)

$$\omega_n^2 = g\lambda_n \frac{1 + J_{n0} \tanh \lambda_n h}{J_{n0} + \tanh \lambda_n h}$$

where

$$J_{n0}(r) = \frac{2}{n\pi^2 r} \left(\int_0^1 \frac{r^2}{u^2 \sqrt{u^2 + r^2}} [1 + 2u + (u-1) \cos(n\pi u) - \frac{3}{n\pi} \sin(n\pi u)] du - \frac{1}{\sin \theta_0} + 1 + 2r \ln \frac{1 + \cos \theta_0}{1 - \cos \theta_0} \right)$$

- $r = b/l$ [-]
 $b =$ width of the gap between vessels [m]
 $l =$ length of the gap (approximated by length of shortest vessel) [m]
 $h =$ draft of vessels (assumed to have similar draft) [m]
 $g =$ acceleration of gravity [m/s²]
 $\lambda_n = n\pi/l$ [m⁻¹]
 $\theta_0 = \tan^{-1}(1/r)$ [rad]

The function J_n versus $n\pi r$ is shown in Fig. 9-3. The corresponding natural periods are given by

$$T_n = 2\pi / \omega_n$$

9.4.1.3 In the piston mode motion, the volume of water between the vessels heaves up and down more or less like a rigid body. This mode of motion is also called the pumping or Helmholtz mode. The eigenfrequency of the piston mode is obtained by setting $n = 1$ in the general expression 9.4.1.2.

9.4.1.4 A simplified expression for the eigenfrequency of the piston mode is given by (Ref. /4/)

$$\omega_1^2 = \frac{g}{d + \frac{b}{\pi} \left(1.5 + \ln \frac{B}{2b} \right)}$$

where B is the total beam of the two vessels including the gap between the vessels.

9.4.1.5 In the longitudinal sloshing modes the water between the vessels moves back and forth in the longitudinal direction. The eigenfrequencies of sloshing modes are obtained by setting $n = 2, 3, 4, \dots$ in the general expression 9.4.1.2.

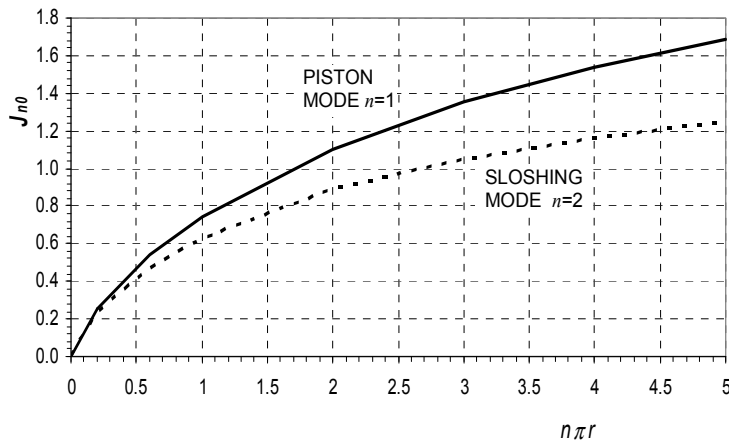


Figure 9-3
Function J_{n0} versus $n\pi r$ for piston mode ($n=1$, solid line) and lowest sloshing mode ($n=2$, dotted line)

Guidance note:

Example: For a gap between two barges of dimensions $l = 80$ m, $b = 4$ m and draft $h = 10$ m, $r = b/l = 0.05$, $\lambda_1 = 0.03927$, $\lambda_2 = 0.07854$, $J_{10} = 0.2067$ and $J_{20} = 0.3089$ resulting in natural periods $T_1 = 7.43$ sec for the piston mode and $T_2 = 6.41$ sec for the lowest sloshing mode.

---e-n-d---of---G-u-i-d-a-n-c-e---n-o-t-e---

9.4.1.6 In the transverse sloshing mode the water motion between the vessels is a standing wave between the vessels with a wave length on the order of the gap width. When vessels are located in close proximity, with a narrow gap, the eigenfrequencies of transverse sloshing are high and may be neglected.

9.4.1.7 The hydrodynamic resonances in the piston mode and the longitudinal/transverse sloshing modes can be identified by a diffraction analysis as peaks in the transfer function for surface elevation at arbitrary points in the gap between the vessels.

9.5 Lift-off of an object

9.5.1 General

9.5.1.1 Since lifting operations takes place in relatively calm weather, the motions of the barge and the crane vessel can be computed from linear wave theory, and the motions can be assumed to be Gaussian distributed.

9.5.1.2 In case the transport has taken place on the crane vessel, the lift off operation itself is a simple operation since the relative motion between the crane-top and the vessel is marginal.

9.5.1.3 When lifting an object from the barge by means of a crane onboard a crane vessel positioned side by side with the barge, a critical parameter is the relative motion between the crane hook and the barge at the position of the lifted object. The statistics of the relative motion determines the probability that the barge will hit the lifted object after lift-off.

9.5.1.4 The parameters determining if the lift-off operation is feasible are the following:

- The hoisting speed of the crane (depends on the weight of the object to be lifted, a lower limit is usually taken to be in the order of 0.1 m/s).
- The combined motion characteristics of the barge and the crane vessel.
- The weather condition, combined with the orientation of the two vessels.

9.5.1.5 Once the object is lifted free of the transporting vessel (barge), the object will be hanging from the crane, and is being subject to the motion of the crane top. Since the length of the wire is short in this case, the dynamic response of the object/wire system will be marginal, and the force in the wire can be estimated from the vertical acceleration of the crane top alone.

9.5.2 Probability of barge hitting lifted object

9.5.2.1 A criterion for characterization of the safety of the lifting operation is that the object is not re-hit by the barge after having been lifted off. The safety of the operation can be assessed by estimating the probability that the lifted object will be hit by the barge and ensuring that the probability is less than a certain prescribed value.

9.5.2.2 The following simplifying assumptions are made for the statistical analysis:

- The motion responses of the two vessels are assumed to be narrow banded.
- The hoisting speed U is constant during lifting
- The lifted object is leaving the barge as the relative vertical motion a between the barge and the crane hook has a maximum.
- The probability that the lifted object will be hit by the barge more than once is practically zero. Consequently only the first possible hit is considered.

9.5.2.3 The probability P that the lifted object will be hit by the barge at the next maximum value of the relative motion can be approximated by

$$P(\tau) = \frac{1}{2} \exp\left(-\frac{\tau^2}{2}\right) \left(1 - \frac{\tau\sqrt{\pi}}{2} \exp\left(\frac{\tau^2}{4}\right) \operatorname{erfc}\left(\frac{\tau}{2}\right)\right)$$

where

$$\tau = \frac{UT_z}{\sigma}$$

- U = hoisting speed [m/s]
 T_z = zero up-crossing period for relative motion [s]
 σ = standard deviation of relative motion [m]

$$\operatorname{erfc}(x) = \frac{2}{\sqrt{\pi}} \int_x^{\infty} e^{-t^2} dt$$

The probability P is plotted in Figure 9-4.

9.5.2.4 The probability of the lifted object hitting the barge is a function of the non-dimensional number

$$\tau = \frac{UT_z}{\sigma}$$

Requiring the probability to be less than a given number ε , gives implicitly a value for the maximum standard deviation σ of the relative motion which is proportional to the significant wave height H_s .

Guidance note:

During a series of 10 lifting operations one may require that the total acceptable probability is 0.01. Hence the required probability P for each lift should be less than 0.001. From Figure 9-5 this requires $UT_z/\sigma > 2.9$.

Assuming hoisting speed $U = 0.3$ m/s and $T_z = 7.0$ sec, the requirement to standard deviation of relative motion is $\sigma < 0.72$ m which is related to significant wave height of the seastate through the relative motion transfer function. If the relative motion as a special case, is equal to the wave motion, the limiting H_s of the operation is in this case given by $H_{s,max} = 4\sigma = 2.9$ m.

---e-n-d---of---G-u-i-d-a-n-c-e---n-o-t-e---

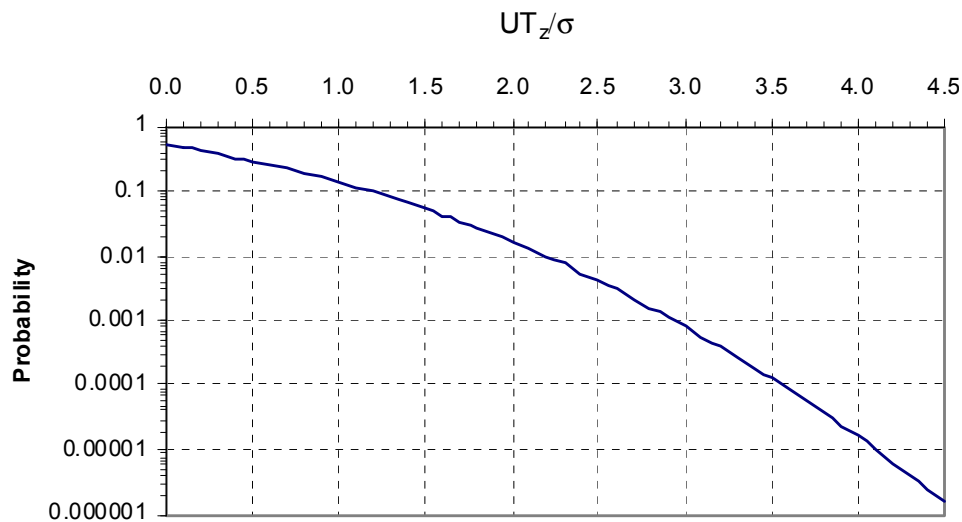


Figure 9-4
Probability of barge hitting lifted object

9.6 References

- /1/ F.G. Nielsen (2007) "Lecture Notes in Marine Operations". NTNU.
- /2/ Recommended Practice DNV-RP-C205 "Environmental Conditions and Environmental Loads". Issued April 2007.
- /3/ Faltinsen, O.M. (1990) "Sea Loads on Ships and Offshore Structures". Cambridge University Press.
- /4/ Molin, B. (2001) "On the piston and sloshing modes in moonpools". J. Fluid Mech. Vol. 430, pp. 27-50.
- /5/ Molin, B. (2002) "Experimental study of the wave propagation and decay in a channel through a rigid ice-sheet". Applied Ocean Research Vol. 24 pp.247-260.
- /6/ Abramowitz, M. and Stegun, I.A. (1965) "Handbook of Mathematical Functions". Dover edition.
- /7/ DNV-OS-H205 (planned issued 2010) "DNV Marine Operations. Lifting Operations".

APPENDIX A

ADDED MASS COEFFICIENTS

Table A-1 Analytical added mass coefficient for two-dimensional bodies, i.e. long cylinders in infinite fluid (far from boundaries). Added mass (per unit length) is $A_{ij} = \rho C_A A_R$ [kg/m] where A_R [m²] is the reference area

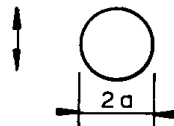
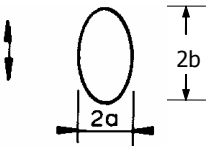
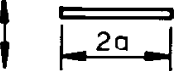
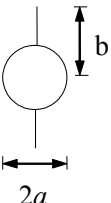
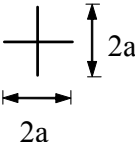
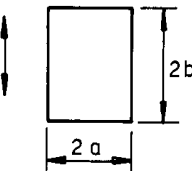
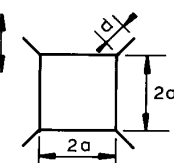
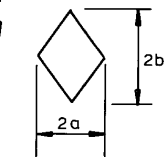
Section through body	Direction of motion	C_A	A_R	Added mass moment of inertia [(kg/m)*m ²]																				
		1.0	πa^2	0																				
	Vertical	1.0	πa^2	$\rho \frac{\pi}{8} (b^2 - a^2)^2$																				
	Horizontal	1.0	πb^2																					
	Vertical	1.0	πa^2	$\rho \frac{\pi}{8} a^4$																				
 Circular cylinder with two fins	Vertical	1.0	πa^2	$\rho a^4 (\csc^4 \alpha f(\alpha) - \pi^2) / 2\pi$ where $f(\alpha) = 2\alpha^2 - \alpha \sin 4\alpha + 0.5 \sin^2 2\alpha$ and $\sin \alpha = 2ab / (a^2 + b^2)$ $\pi / 2 < \alpha < \pi$																				
	Horizontal	$1 - \left(\frac{a}{b}\right)^2 + \left(\frac{a}{b}\right)^4$	πb^2																					
	Horizontal or Vertical	1.0	πa^2	$\frac{2}{\pi} \rho a^4$																				
	Vertical	1.0	πa^2	$\beta_1 \rho \pi a^4$ or $\beta_2 \rho \pi b^4$																				
				<table><tr><th>a/b</th><th>β_1</th><th>β_2</th></tr><tr><td>0.1</td><td>-</td><td>0.147</td></tr><tr><td>0.2</td><td>-</td><td>0.15</td></tr><tr><td>0.5</td><td>-</td><td>0.15</td></tr><tr><td>1.0</td><td>0.234</td><td>0.234</td></tr><tr><td>2.0</td><td>0.15</td><td>-</td></tr><tr><td>5.0</td><td>0.15</td><td>-</td></tr><tr><td>∞</td><td>0.125</td><td>-</td></tr></table>	a/b	β_1	β_2	0.1	-	0.147	0.2	-	0.15	0.5	-	0.15	1.0	0.234	0.234	2.0	0.15	-	5.0	0.15
a/b	β_1	β_2																						
0.1	-	0.147																						
0.2	-	0.15																						
0.5	-	0.15																						
1.0	0.234	0.234																						
2.0	0.15	-																						
5.0	0.15	-																						
∞	0.125	-																						
	Vertical	1.61 1.72 2.19	πa^2	$\beta \rho \pi a^4$																				
				<table><tr><th>d/a</th><th>β</th></tr><tr><td>0.05</td><td>0.31</td></tr><tr><td>0.10</td><td>0.40</td></tr><tr><td>0.10</td><td>0.69</td></tr></table>	d/a	β	0.05	0.31	0.10	0.40	0.10	0.69												
d/a	β																							
0.05	0.31																							
0.10	0.40																							
0.10	0.69																							
	Vertical	0.85 0.76 0.67 0.61	πa^2	$0.059 \rho \pi a^4$ for $a = b$ only																				

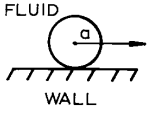
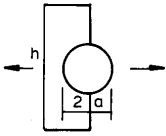
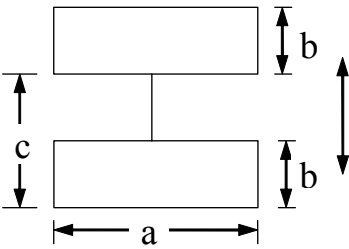
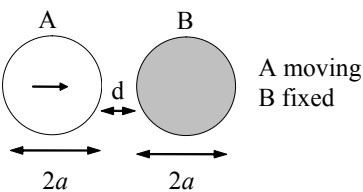
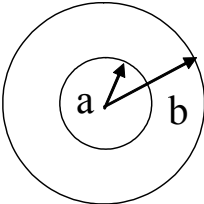
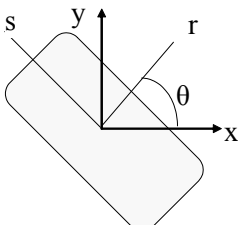
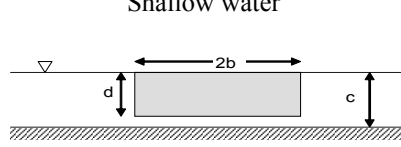
Table A-1 Analytical added mass coefficient for two-dimensional bodies, i.e. long cylinders in infinite fluid (far from boundaries). Added mass (per unit length) is $A_{ij} = \rho C_A A_R$ [kg/m] where A_R [m ²] is the reference area								
Section through body	Direction of motion	C_A		A_R	Added mass moment of inertia [(kg/m)*m ²]			
	Horizontal	$\frac{\pi^2}{3} - 1$		πa^2				
	Horizontal	$1 + \left(\frac{h}{2a} - \frac{2a}{h} \right)^2$		πa^2				
	Vertical	c/a	b/a				$2ab$	
			0.1	0.2	0.4	1.0		
		0.5	4.7	2.6	1.3	-		
		1.0	5.2	3.2	1.7	0.6		
		1.5	5.8	3.7	2.0	0.7		
		2.0	6.4	4.0	2.3	0.9		
		3.0	7.2	4.6	2.5	1.1		
		4.0	-	4.8	-	-		
	Horizontal	$d/a = \infty$ $d/a = 1.2$ $d/a = 0.8$ $d/a = 0.4$ $d/a = 0.2$ $d/a = 0.1$		1.000 1.024 1.044 1.096 1.160 1.224	πa^2			
		$\frac{b^2 + a^2}{b^2 - a^2}$		πa^2				
	Cross section is symmetric about r and s axes							
		$m_{yy}^a = m_{rr}^a \sin^2 \theta + m_{ss}^a \cos^2 \theta$ $m_{xx}^a = m_{rr}^a \cos^2 \theta + m_{ss}^a \sin^2 \theta$ $m_{xy}^a = \frac{1}{2} (m_{rr}^a - m_{ss}^a) \sin 2\theta$						
	Shallow water	$\frac{b}{c\varepsilon} - \frac{2}{\pi} \ln 4\varepsilon + \frac{2}{\pi} - \frac{2b}{c} + \varepsilon \frac{b}{c} + \frac{2}{3\pi} \varepsilon^2$ $\frac{d}{c} = 1 - \varepsilon$ where $\varepsilon \ll 1$			$2\rho c^2$			


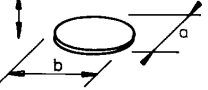
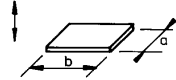
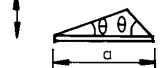
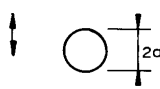
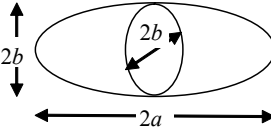
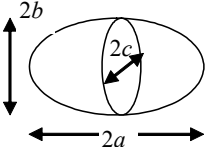
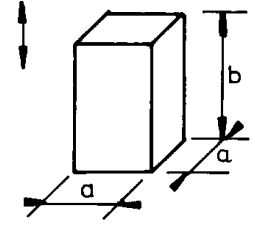
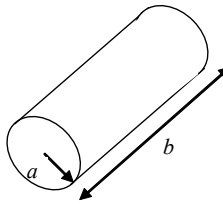
Table A-2 Analytical added mass coefficient for three-dimensional bodies in infinite fluid (far from boundaries). Added mass is $A_{ij}=\rho C_A V_R$ [kg] where V_R [m ³] is reference volume							
Body shape		Direction of motion	C_A				V_R
Flat plates	Circular disc 	Vertical	$2/\pi$				$\frac{4}{3} \pi a^3$
	Elliptical disc 	Vertical	b/a	C_A	b/a	C_A	$\frac{\pi}{6} a^2 b$
			∞	1.000	5.0	0.952	
			14.3	0.991	4.0	0.933	
			12.8	0.989	3.0	0.900	
			10.0	0.984	2.0	0.826	
			7.0	0.972	1.5	0.758	
	6.0	0.964	1.0	0.637			
	Rectangular plates 	Vertical	b/a	C_A	b/a	C_A	$\frac{\pi}{4} a^2 b$
			1.00	0.579	3.17	0.840	
1.25			0.642	4.00	0.872		
1.50			0.690	5.00	0.897		
1.59			0.704	6.25	0.917		
2.00			0.757	8.00	0.934		
2.50	0.801	10.00	0.947				
3.00	0.830	∞	1.000				
Triangular plates 	Vertical	$\frac{1}{\pi} (\tan \theta)^{3/2}$				$\frac{a^3}{3}$	
Bodies of revolution	Spheres 	Any direction	$\frac{1}{2}$				$\frac{4}{3} \pi a^3$
	Spheroids 	Lateral or axial	a/b	C_A		$\frac{4}{3} \pi b^2 a$	
			1.0 1.5 2.0 2.5 4.0 5.0 6.0 7.0 8.0	Axial	Lateral		
				0.500	0.500		
				0.304	0.622		
				0.210	0.704		
				0.156	0.762		
				0.082	0.860		
				0.059	0.894		
				0.045	0.917		
0.036				0.933			
0.029	0.945						
Ellipsoid  Axis $a > b > c$	Axial	$C_A = \frac{\alpha_0}{2 - \alpha_0}$ where $\alpha_0 = \varepsilon \delta \int_0^\infty (1+u)^{-3/2} (\varepsilon^2 + u)^{-1/2} (\delta^2 + u)^{-1/2} du$ $\varepsilon = b/a \quad \delta = c/a$				$\frac{4}{3} \pi abc$	
Square prisms 	Vertical	b/a 1.0 2.0 3.0 4.0 5.0 6.0 7.0 10.0	C_A 0.68 0.36 0.24 0.19 0.15 0.13 0.11 0.08		$a^2 b$		

Table A-2 Analytical added mass coefficient for three-dimensional bodies in infinite fluid (far from boundaries). Added mass is $A_{ij}=\rho C_A V_R$ [kg] where V_R [m ³] is reference volume (Continued)					
Body shape		Direction of motion	C_A		V_R
Right circular cylinder		Vertical	$b/2a$	C_A	$\pi a^2 b$
			1.2	0.62	
			2.5	0.78	
			5.0	0.90	
			9.0	0.96	
			∞	1.00	

APPENDIX B

DRAG COEFFICIENTS

Table B-1Drag coefficient on non-circular cross-sections for steady flow C_{DS} .Drag force per unit length of slender element is $f = \frac{1}{2} \rho C_{DS} D u^2$. D = characteristic width [m]. $Re = uD/\nu$ = Reynolds number.Adopted from Blevins, R.D. (1984) *Applied Fluid Dynamics Handbook*. Krieger Publishing Co.

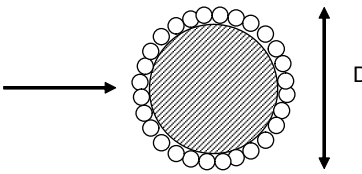
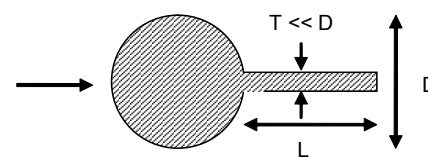
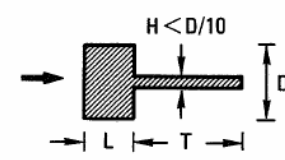
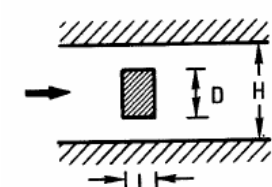
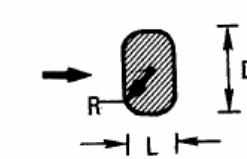
Geometry	Drag coefficient, C_{DS}							
1. Wire and chains 	Type ($R_e = 10^4 - 10^7$)				C_{DS}			
	Wire, six strand				1.5 - 1.8			
	Wire, spiral no sheathing				1.4 - 1.6			
	Wire, spiral with sheathing				1.0 - 1.2			
	Chain, stud (relative chain diameter)				2.2 - 2.6			
Chain stud less (relative chain diameter)				2.0 - 2.4				
2. Circular cylinder with thin fin 	L/D	0	0.33	0.67	1.0	1.5	2.0	2.5
	C_{DS}	1.25	1.2	1.15	1.1	1.07	1.02	1.0
	$R_e \sim 10^5$							
3. Rectangle with thin splitter plate 	L/D		T/D					
			0	5	10			
	0.1	1.9	1.4	1.38				
	0.2	2.1	1.4	1.43				
	0.4	2.35	1.39	1.46				
	0.6	1.8	1.38	1.48				
	0.8	2.3	1.36	1.47				
	1.0	2.0	1.33	1.45				
	1.5	1.8	1.30	1.40				
	2.0	1.6	-	1.33				
$R_e \sim 5 \times 10^4$								
4. Rectangle in a channel 	$C_{DS} = (1-D/H)^n C_D \mid H = \infty \text{ for } 0 < D/H < 0.25$							
	L/D	0.1	0.25	0.50	1.0	2.0		
	n	2.3	2.2	2.1	1.2	0.4		
	$R_e > 10^3$							
5. Rectangle with rounded corners 	L/D	R/D	C_{DS}	L/D	R/D	C_{DS}		
	0.5	0	2.5	2.0	0	1.6		
		0.021	2.2		0.042	1.4		
		0.083	1.9		0.167	0.7		
		0.250	1.6		0.50	0.4		
	1.0	0	2.2	6.0	0	0.89		
		0.021	2.0		0.5	0.29		
		0.167	1.2					
		0.333	1.0					
	$R_e \sim 10^5$							

Table B-1 (Continued)Drag coefficient on non-circular cross-sections for steady flow C_{DS} .Drag force per unit length of slender element is $f = \frac{1}{2} \rho C_{DS} D u^2$. D = characteristic width [m]. $R_e = uD/\nu$ = Reynolds number.Adopted from Blevins, R.D. (1984) *Applied Fluid Dynamics Handbook*. Krieger Publishing Co.

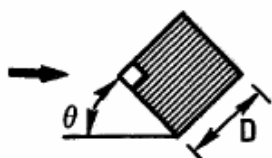
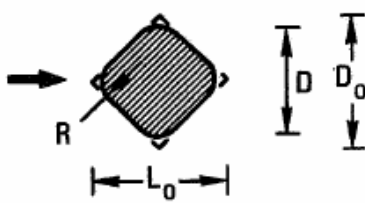
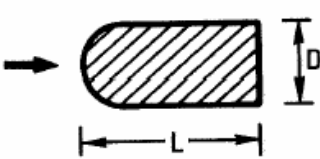
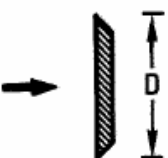
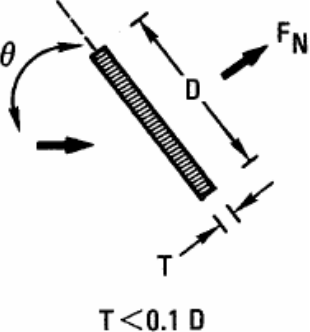
Geometry	Drag coefficient, C_{DS}										
6. Inclined square	θ	0	5	10	15	20	25	30	35	40	45
	C_{DS}	2.2	2.1	1.8	1.3	1.9	2.1	2.2	2.3	2.4	2.4
	$R_e \sim 4.7 \times 10^4$										
7. Diamond with rounded corners	L_0/D_0	R/D_0		C_{DS}							
	0.5	0.021 0.083 0.167		1.8 1.7 1.7		Fore and aft corners not rounded					
	1.0	0.015 0.118 0.235		1.5 1.5 1.5							
	2.0	0.040 0.167 0.335		1.1 1.1 1.1		Lateral corners not rounded					
	$R_e \sim 10^5$										
8. Rounded nose section	L/D					C_{DS}					
	0.5 1.0 2.0 4.0 6.0					1.16 0.90 0.70 0.68 0.64					
9. Thin flat plate normal to flow		$C_{DS} = 1.9, R_e > 10^4$									
10. Thin flat plate inclined to flow		$C_N = \begin{cases} 2\pi \tan \theta, & \theta < 8^\circ \\ 1, & 90^\circ \geq \theta > 12^\circ \\ 0.222 + 0.283/\sin \theta, & \end{cases}$ $C_L = C_N \cos \theta$ $C_{DS} = C_N \sin \theta$ <p>$T < 0.1 D$</p>									

Table B-1 (Continued)Drag coefficient on non-circular cross-sections for steady flow C_{DS} .Drag force per unit length of slender element is $f = \frac{1}{2} \rho C_{DS} D u^2$. D = characteristic width [m]. $R_e = uD/\nu$ = Reynolds number.Adopted from Blevins, R.D. (1984) *Applied Fluid Dynamics Handbook*. Krieger Publishing Co.

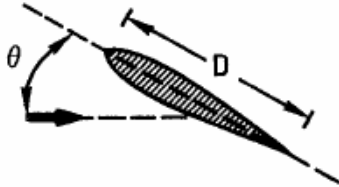
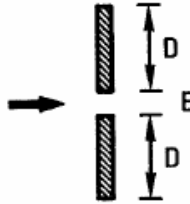
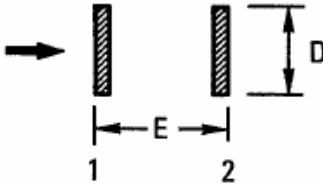
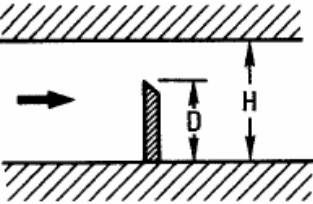
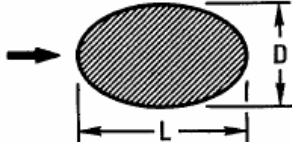
Geometry	Drag coefficient, C_{DS}		
11. Thin lifting foil 	$C_{DS} \sim 0.01$ $C_L = 2\pi \sin \theta$ $C_M = (\pi/4) \sin 2\theta$ (moment about leading edge) $C_M = 0$ about point $D/4$ behind leading edge		
12. Two thin plates side by side 	E/D 0.5 1.0 2.0 3.0 5.0 10.0 15.0	C_{DS} 1.42 or 2.20 1.52 or 2.13 1.9 or 2.10 2.0 1.96 1.9 1.9	multiple values due to jet switch Drag on each plate.
$R_e \sim 4 \times 10^3$			
13. Two thin plates in tandem 	E/D 2 3 4 6 10 20 30 ∞	C_{DS1} 1.80 1.70 1.65 1.65 1.9 1.9 1.9 1.9	C_{DS2} 0.10 0.67 0.76 0.95 1.00 1.15 1.33 1.90
$R_e \sim 4 \times 10^3$			
14. Thin plate extending part way across a channel 	$C_{DS} = \frac{1.4}{(1 - D/H)^{2.85}}$ for $0 < D/H < 0.25$ $R_e > 10^3$		
15. Ellipse 	D/L 0.125 0.25 0.50 1.00 2.0	C_{DS} ($R_e \sim 10^5$) 0.22 0.3 0.6 1.0 1.6	

Table B-1 (Continued)Drag coefficient on non-circular cross-sections for steady flow C_{DS} .Drag force per unit length of slender element is $f = \frac{1}{2}\rho C_{DS} Du^2$. D = characteristic width [m]. $Re = uD/\nu$ = Reynolds number.Adopted from Blevins, R.D. (1984) *Applied Fluid Dynamics Handbook*. Krieger Publishing Co.

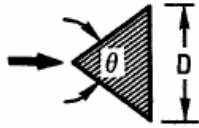
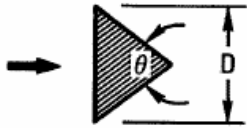
Geometry		Drag coefficient, C_{DS}	
16. Isosceles triangle 		θ	$C_{DS} (Re \sim 10^4)$
		30	1.1
		60	1.4
		90	1.6
		120	1.75
17. Isosceles triangle 		θ	$C_{DS} (Re = 10^4)$
		30	1.9
		60	2.1
		90	2.15
		120	2.05

Table B-2Drag coefficient on three-dimensional objects for steady flow C_{DS} .Drag force is defined as $F_D = \frac{1}{2}\rho C_{DS} S u^2$. S = projected area normal to flow direction [m^2]. $Re = uD/\nu$ = Reynolds number where D = characteristic dimension.

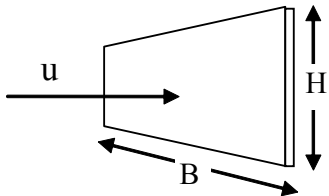
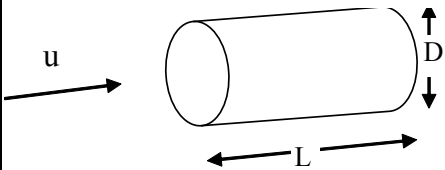
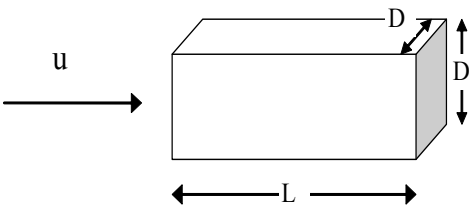
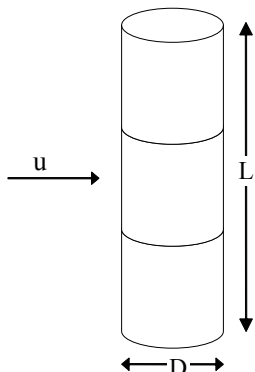
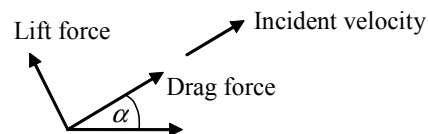
Geometry	Dimensions	C_{DS}	
Rectangular plate normal to flow direction 	B/H 1 5 10 ∞	1.16 1.20 1.50 1.90 $Re > 10^3$	
Circular cylinder. Axis parallel to flow. 	L/D 0 1 2 4 7	1.12 0.91 0.85 0.87 0.99 $Re > 10^3$	
Square rod parallel to flow 	L/D 1.0 1.5 2.0 2.5 3.0 4.0 5.0	1.15 0.97 0.87 0.90 0.93 0.95 0.95 $Re = 1.7 \cdot 10^5$	
Circular cylinder normal to flow. 	L/D 2 5 10 20 40 50 100	Sub critical flow $Re < 10^5$	Supercritical flow $Re > 5 \cdot 10^5$
		κ 0.58 0.62 0.68 0.74 0.82 0.87 0.98	κ 0.80 0.80 0.82 0.90 0.98 0.99 1.00
	$C_{DS} = \kappa C_{DS}^{\infty}$ κ is the reduction factor due to finite length. C_{DS}^{∞} is the 2D steady drag coefficient.		

Table B-3 Drag-lift force on two-dimensional profiles for steady flow

Force components are defined as $P_{d1} = \frac{1}{2}\rho C_{d1} b U^2$ and $P_{d2} = \frac{1}{2}\rho C_{d2} b U^2$ (note that the same characteristic dimension b is used for both components) where U is the incident velocity at angle α . If the lift force is positive, as shown, the total drag and lift coefficients on the profile are given by

$$C_D = C_{d1} \cos \alpha + C_{d2} \sin \alpha$$

$$C_L = -C_{d1} \sin \alpha + C_{d2} \cos \alpha$$



Profile	α (deg)	C_{d1}	C_{d2}	Profile	α (deg)	C_{d1}	C_{d2}
	0 45 90 135 180	1.9 1.8 2.0 -1.8 -2.0	1.0 0.8 1.7 -0.1 0.1		0 45 90 135 180	2.1 1.9 0 -1.6 -1.8	0 0.6 0.6 0.4 0
	0 45 90 135 180	1.8 2.1 -1.9 -2.0 -1.4	1.8 1.8 -1.0 0.3 -1.4		0 45 90	2.1 2.0 0	0 0.6 0.9
	0 45 90 135 180	1.7 0.8 0 -0.8 -1.7	0 0.8 1.7 0.8 0		0 45 90	1.6 1.5 0	0 1.5 1.9
	0 45 90 135 180	2.0 1.2 -1.6 -1.1 -1.7	0 0.9 2.2 -2.4 0		0 180	1.8 -1.3	0 0

APPENDIX C

PHYSICAL CONSTANTS

Table C-1 Density and viscosity of fresh water, sea water and dry air						
<i>Temperature deg [C]</i>	<i>Density, ρ, [kg/m³]</i>			<i>Kinematic viscosity, ν, [m²/s]</i>		
	<i>Fresh water</i>	<i>Salt water</i>	<i>Dry air</i>	<i>Fresh water</i>	<i>Salt water</i>	<i>Dry air</i>
0	999.8	1028.0	1.293	$1.79 \cdot 10^{-6}$	$1.83 \cdot 10^{-6}$	$1.32 \cdot 10^{-5}$
5	1000.0	1027.6	1.270	1.52	1.56	1.36
10	999.7	1026.9	1.247	1.31	1.35	1.41
15	999.1	1025.9	1.226	1.14	1.19	1.45
20	998.2	1024.7	1.205	1.00	1.05	1.50
25	997.0	1023.2	1.184	0.89	0.94	1.55
30	995.6	1021.7	1.165	0.80	0.85	1.60